



**Provisional Manuscript – Private Defense**

# **COMPARISON OF DIFFERENT METHODS FOR SHAPING AMORPHOUS SOLID DISPERSIONS**

---

Olivier Jennotte

Pharmacist

Promotor: Prof. **B. Evrard**

Co-promotor: Prof. **G. Piel**

Doctoral thesis presented with the purpose of being awarded the degree of  
PhD in Biomedical and Pharmaceutical Sciences

Academic year 2022-2023



## Remerciements

*Au terme de ce travail, je voudrais remercier toutes les personnes qui, d'une manière ou d'une autre, ont contribué à sa réalisation et qui m'ont permis, par leurs conseils mais aussi leur soutien, de le mener à bien.*

*Je désire tout d'abord adresser mes sincères remerciements à la Professeure Brigitte Evrard, ma promotrice, de m'avoir donné l'opportunité de réaliser une thèse au sein du Laboratoire de Technologie Pharmaceutique, combinée à l'assistanat qui m'a donné goût à cette forme d'enseignement.*

*J'exprime également ma gratitude à la Professeure Géraldine Piel, ma co-promotrice, pour ses conseils avisés lors de la réalisation et la rédaction de ce projet, mais aussi pour sa guidance lors de mes premières années d'assistanat.*

*J'aimerais ensuite remercier la Docteure Anna Lenchanteur pour tout le temps consacré à suivre mon projet ainsi qu'aux nombreuses relectures effectuées.*

*Je remercie vivement les autres membres de mon comité de thèse: le Professeur Philippe Hubert, la Professeure Christine Jérôme, le Professeur Patrick Herné et le Docteur Pierre Lebrun de m'avoir prodigué de précieux conseils et encouragements lors de notre réunion annuelle. Je remercie également les membres du jury extérieur, le Professeur Jonathan Goole et le Professeur Assistant Julian Quodbach d'avoir accepté de juger ce travail.*

*Ces derniers mois «d'isolement» passés à rédiger cette thèse m'ont permis de me rendre compte que l'ambiance de tous les jours qui règne au sein du laboratoire allait me manquer. Je remercie dès lors tous mes collègues, anciens et actuels, d'avoir rendu cette atmosphère de travail si agréable. Merci à Laurence Collard, Françoise Léonard, Martine Cao, Natacha Rocks, Claudio Palazzo, Justine Thiry, Aude Pestieau, Charline Defourny, William Bigazzi, Chloé Parulski, Manon Berger, Eva Gresse, Laure-Anne Bya, Tuan Nghia Dinh, Chloé Gauthy, Hope Sounouvou, Ange Ilangalabooka, Luc Delma, Isaïe Nyamba, Cindy Chaballe, Robin Crunenbergen et Vanessa Strauven.*

*Mention spéciale à Coralie Bellefroid, Nathan Koch et Noémie Penoy pour ces moments formidables passés avec vous. Cette phrase est ultra bateau, mais pourtant si vraie, toutes ces années n'auraient pas été d'une telle qualité sans votre compagnie.*

*Merci à mes amis, ma famille et en particulier à mes parents qui m'ont permis d'en arriver jusqu'ici.*

*Enfin, je tiens à remercier Marie, qui par sa patience et sa bonne humeur sans faille, a réussi à gérer mes énormes périodes de stress. Ton écoute (quand je parle) et ton soutien sont pour moi inestimables. Merci aussi à Louis, qui, plus récemment, a été une grande source de motivation pour la finalisation de ce projet.*

*Du fond du cœur, merci.*

Olivier

## TABLE OF CONTENTS

Remerciements .....	2
INTRODUCTION.....	8
Chapter I. BCS II DRUG FORMULATION .....	10
1 Introduction.....	10
2 Biopharmaceutics Classification System.....	10
3 Formulation Strategies for BCS II Drugs .....	13
3.1 Crystal Modifications.....	13
3.2 Cyclodextrin Complexation .....	17
3.3 Self-emulsification .....	18
3.4 pH Modification.....	19
3.5 Amorphization.....	19
3.6 Solid Dispersions .....	22
Chapter II. MANUFACTURING PROCESSES FOR AMORPHOUS SOLID DISPERSIONS.....	25
1 Solvent-Based Methods.....	25
1.1 Spray-Drying.....	25
1.2 Freeze-drying .....	26
1.3 Supercritical Fluids .....	26
1.4 Electrospinning .....	26
2 Photopolymerization-Based Method (stereolithography) .....	27
3 Melting-Based Methods .....	29
3.1 KinetiSol®.....	29
3.2 Microwave Heating .....	30
3.3 Selective Laser Sintering .....	30
3.4 Direct Powder Extrusion .....	32
3.5 Hot-Melt Extrusion .....	33
Chapter III. SHAPING OF EXTRUDED AMORPHOUS SOLID DISPERSIONS.....	36
1 Milling and Tableting or Capsule Filling.....	36
2 Injection Moulding.....	37
3 Calendaring and Cutting .....	37
4 Pelletizing and Tableting/Capsule Filling.....	38
5 Three Dimensional Printing.....	39

5.1 Fused Deposition Modeling (FDM) .....	40
5.2 Conclusion .....	53
6 References.....	55
OBJECTIVES .....	66
RESULTS .....	70
Chapter I. SELECTION OF A SUITABLE AMORPHOUS SOLID DISPERSION METHOD .....	72
1. Context and purpose of the study.....	72
2. Publication .....	74
2.1 Abstract.....	75
2.2 Introduction .....	76
2.3 Materials and methods.....	77
2.4 Results.....	82
2.5 Conclusion .....	92
2.6 Acknowledgements .....	92
2.7 References.....	93
Chapter II. PRODUCTION AND SHAPING OF ASDs BY HOT-MELT EXTRUSION AND CAPSULE FILLING .....	97
1. Context and purpose of the study.....	97
2. Publication .....	100
2.1 Abstract.....	101
2.2 Introduction .....	102
2.3 Material and methods.....	104
2.4 Results and Discussion .....	107
2.5 Conclusion .....	116
2.6 Acknowledgments .....	116
2.7 References.....	117
Chapter III. USE OF FUSED-DEPOSITION MODELING 3D PRINTING COUPLED WITH HOT-MELT EXTRUSION FOR THE PRODUCTION OF IMMEDIATE RELEASE SOLID FORMS .....	122
1. Context and purpose of the study.....	122
2. Publication .....	125
2.1 Abstract.....	126
2.2 Introduction .....	127
2.3 Material and methods.....	129

2.4	Results and discussion .....	135
2.5	Conclusion.....	144
2.6	Acknowledgments .....	145
2.7	References .....	146
Chapter IV. FEASIBILITY STUDY OF THE USE OF A HOMEMADE 3D POWDER PRINTER FOR THE PRODUCTION OF SOLID FORMS WITH IMMEDIATE RELEASE OF CANNABIDIOL .....		
		151
1.	Context and purpose of the study .....	151
2.	Publication .....	154
2.1.	Abstract .....	155
2.2.	Introduction.....	156
2.3.	Material and methods .....	159
2.4	Results and discussion .....	165
2.5	Conclusion .....	172
2.6	Acknowledgments .....	173
2.7	References .....	174
DISCUSSION.....		179
CONCLUSIONS AND PERSPECTIVES .....		206
Summary.....		211
APPENDICES .....		214
APPENDIX I. VALIDATION OF HPLC METHOD FOR DOSING CBD <i>IN VITRO</i> .....		
		215
1.	Calibration solutions .....	215
2.	Validation report .....	216
2.1	Experimental design .....	216
2.2	Response function.....	217
2.3	Trueness .....	220
2.4	Precision .....	220
2.5	Uncertainty of measurements .....	222
2.6	Accuracy.....	223
2.7	Linearity of results .....	225
2.8	Limit of detection (LOD), limits of quantification (LOQ) and dosing range	227
APPENDIX II. ADDITIONAL STUDIES ON CAPSULES.....		228
1.	Pharmacotechnical Tests.....	228

2. Stability of CBD Physical State.....	228
APPENDIX III. ADDITIONAL STUDIES ON FILAMENTS AND PRINTED TABLETS .....	231
1. Stability of CBD Physical State.....	231
2. Evaluation of degradation temperature of raw materials.....	233
3. In vivo considerations.....	233
APPENDIX IV. ADDITIONAL STUDIES ON PRINTED TABLETS PRODUCED BY DPE .....	235
1. Stability of CBD Physical State.....	235
2. Evaluation of degradation temperature of raw materials.....	237
APPENDIX V. <i>IN VITRO</i> DISSOLUTION TEST WITH ASD MANUFACTURED WITH THREE PROCESSING TECHNOLOGIES .....	238
APPENDIX VI. 3D PRINTING TECHNOLOGIES FOR SOLUBILITY INCREASE .....	240
1. Introduction .....	241
2. Three-dimensional Printing Techniques .....	242
2.1 Nozzle-deposition models .....	244
2.2 Laser-based printing .....	259
3. Conclusion .....	262
4. References.....	265
ABBREVIATIONS.....	272
CURRICULUM VITAE .....	275
Education .....	276
Bibliography .....	276

# INTRODUCTION

---





## Chapter I. BCS II DRUG FORMULATION

### 1 Introduction

Before the 1990s, the discovery of molecules of therapeutic interest was rather done through empirical methods. Since then, computational chemistry combined with high-throughput screening (HTS) has made the research for new molecules more rational. However, the trend towards computational modification of the structure of molecules of interest, in order to more closely match the target, leads to the synthesis of molecules with poor drug-like properties, namely increased molecular weight, greater LogP and consequently lower aqueous solubility [1–3]. While HTS is useful to test these multiple drug candidates in a reasonable time, current HTS techniques usually require dimethyl sulfoxide (DMSO), sometimes added with surfactants, to solubilize the drug candidate, which is different from human physiological fluids. As an example, HTS results may highlight the potential of drug candidates in terms of in vitro drug-receptor interaction without considering the in vivo aspect. Consequently, poorly water-soluble molecules could be wrongly considered drug-able. To integrate the notion of solubility, biorelevant media, composed of physiological components to simulate as close as possible the in vivo conditions are nowadays more and more investigated. Nevertheless, despite the growing use of biorelevant media in order to better predict the solubility of drug candidates, it is estimated that 75-90% of drug products in development are considered as poorly water-soluble [4–9]. Therefore, increasing the water solubility of these drugs during the preformulation and optimization steps is crucial before the conduction of clinical trials. The discovery and the improvement of strategies to enhance water-solubility of drugs has contributed to reduce the impact of poor solubility on clinical trials failure. Indeed, of 90% of the drug candidates that fail during phase I, II or III of clinical studies, the impact of molecules with poor drug-like properties decreased from 30% - 40% in the 1990s to 10% - 15% today [3]. However, this percentage remains high and preformulation/optimization methods should continue to be investigated.

### 2 Biopharmaceutics Classification System

In 1995, Amidon and his team developed the Biopharmaceutics Classification System (BCS) with the aim of having a theoretical basis for the correlation of in vitro dissolution with in vivo bioavailability of an active pharmaceutical ingredient (API). The bioavailability is defined by the rate and the extent at which the drug is absorbed from a formulation and made available at the site of pharmacological action. This model is based on the two key factors that have the most significant influence on the absorption

rate and extent of a drug, namely its aqueous solubility and its gastrointestinal permeability. These two properties were used to classify drug substances into four classes, each with different formulation options, as shown in Fig. 1 and discussed below [10].

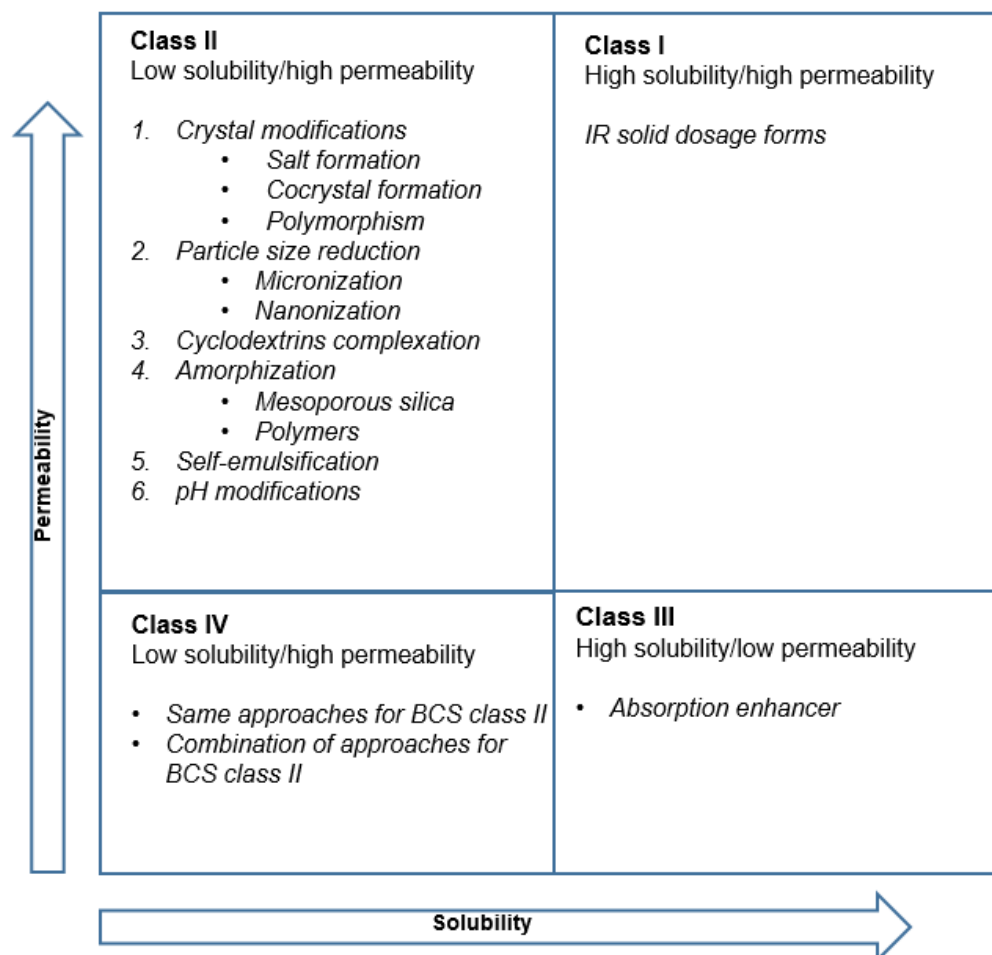


Figure 1 - Formulation options based on BCS. Adapted from [11].

According to the Food and Drug Administration (FDA), a drug is classified as highly soluble drug if the highest drug product's strength is soluble in 250 mL of aqueous media in the gastrointestinal pH range (1 – 6.8) at a temperature of 37 °C ± 1 °C and highly permeable meaning that the systemic bioavailability or absorption of an orally administered dose in humans is equal or higher than 85%. This dose is based on a mass balance determination or in comparison to an intravenous reference dose [12,13]. Based on these definitions, drugs can be divided into four classes, allowing a better prediction of the *in vitro-in vivo* correlations (IVIVC) [10]:

- **Class I** gathers drugs with high solubility and high permeability. The factor limiting the drug absorption is the drug dissolution or the gastric emptying if the dissolution is very fast. The IVIVC is possible only if the dissolution rate is slower than the gastric emptying rate.
- **Class II** gathers drugs with low solubility and high permeability. The factor controlling the drug absorption is the *in vivo* drug dissolution. The IVIVC is possible if the *in vitro* dissolution rate is similar to *in vivo* dissolution rate, unless administering a very high dose.
- However, while the BCS system is recognized as the pioneer classification, many works have adapted this system to improve the *in vivo* correlation. In particular, the Developability Classification System (DCS) was introduced by Butler and Dressman in 2010 and subdivided the second class in two in order to take into account the human physiology [14]. The BCS system categorizes a drug as non-soluble if it does not reach sufficient solubility in a broad range of pH (1 – 6.8). However, many drugs are weak acids or bases, and their solubility varies significantly depending on whether it is measured in a gastric or intestinal environment. As an example, ibuprofen is classified in BCS class II due to its poor solubility at low pH, while its high solubility in intestinal environment gives this molecule a good bioavailability.
- Therefore, DCS splits the BCS II class in two:
  - *I/a* gathers drugs with a limited dissolution rate. Because they are highly permeable, the formulation can usually be designed to achieve complete oral absorption from a standard solid oral dosage form containing the drug in its crystalline state. Indeed, the solubility and permeability are compensatory, leading to a continuous absorption of the slowly dissolving drug.
  - *I/b* gathers drugs with a limited solubility. They tend to be incompletely absorbed if they are in their crystalline state in the formulation.
- **Class III** gathers drugs with high solubility and low permeability. The factor controlling the drug absorption is the drug permeability. The IVIVC with the dissolution rate is limited.
- **Class IV** gathers drugs with low solubility and low permeability. The drug absorption is limited by the solubility and the permeability. There is limited or no expected IVIVC.

Three main purposes of BCS can be highlighted [15]:

- 1 Allowing the prediction of *in vivo* pharmacokinetic performance of drugs by measuring their solubility and permeability;
- 2 Reducing expensive and time-consuming *in vivo* bioequivalence studies with the BCS-based Biowaivers approach whereby the equivalence of two products can be decided following an *in vitro* dissolution test;
- 3 Facilitate the formulation design in drug development by proposing leads of formulation for each class of drugs:
  - 3.1 Class I: conventional formulations such as capsules or tablets are generally sufficient to ensure the rapid dissolution of class I drugs, as there are highly water-soluble and highly permeable to the gastrointestinal tract (GIT).
  - 3.2 Class II: Depending on the drug, the bioavailability could be improved by increasing the dissolution rate (IIa) or by increasing the aqueous solubility of the drug (IIb). The strategies used for class II are described in the next chapter.
  - 3.3 Class III: This class orients the formulator to the use of absorption enhancer such as polysaccharides or bile salt.
  - 3.4 Class IV: This challenging class regroups drugs with low solubility combined with low permeability. The formulators must combined strategies derived from class II and III.

### 3 Formulation Strategies for BCS II Drugs

Increasing the aqueous solubility and/or the dissolution rate is essential to improve the bioavailability of molecules belonging to the BCS II class, as they have good intestinal permeability, only limited by the rate of dissolution and/or the solubility. Several strategies are used to increase these two parameters. For molecules classified as DCS IIa, drug dissolution can be optimized by controlling the particle size. For molecules classified as DCS IIb, improvement can be achieved by using thermodynamically more soluble drugs, such as modified crystals, amorphous forms, or by the use of excipients that promote solubility such as cyclodextrins (CDs) or lipids. Each strategy is described hereunder.

#### 3.1 Crystal Modifications

##### 3.1.1 Salt Formation

Salts of acidic and basic drugs have, in general, a higher solubility than their corresponding acid or base forms. The use of salt form of poorly water-soluble drugs

has been widely used in drug development to increase their solubility and dissolution rate. For example, Cristofaletti and Dressman compared the dissolution of ibuprofen and two of its salts, namely ibuprofen sodium dihydrate and ibuprofen lysinate [16]. The dissolution test of these three entities in a 50 mM phosphate buffer showed a virtually instantaneous dissolution of the two salts while ibuprofen suffered from wettability issues, resulting in a slower dissolution.

Salt formation is considered as the most widely used technique to increase the solubility and dissolution rate of drugs in development [17]. However, this technique has some drawbacks. Salt formation is only applicable to molecules possessing acidic or basic character. Additionally, salts of acidic or basic drugs can precipitate in the gastric or intestinal pH, respectively, necessitating the combination of salt formation with other solubility-enhancing techniques. Finally, the salts are generally manufactured using “non-green” organic solvents [18].

More than 50 API salts are currently commercialized. As examples *Glivec*® contains a mesilate salt of imatinib. The API contained in *Plavix*® is clopidogrel hydrogen sulfate, an anti-platelet. Another example is metoprolol tartrate that is used as a  $\beta$ -blocker in *Seloken*®.

### 3.1.2 Cocrystal Formation

A pharmaceutical cocrystal is a structurally homogeneous multicomponent system composed of at least one API connected by weak bonds, generally hydrogen bonds, to one or more coformer(s) [19]. They are used in drug development to address problems of poorly soluble drugs. Once in a biological medium, the coformer will quickly dissociate from the API, due to the weak interaction forces. The coformer, being generally more water-soluble than the API, will be removed from the crystal lattice, leading to a more soluble API crystal architecture. This results in a supersaturated solution in which the API is available for absorption.

Unlike salts, cocrystals can be formed with non-ionizable molecules without any alteration of the drug molecular structure. However, the formation of cocrystals has some limitations. Among them, solvent selection is critical and it is hardly transferable in large scale of production because it requires a large amount of material and it is time consuming. Many studies concerning cocrystals formation can be found in the literature. As an example, Ma *et al.* used the technique of solvent drop grinding to develop a cocrystal of apigenin, a flavonoid used to reduce the inflammation associated with chronic aging diseases, and bipyridine in order to improve the aqueous solubility and bioavailability of apigenin. *In vivo*, the cocrystal exhibited an anti-inflammatory response

of 56%, which was significantly higher than the response of pure apigenin, which was only 26% [20].

Examples of the few marketed products containing cocrystals are: *Odomzo*<sup>®</sup> (cocrystal of sonidegib and phosphoric acid, antitumor), *Entresto*<sup>®</sup> (cocrystal of valsartan and sacubitril, antihypertensive) and *Steglatro*<sup>®</sup> (antidiabetic, cocrystal of ertugliflozin and L-pyrogutamic acid, antidiabetic).

### 3.1.3 Polymorphism

Polymorphs are crystalline solids that share the same chemical composition, but differ in their internal crystal structures [21]. Each polymorph of a given compound exhibits unique physicochemical properties, such as distinct mechanical behavior, physical and chemical stability, solubility and dissolution rate [22]. In most cases, the solubility of metastable forms is higher than the one of the corresponding stable forms, but they tend to return to a thermodynamically stable state in a relatively short time [23]. Therefore, the polymorphic transformation has to be controlled in dosage forms containing metastable forms, in order to keep reproducibility in terms of solubility, dissolution rate and stability [24]. For example, Zhang and Chen produced two forms of amisulpride and showed that the metastable form II possesses a higher aqueous solubility than the stable form I [25].

### 3.1.4 Particle Size Reduction

If the bioavailability of molecules is limited by the dissolution rate, it can be improved by increasing the dissolution rate. The dissolution rate is defined by the equation developed in 1897 by Noyes and Whitney (**Eq. 1**) [26]:

$$\frac{dC}{dt} = \frac{D}{h} \times S \times (C_s - C) \quad \text{Eq. 1}$$

where  $dC/dt$  represents the dissolution rate,  $D$  is the diffusion coefficient of the drug,  $h$  is the thickness of the diffusion layer,  $S$  is the surface area of the compound undergoing dissolution,  $C_s$  is the aqueous solubility of the drug and  $C$  the concentration of the drug at time  $t$ .

Two approaches are currently used to increase the surface area of the drug particle, namely the micronization and the nanonization.

#### 3.1.4.1 Micronization

Particles micronization has been widely used for the enhancement of the dissolution rate of poorly water-soluble drugs. Micronization can enhance the dissolution rate of a

substance through two mechanisms. First, it increases the surface area of the particle that comes into contact with biological fluids, as described by Eq. 1. Second, reducing the particle size decreases the thickness of the diffusion layer, leading to faster dissolution, particularly when the thickness of the diffusion layer is reduced to less than 5  $\mu\text{m}$ , as suggested by the Prandtl boundary layer equation (Eq. 2) [11,27].

$$h_H = k \left( \frac{L^{1/2}}{V^{1/2}} \right) \quad \text{Eq. 2}$$

where  $h_H$  represents the hydrodynamic boundary layer thickness,  $L$  is the length of the surface in the direction of the flow,  $k$  denotes a constant and  $V$  is the relative velocity of the flowing against the flat surface.

The most used method for particles micronization is the milling, such as air jet milling or the ball milling [28]. This can also be conducted by spray-drying [29] or by a supercritical fluid technology [30], but these two techniques require expensive equipment and are time-consuming [31].

Micronization does not always induce an increase of the dissolution rate. Indeed, the large induced surface area of the particles can promote the agglomeration of them, resulting in a slower dissolution of the drug. In order to avoid this phenomenon, adjuvants such as hydrophilic polymers or surfactants, can be added to the formulation to prevent agglomeration [32].

Example of the few marketed products containing micronized API: *Lofibra*<sup>®</sup> (fenofibrate, hypolipidemic).

### 3.1.4.2 Nanonization

Nanonization is the process of reduction of an active drug in nanoparticles or in sub-micron particles, with sizes of 1-100 and 100-1000 nm, respectively [33]. Three categories of techniques are used to produce these particles: bottom-up, top-down or a combination of these two approaches [34]. The bottom-up processes involve the building of nanoparticles by precipitation of dissolved molecules and the top-down processes involve particle reduction of larger crystals. Particles produced through nanonization offer similar benefits to micronized particles. In addition, they can increase the solubility at saturation. This is due to the fact that, according to Ostwald-Freundlich equation (Eq. 3), saturation solubility  $C_s$  is inversely proportional to the particle size [35].



$$\log \frac{C_s}{C_\infty} = \frac{2 \times \sigma V}{2.303 \times RT\rho r} \quad \text{Eq. 3}$$

where  $C_s$  is the solubility of a small solid particle,  $C_\infty$  is the relative concentration of the solute at the interface,  $\sigma$  is the interfacial tension substance,  $V$  is the molar volume of the particle material,  $R$  is the gas constant,  $T$  is the absolute temperature,  $\rho$  is the density of the solid and  $r$  is the radius.

The property of nanoparticles to induce a supersaturated solution of the drug can also induce recrystallization into larger insoluble particles, called the Ostwald ripening [31]. Moreover, as the high surface area of the nanoparticles gives them a high free energy, agglomeration can occur by particles attraction. Like for the micronized formulations, hydrophilic polymers and/or surfactants can be added in order to prevent this phenomenon [36].

Examples of the few marketed products containing nanonized API: *Triglide*® (fenofibrate, hypolipidemic) or *Avinza*® (morphine sulfate, painkiller).

### 3.2 Cyclodextrin Complexation

CDs are cyclic, torus shaped, oligosaccharides containing six ( $\alpha$ CD), seven ( $\beta$ CD), eight ( $\gamma$ CD) or more glucopyranose units (Fig. 2) [37]. The orientation of the hydroxyl functions of the glucopyranose monomers makes the outer of the torus hydrophilic while the inner is formed by the more hydrophobic parts. This configuration allows the CDs to form water-soluble inclusion complexes with poorly-soluble drugs by taking up the hydrophobic part of the molecule in the inner part of the CD [38]. The formation and dissociation of the CD-drug complex does not induce the formation or breaking of covalent bonds, resulting in an easy release of the molecule once in contact with aqueous media [39,40]. The chemical structures and the physicochemical properties of both drug and CD will influence the formation of a drug-CD complex. For example, even if ionizable drugs are able to form an inclusion complex with CDs, non-ionizable drugs usually form more stable complexes [41].

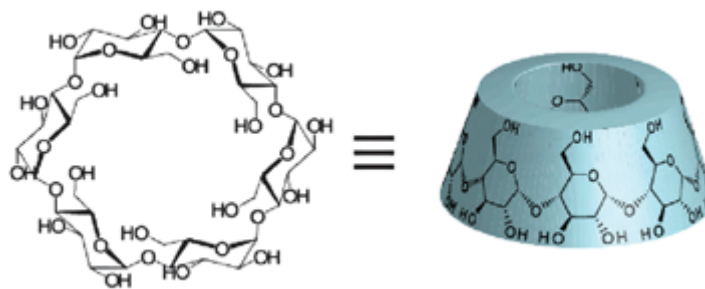


Figure 2 - Structure of αCD [42].

Multiple methods for the formation of inclusion complex can be found in the literature, such as rapid mixing, spray-drying [43], freeze-drying (FD) [44], supercritical antisolvent technology [45] or hot-melt extrusion (HME) [46].

As an example, Thiry *et al.* compared six types of CDs for the production by HME of ternary inclusion complexes of itraconazole (ITZ), a poorly water-soluble API and Soluplus® (SOL), a polymeric complex stabilizer [47]. The ternary complexes were compared to an amorphous binary formulation composed of ITZ and SOL. The improvement of the solubility and the dissolution rate of ITZ from the ternary complexes was reported to be higher than that from the binary formulation.

A recent review listed more than 100 marketed formulations containing API-CDs complex. As examples *Brexine*® (piroxicam, anti-inflammatory), *Indocollyre*® (indomethacin, anti-inflammatory), *Fluner*® (flunarizine, calcium antagonist) or *Bisolvon*® tablet (Bromhexin, mucolytic) can be cited.

### 3.3 Self-emulsification

Self-emulsifying drug delivery systems (SEDDS) are lipid-based formulations composed of oils, surfactants and co-solvents. They are prepared by gentle mixing of oil and surfactant to produce an isotropic mixture. The resulting formulation is able to emulsify *in vivo* once in contact with aqueous fluid, leading to the dissolution of hydrophobic drugs. Depending on the manufacturing method and the composition, SEDDS can be categorized in self-microemulsifying drug delivery systems (SMEDDS) or self-nanoemulsifying drug delivery systems (SNEDDS) [48]. Once in contact with the physiological fluids, SMEDDS will spontaneously emulsify in microemulsions while SNEDDS will form nanoemulsions [49].

The SEDDS provide an effective approach for poorly soluble and poorly permeable drugs. Indeed, their lipid-based structure enhances both the drug intestinal permeability and the drug lymphatic transport to avoid first-pass hepatic metabolism. Moreover, the large surface area of the droplets improves the aqueous solubility of the drug. However,

conventional SEDDS have some drawbacks such as high surfactant concentration that irritates the GIT or a lack of suitable *in vitro* models for the assessment of SEDDS formulations. Several new methods for the formulation of SEDDS have been developed to overcome these problems [48]. As an example, Madagul *et al.* formulated a solid SMEDDS of chlorthalidone by spray-drying technology. In addition to provide a better solubility of the drug, the solid SMEDDS was stable for at least three months [50]. Less than 20 marketed drug products containing SEDDS were found. Some examples are: *Fortovase*® (saquinavir, treatment of HIV), *Depakene*® (valproic acid, treatment of seizures) and *Accutane*® (isotretinoin, treatment of acne).

### 3.4 pH Modification

According to Vo *et al.*, two thirds of poorly water-soluble drugs are weak acids or bases with a pH-dependent solubility [51]. The microenvironment pH has been defined as “a microscopic layer surrounding a solid particle in which the solid forms a saturated solution with the absorbed water” [52]. Adding pH modifiers in this diffusion area could improve the stability and the dissolution behavior of the ionizable drugs.

Organic acids, such as fumaric acid, citric acid or succinic acid have often been used as pH modifiers for formulations containing weakly basic drugs. Concerning the formulations of weakly acidic drugs, alkalizers such as sodium hydroxide, magnesium hydroxide, calcium phosphate or sodium carbonate have been used [53].

If there is an incompatibility between a drug and pH modifier, or if the drug recrystallizes after being rapidly released from a pH-modified formulation, pellets can be produced to separate the drug from the pH modifier and polymeric-based formulation can be used to stabilize the drug in solution, respectively.

Examples of the few marketed products containing pH modifiers are: *Micardis*® (telmisartan, meglumine and sodium hydroxide as alkalizers, antihypertensive). *Prandin*® (repaglinide, meglumine as alkilizer, antidiabetic).

### 3.5 Amorphization

Solids in their amorphous state are characterized by short-range order over a few molecular dimensions in opposition to their crystalline state which have a three-dimensional (3D) long-range order. Hancock and Zografi illustrated the variations in enthalpy (H) and volume (V) of a solid substance with respect to temperature (**Fig. 3**) [54]. At very low temperatures, a crystalline solid exhibits a certain heat capacity and thermal expansion, resulting in a slight increase in both enthalpy and volume. When the temperature reaches the melting point ( $T_m$ ), there is a sharp increase in both H and V, representing the first-order phase transition to the liquid state. If the liquid is rapidly

cooled, the H and V values may follow the equilibrium line for the liquid, extending beyond the  $T_m$  into a "supercooled" liquid region until it reaches the glass transition temperature ( $T_g$ ). At  $T_g$ , the properties of the glassy material deviate from those of the equilibrium supercooled liquid, resulting in a nonequilibrium state with even higher V and H values than the supercooled liquid.

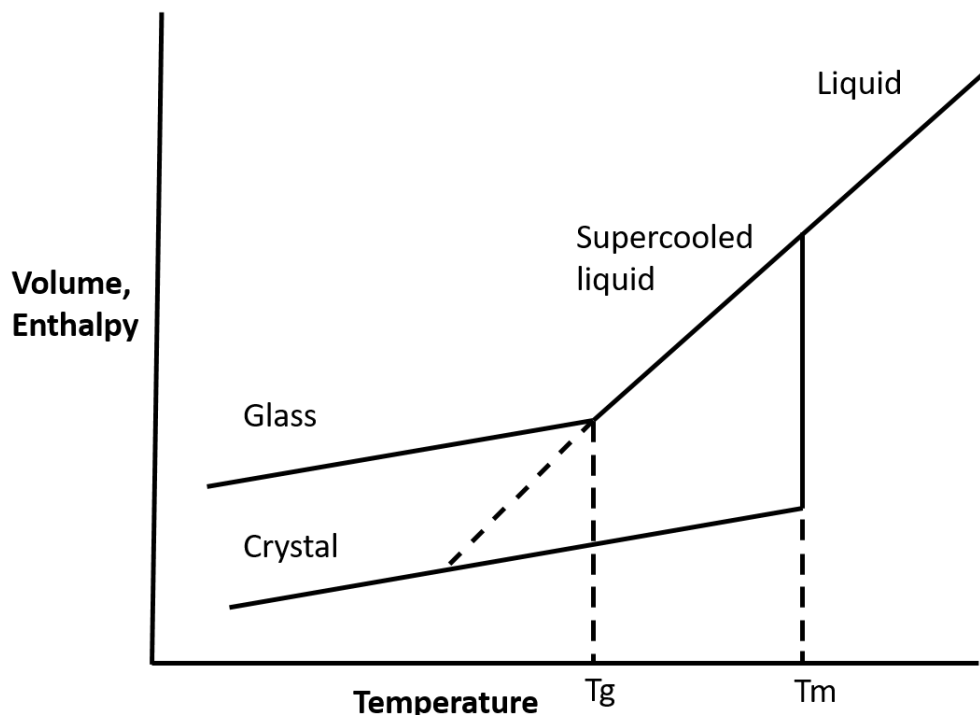


Figure 3 - Representation of the evolution of enthalpy or volume in a function of the temperature. Adapted from [54].

Having higher intern energy, the amorphous state has enhanced thermodynamic properties, such as solubility and dissolution, compared to the crystal state. This high intern energy added to the high molecular motion stands for a high chemical reactivity and a risk of spontaneous crystallization. This instability explains why the application of pure amorphous drugs is limited in the pharmaceutical market. Some of the few examples are *Ceftin*<sup>®</sup> (cefuroxime axetil, naturally amorphous) and *Accolate*<sup>®</sup> (Zafirlukast, produced by spray-drying).

However, a drug in its amorphous state can be stabilized and prevented from recrystallization by the molecular dispersion of the amorphous drug in a hydrophilic carrier, forming a drug-carrier system with a negative Gibbs free energy [55]. According

to Gibbs equation (Eq. 4), a system with a negative free energy allows the stabilization of the amorphous state of the drug [56].

$$\Delta G = \Delta H - T\Delta S \quad \text{Eq. 4}$$

where  $\Delta G$  is Gibbs free energy,  $\Delta H$  is the enthalpy,  $T$  the temperature and  $\Delta S$  the entropy of the system.

The role of the carrier is vital in the performance of the amorphous formulations, as it influences the amorphous degree, the physical and chemical stability of the amorphous drug and its solubility. Indeed, the drug-carrier affinity is a key aspect, especially when aiming for bioavailability enhancement [57]. Different types of drug-carrier are detailed hereunder.

### 3.5.1 Mesoporous Silica

Mesoporous silica (MS) can be defined as silica-based materials containing pores with a diameter between 2 and 50 nm [58]. They have high surface area, large pore volume and ordered pore networks [59]. These properties allow impregnation of MS by large numbers of molecules, generally in their amorphous state, leading to the fast release of them. Moreover, they prevent recrystallization and premature degradation of impregnated molecules [60,61].

Drugs can be impregnated into mesoporous carriers by different methods, such as melting [62], organic solvent impregnation [63] or supercritical fluid processes [64]. The drug loading capacity depends on the loading method, the surface area and the affinity of the drug for the mesoporous carrier [65].

As an example Koch *et al.* impregnated a MS carrier with 40% of fenofibrate, a BCS II drug used in the treatment of hypertriglyceridemia, with pressurized carbon dioxide. The resulting dosage forms allowed the supersaturation of fenofibrate during at least 2 hours [66].

### 3.3.2 Polymers

Polymers are the most commonly used carriers for the formulation of second generation solid dispersions (SDs), called amorphous solid dispersions (ASDs), discussed below. These dispersions involve incorporating a drug in its amorphous state into a carrier, typically a single polymer or a mixture of polymers [67]. These formulations allow the drug to remain amorphous, mainly by decreasing the molecular mobility. Dissolution of the drug from an ASD leads to supersaturated solutions by a mechanism that is not yet fully understood. However, it is generally considered important that the polymer should be constituted of hydrophobic functions in order to interact with the drug in aqueous environment and of hydrophilic functions that interact with water to facilitate the drug release [68]. The polymers commonly used for forming ASDs are biologically inactive and have low absorption in the GIT [69]. Among them are the cellulose derivatives such as hydroxypropyl methylcellulose (HPMC), hypromellose acetate succinate (HPMCAS), hydroxypropylcellulose (HPC), but also polyvinylpyrrolidone (PVP), polyvinylpyrrolidone-vinyl acetate (PVP/VA) copolymer, polymethacrylates (Eudragit® E, L, S, FS), polyvinyl alcohol (PVA), Polyvinyl caprolactam-polyvinyl acetate-polyethylene glycol graft copolymer (SOL) and other polyethylene glycol (PEG) derivatives [70].

ASD can be manufactured by several techniques which will be discussed in the next chapter.

### 3.6 Solid Dispersions

SDs have been defined by Chiou and Riegelmanas as “dispersions of one or more active ingredients in an inert carrier at the solid state, prepared by the melting, the solvent or the melting solvent method” [71]. Depending on their composition, the SDs can be classified into five categories [51,72,73]. ASDs are classified in the second generation.

- *First generation SDs* are crystalline SDs in which the crystalline drug is dispersed into a crystalline carrier, such as urea or sugars, forming eutectic or monotectic mixture. Due to the lower melting point of the eutectic mixture compared to the melting point of the drug and carrier, these latter will crystallize simultaneously during the cooling process, resulting in a homogeneous dispersion of the drug in the carrier, enhancing its dissolution rate.
- *Second generation SDs*, named ASDs, contain amorphous carriers, especially polymers such as HPMC, PVP/VA or PVP. The drug is finely dispersed into the carrier, resulting in a reduction of drug particle size to nearly molecular level

and in a better wettability and dispersibility of the drug. These properties, along with the thermodynamically unstable amorphous state of both the drug and carrier allow an enhancement of the solubility and the dissolution rate of the drug. Depending on drug-carrier miscibility, ASD can be separated into two classes; amorphous solid solutions in which the drug is completely miscible with the carrier and amorphous solid suspensions in which the drug has either poor carrier miscibility or a high melting point. Among these five generations of SDs, ASDs have proven their superiority as a strategy to increase the solubility and dissolution rate of poorly soluble molecules and have attracted the interest of research groups and industries for several years. Examples of approved drug products by FDA and/or European Medicines Agency (EMA) are gathered in [Table 1](#).

- As the drug in the ASDs can lead to a supersaturated state upon dissolution process, it tends to recrystallize and decrease the *in vitro* or *in vivo* drug concentration. Third generation SDs are second generation SDs to which emulsifiers or surfactants such as poloxamer, SOL or Gelucire® 44/14 are added to prevent the drug from recrystallizing upon storage by increasing the miscibility of the drug in the carrier. Moreover, the emulsifiers or surfactants are able to improve the wettability of the drug and prevent its precipitation by absorbing the outer layer of drugs particles or by forming micelles that encapsulate the drug and increase its solubility.
- *Fourth generation SDs* are controlled release SDs composed of swellable polymers such as ethylcellulose or HPC. The molecular dispersion of the poorly soluble drug increases the drug solubility and the polymers delay the drug release in the dissolution medium.
- *Fifth generation SDs* are characterized by the use of micro- or nanostructures in addition to the functional performance of the formulation. The fourth generation SDs are monolithic homogeneous systems that often result in an initial burst release of the drug present at the surface, followed by a continuous release to maintain the API concentration in the plasma. Burst release is difficult to predict and control, which can modify the properties of the formulation. Fifth generation SDs allow to overcome this challenge by having a core-shell structure with different inner and exterior components. The composition of these two compartments can be tailored so that the performance of the fifth generation SDs, compared to the others, does not depend only on the physicochemical properties of the carriers/excipients, but also on the production of complex and controllable nanoscale structures.

## INTRODUCTION

*Table 1 – Examples of FDA and/or (EMA) approved marketed drug products containing ASD, adapted from [7,70,74,75]*

Production method	Product name	API	Stabilizer
Co-precipitation	Zelboraf® (FDA/EMA)	Vemurafenib	HPMCAS
Granulation	Samsca® (FDA/EMA)	Tolvaptan	N.A.
Melt extrusion	Gris-PEG™ (FDA)	Griseofluvin	PEG
	Onmel® (FDA)	Itraconazole	HPMC
	Kaletra® (FDA/EMA)	Lopinavir/Ritonavir	PVP/VA
	Viekira™/Viekirax® (FDA/EMA)	Ombitasvir/Paritaprevir/Ritonavir	PVP/VA and TPGS
	Noxafil® (FDA/EMA)	Posaconazole	HPMCAS
	Norvir® (FDA/EMA)	Ritonavir	PVP/VA
	Eucreas®/Galvumet™ (EMA)	Vildagliptin/Metformin HCL	HPC
	Belsomra® (FDA)	Suvorexant	PVP/VA
	Venclexta® (FDA)	Venetoclax	PVP/VA
	Maviret® (EMA) Mavyret® (FDA)	Glecaprevir/Pibrentasvir	PVP/VA
	Intelence® (FDA/EMA)	Etravirine	HPMC
N.A.	Cesamet®/Canemes® (FDA)	Nabilone	PVP
Spray-drying	Zotress®/Certican®/Votubia® (FDA/EMA)	Everolimus	HPMC
	Kalydeco® (FDA/EMA)	Ivacaftor	HPMCAS and SDS
	Orkambi® (FDA/EMA)	Lumacaftor/Ivacaftor	HPMCAS and SDS
	Crestor® (FDA/EMA)	Rosuvastatin	HPMC
	Modigraf® (EMA) Prograf™ (FDA)	Tacrolimus	HPMC
	Incivek™/Incivo® (FDA/EMA)	Telaprevir	HPMCAS
	Sporanox® (FDA)	Itraconazole	HPMC
	Zepatier® (FDA/EMA)	Elbasvir/grazoprevir	HPMC
	Delstrigo™ (FDA/EMA)	Doravirine/lamivudine/tenefovir fumarate	HPMCAS
	Epclusa® (FDA/EMA)	Sofosbuvir/velpatasvir	PVP/VA
	Harvoni® (FDA/EMA)	Ledipasvir/Sofosbuvir	PVP/VA
Spray-melt	Fenoglide™ (FDA)	Fenofibrate	PEG/Poloxamer 188
Wet granulation	Advagraf®/Astagraf® (FDA/EMA)	Tacrolimus	HPMC



## Chapter II. MANUFACTURING PROCESSES FOR AMORPHOUS SOLID DISPERSIONS

Many methods for producing ASDs are available, each with advantages and limitations, but the basic principle remains the same. The crystal lattice of the drug is broken by fusion or dissolution in a solvent. The system is then quench cooled (in case of heating) or dried (in case of using a solvent) to obtain a solid drug in its amorphous state. The methods for the production of ASDs can be classically classified into solvent-based methods, photopolymerization-based method and melting-based methods [76].

### 1 Solvent-Based Methods

The solvent processes for the manufacturing of ASDs are based on the dissolution of the drug-polymer mixture, generally in an organic solvent, even if aqueous solvents can be added to increase the polymer solubility or to reduce the use of organic solvents. The solvent is then quickly evaporated at a generally low temperature suitable for thermosensitive drugs. The solvent selection is the most challenging step of the solvent-based methods, as it has to solubilize both drug and polymer [77].

#### 1.1 Spray-Drying

Spray-drying is a continuous and scalable drying process that allows the manufacture of ASDs particles with adequate granulometry. The equipment is generally composed of a container, filled with the components to process, connected to a drying chamber by a nozzle. ASD components, generally an organic solution or a suspension of API and polymer(s), are pumped and atomized into droplets in the drying chamber through the nozzle. A hot gas is circulating at an adequate flow in the chamber, creating a favorable environment that promotes energy-mass transfer. The contact between the formed droplets and the gas promotes solvent evaporation and size controlled dry particles of ASD generation. These particles are finally separated from the drying medium in a cyclone and collected into a collector vessel. Optimization of each step (pump flow, gas flow, and nozzle diameter, drying temperature...) is required to obtain particles with targeted API physical state. A variety of carriers are processed by this technique to produce SDs and can be categorized into four categories: crystalline first generation, such as urea or sugars, amorphous polymers second generation, such as PVP, PEG or HPMC, surfactant third generation, such as glyceryl behenate or poloxamer and controlled release fourth generation, such as ethylcellulose [78]. Spray-drying is a reproducible, rapid and single-step technique that allows the manufacture of various

ASDs. Moreover, heat-sensitive compounds can be spray-dried without any degradation. Nevertheless, the process yield is generally low due to the loss of products onto the equipment surfaces [79].

### 1.2 Freeze-drying

The production of ASD by FD, or lyophilization, consists of several steps. First, the API and the carrier are solubilized in a common solvent. The resulting solution is then frozen before primary drying and secondary drying. As the cooling is very fast, the nucleation of crystals is reduced or completely prevented [80]. FD process offers the advantage of operating at low temperatures, enabling the lyophilization of thermosensitive molecules. The FD process has the advantage of working at low temperatures, making possible the lyophilization of thermosensitive molecules. However, the low temperatures of drying extend the process time, which can take up to several days.

Hassouna et al. managed to produce ASD of ibuprofen and Eudragit® L100-55 from freeze-dried nanoparticles suspension in which the amorphous state of the ibuprofen was stabilized during at least 12 months [81].

### 1.3 Supercritical Fluids

Supercritical fluids are fluids set at pressure and temperature above their critical point. From this point, interface between liquid and gas disappears to provide a homogenous phase with both gas and liquid properties, especially high density but low viscosity that vary depending on the pressure and temperature. Supercritical carbon dioxide (sc-CO<sub>2</sub>) is by far the most employed component thanks to its easily reached critical parameters (31.3 °C and 72.9 bar) and because it is non-toxic and non-inflammable. Due to its properties, sc-CO<sub>2</sub> can be used as solvent or anti-solvent to produced ASDs by precipitation during the depressurization which causes CO<sub>2</sub> to return to its gaseous state. It can also act as a plasticizer to decrease the T<sub>g</sub> of polymers. Such methods allow the production of ASDs with controlled and adjustable process conditions and good reproducibility. In addition, no organic solvent is required in many cases. However, poor solubility of polymers and drugs in sc-CO<sub>2</sub> constitutes the major drawback of this method [82,83].

### 1.4 Electrospinning

The development of ASDs by electrospinning is based on the transformation of a liquid (solution or melt) containing API, polymers and other additives, into solid ASD-based nanofibers. The liquid is held at the end of a capillary by its surface tension and is subjected to an electric field. When the intensity of the electric field increases, the

hemispherical surface of the liquid elongates to form a cone called the Taylor cone. When the electric field reaches a critical value, a charged jet of solution is ejected from the Taylor cone and will settle on a metal collector screen. During its journey in the open air, the solvent evaporates to leave only a solid fiber [84]. The electrospinning process has many advantages, such as the production of nanostructured architectures with a large surface area and high porosity (fifth generation SD), the possibility of working with thermosensitive APIs as well as the high speed of solvent evaporation [73].

PVA has already been studied as a filament forming polymer and drug carrier to produce nanofibers containing amorphous riboflavin [85]. Dissolution tests showed a burst release (40%) of the drug during the first 40 seconds and the complete release after 260 seconds. Confirming the ability of electrospinning process to produce fast dissolving oral solid dosage forms.

## 2 Photopolymerization-Based Method (stereolithography)

Stereolithography (SLA) is one of the many 3D printing techniques [86]. 3D printing is a method of additive manufacturing that produces 3D structures by depositing or binding materials layer by layer under control of computer software [115,116]. Since the first method for the 3D printing of objects, using SLA, developed by Charles Hull in the early '80s (Hull, 1986), many other methods emerged and their accessibility increased for the industrial, but also the general public [117,118]. Among them, drop-on-powder deposition, fused-deposition modeling (FDM) and laser-based writing systems can be cited [114]. Due to its multitude of features and its flexibility, 3D printing has been applied to a great number of diverse domains like construction, biomedical, aerospace, protective structures, but also pharmacy [119]. The first publication combining 3D printing and drug delivery dates from 1996 by Benjamin M. Wu and his team [120]. Since then, the interest was growing for this kind of research, but it really exploded over the last four years. Indeed, since the FDA approval of a tablet with accelerated release manufactured by 3D printing (Spritam®, Aprelia Pharmaceuticals) in 2015, the number of publications concerning the “3D printing and drug delivery” has increased more than three times. The different methods for 3D printing offer a large panel of advantages for the pharmaceutical field, like the personalized medicine [121], the manufacturing of multi-compartment dosage forms [122,123], complex geometries [124,125], implants [126] or tablets with a high porosity [127].

Some 3D printing techniques, namely SLA, selective laser sintering (SLS) and direct powder extrusion 3D printing (DPE) are used for the production of oral solid dosage forms containing ASDs, without further additional steps. FDM may also be used for the

production of ASDs, but amorphization occurs more often during the HME stage rather than during the printing stage [87].

3D printing SLA is a technology that uses a laser which produces the photopolymerization and the solidification of a liquid resin. The laser is focused on the specific area to densify. The solidification is repeated layer-by-layer in order to construct the desired free form (Fig. 4) [88].

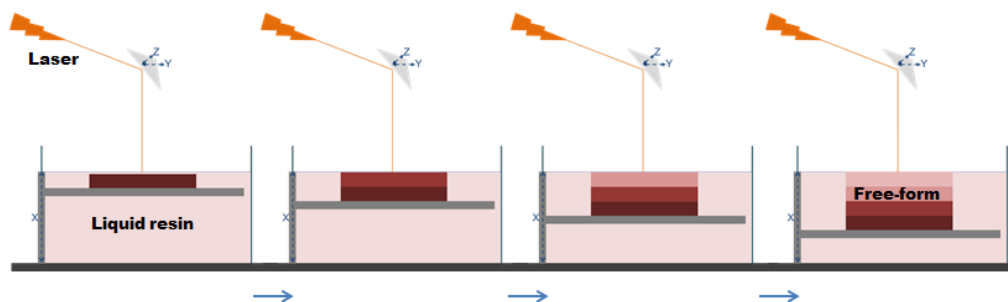


Figure 4– Principle of SLA 3D printing. A laser is focused in a vat that contains a liquid resin with a specific depth. The region in which the laser is focused polymerizes and provides a solid layer. The depth increases progressively in order to build layer-by-layer the desired free form [89].

Several crosslinkable monomers have been used in order to prepare free-form dosages. In most cases, acrylate entities are used. Actually, the photopolymerization can be divided in two groups: cationic polymerization mostly used with vinyl ether, epoxides or lactones, and radical polymerization, mostly used for acrylate derivatives. Basically, a first initiating phase occurs with photo sensible initiator that provides a cation or a radical contact of light [90].

In general, aromatic ketones are used to provide two radical species by a homolytic cut. Once the monomers are activated, the polymerization occurs in a chain reaction like any classical polymer formation. The reactive monomers link to form a chain until the rigidity becomes too high to continue the reaction and reach the termination phase.

To initiate polymerization, a photoinitiator must possess certain properties. Firstly, it should have minimal absorption in the wavelength range of the laser being used to provide excited states with a very short lifetime, preventing deactivation by oxygen. Additionally, the photoinitiator should have a highest possible yield [88]. Besides, monomers can be divided in two groups based on the initiation mechanism, as mentioned above. Polyethylene glycol diacrylate (PEGDA) is the most used polymer when SLA is considered. However, other acrylate entities could be used. For example, theophylline was treated with the photoinitiator 2-hydroxy-4-(2-hydroxyethoxy)-2-methylpropiophenone and photoactive monomers PEDGA and polyethylene glycol

methacrylate (PEGMA). The aim of this study was to compare the two types of acrylate entities. It was observed that PEGMA provided translucent printed free form while those produced with PEGDA were opaque, explained by a modification of the refractive index. However, both acrylate entities were easily photopolymerized [91].

To cite a further example of initiator, diphenyl (2,4,6-trimethylbenzoyl) phosphine oxide has been used to initiate the polymerization of PEGDA and PEG 300 to produce paracetamol and 4 amino salicylic acid amorphous formulations [88]. Different PEGDA/PEG 300 ratios were used in order to study the impact of these two polymers on the release of both drugs. It was shown that the less PEGDA in the formulation, the faster the drug release.

### 3 Melting-Based Methods

Melting methods are solvent-free processes which involve the melt of the drug-polymer mixture, followed by its solidification by cooling. The major drawback of these manufacturing methods is the melting temperature of the materials that may be high and cause drug degradation. Moreover, the melting-based methods require a certain solubility/miscibility of the drug in the polymer, which can be difficult to achieve for certain molecule [76].

#### 3.1 KinetiSol®

The schematic representation of KinetiSol® technology is shown in [Fig. 5](#) [92]. It involves paddles rotating in a cylindrical vessel and shaft with high-speed mixing elements which produce a great amount of frictional and shear energy. These mechanical forces induce a rapid increase of the temperature which melts the drug-polymer mixture. The molten mass is immediately quenched and ejected from the vessel. The process duration is normally < 20 s and the material is generally exposed to high temperatures for less than 5 s. This low exposure to thermal stress makes KinetiSol® technology suitable for the manufacturing of ASDs with thermosensitive drugs. Moreover, this technology is applicable to molecules with high melting points and low solubility in solvents and it enables the elimination of plasticizers [76].

Abiraterone is a BCS IV molecule with a high melting point 227.85 °C and a poor solubility in organic solvents, making difficult the use of conventional ASD manufacturing techniques to improve its aqueous solubility. Gala *et al.* managed to produce an ASD of abiraterone with hydroxypropyl- $\beta$ -cyclodextrin (HP $\beta$ CD) and HPMC using KinetiSol® technique. The results of a pharmacokinetic study highlighted an increase of the abiraterone bioavailability by 13.8-fold compared to a generic abiraterone tablet [93].

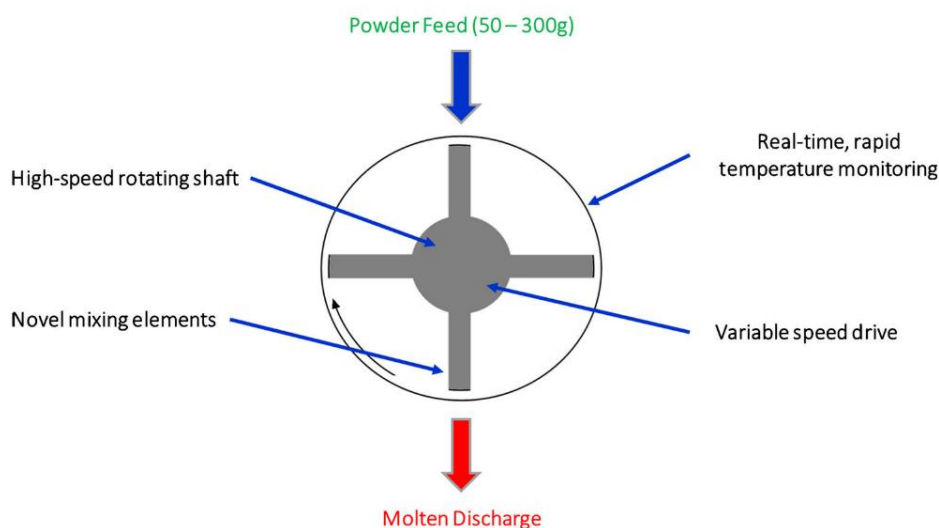


Figure 5 - Simplified schematic diagram for a KinetiSol® compounder. Reprinted from [92].

### 3.2 Microwave Heating

Microwave-induced heating of drug-polymer mixtures has been investigated for the manufacturing of ASDs. Although a microwave is not inherently hot, the dipole rotations within the carrier matrices can generate heat when exposed to microwaves. With a sufficient heating, the drug can be converted *in situ* into its amorphous state in its final dosage form. Zhang *et al.* compared the dissolution profiles of ASDs tablets of indomethacin and different polymers, produced by direct compression followed by a microwave irradiation in a household microwave, with conventional indomethacin tablets [94]. The *in vitro* dissolution tests highlighted a faster indomethacin dissolution from the ASD tablets.

Along the ASD production combined with an increased dissolution rate, microwave-based method is easy to use and cost-efficient compared to the other ASD manufacturing techniques. The possibility of producing ASDs *in situ* with a household microwave could prevent from drug recrystallization and amorphous-amorphous phase separation and is feasible by the patients. However, this technique suffers from some drawbacks such as a possible thermal degradation of the drug, potential chemical reactions and a reproducibility that needs to be improved.

### 3.3 Selective Laser Sintering

SLS is an alternative laser 3D printing technique for which light energy is used to bind powder particles together (Fig. 6) [86]. The specific pattern introduced in the computer will guide the laser in order to draw the specific free forms from the powder bed. The

goal is to reach a solid-state sintering obtained with a local temperature between the melting point ( $T_m$ ) of the material and to obtain the maximum of porosity [95].

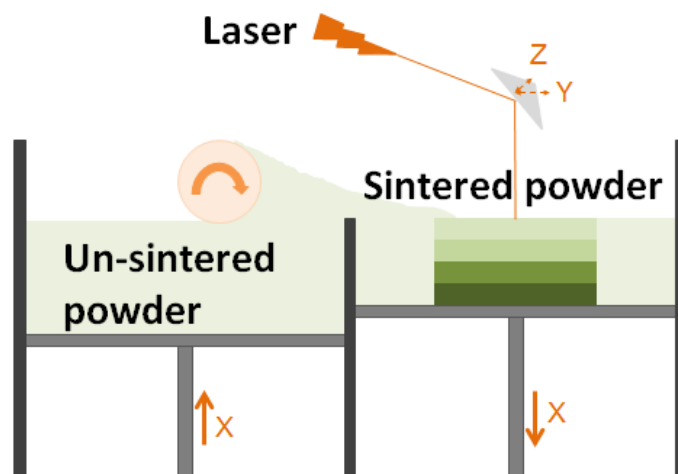


*Figure 6 – Illustration of the SLS technique. A laser is focused on a specific region and in a specific depth of the powder to sinter. A vat that contains un-sintered powder feeds the compartment containing the powder to be sintered with a rising piston and a roller. The number of solid layers of the free form is increased by the extent of the depth of the treated container [86].*

The first study concerning this technique in the pharmaceutical field is very recent. SLS has been employed in 2017 to construct a SD of paracetamol with Kollicoat® IR and Eudragit® L100-55. An approved pharmaceutical absorbent excipient, Candurin® Gold Sheen (3% w/w), was used to enhance the energy of absorption of the system. No degradation could be observed. Thermograms and diffractograms showed paracetamol crystallinity in the Kollicoat® but no peaks were observed with Eudragit®. As expected, Kollicoat® formulation allowed the API dissolution in the acidic media while only low releases were observed with Eudragit® formulation in the same fluid. Finally, it has been demonstrated that an increasing drug content provides less porosity and so requires more time to release the entire loading [96].

Later, SLS was successfully used to manufacture ASDs of a model drug blended with inorganic carriers, KVA64 and Candurin®. The authors highlighted the impact of the laser speed and the drug particle size on the amorphization of the drug and therefore on its dissolution performance.

This promising technique offers the possibility to produce extremely precise free forms without the requirement of any support.

### 3.4 Direct Powder Extrusion

DPE is a recent technique, which could be defined as a combination between single screw HME and 3D printing. The ASD is produced in the machine that will directly shape it in its final form [97]. The process is shown on [Fig. 7](#). A powder mixture composed of an API, polymers and eventual other additives is introduced in a hopper which discards the powder in a vertical heated barrel which contains a screw. The ASD is formed in the barrel and directly printed through a nozzle, layer by layer on a heating bed. DPE is similar to FDM, but without the need of a filament preparation by HME, which reduces the risk of degradation of thermosensitive compounds, reduces the process time, waste and cost. Moreover, it increases the choice of printable excipients, as they do not have to possess the mechanical properties that are mandatory for printable filament manufacturing, such as suitable brittleness and flexibility.

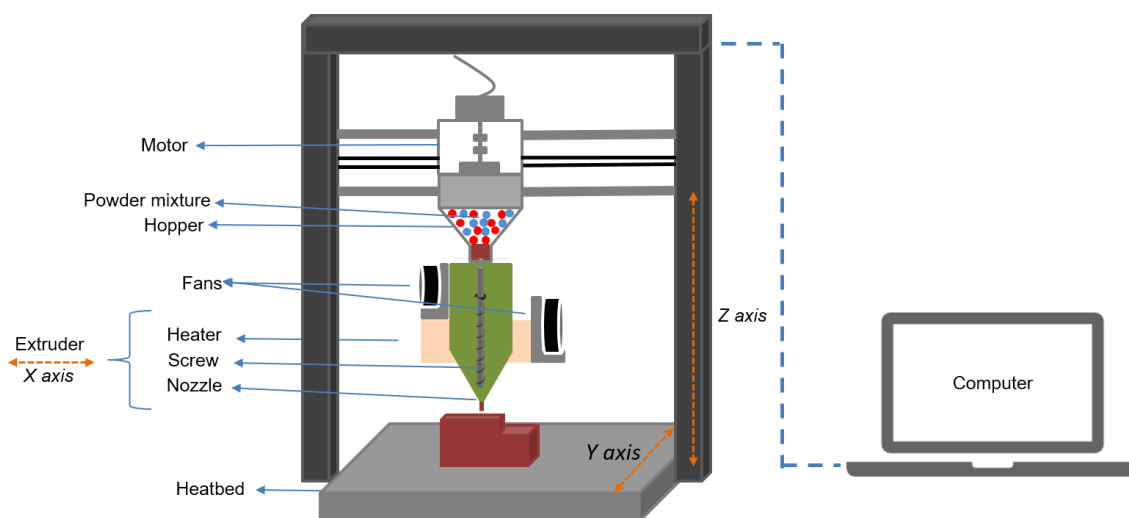


*Figure 7 - Illustration of the DPE technique. A powder mixture is delivered from a hopper through an extruder composed of one screw, a nozzle and a heater. The structure is directly created from a computer-aided design (CAD) model which controls the layer-by-layer.*

This technique has already demonstrated its ability to produce immediate-release formulations of BCS I molecules. Indeed, Fanous *et al.* produced printed tablets of caffeine using HPC-SSL as the polymeric matrix, PEG 4000 as plasticizer/pore former and Kollidon® VA64 (KVA46) as rapidly dissolving polymer [98]. The printed tablets dissolved rapidly at pH 2 (at least 85% drug dissolved in 30 min).

In another study, praziquantel, the standard treatment for schistosomiasis, a parasitic disease, was directly printed into pediatric printed tablets [99]. ASDs of the API with



KVA64 and surfactants were prepared before being printed. In addition to providing enhanced release of praziquantel, the printed tablets showed a good tolerability in palatability without the need for additional taste masking excipients, highlighting the capabilities of DPE for the manufacturing of pediatric printed tablets.

DPE also makes it possible to print formulations with a high percentage of API, as demonstrated by Goyanes and his team [97]. They managed to directly print powder blends containing 35% of ITZ with different grades of HPC - UL, SSL, SL and L, without the use of additional excipients. This development overcomes the limitations of HME, which often requires the addition of excipients such as plasticizers to prevent the formation of a filament that is either too brittle or too flexible.

Beside all these advantages of DPE, investigations have to be conducted concerning the weight uniformity of the printed tablets, which depends on the flowability of the powder mixtures [100]. Moreover, to fully realize the potential of direct printing technology for pharmaceutical applications, it is necessary to optimize and standardize the equipment used in the process. Currently, many studies have utilized custom-built equipment, making it difficult to compare results across studies. Despite this limitation, direct printing technology still presents a promising opportunity to accelerate the development of drug formulations by tailoring them to the unique requirements of the printing process, thereby increasing their bioavailability and overall effectiveness.

### 3.5 Hot-Melt Extrusion

HME is a process known and used for nearly a century. In addition to its application in the plastics, rubber and food industry, HME is used in the pharmaceutical field for a wide range of applications. Some of the more common applications are for taste masking, enhancement of the solubility of poorly water-soluble drugs, controlled, sustained and targeted drug delivery [101]. A Pharma 11 twin-screw extruder (ThermoFisher Scientific, Germany) equipment is represented on [Fig. 8](#). During a classical HME process, a mixture of drug and thermoplastic polymer is mixed, melted, dispersed, and forced through a die under specific conditions. The mixture is first introduced into a feeder which will discharge it in a heated barrel which contains one or two screws. While being conveyed along the screw(s), the mixture is melted and kneaded, until being pushed out of the barrel through the die, mostly in cylindrical or film shape, depending on the die shape. Finally, the extrudate is cooled along a conveyor belt, with or without pressurized air until eventual further downstream processes. HME is a continuous, solvent-free method easy to scale up [102]. Moreover, in-line analysis techniques such as Raman, near-infrared and ultrasonic and dielectric

spectroscopy can be added to the equipment to have a direct quality-control of the product [103].

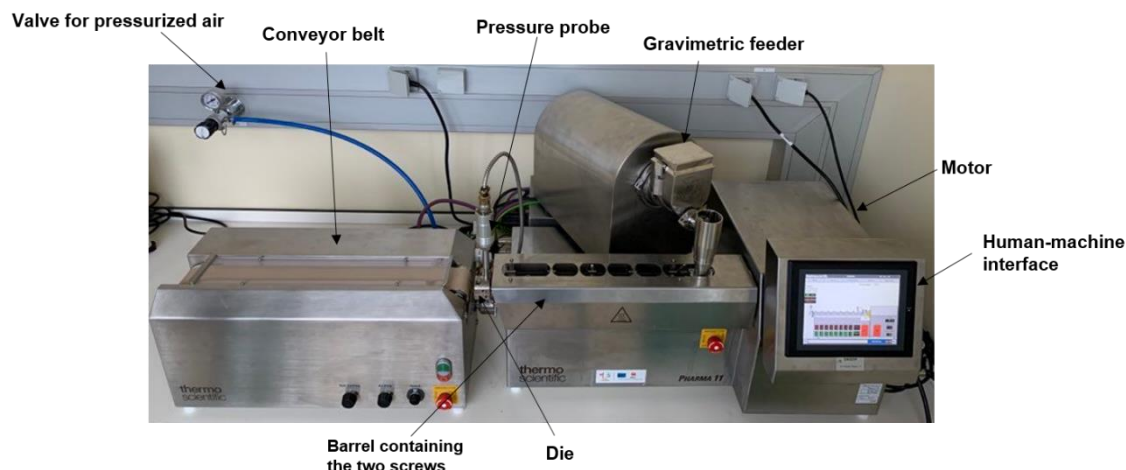


Figure 8 - Pharma 11 twin-screw extruder equipment (ThermoFisher Scientific, Germany).

The elements that most influence the final product are the screws. Depending on the number of screws, the HME process is referred to as single-screw or twin-screw extrusion. Twin-screw extrusion is the most preferred configuration for the manufacturing of ASDs [75]. Indeed, compared to the single-screw extrusion, the use of two screws gives the advantage of a reduced residence time inside the barrel, a facilitated continuous mass flow and a better mixing of the different components [104]. Moreover, twin-screw HME offers greater versatility due to changeable screw elements to achieve the proper level of mixing and kneading, according to the desired final product. These elements are conveying, kneading or building pressure elements (Fig. 9) [102].

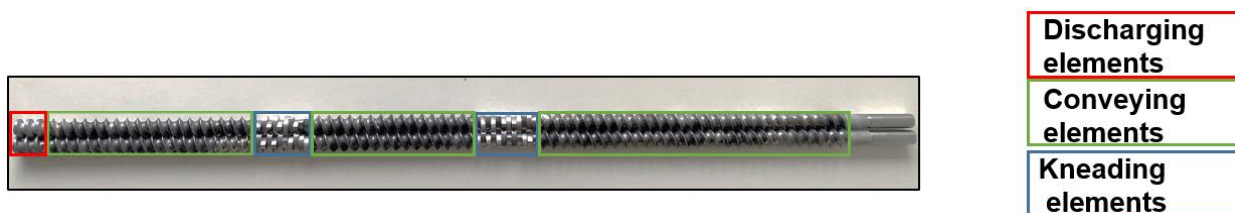


Figure 9 - Twin-screw with different screw elements.

To achieve complete amorphization of the API in the manufacturing of ASDs, the mixture needs to be subjected to the thermal conditions of the barrel for a specific duration and, in most cases, pass through one or more kneading zones. Hanada *et al.* studied the influence of these extrusion parameters with ternary ASDs containing indomethacin, HPMC and XDP MS. The powder blends were extruded at 3 different screw speeds (50, 100 or 150 rpm) and an increasing number of kneading zones (0, 1,

2 or 3). Modulated differential scanning calorimetry (mDSC) studies were conducted to characterize formulations thermal behavior. It appeared that every formulation was completely amorphous, except for the formulations extruded at 0 kneading zone/100 rpm, 0 kneading zone/150 rpm and 1 kneading zone/150 rpm which showed an endothermic peak, characteristic of an incomplete amorphization of the API. This study highlighted the importance of the kneading zones and the residence time of the API in the extruder for the amorphization of it [105]. These parameters have to be optimized for each mixture, depending on the degradation risk for each component.

The screws can rotate in the same direction (co-rotating extruder) or in the opposite direction (counter-rotating extruder) [106]. The co-rotating extruders are generally preferred to the counter-rotating extruders concerning the manufacturing of ASDs. Indeed, they have a higher maximum speed screw, a better output and they induce lower shear forces, which reduce the risk of drug degradation compared to the counter-rotating extruders.

Thermo-sensitive components are difficult to extrude, because the extrusion temperature has to be above the  $T_g$  of the polymer and as far as possible from the temperature of degradation of each component. If these two temperatures are too close, plasticizers can be added to the mixture in order to reduce the  $T_g$  of the polymer [107]. The addition of plasticizers is also interesting concerning the materials with a high molecular weight, inducing a high torque during the extrusion process, as the plasticizing of the mixture allow a reduction of the torque.

From an industrial point of view, HME is, along with the spray-drying, the most used continuous manufacturing (CM) method for the production of approved marketed products containing ASDs, with the advantage of being a solvent-free method. Next to these interests for HME, it is important to mention the technology requires a down-stream process which constitute an additional step. The next chapter will only deal with the shaping of extruded ASDs

## Chapter III. SHAPING OF EXTRUDED AMORPHOUS SOLID DISPERSIONS

Once extruded, the ASDs have to be shaped in their final oral dosage form. Indeed, extrudates are generally in a spaghetti form and have to be processed in order to be more swallowable or insertable (**Fig. 10**).

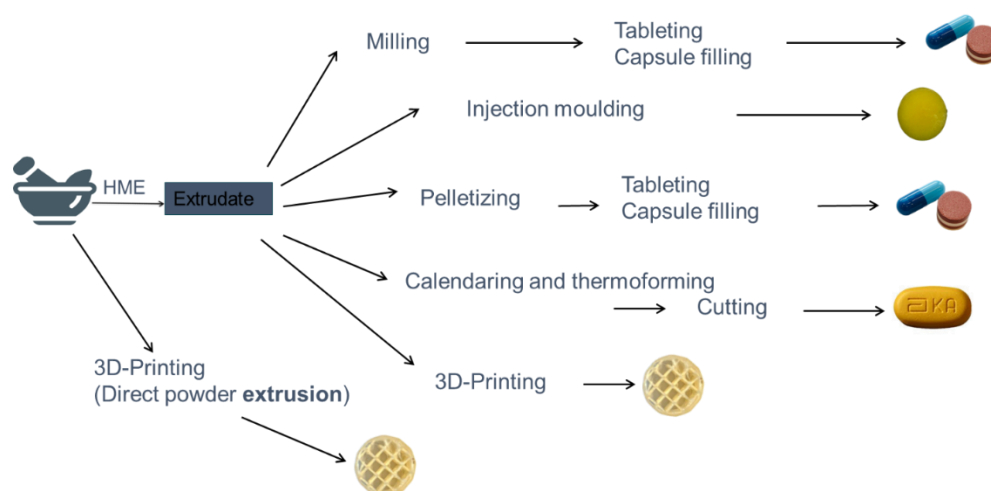


Figure 10 – Processes to shape ASDs [108].

Currently, the following processes are used to transform the extrudate strand into a final dosage form:

### 1 Milling and Tableting or Capsule Filling

Milling process converts HME filaments into free-flowing ASD powder. This powder can be further manipulated to fill capsule or to be compressed. Parameters such as cutting speed or process temperature must be studied and optimized in order to obtain good process reproducibility. Indeed, the obtained particle size has a crucial role on the flowability, dissolution and compaction and must be fully controlled. In addition, the glassy nature of HME-based ASDs can be challenging because of the heating induced by the process that could produce sticking material in the hammer if the temperature reaches the  $T_g$  polymer. Cryogenic milling or air classifier mill can be used to reduce the temperature process and avoid the melting or softening of polymers [109]. Nevertheless, particular attention is required on the API physical state during milling process since high amount of energy is brought and could lead to API recrystallization.

Among the different tableting methods, namely wet or dry granulation tableting and direct tableting, the latter is the most desired compaction method since no particle engineering (granulation) step is required. Indeed, usually, granulation of such material is not necessary since milling of HME based formulations produce particles with appropriate flowing properties and high bulk density. Moreover, this method is cheap and fast. On one hand, the direct tableting of HME-based ASDs takes advantage of extrudates milled properties (especially high bulk density). On the other hand, tableting can be challenging since the process produces heat energy that can induce, as during the milling step, melting or softening of ASDs. This compression energy can also influence the physical state of the ASD due to mechanical stress. As an example, Singh et al. showed a reduced interaction of polymer and API during compression leading to significant recrystallization [110]. Since the compression force impacts tablet properties, it must be optimized to obtain tablets with sufficient hardness while maintaining fast disintegration and high stability. Depending on the ASD to compress, the formulation should also be adapted with excipients such as fillers (e.g. lactose), binders (e.g. microcrystalline cellulose), disintegrants (e.g. croscarmellose natrium) or lubricant (e.g. magnesium stearate).

## 2 Injection Moulding

Injection moulding is a useful technique for producing complex shapes. One of its main advantages is the non-necessity of additional steps after the HME, such as cutting, milling or pelletizing. The extrudate is directly inserted into a closed, shape-specific, cooled mold. The molten polymer fills the cavity of the mold and will duplicate its shape as it solidifies [111]. The final product is then ejected from the mold, to make space for the following molten mixture. It takes only a few seconds to produce the final product, making this technology suitable for mass production. The pharmaceutical applicability of injection moulding was demonstrated for immediate and sustained release formulations [112].

## 3 Calendaring and Cutting

A continuous SD manufacturing process based on HME has been patented as Metlrex™ technology (Fig. 11) [113]. A special twin-screw design combined to a large and flat die allow the production of a thin ASD slice, which is further and in continuously conducted through two rollers. Roller design ducted the future extrudates form. Calendaring is obtained by rollers with preformed holes that can be seen as imprint of future tablets leading to the formation of a sheet of tablets. Besides, thins films are

obtained with rollers with no holes. The sheet must finally be cut to obtain single dosage forms.

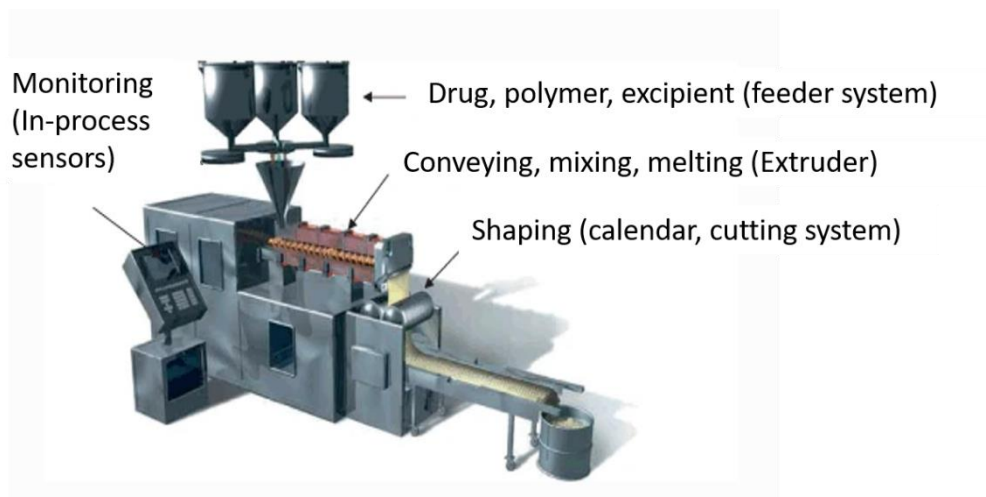


*Figure 11 - Meltrex™ process technology reprinted from Shah and Breitenbach [113].*

#### 4 Pelletizing and Tableting/Capsule Filling

Pelletizing process is the manufacture of pellets, multiparticulate forms produced by the agglomeration of mixture of excipient and drug powders leading to small free flowing and generally spherical particles. In the pelletizing coupled with HME process, a pelletizer composed of knives is placed at the end of the extrusion process. There are two types of pelletizers that are compatible with HME, which differ in whether the cut is made with the cooled or the molten filament. With the strand pelletizer, the cooled extrudates is directed through the knives roll that cut the filament. Depending on the roll speed, different granulometries are obtained. The second one, the face die pelletizer, cuts the extrudates in its molten state just at the exit die. Depending on the cutting parameters, pellets with various shaped, size and polydispersity can be obtained, influencing notably the flowing properties and compaction of the powder. These parameters must be fully controlled. Indeed, the obtained pellets can be further processed to fill capsules or to be tableted [114].

### 5 Three Dimensional Printing

There are many 3D printing techniques, each with a well-defined process, but always based on the layer-by-layer construction of a form previously developed by CAD. They are used to shape and/or produce drug formulations, initially in liquid, semi-solid or solid into solid forms. Adaptability is the main advantage of 3D printing for medicine manufacturing. It includes ability to manufacture complex geometries, impossible to create with conventional techniques such as capsule filling or tableting [115]. The adaptability may also be applied for precise and unique drug dosage production, by varying the printed form size [116]. Moreover, multiple doses or multiple drugs can be printed in a single dosage form [117]. 3D printing is also able to produce dosage forms with tailored drug release [118]. Finally, it allows adaptable on-demand drug production which has major applications in emergency medicine or for drugs with short shelf-life [119]. Versatility and flexibility of 3D printing technology makes it suitable for the medicines individualization and for moving away from one-size-fits-all drug products.

Among the various 3D printing techniques, FDM is one of the most reported for shaping ASDs, as described below.

## 5.1 Fused Deposition Modeling (FDM)

FDM (Fig. 12) is a rapid prototyping technology in which a thermoplastic filament polymer, which can contain drug(s) or additive(s), is pulled by two gears through a small die diameter heated nozzle. The molten, extruded filament solidifies itself on a bed which can be heated [120]. The printed structure is previously designed thanks to a slicing software. The extruder can move within the x- and z-axes while the heat bed can move in the y-axis in order to create a 3D structure [121].

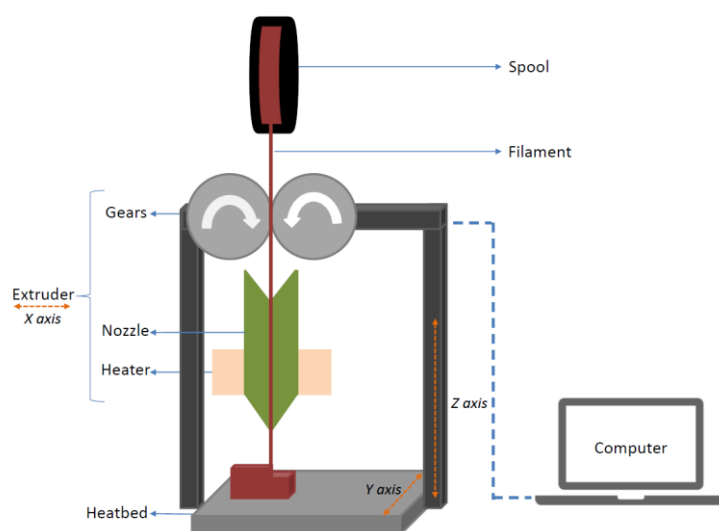


*Figure 12 – Illustration of the FDM technique. A filament is delivered from a spool through an extruder composed of two gears, a nozzle and a heater. The structure is directly created from a CAD model which controls the layer-by-layer deposition of a filament extruded through the nozzle. The deposition occurs on a building platform which can be heated.*

It is quite easy to modify the drug release from FDM 3D printed formulations, even if this technique is mostly used to manufacture sustained release formulations [122–124]. FDM is less used for the enhancement of the dissolution speed of poorly soluble drugs because, among others, of the compactness of the solidified melt, which slows the drug release. However, some authors showed that it seems possible to produce drug dosage forms with a release profile that matches the Pharmacopeia specifications for immediate release formulations, by modifying some critical parameters. These parameters are described in this chapter.

### 5.1.1 Formulation and Printing Parameters

When drugs have a poor aqueous solubility due to their high crystallinity cohesion, the use of related amorphous forms provides higher aqueous solubility than crystalline forms. Indeed, amorphous forms translate no long-range order molecular structure and



have more enthalpy than crystal forms. The energy required to tear molecules out of the disorganized structure is lower with amorphous form, which provides higher solubility [55].

However, amorphous forms are thermodynamically unstable due to their high internal energy. They tend to return to the crystalline state which is more stable. One of the solutions for stabilizing the amorphous state is to minimize the molecular mobility. The incorporation into a polymeric matrix is a suitable option. Such entities are called ASDs [125].

ASD allow the solvation of each individual API molecule and provide potential supersaturated concentration. This metastable state is a driving force for the nucleation and crystal growth of API in order to reach the thermodynamically stable concentration. This phenomenon, called “spring effect”, can be avoided by soluble polymers that may increase the viscosity and act as precipitation inhibitors or by drug-polymer interactions which inhibit nucleation and crystal growth. **Fig. 13** shows this behavior which is called “spring and parachute effect” [126].

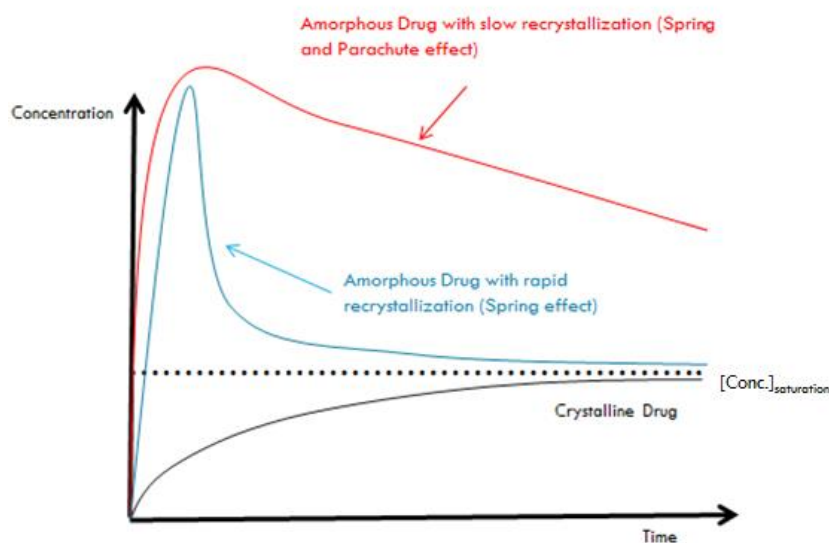


*Figure 13– Spring and parachute effect. The crystalline drug (black curve) doesn't allow to reach a supersaturated solution. The non-stabilized amorphous drug (blue curve) allows to reach a supersaturated solution, but a spring effect is observed because of the rapid recrystallization. The amorphous drug stabilized by a polymer (red curve) allows to reach a supersaturated solution which is maintained during a certain time and provides a spring with parachute effect. Adapted from [127], with permission of Elsevier.*

In order to produce an ASD, it is important to reach a molecular dispersion of API and/or additive in the polymer. Drug-polymer, polymer-polymer and additive-polymer miscibility studies have to be conducted. Indeed, the stability of ASD below polymer  $T_g$  is highly

dependent on phase separation kinetics [128]. Immiscibility may lead to API recrystallization, or non-homogeneity of mechanical properties such as flexibility due to unequal repartition of the plasticizer. The miscibility involves a whole series of forces binding the drug and the polymer, each with a more or less important influence. It is important to study the strength of drug-polymer interactions, as they play a role on the ASD properties, such as its dissolution profiles or its stability [129]. Stability of ASD at temperature near  $T_g$  could be attributed to the drug-polymer bonding which makes recrystallization more difficult [130]. Besides, drug-polymer interactions have impacts on the dissolution profiles of the filaments. As an example, improvement of indomethacin acidic solubility has been obtained by using cationic Eudragit® EPO (EPO), unlike with the use of other mixtures of indomethacin and non-ionic polymers, while all the compared formulations were miscible and maintained the amorphous form of indomethacin [131]. The miscibility studies can be conducted by several methods, such as the Van Krevelen and Hoftyzer's group contribution method which allows to calculate a solubility parameter, depending on cohesive forces. Solubility parameters of both API and polymers are then compared to predict the miscibility [132,133]. DSC is useful since miscible binary mixture provides one single  $T_g$  endotherm event while immiscibility can be detected by highlighting the separate  $T_g$  of mixture components [134].

Alhijaj and his team studied the possibility of using pharmaceutical approved polymer miscible blends in FDM 3D printing of oral solid dosage forms [135]. PVA, EPO and SOL were used as polymeric matrices to improve the aqueous solubility of felodipine and polysorbate 80 (Tween® 80), polyethylene oxide and PEG, which are the same polymer but with different chain lengths, were used as plasticizers. The miscibility predictions revealed that SOL and EPO are miscible with PEG/PEO and Tween® 80 while PVA is only partially miscible with Tween® 80. The mixture of PVA and Tween® 80 showed a weak stiffness that may be attributed to the discontinuity of the Tween® 80 phase in the PVA due to the low miscibility.

While a significant improvement of the dissolution of felodipine in a pH 1.2 HCl medium was observed with EPO formulation (release of 84.3% of API within 30 min) in comparison with crystalline felodipine, SOL and PVA formulations showed significantly slower drug release profiles. These facts could be explained by two principles. First, the salts strength of the medium may depress the polymer solubility of SOL and PVA [136]. Secondly, the excipients miscibility seems to have a very important role. Indeed, percentage of PEO/PEG used in EPO allows its complete dissolution in the polymer in contrary to the SOL formulations for which PEO/PEG crystallinity has been observed. This crystalline form requires wetting and hydration before the dissolution, which is not necessary when complete dissolution in the polymer is achieved and delayed the drug release [135].

One of the most appropriate techniques used for the manufacturing of ASD is the HME which is the process of converting a raw material into a product of uniform shape and density by forcing it through a die under defined conditions of heating, kneading and pressure [137]. It allows to produce filaments containing the drug dispersed or dissolved in a polymeric matrix which can be shaped using FDM 3D printing. The problem with most of the water-soluble polymers that are used in FDM ([Table 2](#)) is that they do not have the appropriate printing properties on their own.

*Table 2 – Most used water-soluble polymers in FDM 3D technology*

Water-soluble polymer	Most used trend names	Publications
Poly (vinyl alcohol)	Parteck® MXP	[135,138–142]
Polyvinylpyrrolidone	Kollidon® 12PF (K12PF)	[143–145]
Polyvinyl caprolactam – polyvinyl acetate – polyethylene glycol graft copolymer	Soluplus®	[135,141,146]
Poloxamer 407	Lutrol® F127, Kolliphor® P407	[145]
Polyethylene oxide	Polyox® WSR	[140,147]
Polyethylene Glycol	/	[145,147]
Basic Butylated Methacrylate Copolymer	Eudragit® E	[135,148]
Polyvinyl Alcohol/Polyethylene Glycol Graft Copolymer	Kollicoat® IR	[141,145]
Polyvinylpyrrolidone-Vinyl Acetate Copolymer	Kollidon® VA64	[143,145]

Therefore, the choice of the polymer is a critical parameter in the development of the FDM process for manufacturing immediate release forms. It has to keep the API in its

amorphous state, allowing a better aqueous solubility. Besides, the polymer has to give appropriate printing properties to the filament, as its “printability” depends on its diameter, its thermal rheology (at printing temperature), its thermal properties (glass, fusion and degradation temperatures) and its mechanical properties (hardness and elasticity) [149,150]. All these parameters are discussed hereunder.

If the filament is not printable, additives, such as plasticizers, will have to be added to the formulation. The plasticizers will lower the  $T_g$  of the polymeric matrix, which will improve the mechanical properties and lower the temperature of extrusion/printing [151]. A plasticizer could be an additive, such as sorbitol or triethylcitrate (TEC), or the API itself, such as theophylline, as explained later in this chapter [138,139,152].

*The filament diameter* is a critical parameter for the feeding through the print head. Indeed, if the diameter exceeds the inner diameter of the hot end of the printer head, it would prevent the filament conduction. If the diameter is too thin, the filament may break because of the traction of the two printer gears [150]. The most common diameter found in the literature is 1.75 mm, but depending on the printer, it can vary between 1.75 and 3.0 mm. In order to have a consistent diameter, different techniques downstream the HME can be used, such as a conveyor belt, a melt pump or a filament maker. The conveyor belt can be placed at the end of the extruder. A high belt speed will stretch the filament, so the diameter will grow shorter and, on the contrary, a small low speed will allow the diameter to grow higher. The melt pump is used to solve the problem of pulsating output of the twin-screw extruder, which makes difficult to maintain a constant filament diameter. This pump will maintain an accurate pulsation-free output, resulting in a constant diameter filament being extruded [153]. At last, a filament maker can be used. This kind of apparatus is equipped with an optical sensor and a dynamic puller system that work together to produce a filament spool with constant diameter [154].

*The rheological properties* of the filament are critical for the printing process, as a too high viscosity could lead to a clogging of the printer nozzle [149]. These properties can be characterized by a rotational rheometer. The viscosity depends on the formulation, but also on *the temperature*. Indeed, it is well known that the temperature impacts the viscosity of the molten material [155]. Besides, depending on the different components of the formulation, the temperature has to be sufficient to melt the material, but not too high, to avoid any degradation. Therefore, an equilibrium has to be found between a high-printing temperature where the viscosity of the melt is low but with a risk of degradation and a low printing temperature with the risk of clogging the printer nozzle because of the high viscosity. The generally used temperatures for FDM 3D printing are between 150 and 230 °C [143]. These temperatures are too high for many APIs, so the

addition of a plasticizer may be necessary to reduce the extrusion and printing temperatures.

Some authors proposed a flowchart for the formulation of rapid drug release forms using HME and FDM (Fig. 14).

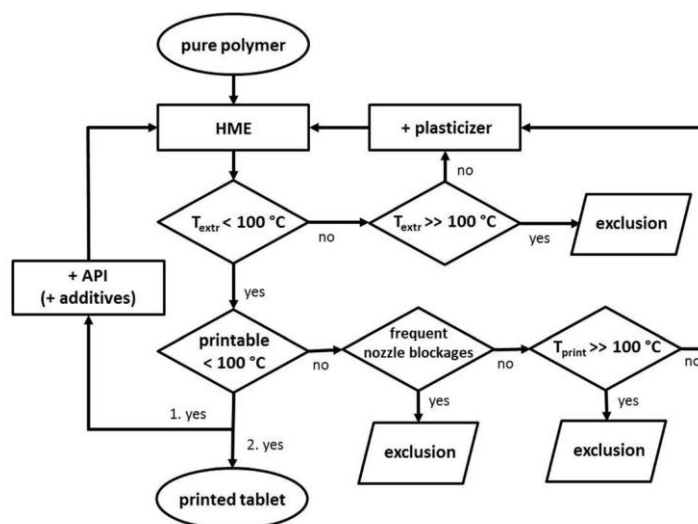


Figure 14– Flowchart for drug loaded tablet formulations;  $T_{extr}$  = temperature required for extrusion;  $T_{print}$  = temperature required for printing. Reprinted from [145], with permission of Springer Nature.

They used this flowchart for pantoprazole sodium. The targeted temperature for both HME and FDM was below 100 °C because the pantoprazole sodium has a degradation temperature at approximately 110 °C [156]. To extrude and print below this temperature, the addition of a plasticizer was recommended. Immediate release formulations of PEG 6000 + 10% of API were printed without the need of any plasticizer while immediate release formulations of PVP K12 + 10% of API were successfully printed after the addition of 15% of TEC, a plasticizer [145].

In the case of 4-aminosalicylic acid, a thermo-sensitive drug, Kollamaram *et al.* managed to produce different immediate release formulations at lower temperatures [143]. All the formulations that were tested contained KVA64 as a water-soluble polymer, PEG 1500 as a plasticizer, magnesium carbonate as a stabilizing agent and mannitol as a secondary plasticizer and a channeling agent. K12PF, another water-soluble polymer, was added to some of the formulations. The tablets were printed at 90 °C, with no degradation of the 4 – aminosalicylic acid. The complete dissolution of the drug was obtained after 20–30 min for each formulation. The release profile of the formulations which contained the K12PF was faster than the others, which led the

authors to suppose that the mechanism of the drug release from these tablets was erosion.

In another study, a mixture of theophylline, Eudragit® E, an acrylate polymer and TEC as a plasticizer was extruded in order to provide printable filaments. Immediate release formulations with a caplet shape were successfully printed. However, the researchers mentioned difficulties to combine optimal HME temperature process and optimal printing temperature process, where ideal values of printing temperature were 40 to 50 °C above the ideal HME temperature process, which was 110 to 120 °C. In this case, the ideal printing temperature would be 170 °C, which is not suitable with acrylate polymers that degrade above 166 °C. Authors found as a solution the use of high melting point compound (in this study, theophylline has a higher melting point, 273 °C, than printing temperature) that acts as a plasticizer and allows consistent flow through the printer's nozzle and a rapid solidification of the printed structure at room temperature [152].

Sadia also proved that it was possible to print immediate release oral formulations, with lower process temperatures [148]. The authors tested four different API's, 5-aminosalicylic acid, captopril, prednisolone and theophylline, to produce FDM 3D printed tablets. They used EPO as the delivery carrier and tri-calcium phosphate (TCP) as a filler. All the formulations were printed with a temperature of 135 °C. The release profile of each formulation showed a drug release of more than 85% after 30 min.

*The mechanical resilience* of the filament is another essential parameter for its feeding through the two gears of the printer without deformation, which could be due to a lack of stiffness, or breakage, when the filament is too brittle ([Fig. 15](#)).

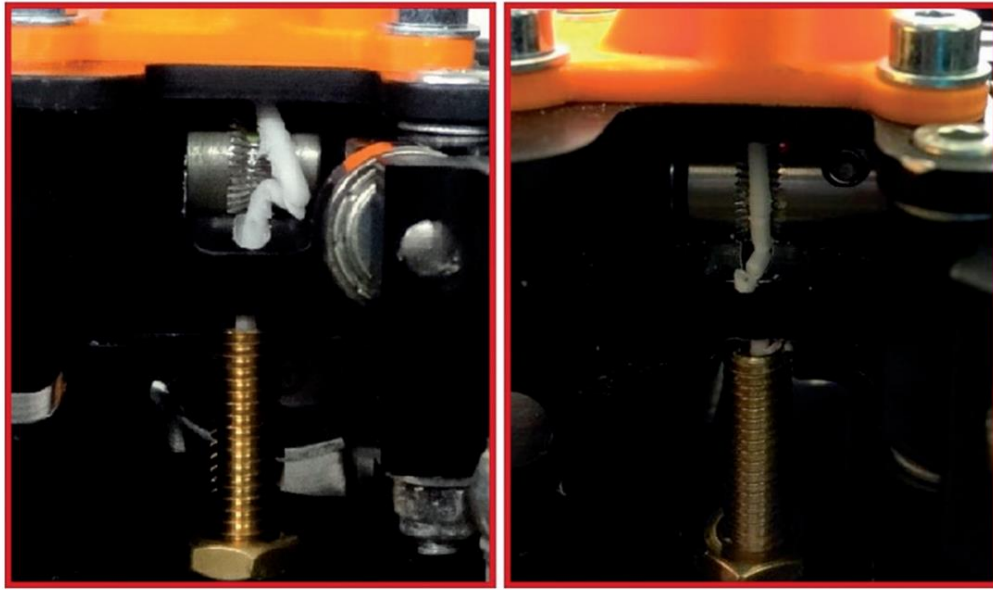


*Figure 15– Open print head with non-printable filaments. The filament on the left is too flexible (contains too much plasticizer), so it cannot be conducted through the print head. The filament on the right is too brittle (not enough plasticizer), so it breaks inside the print head, mainly because of the transversally applied pressure of the two gears. Reprinted from [150], with permission of Taylor & Francis.*

To determine this resilience, the tensile test and the three-point bend test can be effectuated on the extruded filaments, using a texture analyzer [150,157]. To fine tune the mechanical behavior of the filaments, plasticizers can be used. By modifying the percentage of plasticizers, the brittleness of the filament can be sufficiently reduced and its flexibility can be improved until obtaining a printable filament.

Melocchi studied the printability of extruded filaments based on a variety of pharmaceutical grade polymers, such as SOL, Kollicoat® IR or PVA [141]. As these polymers were not “feedable” on their own in the printer because of inappropriate mechanical properties, plasticizers had to be added before the extrusion as follow: SOL + 10% PEG 400, Kollicoat® IR + 12% glycerol and PVA + 5% glycerol. Disk-shaped structures were successfully printed with these mixtures.

In another study, authors showed that a concentration of sorbitol, used as a plasticizer, could be adjusted in a mixture with PVA in order to produce filaments with desired mechanical properties for printing. Sorbitol 10% (w/w) reduced the maximum forces during three-point test from 7.3 N to 2.2 N at a maximum distance of 3.9 mm. With 20% (w/w) of sorbitol, maximum force decreased until 0.6 N. Nevertheless, higher sorbitol concentrations provided too flexible filaments, unsuitable for printing [139].

### 5.1.2 Structure of the printed forms

#### *Infill*

In FDM 3D printing, the infill represents the inner support of the printed structure. An infill of 0% is characterized by a completely hollow structure while 100% of infill is characterized by a fully solid filled structure [158]. A compromise has to be found between a low percentage of infill, which presents a high porosity but a low capacity of dosage of the API, and a high percentage of infill, which allows a high dosage of the API but with lower porosity and therefore a smaller surface of contact with the aqueous media.

In a study conducted by Solanki, a 1/1 (w/w) mixture of KVA64 and Affinisol® was selected to stabilize haloperidol in its amorphous state [159]. Tablets with different percentages of infill were printed. Complete release was obtained after 45 min with 60% infilled printed tablets while the 100% infilled printed tablets completely dissolved after 3 hours. This study showed that a higher porosity, and so a higher specific surface, improve the dissolution rate. However, Kempin showed that modifying the percentage of infill doesn't always influence the dissolution time of drugs [145]. They printed PEG 6000 and PVP K12 tablets with three different percentages of infill (50%, 90% and 100%). There was no significant change in the dissolution time for the PEG 6000 printed tablets. The authors suggested that it could be due to the low viscosity of the PEG 6000 melt, which makes the PEG strands tighter, decreasing the contact area with the aqueous fluids. However, the PVP K12 printed tablets with 50% infill were completely dissolved in 3 min, which is 7 min faster than the printed tablets with 100% infill [159].

#### *Geometry of the Printed Tablet*

In addition to the porosity or the polymer that can be changed in order to modify the dissolution behavior of a printed tablet, the geometry of the printed structure also has an important impact. Following this idea, paracetamol has been extruded with PVA through single-screw extruder and the formed filaments have been used to print different geometries. A drug loading of 3.95% (w/w) has shown to provide optimal mechanical behavior while higher drug loading required the use of plasticizers to give a filament with optimal softness. Following this composition optimization, five shapes have been successfully constructed (cube, pyramid, cylinder, sphere and torus) (**Fig. 16**) [160].



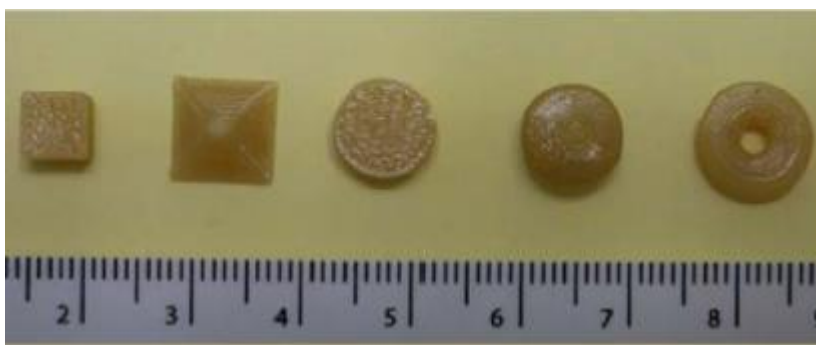


Figure 16– Picture of different shapes of paracetamol (3.78%)-PVA formulations obtained by FDM: cube, pyramid, cylinder, sphere and torus (from left to right). Reprinted from [161], with permission of Elsevier.

Researchers showed that the fastest release rates were obtained with geometries characterized by a high surface area/volume (SA/V) ratio. Indeed, the pyramid form had the fastest rate while the sphere had the slowest, with a similar surface area, but a different volume. When this SA/V ratio was kept constant, the results were radically different with the faster release obtained with the sphere (and cubic) forms while the pyramid forms gave the slower release. Erosion of the matrix could be an explanation. This study shown that drug release kinetic is more influenced by the ratio SA/V rather than the surface area alone, which highlighted the importance of the geometry. In this point of view, FDM is one of the most suitable techniques to provide very complex tablets form in order to optimize the desired ratio [160].

In another study, channeled tablets containing hydrochlorothiazide were also produced by FDM [162]. Five widths of channel section were tested (0.2, 0.4, 0.6, 0.8 and 1.0 mm). Besides, in order to measure the influence of the length and orientation of the channels, 9-long channels parallel to the long axis of the caplet design or 18-shorter channels at right angles to the long axis of the caplet design were applied (Fig. 17). It was shown that the printed tablet design has an influence on the *in vitro* drug release. Indeed, the short channels (0.2-0.4 mm) showed a limited improvement in the dissolution rate in comparison to the wider channels. This latter allowed a release of hydrochlorothiazide reaching a maximum, after 30 min, of 92.3% for 9-long channel designs and of 93.4% for the 18-short channel designs. As it has been written above, the dissolution rate is often directly linked to the surface area of the printed structure. Here, the release of hydrochlorothiazide is faster for the 18-short channel tablets while they have a lower surface/volume ratio in comparison to 9-long channel tablets. In this study, the release of the drug is rather depending on the length of the channels which eroded faster for the 18-short channels than for the 9-long channels.

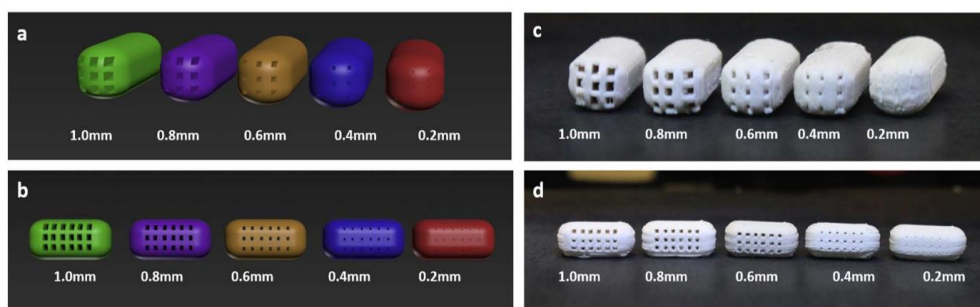


Figure 17– Rendered images of caplet designs with decreasing channel size with a) 9-long channels b) 18-short channels, photographs of tablets with decreasing channel size c) 9-long channels d) 18-short channels. Reprinted from [162], with permission of Elsevier.

**Fig. 18** shows capsule-like structure designed by Arafat and his team [163]. This design was divided into nine blocks with determined light spaces in between (0, 0.2, 0.4, 0.6, 0.8, 1.0 or 1.2 mm). The distance between the blocks was of most importance for the drug liberation. A distance of 1.0 mm between the different blocks was necessary to allow a sufficient flow of medium in the structure and to meet the Pharmacopeia criteria concerning the dissolution of immediate release formulations. In this study, the increase of the dissolution rate of the different structures is not only due to the increase of the surface/mass ratio. Indeed, the difference of the surface/mass ratio of tablets with inter-blocks spaces of more than 0.6 mm and the others is negligible. According to the authors, the reason that explains the different dissolution profiles is the structural change of the tablets during the dissolution. Wide angle laser imaging was performed during the dissolution tests in order to measure the time-to-break of the tablets. It appeared that the larger the inter-block, the faster the tablet broke, allowing a greater contact with the aqueous medium, so a faster release of the drug.

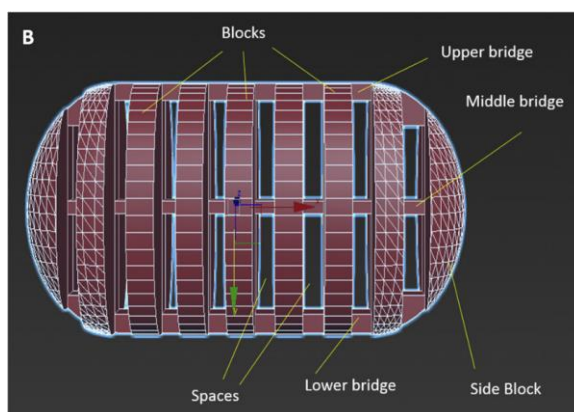


Figure 18– Illustration of the novel design based on 9 repeating units (blocks) with determined light spaces in between (0, 0.2, 0.4, 0.6, 0.8, 1.0 or 1.2 mm). The capsule-like general shape was maintained by using curved side units. Reprinted from [163], with permission of Elsevier.

Another complex geometry that was studied is radiator-like printed structures (Fig. 19) [164].

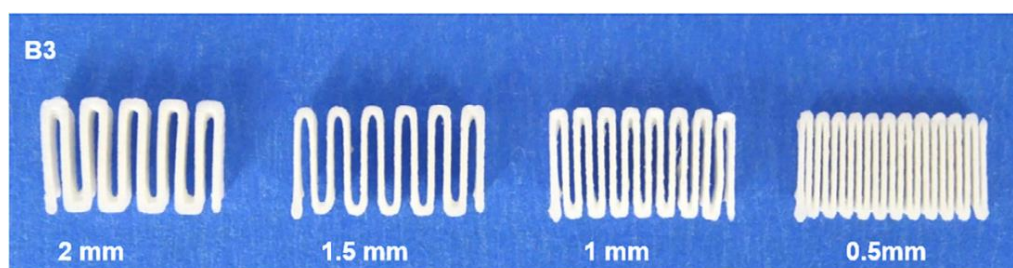


Figure 19– Radiator-like doses containing theophylline, PEG 6 K and PEO 600 K. These four designs have the same overall dimensions, but with increasing spaces (2.0, 1.5, 1.0 and 0.5 mm). Reprinted from [164], with permission of Elsevier.

PEO has already been used in FDM 3D printing in order to print immediate release formulations [135,140]. Isreb evaluated the ability of PEO 600,000 to be the backbone polymer of original FDM 3D printed structures with fast drug release [164]. PEG 6000 was used as a plasticizer in the tested formulations. Compressed PEO/PEG blends, in contact with aqueous media, tend to form a gel layer which slows the drug release down [165]. To overcome this dissolution speed reduction, the authors designed FDM 3D printed radiator-like structures with different spaces between the plates. These structures allow to have an increased surface/mass ratio. Besides, the thinness of the plates makes the formed gel layer thinner, allowing the drug to be released faster. Four different spaces were tested (0.5, 1.0, 1.5 and 2.0 mm). To be in accordance with the USP criteria for immediate release formulations, namely reaching 80% of the API

dissolution in 500 mL of HCl 0.1 N in aqueous medium within 30 minutes, the space between the plates had to be 1.0 mm long minimum. The last four studies of the previous chapter proved that the dissolution rate of the printed structures is not only influenced by the surface area, but also by the geometry of the structure. Indeed, for a same surface area, different geometries can have different dissolution behavior.

This chapter highlighted one of the advantages of FDM compared to the traditional tablets manufacturing techniques such as powder compression. Indeed, elaborated geometries, impossible to make by simple compression, are easily manufactured by FDM 3D printing. This makes it possible to increase the surface of contact with the physiological fluids and so to increase the dissolution rate. But this surface area is not the only parameter that modifies the dissolution rate of printed tablets. Indeed, recent studies showed that it was not always the structures with the highest surface area that dissolved the fastest.

### *5.1.3 Alternatives to Hardly Swallowable Immediate Release Forms*

All elaborated, complex structures described in this review article have proved their ability to form immediate release formulations, due to an increase of the surface area, a particular design or an acceleration of the polymeric erosion. However, one issue that we want to raise is that these unconventional structures would be difficult to swallow. To overcome this problem, authors tried to build orodispersible 3D forms that avoid any swallowable step.

Ehtezazi used a FDM 3D printer to produce fast dissolving oral films which have the advantage to be easily taken by the patient who presents difficulties to swallow, like the children or the elderly compared to the printed tablets [140]. Besides, they allow to avoid the hepatic first-pass metabolism if the drug is absorbed by the sublingual route [166]. The authors designed plain and mesh films, with or without taste-masking layer. The study showed that the drug release was impacted by the design of the film as well as by the presence or not of the taste-masking layer. Indeed, the films without this layer showed a faster release profile than those which contained the taste-masking layer which acts like a barrier, delaying the contact between the drug and the physiological fluids. It can also be seen that the mesh films had a faster release profile than the plain films, the surface of contact area being more important.

Following the same idea, other researchers used FDM to manufacture perforated orodispersible films with aripiprazole and compare them to orodispersible films made with standard solvent casting method. Concerning the dissolution studies, it appeared that the drug release profile was faster for the 3D printed orodispersible films, 95% of

the aripiprazole was released after 15 min while 75% of the API contained in the cast films was released after the same time. The difference between the two release profiles can be explained by the higher surface area of the printed orodispersible films. Besides, the DSC measurements showed a fully amorphization of the aripiprazole in the printed orodispersible films, while it is only partially amorphous in the cast films [142].

To summarize, even if the studies about the manufacture of formulations with a sustained release profile are far more numerous than studies dealing with FDM for immediate release oral drugs, this chapter showed that more and more research are conducted to accelerate the drug release, using this technique. By modifying process parameters such as the design, the porosity or the temperature, FDM can be used to produce such oral drug dosage forms.

### 5.2 Conclusion

The poor aqueous solubility of active ingredients is one of the most challenging issues in the pharmaceutical field. This leads to low and erratic absorption of API and may occult numerous promising new drugs. Researchers have developed many strategies to overcome the low solubility such as the use of polymers, CDs or by reducing the particle size. The 3D printing technologies are recent methods exploding in a lot of scientific fields. They offer several advantages such as the possibility of the ultra-precise construction of complex oral dosage forms used to optimize specific surface area of medicines. Moreover, techniques like FDM are relatively cheap and could be used to produce personalized medicines. The drop-on-powder 3D printing technique allowed to produce the Spritam®, the unique FDA approved 3D printed medicine, which may be the first in a long series of innovative medicines with an immediate release. Despite this, the FDM is by far the most used technique, especially to manufacture ASDs with optimized surface area. The critical parameter is to obtain filaments with optimal flexibility and API homogeneity. A huge work of filaments optimization is still needed and essential since many commonly used polymers in the field of solubility enhancement do not allow the formation of printable filaments. This could be settled by the development of new polymers, more appropriated for 3 DP, or by varying proportions of solubility enhancers, plasticizers and API. By solving this issue, medicine could be produced as filaments that can be shaped with a precise design and a precise dosage leading the way to personalized medicine. Concerning the laser-based printing techniques, the major limitation is the lack of pharmaceutical approved excipients. Further studies have to be conducted in order to obtain safety information of photopolymerizable polymer as well as a photoinitiator in the perspective of a scale-up for human consumption. Other photoreactive monomers must also be developed in

order to provide a wider range of excipients and so cope with potential API-polymer compatibility issues. Inkjet printing suffers from the need of solvents which will pose more and more problems because of the more important restrictions of residual solvent in medicines as well as environmental concern. Moreover, as inks are liquid forms, stability issues will occur more often compared to the use of dry forms. To conclude, 3D printing technologies offer the possibility to build very precise architecture which benefits the dissolution rate by optimizing the ratio  $SA/V$  but also provided all-in-one processes using known solubility enhancement strategies.

## 6 References

- [1] C.A. Lipinski, F. Lombardo, B.W. Dominy, P.J. Feeney, Experimental and computational approaches to estimate solubility and permeability in drug discovery and development settings, *Adv. Drug Deliv. Rev.* 64 (2012) 4–17. <https://doi.org/10.1016/j.addr.2012.09.019>.
- [2] P. Gribbon, S. Andreas, High-throughput drug discovery: What can we expect from HTS?, *Drug Discov. Today*. 10 (2005) 17–22. [https://doi.org/10.1016/S1359-6446\(04\)03275-1](https://doi.org/10.1016/S1359-6446(04)03275-1).
- [3] D. Sun, W. Gao, H. Hu, S. Zhou, Why 90% of clinical drug development fails and how to improve it?, *Acta Pharm. Sin. B*. 12 (2022) 3049–3062. <https://doi.org/10.1016/j.apsb.2022.02.002>.
- [4] C.A.S. Bergström, P. Larsson, Computational prediction of drug solubility in water-based systems: Qualitative and quantitative approaches used in the current drug discovery and development setting, *Int. J. Pharm.* 540 (2018) 185–193. <https://doi.org/10.1016/j.ijpharm.2018.01.044>.
- [5] B. Dong, K. Hadinoto, Carboxymethyl cellulose is a superior polyanion to dextran sulfate in stabilizing and enhancing the solubility of amorphous drug-polyelectrolyte nanoparticle complex, *Int. J. Biol. Macromol.* 139 (2019) 500–508. <https://doi.org/10.1016/j.ijbiomac.2019.08.023>.
- [6] Y. Liu, T. Wang, W. Ding, C. Dong, X. Wang, J. Chen, Y. Li, Dissolution and oral bioavailability enhancement of praziquantel by solid dispersions, *Drug Deliv. Transl. Res.* 8 (2018) 580–590. <https://doi.org/10.1007/s13346-018-0487-7>.
- [7] S. V. Jermain, C. Brough, R.O. Williams, Amorphous solid dispersions and nanocrystal technologies for poorly water-soluble drug delivery – An update, *Int. J. Pharm.* 535 (2018) 379–392. <https://doi.org/10.1016/j.ijpharm.2017.10.051>.
- [8] Y. Xie, Y. Yao, Octenylsuccinate hydroxypropyl phytoglycogen, a dendrimer-like biopolymer, solubilizes poorly water-soluble active pharmaceutical ingredients, *Carbohydr. Polym.* 180 (2018) 29–37. <https://doi.org/10.1016/j.carbpol.2017.10.004>.
- [9] H. Abdelkader, Z. Fathalla, Investigation into the Emerging Role of the Basic Amino Acid L-Lysine in Enhancing Solubility and Permeability of BCS Class II and BCS Class IV Drugs, *Pharm. Res.* 35 (2018). <https://doi.org/10.1007/s11095-018-2443-0>.
- [10] G.L. Amidon, H. Lennernäs, V.P. Shah, J.R. Crison, A Theoretical Basis for a Biopharmaceutic Drug Classification: The Correlation of in Vitro Drug Product Dissolution and in Vivo Bioavailability, *Pharm. Res. An Off. J. Am. Assoc. Pharm. Sci.* 12 (1995) 413–420. <https://doi.org/10.1023/A:1016212804288>.
- [11] Y. Kawabata, K. Wada, M. Nakatani, S. Yamada, S. Onoue, Formulation design for poorly water-soluble drugs based on biopharmaceutics classification system: Basic approaches and practical applications, *Int. J. Pharm.* 420 (2011) 1–10. <https://doi.org/10.1016/j.ijpharm.2011.08.032>.
- [12] FDA, Dissolution Testing and Acceptance Criteria for Immediate-Release Solid Oral Dosage Form Drug Products Containing High Solubility Drug Substances Guidance for Industry, 8 (2018). [http://www.fda.gov/Drugs/GuidanceComplianceRegulatoryInformation/Guidances/default.htm%0Afile:///C:/Users/ASUS/Desktop/Rujukan PhD/Drug Release/1074043 FNL\\_clean.pdf](http://www.fda.gov/Drugs/GuidanceComplianceRegulatoryInformation/Guidances/default.htm%0Afile:///C:/Users/ASUS/Desktop/Rujukan%20PhD/Drug%20Release/1074043%20FNL_clean.pdf).
- [13] FDA, U.S. Department of Health and Human Services Food and Drug Administration Center for Evaluation and Research (CDER), Guid. Ind. Vitro. Metab. Mediat. Drug-Drug Transp. Interact. Stud. Draft Guid. (2017) 1–16. <https://www.fda.gov/drugs/guidances-drugs/all-guidances-drugs>.
- [14] J.B.D. James M. Butler, The Developability Classification System: Application of Biopharmaceutics Concepts to Formulation Development, *J. Pharm. Sci.* 99 (2010) 4940–4954. <https://doi.org/10.1002/jps>.
- [15] A. Charalabidis, M. Sfouni, C. Bergström, P. Macheras, The Biopharmaceutics Classification System (BCS) and the Biopharmaceutics Drug Disposition Classification System (BDDCS): Beyond guidelines, *Int. J. Pharm.* 566 (2019) 264–281. <https://doi.org/10.1016/j.ijpharm.2019.05.041>.
- [16] R. Cristofolletti, J.B. Dressman, Dissolution Methods to Increasing Discriminatory Power of In Vitro Dissolution Testing for Ibuprofen Free Acid and Its Salts, *J. Pharm. Sci.* 106 (2017) 92–99. <https://doi.org/10.1016/j.xphs.2016.06.001>.
- [17] A.T.M. Serajuddin, Salt formation to improve drug solubility, *Adv. Drug Deliv. Rev.* 59 (2007) 603–616. <https://doi.org/10.1016/j.addr.2007.05.010>.
- [18] M.S. Hossain Mithu, S. Economidou, V. Trivedi, S. Bhatt, D. Douroumis, Advanced Methodologies for Pharmaceutical Salt Synthesis, *Cryst. Growth Des.* 21 (2021) 1358–1374.

- <https://doi.org/10.1021/acs.cgd.0c01427>.
- [19] M. Guo, X. Sun, J. Chen, T. Cai, Pharmaceutical cocrystals: A review of preparations, physicochemical properties and applications, *Acta Pharm. Sin. B.* 11 (2021) 2537–2564. <https://doi.org/10.1016/j.apsb.2021.03.030>.
  - [20] X.Q. Ma, C. Zhuang, B.C. Wang, Y.F. Huang, Q. Chen, N. Lin, Cocrystal of Apigenin with Higher Solubility, Enhanced Oral Bioavailability, and Anti-inflammatory Effect, *Cryst. Growth Des.* 19 (2019) 5531–5537. <https://doi.org/10.1021/acs.cgd.9b00249>.
  - [21] S.R. Vippagunta, H.G. Brittain, D.J.W. Grant, Crystalline solids, *Adv. Drug Deliv. Rev.* 48 (2001) 3–26. [https://doi.org/10.1016/S0169-409X\(01\)00097-7](https://doi.org/10.1016/S0169-409X(01)00097-7).
  - [22] B. Rodríguez-Spong, C.P. Price, A. Jayasankar, A.J. Matzger, N. Rodríguez-Hornedo, General principles of pharmaceutical solid polymorphism: A supramolecular perspective, *Adv. Drug Deliv. Rev.* 56 (2004) 241–274. <https://doi.org/10.1016/j.addr.2003.10.005>.
  - [23] S.B. Murdande, M.J. Pikal, R.M. Shanker, R.H. Bogner, Aqueous solubility of crystalline and amorphous drugs: Challenges in measurement, *Pharm. Dev. Technol.* 16 (2011) 187–200. <https://doi.org/10.3109/10837451003774377>.
  - [24] R. Censi, P. Di Martino, Polymorph impact on the bioavailability and stability of poorly soluble drugs, *Molecules.* 20 (2015) 18759–18776. <https://doi.org/10.3390/molecules201018759>.
  - [25] W. Zhang, D. Chen, Crystal structures and physicochemical properties of amisulpride polymorphs, *J. Pharm. Biomed. Anal.* 140 (2017) 252–257. <https://doi.org/10.1016/j.jpba.2017.03.030>.
  - [26] A.A. Noyes, W.R. Whitney, The rate of solution of solid substances in their own solutions, *J. Am. Chem. Soc.* 19 (1897) 930–934. <https://doi.org/10.1021/ja02086a003>.
  - [27] M. Mosharraf, C. Nyström, The effect of particle size and shape on the surface specific dissolution rate of micro-sized practically insoluble drugs, *Int. J. Pharm.* 122 (1995) 35–47. [https://doi.org/10.1016/0378-5173\(95\)00033-F](https://doi.org/10.1016/0378-5173(95)00033-F).
  - [28] I.Y. Saleem, H.D.C. Smyth, Micronization of a soft material: Air-jet and micro-ball milling, *AAPS PharmSciTech.* 11 (2010) 1642–1649. <https://doi.org/10.1208/s12249-010-9542-5>.
  - [29] N. Rasenack, H. Hartenhauer, B.W. Müller, Microcrystals for dissolution rate enhancement of poorly water-soluble drugs, *Int. J. Pharm.* 254 (2003) 137–145. [https://doi.org/10.1016/S0378-5173\(03\)00005-X](https://doi.org/10.1016/S0378-5173(03)00005-X).
  - [30] A. Martín, M.J. Cocero, Micronization processes with supercritical fluids: Fundamentals and mechanisms, *Adv. Drug Deliv. Rev.* 60 (2008) 339–350. <https://doi.org/10.1016/j.addr.2007.06.019>.
  - [31] F.L.O. Da Silva, M.B.D.F. Marques, K.C. Kato, G. Carneiro, Nanonization techniques to overcome poor water-solubility with drugs, *Expert Opin. Drug Discov.* 15 (2020) 853–864. <https://doi.org/10.1080/17460441.2020.1750591>.
  - [32] Z.H. Loh, A.K. Samanta, P.W. Sia Heng, Overview of milling techniques for improving the solubility of poorly water-soluble drugs, *Asian J. Pharm. Sci.* 10 (2014) 255–274. <https://doi.org/10.1016/j.ajps.2014.12.006>.
  - [33] D. Manzanares, V. Ceña, Endocytosis: The nanoparticle and submicron nanocompounds gateway into the cell, *Pharmaceutics.* 12 (2020) 1–22. <https://doi.org/10.3390/pharmaceutics12040371>.
  - [34] B. Van Eerdenbrugh, G. Van den Mooter, P. Augustijns, Top-down production of drug nanocrystals: Nanosuspension stabilization, miniaturization and transformation into solid products, *Int. J. Pharm.* 364 (2008) 64–75. <https://doi.org/10.1016/j.ijpharm.2008.07.023>.
  - [35] R.H. Müller, K. Peters, Nanosuspensions for the formulation of poorly soluble drugs. I. Preparation by a size-reduction technique, *Int. J. Pharm.* 160 (1998) 229–237. [https://doi.org/10.1016/S0378-5173\(97\)00311-6](https://doi.org/10.1016/S0378-5173(97)00311-6).
  - [36] Y. Lu, K. Park, Polymeric micelles and alternative nanonized delivery vehicles for poorly soluble drugs, *Int. J. Pharm.* 453 (2013) 198–214. <https://doi.org/10.1016/j.ijpharm.2012.08.042>.
  - [37] M.E. Brewster, T. Loftsson, Cyclodextrins as pharmaceutical solubilizers, *Adv. Drug Deliv. Rev.* 59 (2007) 645–666. <https://doi.org/10.1016/j.addr.2007.05.012>.
  - [38] S. V. Kurkov, T. Loftsson, Cyclodextrins, *Int. J. Pharm.* 453 (2013) 167–180. <https://doi.org/10.1016/j.ijpharm.2012.06.055>.



- [39] V.J. Stella, V.M. Rao, E.A. Zannou, V. Zia, Mechanisms of drug release from cyclodextrin complexes, *Adv. Drug Deliv. Rev.* 36 (1999) 3–16. [https://doi.org/10.1016/S0169-409X\(98\)00052-0](https://doi.org/10.1016/S0169-409X(98)00052-0).
- [40] G. Tiwari, R. Tiwari, A. Rai, Cyclodextrins in delivery systems: Applications, *J. Pharm. Bioallied Sci.* 2 (2010) 72. <https://doi.org/10.4103/0975-7406.67003>.
- [41] S.S. Jambhekar, P. Breen, Cyclodextrins in pharmaceutical formulations II: Solubilization, binding constant, and complexation efficiency, *Drug Discov. Today*. 21 (2016) 363–368. <https://doi.org/10.1016/j.drudis.2015.11.016>.
- [42] A. Harada, Y. Takashima, H. Yamaguchi, Cyclodextrin-based supramolecular polymers, *Chem. Soc. Rev.* 38 (2009) 875–882. <https://doi.org/10.1039/b705458k>.
- [43] K. Pongsamart, W. Limwikrant, U.R. Ruktanonchai, N. Charoenthai, S. Puttipipatkachorn, Preparation, characterization and antimalarial activity of dihydroartemisinin /  $\beta$ -cyclodextrin spray-dried powder, *J. Drug Deliv. Sci. Technol.* 73 (2022) 103434. <https://doi.org/10.1016/j.jddst.2022.103434>.
- [44] N.N.S. Mai, R. Nakai, Y. Kawano, T. Hanawa, Enhancing the Solubility of Curcumin Using a Solid Dispersion System with, *Pharmacy*. 8 (2020) 14.
- [45] T. Yan, M. Ji, Y. Sun, T. Yan, J. Zhao, H. Zhang, Z. Wang, Preparation and characterization of baicalein/hydroxypropyl- $\beta$ -cyclodextrin inclusion complex for enhancement of solubility, antioxidant activity and antibacterial activity using supercritical antisolvent technology, *J. Incl. Phenom. Macrocycl. Chem.* 96 (2020) 285–295. <https://doi.org/10.1007/s10847-019-00970-2>.
- [46] P.A. Granados, L.A.G. Pinho, L.L. Sa-Barreto, T. Gratieri, G.M. Gelfuso, M. Cunha-Filho, Application of hot-melt extrusion in the complexation of naringenin with cyclodextrin using hydrophilic polymers, *Adv. Powder Technol.* 33 (2022) 103380. <https://doi.org/10.1016/j.apt.2021.11.032>.
- [47] J. Thiry, F. Krier, S. Ratwatte, J. Thomassin, C. Jerome, B. Evrard, Hot-melt extrusion as a continuous manufacturing process to form ternary cyclodextrin inclusion complexes, *Eur. J. Pharm. Sci.* 96 (2017) 590–597. <https://doi.org/10.1016/j.ejps.2016.09.032>.
- [48] P. Tran, J.-S. Park, Recent trends of self-emulsifying drug delivery system for enhancing the oral bioavailability of poorly water-soluble drugs, *J. Pharm. Investig.* 51 (2021) 439–463. <https://doi.org/10.1007/s40005-021-00516-0>.
- [49] K. Kohli, S. Chopra, D. Dhar, S. Arora, R.K. Khar, Self-emulsifying drug delivery systems: An approach to enhance oral bioavailability, *Drug Discov. Today*. 15 (2010) 958–965. <https://doi.org/10.1016/j.drudis.2010.08.007>.
- [50] J.K. Madagul, D.R. Parakh, R.S. Kumar, R.R. Abhang, Formulation and evaluation of solid self-microemulsifying drug delivery system of chlorthalidone by spray drying technology, *Dry. Technol.* 35 (2017) 1433–1449. <https://doi.org/10.1080/07373937.2016.1201833>.
- [51] C.L.N. Vo, C. Park, B.J. Lee, Current trends and future perspectives of solid dispersions containing poorly water-soluble drugs, *Eur. J. Pharm. Biopharm.* 85 (2013) 799–813. <https://doi.org/10.1016/j.ejpb.2013.09.007>.
- [52] M. Yang, S. He, Y. Fan, Y. Wang, Z. Ge, L. Shan, W. Gong, X. Huang, Y. Tong, C. Gao, Microenvironmental pH-modified solid dispersions to enhance the dissolution and bioavailability of poorly water-soluble weakly basic GT0918, a developing anti-prostate cancer drug: Preparation, characterization and evaluation in vivo, *Int. J. Pharm.* 475 (2014) 97–109. <https://doi.org/10.1016/j.ijpharm.2014.08.047>.
- [53] C. Taniguchi, Y. Kawabata, K. Wada, S. Yamada, S. Onoue, Microenvironmental pH-modification to improve dissolution behavior and oral absorption for drugs with pH-dependent solubility, *Expert Opin. Drug Deliv.* 11 (2014) 505–516. <https://doi.org/10.1517/17425247.2014.881798>.
- [54] B.C. Hancock, G. Zografi, Characteristics and Significance of the Amorphous State in Pharmaceutical Systems, *J. Pharm. Sci.* 86 (1997) 1. <https://doi.org/10.1021/js9601896>.
- [55] G. Van Den Mooter, The use of amorphous solid dispersions: A formulation strategy to overcome poor solubility and dissolution rate, *Drug Discov. Today Technol.* 9 (2012) e79–e85. <https://doi.org/10.1016/j.ddtec.2011.10.002>.
- [56] J.G. Calvert, Glossary of atmospheric chemistry terms, *Pure Appl. Chem.* 62 (1990) 2167–2219. <https://doi.org/10.1351/pac199062112167>.
- [57] T. Van Duong, G. Van den Mooter, The role of the carrier in the formulation of pharmaceutical solid dispersions. Part II: amorphous carriers, *Expert Opin. Drug Deliv.* 13 (2016) 1681–1694.

- <https://doi.org/10.1080/17425247.2016.1198769>.
- [58] S. Kumar, M.M. Malik, R. Purohit, Synthesis Methods of Mesoporous Silica Materials, *Mater. Today Proc.* 4 (2017) 350–357. <https://doi.org/10.1016/j.matpr.2017.01.032>.
  - [59] C.A. McCarthy, R.J. Ahern, R. Dontireddy, K.B. Ryan, A.M. Crean, Mesoporous silica formulation strategies for drug dissolution enhancement: A review, *Expert Opin. Drug Deliv.* 13 (2016) 93–108. <https://doi.org/10.1517/17425247.2016.1100165>.
  - [60] A. Baumgartner, O. Planinšek, Application of commercially available mesoporous silica for drug dissolution enhancement in oral drug delivery, *Eur. J. Pharm. Sci.* 167 (2021). <https://doi.org/10.1016/j.ejps.2021.106015>.
  - [61] K.E. Bremmell, C.A. Prestidge, Enhancing oral bioavailability of poorly soluble drugs with mesoporous silica based systems: opportunities and challenges, *Drug Dev. Ind. Pharm.* 45 (2019) 349–358. <https://doi.org/10.1080/03639045.2018.1542709>.
  - [62] R. Mellaerts, J.A.G. Jammaer, M. Van Speybroeck, H. Chen, J. Van Humbeeck, P. Augustijns, G. Van Den Mooter, J.A. Martens, Physical State of Poorly Water Soluble Therapeutic Molecules Loaded into SBA-15 Ordered Mesoporous Silica Carriers: A Case Study with Itraconazole and Ibuprofen, (n.d.). <https://doi.org/10.1021/la801161g>.
  - [63] F. Qu, G. Zhu, H. Lin, W. Zhang, J. Sun, S. Li, S. Qiu, A controlled release of ibuprofen by systematically tailoring the morphology of mesoporous silica materials, *J. Solid State Chem.* 179 (2006) 2027–2035. <https://doi.org/10.1016/j.jssc.2006.04.002>.
  - [64] A. Gignone, L. Manna, S. Ronchetti, M. Banchero, B. Onida, Incorporation of clotrimazole in Ordered Mesoporous Silica by supercritical CO<sub>2</sub>, *Microporous Mesoporous Mater.* 200 (2014) 291–296. <https://doi.org/10.1016/j.micromeso.2014.05.031>.
  - [65] J. Andersson, J. Rosenholm, S. Areva, M. Lindén, Influences of Material Characteristics on Ibuprofen Drug Loading and Release Profiles from Ordered Micro-and Mesoporous Silica Matrices, *Chem. Mater.* 16 (2004) 4160–4167. <https://doi.org/10.1021/cm0401490>.
  - [66] N. Koch, O. Jennotte, B. Grignard, A. Lechanteur, B. Evrard, Impregnation of mesoporous silica with poor aqueous soluble molecule using pressurized carbon dioxide: is the solubility in the supercritical and subcritical phase a critical parameter?, *Eur. J. Pharm. Sci.* (2020) 105332. <https://doi.org/https://doi.org/10.1016/j.ejps.2020.105332>.
  - [67] G.Z. A. Newman, G. Knipp, Assessing the Performance of Amorphous Solid Dispersions, *J. Pharm. Sci.* 101 (2012) 1355–1377. <https://doi.org/10.1002/jps>.
  - [68] V.R. Wilson, X. Lou, D.J. Osterling, D.A.F. Stolarik, G.J. Jenkins, B.L.B. Nichols, Y. Dong, K.J. Edgar, G.G.Z. Zhang, L.S. Taylor, Amorphous solid dispersions of enzalutamide and novel polysaccharide derivatives: investigation of relationships between polymer structure and performance, *Sci. Rep.* 10 (2020) 1–12. <https://doi.org/10.1038/s41598-020-75077-7>.
  - [69] V. Sihorkar, T. Dürig, The role of polymers and excipients in developing amorphous solid dispersions: An industrial perspective, 2020. <https://doi.org/10.1016/B978-0-12-821222-6.00005-1>.
  - [70] P. Pandi, R. Bulusu, N. Kommineni, W. Khan, M. Singh, Amorphous solid dispersions: An update for preparation, characterization, mechanism on bioavailability, stability, regulatory considerations and marketed products, *Int. J. Pharm.* 586 (2020) 119560. <https://doi.org/10.1016/j.ijpharm.2020.119560>.
  - [71] W. L. Chiou and S. Riegelman, Pharmaceutical Applications of Solid Dispersion Systems, *J. Pharm. Sci.* 60 (1971) 1281–1302. <https://doi.org/10.1002/jps.2600600902>.
  - [72] T. Vasconcelos, F. Prezotti, F. Araújo, C. Lopes, A. Loureiro, S. Marques, B. Sarmento, Third-generation solid dispersion combining Soluplus and poloxamer 407 enhances the oral bioavailability of resveratrol, *Int. J. Pharm.* 595 (2021). <https://doi.org/10.1016/j.ijpharm.2021.120245>.
  - [73] D.G. Yu, J.J. Li, G.R. Williams, M. Zhao, Electrospun amorphous solid dispersions of poorly water-soluble drugs: A review, *J. Control. Release.* 292 (2018) 91–110. <https://doi.org/10.1016/j.jconrel.2018.08.016>.
  - [74] T. Vasconcelos, S. Marques, J. das Neves, B. Sarmento, Amorphous solid dispersions: Rational selection of a manufacturing process, *Adv. Drug Deliv. Rev.* 100 (2016) 85–101. <https://doi.org/10.1016/j.addr.2016.01.012>.
  - [75] N. Mendonsa, B. Almutairy, V.R. Kallakunta, S. Sarabu, P. Thipsay, S. Bandari, M.A. Repka, Manufacturing strategies to develop amorphous solid dispersions: An overview, *J. Drug Deliv. Sci.*

- Technol. 55 (2020) 101459. <https://doi.org/10.1016/j.jddst.2019.101459>.
- [76] S. V. Bhujbal, B. Mitra, U. Jain, Y. Gong, A. Agrawal, S. Karki, L.S. Taylor, S. Kumar, Q. (Tony) Zhou, Pharmaceutical amorphous solid dispersion: A review of manufacturing strategies, *Acta Pharm. Sin. B.* 11 (2021) 2505–2536. <https://doi.org/10.1016/j.apsb.2021.05.014>.
  - [77] D.H. Won, M.S. Kim, S. Lee, J.S. Park, S.J. Hwang, Improved physicochemical characteristics of felodipine solid dispersion particles by supercritical anti-solvent precipitation process, *Int. J. Pharm.* 301 (2005) 199–208. <https://doi.org/10.1016/j.ijpharm.2005.05.017>.
  - [78] A. Singh, G. Van Den Mooter, Spray drying formulation of amorphous solid dispersions ☆, *Adv. Drug Deliv. Rev.* 100 (2016) 27–50. <https://doi.org/10.1016/j.addr.2015.12.010>.
  - [79] A. Sosnik, K.P. Seremeta, Advantages and challenges of the spray-drying technology for the production of pure drug particles and drug-loaded polymeric carriers, *Adv. Colloid Interface Sci.* 223 (2015) 40–54. <https://doi.org/10.1016/j.cis.2015.05.003>.
  - [80] E. Jakubowska, J. Lulek, The application of freeze-drying as a production method of drug nanocrystals and solid dispersions – A review, *J. Drug Deliv. Sci. Technol.* 62 (2021) 102357. <https://doi.org/10.1016/j.jddst.2021.102357>.
  - [81] F. Hassouna, M. Abo El Dahab, M. Fulem, A. De Lima Haiek, A. Laachachi, D. Kopecký, M. Šoóš, Multi-scale analysis of amorphous solid dispersions prepared by freeze drying of ibuprofen loaded acrylic polymer nanoparticles, *J. Drug Deliv. Sci. Technol.* 53 (2019) 101182. <https://doi.org/10.1016/j.jddst.2019.101182>.
  - [82] P. Tran, J.S. Park, Application of supercritical fluid technology for solid dispersion to enhance solubility and bioavailability of poorly water-soluble drugs, *Int. J. Pharm.* 610 (2021) 121247. <https://doi.org/10.1016/j.ijpharm.2021.121247>.
  - [83] F. Han, W. Zhang, Y. Wang, Z. Xi, L. Chen, S. Li, L. Xu, Applying supercritical fluid technology to prepare ibuprofen solid dispersions with improved oral bioavailability, *Pharmaceutics*. 11 (2019). <https://doi.org/10.3390/pharmaceutics11020067>.
  - [84] J. Doshi, D.H. Reneker, Electrospinning process and applications of electrospun fibers, *Conf. Rec. - IAS Annu. Meet. (IEEE Ind. Appl. Soc.* 3 (1995) 1698–1703. <https://doi.org/10.1109/ias.1993.299067>.
  - [85] X. Li, M.A. Kanjwal, L. Lin, I.S. Chronakis, Electrospun polyvinyl-alcohol nanofibers as oral fast-dissolving delivery system of caffeine and riboflavin, *Colloids Surfaces B Biointerfaces*. 103 (2013) 182–188. <https://doi.org/10.1016/j.colsurfb.2012.10.016>.
  - [86] O. Jennotte, N. Koch, A. Lechanteur, B. Evrard, Three-dimensional printing technology as a promising tool in bioavailability enhancement of poorly water-soluble molecules: A review, *Int. J. Pharm.* 580 (2020). <https://doi.org/10.1016/j.ijpharm.2020.119200>.
  - [87] E. Prasad, M.T. Islam, D.J. Goodwin, A.J. Megarry, G.W. Halbert, A.J. Florence, J. Robertson, Development of a hot-melt extrusion (HME) process to produce drug loaded Affinisol™ 15LV filaments for fused filament fabrication (FFF) 3D printing, *Addit. Manuf.* 29 (2019) 100776. <https://doi.org/10.1016/j.addma.2019.06.027>.
  - [88] J. Wang, A. Goyanes, S. Gaisford, A.W. Basit, Stereolithographic (SLA) 3D printing of oral modified-release dosage forms, *Int. J. Pharm.* 503 (2016) 207–212. <https://doi.org/10.1016/j.ijpharm.2016.03.016>.
  - [89] O. Jennotte, N. Koch, A. Lechanteur, B. Evrard, Three-dimensional printing technology as a promising tool in bioavailability enhancement of poorly water-soluble molecules: A review, *Int. J. Pharm.* 580 (2020) 119200. <https://doi.org/10.1016/j.ijpharm.2020.119200>.
  - [90] E. Andrzejewska, Photopolymerization kinetics of multifunctional monomers, *Prog. Polym. Sci.* 26 (2001) 605–665.
  - [91] H. Kadry, S. Wadnap, C. Xu, F. Ahsan, Digital light processing ( DLP ) 3D-printing technology and photoreactive polymers in fabrication of modified-release tablets, *Eur. J. Pharm. Sci.* 135 (2019) 60–67. <https://doi.org/10.1016/j.ejps.2019.05.008>.
  - [92] D.J. Ellenberger, D.A. Miller, R.O. Williams, Expanding the Application and Formulation Space of Amorphous Solid Dispersions with KinetiSol®: a Review, *AAPS PharmSciTech.* 19 (2018) 1933–1956. <https://doi.org/10.1208/s12249-018-1007-2>.
  - [93] U. Gala, D. Miller, R.O. Williams, Improved dissolution and pharmacokinetics of abiraterone through kinetisol® enabled amorphous solid dispersions, *Pharmaceutics*. 12 (2020).

- <https://doi.org/10.3390/pharmaceutics12040357>.
- [94] J. Zhang, R. Thakkar, Y. Zhang, M. Maniruzzaman, Microwave induced dielectric heating for the on-demand development of indomethacin amorphous solid dispersion tablets, *J. Drug Deliv. Sci. Technol.* 61 (2021) 102109. <https://doi.org/10.1016/j.jddst.2020.102109>.
  - [95] S.F.S. Shirazi, S. Gharekhani, M. Mehrli, H. Yarmand, H.S.C. Metselaar, N.A. Kadri, N.A.A.N.A. Osman, A review on powder-based additive manufacturing for tissue engineering : selective laser sintering and inkjet 3D printing A review on powder-based additive manufacturing for tissue engineering : selective laser sintering and inkjet 3D printing, *Sci. Technol. Adv. Mater.* 16 (2015) 1–20. <https://doi.org/10.1088/1468-6996/16/3/033502>.
  - [96] F. Fina, A. Goyanes, S. Gaisford, A.W. Basit, Selective laser sintering (SLS) 3D printing of medicines, *Int. J. Pharm.* 529 (2017) 285–293. <https://doi.org/10.1016/j.ijpharm.2017.06.082>.
  - [97] A. Goyanes, N. Allahham, S.J. Trenfield, E. Stoyanov, S. Gaisford, A.W. Basit, Direct powder extrusion 3D printing: Fabrication of drug products using a novel single-step process, *Int. J. Pharm.* 567 (2019). <https://doi.org/10.1016/j.ijpharm.2019.118471>.
  - [98] M. Fanous, S. Gold, S. Muller, S. Hirsch, J. Ogorka, G. Imanidis, Simplification of fused deposition modeling 3D-printing paradigm: Feasibility of 1-step direct powder printing for immediate release dosage form production, *Int. J. Pharm.* 578 (2020) 119124. <https://doi.org/10.1016/j.ijpharm.2020.119124>.
  - [99] J. Boniatti, P. Januskaite, L.B. da Fonseca, A.L. Viçosa, F.C. Amendoeira, C. Tuleu, A.W. Basit, A. Goyanes, M.I. Ré, Direct powder extrusion 3d printing of praziquantel to overcome neglected disease formulation challenges in paediatric populations, *Pharmaceutics*. 13 (2021). <https://doi.org/10.3390/pharmaceutics13081114>.
  - [100] M. Pistone, G.F. Racaniello, I. Arduino, V. Laquintana, A. Lopalco, A. Cutrignelli, R. Rizzi, M. Franco, A. Lopodota, N. Denora, Direct cyclodextrin-based powder extrusion 3D printing for one-step production of the BCS class II model drug niclosamide, *Drug Deliv. Transl. Res.* 12 (2022) 1895–1910. <https://doi.org/10.1007/s13346-022-01124-7>.
  - [101] M.F. Simões, R.M.A. Pinto, S. Simões, Hot-melt extrusion in the pharmaceutical industry: toward filling a new drug application, *Drug Discov. Today*. 24 (2019) 1749–1768. <https://doi.org/10.1016/j.drudis.2019.05.013>.
  - [102] J. Thiry, F. Krier, B. Evrard, A review of pharmaceutical extrusion : Critical process parameters and, *Int. J. Pharm.* 479 (2015) 227–240. <https://doi.org/10.1016/j.ijpharm.2014.12.036>.
  - [103] I. Alig, D. Fischer, D. Lellinger, B. Steinhoff, Combination of NIR, Raman, ultrasonic and dielectric spectroscopy for in-line monitoring of the extrusion process, *Macromol. Symp.* 230 (2005) 51–58. <https://doi.org/10.1002/masy.200551141>.
  - [104] K. Nakamichi, T. Nakano, H. Yasuura, S. Izumi, Y. Kawashima, The role of the kneading paddle and the effects of screw revolution speed and water content on the preparation of solid dispersions using a twin-screw extruder, *Int. J. Pharm.* 241 (2002) 203–211. [https://doi.org/10.1016/S0378-5173\(02\)00134-5](https://doi.org/10.1016/S0378-5173(02)00134-5).
  - [105] M. Hanada, S. V. Jermain, X. Lu, Y. Su, R.O. Williams, Predicting physical stability of ternary amorphous solid dispersions using specific mechanical energy in a hot melt extrusion process, *Int. J. Pharm.* 548 (2018) 571–585. <https://doi.org/10.1016/j.ijpharm.2018.07.029>.
  - [106] M.M. Crowley, F. Zhang, M.A. Repka, S. Thumma, S.B. Upadhye, S.K. Battu, J.W. McGinity, C. Martin, Pharmaceutical applications of hot-melt extrusion: Part I, *Drug Dev. Ind. Pharm.* 33 (2007) 909–926. <https://doi.org/10.1080/03639040701498759>.
  - [107] D. Desai, H. Sandhu, N. Shah, W. Malick, H. Zia, W. Phuapradit, S.R.K. Vaka, Selection of Solid-State Plasticizers as Processing Aids for Hot-Melt Extrusion, *J. Pharm. Sci.* 107 (2018) 372–379. <https://doi.org/10.1016/j.xphs.2017.09.004>.
  - [108] R. Pezzoli, M. Hopkins, G. Direur, N. Gately, J.G. Lyons, C.L. Higginbotham, Micro-injection moulding of poly(Vinylpyrrolidone-vinyl acetate) binary and ternary amorphous solid dispersions, *Pharmaceutics*. 11 (2019). <https://doi.org/10.3390/pharmaceutics11050240>.
  - [109] A. Singh, A. Bharati, P. Frederiks, O. Verkinderen, B. Goderis, R. Cardinaels, P. Moldenaers, J. Van Humbeeck, G. Van Den Mooter, Effect of Compression on the Molecular Arrangement of Itraconazole-Soluplus Solid Dispersions: Induction of Liquid Crystals or Exacerbation of Phase Separation?, *Mol. Pharm.* 13 (2016) 1879–1893. <https://doi.org/10.1021/acs.molpharmaceut.6b00046>.

- [110] S.M. Mishra, M. Richter, L. Mejia, A. Sauer, Downstream Processing of Itraconazole:HPMCAS Amorphous Solid Dispersion: From Hot-Melt Extrudate to Tablet Using a Quality by Design Approach, *Pharmaceutics*. 14 (2022). <https://doi.org/10.3390/pharmaceutics14071429>.
- [111] T. Quinten, Y. Gonnissen, E. Adriaens, T. De Beer, V. Cnudde, B. Masschaele, L. Van Hoorebeke, J. Siepmann, J.P. Remon, C. Vervaet, Development of injection moulded matrix tablets based on mixtures of ethylcellulose and low-substituted hydroxypropylcellulose, *Eur. J. Pharm. Sci.* 37 (2009) 207–216. <https://doi.org/10.1016/j.ejps.2009.02.006>.
- [112] J. Van Renterghem, H. Dhondt, G. Verstraete, M. De Bruyne, C. Vervaet, T. De Beer, The impact of the injection mold temperature upon polymer crystallization and resulting drug release from immediate and sustained release tablets, *Int. J. Pharm.* 541 (2018) 108–116. <https://doi.org/10.1016/j.ijpharm.2018.01.053>.
- [113] P.S. Shah, J. Breitenbach, Melt Extrusion: A Commercial Perception to Practicality, in: A.M. Repka, N. Langley, J. DiNunzio (Eds.) *Melt extrusion: Materials, Technology and Drug Product Design*, in: Springer New York, New York, NY, 2013: pp. 447–458.
- [114] R. Chopra, F. Podczek, J.M. Newton, G. Alderborn, The influence of pellet shape and film coating on the filling of pellets into hard shell capsules, *Eur. J. Pharm. Biopharm.* 53 (2002) 327–333. [https://doi.org/10.1016/S0939-6411\(02\)00015-2](https://doi.org/10.1016/S0939-6411(02)00015-2).
- [115] L.K. Prasad, H. Smyth, L.K. Prasad, H. Smyth, 3D Printing technologies for drug delivery : a review 3D Printing technologies for drug delivery : a review, 9045 (2016). <https://doi.org/10.3109/03639045.2015.1120743>.
- [116] E. Lepowsky, S. Tasoglu, 3D printing for drug manufacturing: A perspective on the future of pharmaceuticals, *Int. J. Bioprinting*. 4 (2018) 1–13. <https://doi.org/10.18063/IJB.v4i1.119>.
- [117] S.A. Khaled, J.C. Burley, M.R. Alexander, J. Yang, C.J. Roberts, 3D printing of tablets containing multiple drugs with defined release profiles, *Int. J. Pharm.* 494 (2015) 643–650. <https://doi.org/10.1016/j.ijpharm.2015.07.067>.
- [118] G. Gorkem Buyukgoz, D. Soffer, J. Defendre, G.M. Pizzano, R.N. Davé, Exploring tablet design options for tailoring drug release and dose via fused deposition modeling (FDM) 3D printing, *Int. J. Pharm.* 591 (2020). <https://doi.org/10.1016/j.ijpharm.2020.119987>.
- [119] J. Norman, R.D. Madurawe, C.M.V. Moore, M.A. Khan, A. Khairuzzaman, A new chapter in pharmaceutical manufacturing: 3D-printed drug products, *Adv. Drug Deliv. Rev.* 108 (2017) 39–50. <https://doi.org/10.1016/j.addr.2016.03.001>.
- [120] H.N. Chia, B.M. Wu, Recent advances in 3D printing of biomaterials, *J. Biol. Eng.* (2015) 1–14. <https://doi.org/10.1186/s13036-015-0001-4>.
- [121] I. Zein, D.W. Hutmacher, K. Cheng, S. Hin, Fused deposition modeling of novel scaffold architectures for tissue engineering applications, 23 (2002) 1169–1185.
- [122] A. Goyanes, A.B.M. Buanz, G.B. Hatton, S. Gaisford, A.W. Basit, 3D printing of modified-release aminosalicylate (4-ASA and 5-ASA) tablets, *Eur. J. Pharm. Biopharm.* 89 (2015) 157–162. <https://doi.org/10.1016/j.ejpb.2014.12.003>.
- [123] Y. Yang, H. Wang, H. Li, Z. Ou, G. Yang, 3D printed tablets with internal scaffold structure using ethyl cellulose to achieve sustained ibuprofen release, *Eur. J. Pharm. Sci.* 115 (2018) 11–18. <https://doi.org/10.1016/j.ejps.2018.01.005>.
- [124] S. ichiro Kimura, T. Ishikawa, Y. Iwao, S. Itai, H. Kondo, Fabrication of zero-order sustained-release floating tablets via fused depositing modeling 3D printer, *Chem. Pharm. Bull.* 67 (2019) 992–999. <https://doi.org/10.1248/cpb.c19-00290>.
- [125] P. Kanaujia, P. Poovizhi, W.K. Ng, R.B.H. Tan, Amorphous formulations for dissolution and bioavailability enhancement of poorly soluble APIs, *Powder Technol.* 285 (2015) 2–15. <https://doi.org/10.1016/j.powtec.2015.05.012>.
- [126] L.I. Blaabjerg, H. Grohgan, E. Lindenberg, K. Löbmann, A. Müllertz, T. Rades, The influence of polymers on the supersaturation potential of poor and good glass formers, *Pharmaceutics*. 10 (2018) 1–14. <https://doi.org/10.3390/pharmaceutics10040164>.
- [127] C. Brough, R.O. Williams, Amorphous solid dispersions and nano-crystal technologies for poorly water-soluble drug delivery, *Int. J. Pharm.* 453 (2013) 157–166. <https://doi.org/10.1016/j.ijpharm.2013.05.061>.
- [128] S. Shah, S. Maddineni, J. Lu, M.A. Repka, Melt extrusion with poorly soluble drugs, *Int. J. Pharm.*

- 453 (2013) 233–252. <https://doi.org/10.1016/j.ijpharm.2012.11.001>.
- [129] S. Baghel, H. Cathcart, N.J. O'Reilly, Theoretical and experimental investigation of drug-polymer interaction and miscibility and its impact on drug supersaturation in aqueous medium, *Eur. J. Pharm. Biopharm.* 107 (2016) 16–31. <https://doi.org/10.1016/j.ejpb.2016.06.024>.
- [130] K. Khougaz, S.D. Clas, Crystallization inhibition in solid dispersions of MK-0591 and poly(vinylpyrrolidone) polymers, *J. Pharm. Sci.* 89 (2000) 1325–1334. [https://doi.org/10.1002/1520-6017\(200010\)89:10<1325::AID-JPS10>3.0.CO;2-5](https://doi.org/10.1002/1520-6017(200010)89:10<1325::AID-JPS10>3.0.CO;2-5).
- [131] A.L. Sarode, H. Sandhu, N. Shah, W. Malick, H. Zia, Hot melt extrusion (HME) for amorphous solid dispersions: Predictive tools for processing and impact of drug-polymer interactions on supersaturation, *Eur. J. Pharm. Sci.* 48 (2013) 371–384. <https://doi.org/10.1016/j.ejps.2012.12.012>.
- [132] K. Adamska, A. Voelkel, Inverse gas chromatographic determination of solubility parameters of excipients, *Int. J. Pharm.* 304 (2005) 11–17. <https://doi.org/10.1016/j.ijpharm.2005.03.040>.
- [133] A. Forster, J. Hempenstall, I. Tucker, T. Rades, Selection of excipients for melt extrusion with two poorly water-soluble drugs by solubility parameter calculation and thermal analysis, *Int. J. Pharm.* 226 (2001) 147–161. [https://doi.org/10.1016/S0378-5173\(01\)00801-8](https://doi.org/10.1016/S0378-5173(01)00801-8).
- [134] A. Forster, J. Hempenstall, I. Tucker, T. Rades, The potential of small-scale fusion experiments and the Gordon-Taylor equation to predict the suitability of drug/polymer blends for melt extrusion, *Drug Dev. Ind. Pharm.* 27 (2001) 549–560. <https://doi.org/10.1081/DDC-100105180>.
- [135] M. Alhijaj, P. Belton, S. Qi, An investigation into the use of polymer blends to improve the printability of and regulate drug release from pharmaceutical solid dispersions prepared via fused deposition modeling (FDM) 3D printing, *Eur. J. Pharm. Biopharm.* 108 (2016) 111–125. <https://doi.org/10.1016/j.ejpb.2016.08.016>.
- [136] J.R. Hughey, J.M. Keen, D.A. Miller, K. Kolter, N. Langley, J.W. McGinity, The use of inorganic salts to improve the dissolution characteristics of tablets containing Soluplus®-based solid dispersions, *Eur. J. Pharm. Sci.* 48 (2013) 758–766. <https://doi.org/10.1016/j.ejps.2013.01.004>.
- [137] J. Thiry, F. Krier, B. Evrard, A review of pharmaceutical extrusion: Critical process parameters and scaling-up, *Int. J. Pharm.* 479 (2015) 227–240. <https://doi.org/10.1016/j.ijpharm.2014.12.036>.
- [138] B.C. Pereira, A. Isreb, R.T. Forbes, F. Dores, R. Habashy, 'Temporary Plasticiser': A novel solution to fabricate 3D printed patient-centred cardiovascular 'Polypill' architectures, *Eur. J. Pharm. Biopharm.* 135 (2019) 94–103. <https://doi.org/10.1016/j.ejpb.2018.12.009>.
- [139] S. Palekar, P. Kumar, S.M. Mishra, T. Kipping, K. Patel, Application of 3D printing technology and quality by design approach for development of age-appropriate pediatric formulation of baclofen, *Int. J. Pharm.* 556 (2019) 106–116. <https://doi.org/10.1016/j.ijpharm.2018.11.062>.
- [140] T. Ehtezazi, M. Algellay, Y. Islam, M. Roberts, N.M. Dempster, S.D. Sarker, The Application of 3D Printing in the Formulation of Multilayered Fast Dissolving Oral Films The Application of 3D Printing in the Formulation of Multilayered Fast Dissolving Oral Films, *J. Pharm. Sci.* (2017). <https://doi.org/10.1016/j.xphs.2017.11.019>.
- [141] A. Melocchi, F. Parietti, A. Maroni, A. Foppoli, A. Gazzaniga, L. Zema, Hot-melt extruded filaments based on pharmaceutical grade polymers for 3D printing by fused deposition modeling, *Int. J. Pharm.* 509 (2016) 255–263. <https://doi.org/10.1016/j.ijpharm.2016.05.036>.
- [142] W. Jamróz, M. Kurek, Ł. Ewelina, J. Szafraniec, J. Knapik-kowalczyk, K. Syrek, M. Paluch, R. Jachowicz, 3D printed orodispersible films with Aripiprazole, 533 (2017) 413–420. <https://doi.org/10.1016/j.ijpharm.2017.05.052>.
- [143] G. Kollamaram, D.M. Croker, G.M. Walker, A. Goyanes, A.W. Basit, S. Gaisford, Low temperature fused deposition modeling (FDM) 3D printing of thermolabile drugs, *Int. J. Pharm.* 545 (2018) 144–152. <https://doi.org/10.1016/j.ijpharm.2018.04.055>.
- [144] T.C. Okwuosa, D. Stefaniak, B. Arafat, A. Isreb, K. Wan, A Lower Temperature FDM 3D Printing for the Manufacture of Patient-Specific Immediate Release Tablets, *Pharm. Res.* 33 (2016) 2704–2712. <https://doi.org/10.1007/s11095-016-1995-0>.
- [145] W. Kempin, V. Domsta, G. Grathoff, I. Brecht, B. Semmling, S. Tillmann, W. Weitschies, A. Seidlitz, Immediate Release 3D-Printed Tablets Produced Via Fused Deposition Modeling of a Thermo-Sensitive Drug, (2018).
- [146] J. Zhang, W. Yang, A.Q. Vo, X. Feng, X. Ye, D. Wuk, M.A. Repka, Hydroxypropyl methylcellulose-based controlled release dosage by melt extrusion and 3D printing: Structure and drug release

- correlation, *Carbohydr. Polym.* 177 (2017) 49–57. <https://doi.org/10.1016/j.carbpol.2017.08.058>.
- [147] A. Isreb, K. Baj, M. Wojsz, M. Isreb, M. Peak, M.A. Alhnan, 3D printed oral theophylline doses with innovative 'radiator-like' design: Impact of polyethylene oxide (PEO) molecular weight, *Int. J. Pharm.* 564 (2019) 98–105. <https://doi.org/10.1016/j.ijpharm.2019.04.017>.
- [148] M. Sadia, A. So, B. Arafat, A. Isreb, W. Ahmed, Adaptation of pharmaceutical excipients to FDM 3D printing for the fabrication of patient-tailored immediate release tablets, *Int. J. Pharm.* 513 (2016) 659–668. <https://doi.org/10.1016/j.ijpharm.2016.09.050>.
- [149] M. Novák, T. Boleslavská, A. Wan, J. Beránek, P. Kova, Virtual Prototyping and Parametric Design of 3D-Printed Tablets Based on the Solution of Inverse Problem, 19 (2018) 3414–3424. <https://doi.org/10.1208/s12249-018-1176-z>.
- [150] C. Korte, J. Quodbach, C. Korte, J. Quodbach, Formulation development and process analysis of drug-loaded filaments manufactured via hot-melt extrusion for 3D-printing of medicines manufactured via hot-melt extrusion for 3D-printing of medicines, *Pharm. Dev. Technol.* 23 (2018) 1117–1127. <https://doi.org/10.1080/10837450.2018.1433208>.
- [151] F.M. Vanin, P.J.A. Sobral, F.C. Menegalli, R.A. Carvalho, A.M.Q.B. Habitante, Effects of plasticizers and their concentrations on thermal and functional properties of gelatin-based films, *Food Hydrocoll.* 19 (2005) 899–907. <https://doi.org/10.1016/j.foodhyd.2004.12.003>.
- [152] K. Pietrzak, A. Isreb, M.A. Alhnan, A flexible-dose dispenser for immediate and extended release 3D printed tablets, *Eur. J. Pharm. Biopharm.* 96 (2015) 380–387. <https://doi.org/10.1016/j.ejpb.2015.07.027>.
- [153] M. Jährling, Application report No. AN53134\_E\_04/19K : Use of melt pump to produce filaments for additive manufacturing (3D printing), (2019).
- [154] T. Wesselink, L. Van Leeuwen, Fused Deposition Modeling Filament Production Apparatus. American Patent No. US20190168436A1., 2019.
- [155] P. Wang, B. Zou, H. Xiao, S. Ding, C. Huang, Effects of printing parameters of fused deposition modeling on mechanical properties , surface quality , and microstructure of PEEK, *J. Mater. Process. Tech.* 271 (2019) 62–74. <https://doi.org/10.1016/j.jmatprotec.2019.03.016>.
- [156] V. Zupancic, N. Ograjsek, B. Kotar-jordan, F. Vreced, Physical characterization of pantoprazole sodium hydrates, 291 (2005) 59–68. <https://doi.org/10.1016/j.ijpharm.2004.07.043>.
- [157] J. Aho, J.P. Bøtker, N. Genina, M. Edinger, L. Arnfast, Roadmap to 3D-Printed Oral Pharmaceutical Dosage Forms : Feedstock Filament Properties and Characterization for Fused Deposition Modeling, *J. Pharm. Sci.* 108 (2019) 26–35. <https://doi.org/10.1016/j.xphs.2018.11.012>.
- [158] X. Chai, H. Chai, X. Wang, J. Yang, J. Li, Y. Zhao, W. Cai, T. Tao, X. Xiang, Fused Deposition Modeling (FDM) 3D Printed Tablets for Intragastric Floating Delivery of Domperidone OPEN, *Sci. Rep.* 7 (2017). <https://doi.org/10.1038/s41598-017-03097-x>.
- [159] N.G. Solanki, M. Tahsin, A. V. Shah, A.T.M. Serajuddin, Formulation of 3D Printed Tablet for Rapid Drug Release by Fused Deposition Modeling: Screening Polymers for Drug Release, Drug-Polymer Miscibility and Printability, *J. Pharm. Sci.* 107 (2018) 390–401. <https://doi.org/10.1016/j.xphs.2017.10.021>.
- [160] A. Goyanes, P. Robles Martinez, A. Buanz, A.W. Basit, S. Gaisford, Effect of geometry on drug release from 3D printed tablets, *Int. J. Pharm.* 494 (2015) 657–663. <https://doi.org/10.1016/j.ijpharm.2015.04.069>.
- [161] A. Goyanes, P. Robles, A. Buanz, A.W. Basit, S. Gaisford, Effect of geometry on drug release from 3D printed tablets, *Int. J. Pharm.* 494 (2015) 657–663. <https://doi.org/10.1016/j.ijpharm.2015.04.069>.
- [162] M. Sadia, B. Arafat, W. Ahmed, R.T. Forbes, M.A. Alhnan, Channelled tablets: An innovative approach to accelerating drug release from 3D printed tablets, *J. Control. Release.* 269 (2018) 355–363. <https://doi.org/10.1016/j.jconrel.2017.11.022>.
- [163] B. Arafat, M. Wojsz, A. Isreb, R.T. Forbes, M. Isreb, Tablet fragmentation without a disintegrant : A novel design approach for accelerating disintegration and drug release from 3D printed cellulosic tablets, 118 (2018) 191–199. <https://doi.org/10.1016/j.ejps.2018.03.019>.
- [164] A. Isreb, K. Baj, M. Wojsz, M. Isreb, M. Peak, 3D printed oral theophylline doses with innovative ' radiator-like ' design : Impact of polyethylene oxide ( PEO ) molecular weight, *Int. J. Pharm.* 564 (2019) 98–105. <https://doi.org/10.1016/j.ijpharm.2019.04.017>.

- [165] L. Maggi, R. Bruni, U. Conte, High molecular weight polyethylene oxides ( PEOs ) as an alternative to HPMC in controlled release dosage forms, 195 (2000) 229–238.
- [166] A. Abdelbary, E.R. Bendas, A.A. Ramadan, D.A. Mostafa, Pharmaceutical and Pharmacokinetic Evaluation of a Novel Fast Dissolving Film Formulation of Flupentixol Dihydrochloride, 15 (2014). <https://doi.org/10.1208/s12249-014-0186-8>.





# OBJECTIVES

---



The main goals of this research thesis is to use different manufacturing/shaping techniques to develop an **oral solid dosage form** containing an **ASD** of cannabidiol (CBD) allowing its **immediate release**. Solid formulations were chosen for this work as there is only liquids CBD drugs on the market while patients are generally more compliant with solid medicines.

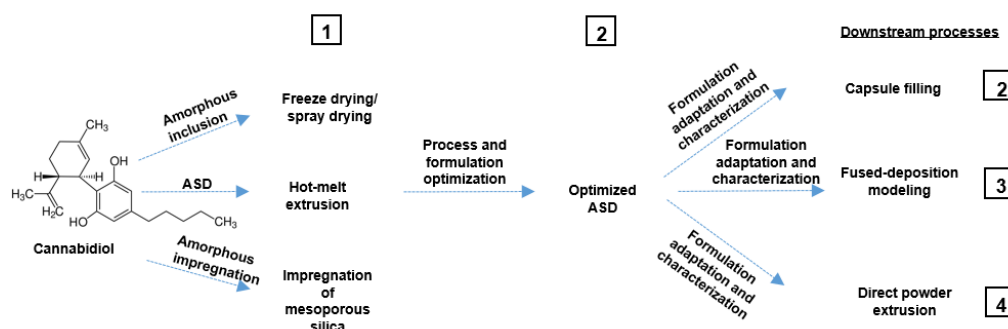


Figure 20 - Aims of the project.

According to these objectives, the project has been divided in four parts summarized on Fig.20:

1. The first part will involve the selection of the most suitable technique to produce of ASD of CBD with an increased aqueous solubility and dissolution rate. HME, solvent evaporation and mesoporous material impregnation will be compared in terms of processability, effectiveness in increasing CBD aqueous solubility, homogeneity and stability.
2. The second part will be the development and optimization of a HME process, the selected manufacturing method from part I, to produce of an ASD of CBD with the requirements described above. The composition, process parameters and stability in terms of amorphous state and drug content will be taken into account in this study.
3. The third part will be the development and optimization of a filament-based 3D printing FDM coupled with HME process to produce an ASD of CBD with the requirements described above. The polymeric carrier and extrusion parameters that allowed an immediate release of CBD in the previous part were chosen for this study. The composition will be adapted to be compatible with FDM 3D printing technique. Evaluation of the influence of the printed form geometry on

dissolution rate as well as process reproducibility and ability of the printer to manufacture printed forms with different doses will be taken into account in this project.

4. The last part of this work will be dedicated to a feasibility study of the use of a modified 3D printer to manufacture ASD of CBD with the requirements described above. The printing will be conducted directly from a powder mixture instead of a filament. Formulation composition will be adapted from the optimized one in part 3 to be compatible with the powder-based printer.

# RESULTS

---



## Chapter I. SELECTION OF A SUITABLE AMORPHOUS SOLID DISPERSION METHOD

### 1. Context and purpose of the study

CBD is a promising molecule to which many therapeutic properties are attributed [1]. However it has a very low aqueous solubility and a large hepatic first pass effect, giving it an oral bioavailability of about 6% [2].

Poorly soluble drugs are currently one of the most critical issue in the pharmaceutical industry. Indeed, it is estimated that 40% of marketed drug products are considered as poorly soluble, with an aqueous solubility of less than 100 µg/mL. This percentage is even higher for drugs in development, as it is estimated that 75-90% have a poor aqueous solubility [3]. These compounds mostly belong to the second and fourth class of the BCS described by Amidon *et al.* [4].

The conversion of these molecules in their amorphous form is one of the possible solutions to overcome the poor solubility problem. Indeed, the amorphous form has a higher intern energy compared to the crystalline form, resulting in enhanced thermodynamic properties such as solubility and dissolution. However, this high energy added to high molecular motion stands for a high chemical reactivity and a risk of spontaneous recrystallization [5]. This phenomenon can be prevented by forming a drug-carrier system with a negative Gibbs free energy in which the amorphous state of the drug is stabilized. Different methods can be used for the manufacture of such systems, such as solvent evaporation, impregnation of melting methods [6–8].

The purpose of this study is to use these three strategies for the production of formulations with stabilized amorphous CBD in order to select the one that allowed the highest increase of its aqueous solubility. The amorphous formulations were produced by spray-drying and FD (solvent evaporation methods), MS impregnation at ambient or subcritical-CO<sub>2</sub> conditions (impregnation method) and by HME (melting method). Each formulation was analyzed in terms of drug content and amorphous state and *in vitro* dissolution performance.

The results of this work are described in the article entitled: “Cannabidiol aqueous solubility enhancement: comparison of three amorphous formulations strategies” published in the International Journal of Pharmaceutics.



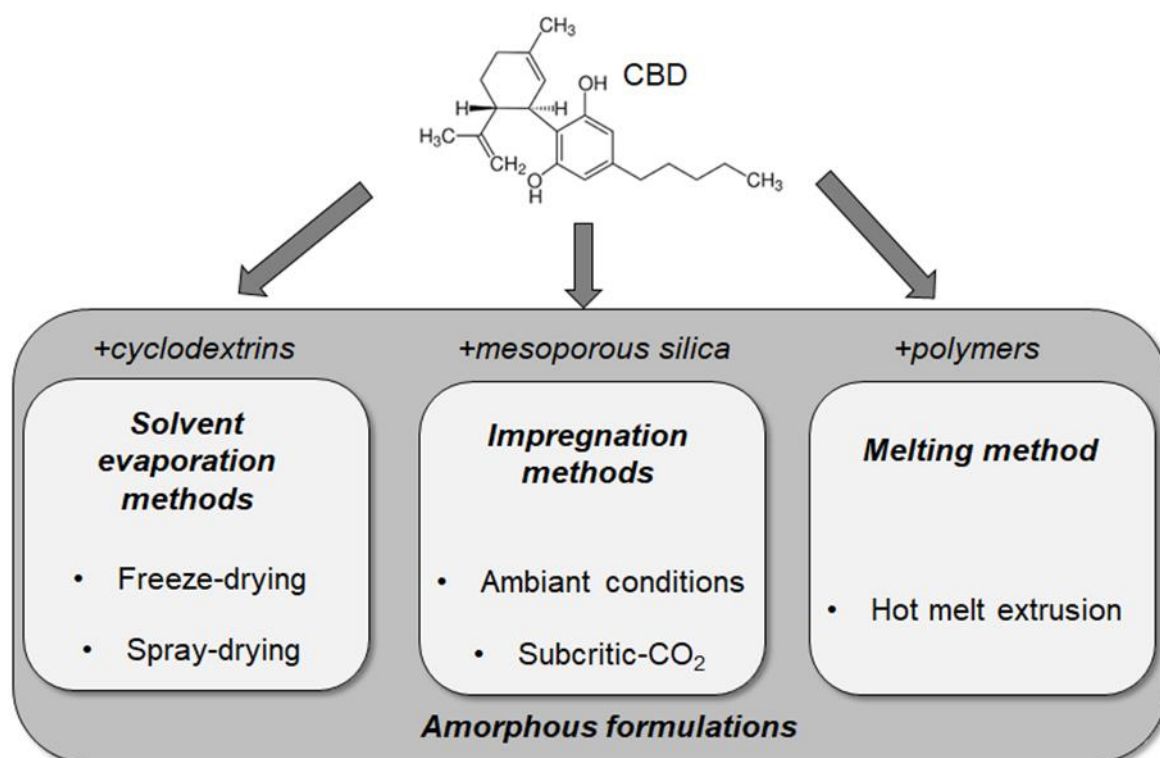
- [1] S. Pisanti, A.M. Malfitano, E. Ciaglia, A. Lamberti, R. Ranieri, G. Cuomo, M. Abate, G. Faggiana, M.C. Proto, D. Fiore, C. Laezza, M. Bifulco, Cannabidiol: State of the art and new challenges for therapeutic applications, *Pharmacol. Ther.* 175 (2017) 133–150. <https://doi.org/10.1016/j.pharmthera.2017.02.041>.
- [2] P.J. J. Mannila, T. Järvinen, K. Järvinen, Precipitation Complexation Method Produces Cannabidiol/b-Cyclodextrin Inclusion Complex Suitable for Sublingual Administration of Cannabidiol, *J. Pharm. Sci.* 101 (2007) 312–319. <https://doi.org/10.1002/jps>.
- [3] B. Dong, K. Hadinoto, Carboxymethyl cellulose is a superior polyanion to dextran sulfate in stabilizing and enhancing the solubility of amorphous drug-polyelectrolyte nanoparticle complex, *Int. J. Biol. Macromol.* 139 (2019) 500–508. <https://doi.org/10.1016/j.ijbiomac.2019.08.023>.
- [4] G.L. Amidon, H. Lennernäs, V.P. Shah, J.R. Crison, A Theoretical Basis for a Biopharmaceutic Drug Classification: The Correlation of in Vitro Drug Product Dissolution and in Vivo Bioavailability, *Pharm. Res. An Off. J. Am. Assoc. Pharm. Sci.* 12 (1995) 413–420. <https://doi.org/10.1023/A:1016212804288>.
- [5] G. Van Den Mooter, The use of amorphous solid dispersions: A formulation strategy to overcome poor solubility and dissolution rate, *Drug Discov. Today Technol.* 9 (2012) e79–e85. <https://doi.org/10.1016/j.ddtec.2011.10.002>.
- [6] D.M. J. Hong, C. Shah, Effect of Cyclodextrin Derivation and Amorphous State of Complex on Accelerated Degradation of Ziprasidone, *J. Pharm. Sci.* 100 (2011) 2703–2716. <https://doi.org/10.1002/jps>.
- [7] S. Chaudhari, A. Gupte, Mesoporous Silica as a Carrier for Amorphous Solid Dispersion, *Br. J. Pharm. Res.* 16 (2017) 1–19. <https://doi.org/10.9734/bjpr/2017/33553>.
- [8] R. Laitinen, K. Loßmann, C.J. Strachan, H. Grohgan, T. Rades, Emerging trends in the stabilization of amorphous drugs, *Int. J. Pharm.* 453 (2013) 65–79. <https://doi.org/10.1016/j.ijpharm.2012.04.066>.

## 2. Publication

### ***“Cannabidiol aqueous solubility enhancement: comparison of three amorphous formulations strategies using different type of polymers”***

**Nathan Koch, Olivier Jennotte**, Youri Gasparrini, Fanny Vandenbroucke, Anna Lechanteur, Brigitte Evrard

**University of Liège**, Laboratory of Pharmaceutical Technology and Biopharmacy, Center for Interdisciplinary Research on Medicines, Avenue Hippocrate B36 (+2) 4000 Liège



Int. J. Pharm. 589 (2020) 119812

<https://doi.org/10.1016/j.ijpharm.2020.119812>

## 2.1 Abstract

Poor aqueous solubility of terpenophenolic compound CBD is a major issue in the widespread use of this promising therapeutic polyphenol. Moreover, choosing the appropriate strategy to overcome this challenge is time-consuming and based on trial-error processes. The amorphous form of CBD provided higher aqueous solubility as well as faster dissolution rate in comparison with crystalline CBD. Nevertheless, amorphous forms of CBD tend to recrystallize. The aim of this study was to use three different strategies based on the stabilization of the amorphous form. CDs ( $\text{CH}_3\alpha\text{CD}$ ,  $\text{HP}\beta\text{CD}$  and hydroxypropyl- $\gamma$ -cyclodextrin ( $\text{HP}\gamma\text{CD}$ )), MS (Silsol® (MS-Silsol) and Syloid® AL-1FP (MS-ALFP)) and water soluble polymers (KVA64, K12PF and SOL) were processed by using the following techniques: FD, spray-drying, subcritical carbon dioxide impregnation or HME. All the obtained formulations provided complete amorphous CBD, although the drug loading depend highly of the excipients. CD-CBD formulations, processed by FD or spray-drying, and CBD-MS formulations, processed by subcritical  $\text{CO}_2$  or by atmospheric impregnation, provided significant increase of aqueous solubility. While the use of K12PF did not provided significant increased solubility within 90 min, KVA64 has been highlighted as the excipient that exhibits the highest increase of aqueous solubility of this study. Finally, all formulations, excepted CBD-ALFP formulations, showed adequate stability within at least two months.

**Keywords:** *Cannabidiol; amorphous dispersion; spray-drying; freeze-drying; hot melt extrusion; impregnation*

## 2.2 Introduction

CBD is a non-psychoactive terpenophenolic compound extracted from *Cannabis sativa* with promising pharmacological activities such as anti-seizures, anxiolytic, antipsychotic, anti-inflammatory or antioxidant properties [1–3]. A first CBD-based medicine, Epidiolex®, has been recently approved by FDA and this lipid solution is used to treat orphan forms of epilepsy [4]. Unlike the more popular cannabinoid compound  $\Delta^9$ -tetrahydrocannabinol (THC), CBD shows no activity on  $\text{CBD}_1$  receptors that explained the non-psychoactivity of this compound and is consequently potentially more benefit for the medical field [5]. However, CBD has bioavailability estimated at 6% explained by its low water solubility, measured at 0.1  $\mu\text{g/mL}$  (Mannila et al., 2007; McArdle, 2004)]. The development of aqueous solubility-enhanced formulations may lead to higher CBD absorption and to a widespread use of this promising molecule. To do so, several strategies are described in the literature and the choice of the optimum one depends on several physicochemical factors such as lipophily, crystallinity, pKa or stability of active molecules [8]. Actually, there is no well-defined decision tree that may help the formulator to select the appropriate strategy based on the poor aqueous solubility of API. Therefore, processes based on trial-and-errors approach have to be investigated which is time-consuming for the formulator [9]. Moreover, the choice of the aqueous solubility enhancement strategy will define the production technique consequently impacting the scale-up capacities of the selected method.

Among the different strategies, the use of the amorphous form of a drug is useful to increase the kinetic aqueous solubility of an API [10]. Nevertheless, this thermodynamically non-stable state is subject to recrystallization. The use of matrices such as polymer or inorganic porous particles could stabilize the amorphous forms [11]. The use of polymers to stabilize the amorphous form of an API has been widely studied in order to obtain what is called ASD [12]. ASD could be defined as a mixture of one or more polymers and an amorphous drug finely and homogeneously dispersed in the polymeric matrix [13]. One of the major techniques used to produce ASD is HME. This technique is based on the introduction of a powder blend composed of a drug and one or more polymers in an oven containing one or two rotating screws set at desired temperature. The blend is then vigorously mixed in a liquid state and finally extruded in order to provide homogeneous glassy extrudates [14].

Another example of amorphous drug mobilization inhibition is the use of mesoporous carriers. More precisely, MS is more and more used to stabilize amorphous state of API [15]. MS are inorganic particles composed of mesoporous network with pore size varying from 2 nm to 50 nm. Such material take advantage of having uniform pore size, high surface area, large pore volume, good biocompatibility and easy surface

functionalization [16,17]. By using the appropriate pore size, entrapped API within the mesopores are immobilized by confinement and/or by silanol-drug interaction [18]. Many methods of impregnation are described in the literature, such as supercritical carbon dioxide or organic solvent [19,20]. Recently, the use of subcritical carbon dioxide has been successfully used to impregnate MS without the requirement of organic solvents and without the requirement of preliminary drug solubilization step [21].

Besides, the amorphous stabilization of an API can be coupled with an increase of the affinity between a drug and a solvent by using CDs [22]. CD are cyclic oligosaccharides composed of 6 ( $\alpha$ ), 7 ( $\beta$ ) or 8 ( $\gamma$ ) D-glucopyranose unit, linked by  $\alpha$ -(1,4) bonds and can be easily tunable by for example methylation or hydroxylation to provide specific physico-chemical properties [23]. Those materials showed a torus shaped in which external surface is hydrophilic while the internal surface is hydrophobic. The hydrophobic part of a molecule is entrapped inside the CD torus shaped and hidden from the aqueous phase [24]. CD-drug complexes are formulated following different processes such as physical mixture, liquid complexation, or more complex techniques such as spray-drying or FD [25].

This article aims to improve the aqueous solubility as well as the dissolution rate of CBD while comparing three different strategies, namely the use of CDs, the use of ASDs and the use of impregnated MS, in order to select the most appropriate strategy taking into account different parameters such as drug loading, increase of aqueous solubility, final stability but also ease of translating these data for large-scale drug production according to the selected strategy.

## 2.3 Materials and methods

### 2.3.1 Materials

CBD was obtained from THC PHARM GmbH (Frankfurt, Germany). CH $\beta$ CD (Rameb<sup>®</sup>, substitution degree of 1.8; Mw 1324.43 g/mol), the HP $\beta$ CD (Kleptose<sup>®</sup>, substitution degree of 0.63; Mw 1395.30 g/mol) and the HP $\gamma$ CD (substitution degree of 0.6; Mw 1575.98 g/mol) were purchased from Sigma-Aldrich (Saint-Louis, USA), Roquette (Lestrem, France) and Ashland Industries Europe GmbH (Schaffhausen, Switzerland), respectively. MS-Silsol (estimated pore sizes: 6.6 nm) and MS-ALFP (estimated pore sizes: 2.5 nm) were kindly provided by W.R. Grace (Worms, Germany). K12PF, KVA64 and SOL were kindly donated by BASF (Ludwigshafen, Germany). All other materials used within the study were of analytical grade.

## 2.3.2 Methods

### 2.3.2.1 Solvent evaporation methods

#### 2.3.2.1.1 Preparation of cyclodextrins-cannabidiol (CD-CBD) inclusion complexes

Different CDs were chosen as the CH $\beta$ CD, the HP $\beta$ CD and the HP $\gamma$ CD. Stock solutions of 200 mM were prepared in milliQ water and diluted to obtain intermediate concentrations. An excess of CBD powder was introduced in 5 mL of each CD solutions. The suspension was then stirred for 24 h in a rotatory water bath at 37°C. Each solution was then filtered on PTFE filter of 0.45  $\mu$ m (Filtre Millex-LCR, Merck-Millipore, Overijse, Belgium) and diluted before high-performance liquid chromatography (HPLC) analysis (see section 2.5).

For comparison, physical mixture of CBD and CH $\beta$ CD was also prepared (CD-CBD PM). For this purpose, an amount of CH $\beta$ CD equal to 200 mM was mixed with CBD powder using a mortar and a pestle.

#### 2.3.2.1.2 Production of powder from CD-CBD complexes

##### 2.3.2.1.2.1 Freeze-drying process

A CBD solution obtained by complexation with of CH $\beta$ CD (at a concentration of 200 mM) was produced using the same method as previously (section 2.2.1). After filtration, the solutions (50 mL) were placed in an open glass container and FD (Epsilon 2-4 LSCplus, Martin Christ Gefriertrocknungsanlagen GmbH, Osterode am Harz, Germany) in order to obtain a powder. In a first step, the samples were frozen from room temperature to -45 °C (pressure of 1000 mbar) over a period of 3 h and 30 min. Primary drying was performed at -45 °C for 10 min (at 0.8 bar pressure) followed by 3 h at -15 °C (at 0.1 bar pressure) and by 12 h at -10 °C (at 0.1 bar pressure). Secondary drying was carried out at 10 °C for 5 h (under 0.1 bar pressure). The complete FD cycle took 23 h and 40 min. The lyophilized powders were weighed in order to evaluate the process yield. In addition, the homogeneity and the CBD content in powders were evaluated. Three individual samples were taken from CD-CBD powders, diluted adequately and analyzed by HPLC (see section 2.5).

##### 2.3.2.1.2.2 Spray-drying process

A CBD solution obtained by complexation with of CH $\beta$ CD (at a concentration of 200 mM) was produced using the same method as explained previously (section 2.2.1). After filtration, the solutions were spray-dried (SD) using the spray-dryer ProCept 4M8-TriX Formatrix (ProCept, Zelzate, Belgium). The CD-CBD solution (50 mL) were driven to the bi-fluid nozzle (1.2 mm) at a speed of 32 rpm (1 g/min) with a nozzle gas pressure

of 1.5 bar. The inlet gas flow was set up at 0.35 m<sup>3</sup>/min with an inlet temperature of 100 °C and a cyclone gas pressure of 0.23 bar (100 L/min). The outlet temperature during the process was of 59.85 ± 1.5 °C, considering all replicates. Once the process was completed, the spray-dried powders were weighed in order to evaluate the process yield. Moreover, the homogeneity and the CBD content in powders were evaluated. Three individual samples were taken from CD-CBD powders, diluted adequately and analyzed by HPLC (see section 2.5).

### 2.3.2.2 Impregnation methods

#### 2.3.2.2.1 Production of mesoporous silica-cannabidiol impregnation formulations

Physical mixtures (PM) were produced by mixing CBD with MS-Silsol or MS-ALFP in fixed proportions by using a mortar and a pestle. One gram of physical mixture was then treated by two different conditions: ambient pressure or subcritical carbon dioxide pressure. To establish the maximum amorphous CBD stabilization capacities of each MS, physical mixtures with decreased percentage of CBD were prepared and treated by using subcritical carbon dioxide pressure until reaching the drug loading that does not provide any endothermic peak (see section 2.4).

##### 2.3.2.2.1.1 Ambient pressure (atm)

One gram of physical mixture was placed in a porcelain cup and left in a heated-controlled oven set at 67 °C, for one hour. The obtained formulations were then cooled at ambient temperature.

##### 2.3.2.2.2 Subcritical carbon dioxide pressure (sub)

One gram of physical mixture was placed in a 20 mL high pressure cell (TOP Industries, France) heated to 50 °C and finally pressurized with a high-pressure pump (SEPAREX, France) to 60 bar for one hour. After this contact time, it was manually depressurized.

The obtained formulations were named as follows: Silsol atm and Silsol sub for the formulations produced by using the MS Silsol, respectively by using the ambient pressure method and the subcritical carbon dioxide pressure method; ALFP atm and ALFP sub for the formulations produced by using the MS-ALFP, respectively by using the ambient pressure method and the subcritical carbon dioxide pressure method.

### 2.3.2.3 Melting method

HME was used to produce ASD composed of CBD (5% m/m) and different polymers. Three polymers were tested: a vinylpyrrolidone-vinyl acetate copolymer, KVA64, a copolymeric solubilizer, SOL and a PVP polymer, K12PF. The binary mixtures of CBD and each polymer were prepared using a mortar and pestle. A co-rotating 11 mm twin screw hot-melt extruder with a screw configuration containing two kneading zones was used (L/D = 40, ThermoFisher Scientific, Karlsruhe, Germany). The extrusion parameters are summarized in [Table 3](#).

*Table 3 – Extrusion parameters*

L/D	40
T° of the different heating zones	50-170-170-170-170-170-170 °C
Screw speed	50 rpm

The obtained extrudates were milled using a crusher (Fredrive-Lab equipped with a Hammerwitt head, Frewitt, Switzerland), the size of the grid was 0.2 mm and the speed was set at speed of 6500 rpm.

The three obtained formulations were named as follows: ASD<sub>1</sub> for the mixture of CBD-KVA64, ASD<sub>2</sub> for CBD-SOL and ASD<sub>3</sub> for CBD-K12PF.

### 2.3.3 Solubility measurements

The solubility of CBD in the phosphate buffer pH 6.8 + 0.5% SLS was assessed via the shake-flask method, which consisted in dispersing an excess amount of CBD in 10 mL of medium and shaking it for 24 h at 37 °C in shaking bath. The obtained samples were filtered and analyzed via HPLC. These solubility measurements were carried out in triplicate, in order to determine the saturation concentration of CBD in the buffer to be used for the dissolution tests.

### 2.3.4 Differential Scanning Calorimetry

DSC was used to evaluate the physical state of CBD within the formulations after production. 5 to 10 mg of powder were accurately weighted, crimped in an aluminum pan and then subjected to one heating ramp at a rate of 20 °C/min ranging from 25 °C to 100 °C. Moreover, a heating rate of 20 °C/min was the optimum one for detecting crystallinity in our formulations. The equipment used for this study was a Mettler-Toledo® DSC 1 (Schwerzenbach, Swiss) controlled by the STARe System software.



### 2.3.5 High-Performance Liquid Chromatography

The quantification of the CBD contained in the different formulations and released in the aqueous media during the dissolution tests was assessed by a validated HPLC method ([Appendix I](#)). The HPLC equipment consisted of an Agilent® 1100 (Santa Clara, USA) with OpenLab CDS LC ChemStation version C.01.05 as the software. A Zorbax® C18 300 SB analytical column with particles of 3,5µm (150 mm × 4.6 mm ID) was used with a mobile phase composed of a mixture of water and acetonitrile (38/62 %v/v). The flow rate was set at 1.0 mL/min and the column temperature was kept constant at 30 °C. 20µL of the samples were injected at room temperature, the chromatographic run time was set to 10 min and the detection wavelength was 240 nm. This present method was successfully validated using the accuracy profile approach and Enoval® software V3.0 (Arlenda, Liège, Belgium). The risk  $\alpha$  was set at 5% with acceptance limits at 10%.

### 2.3.6 Homogeneity and Process Recovery

The homogeneity of each formulation has been performed by analyzing three powder samplings per each batch. Briefly, each sample has been suspended or dissolved in a fixed volume of acetonitrile and sonicated. The obtained solutions and the filtered suspensions were then analyzed by the validated HPLC method (see section 2.5).

Following each powder method production, the homogeneity of the powder was evaluated and the CBD recovery quantified by using [Eq. 5](#):

$$\text{Recovery (\%)} = \frac{\% \text{ CBD after treatment}}{\% \text{ CBD before treatment}} \times 100 \quad \text{Eq. 5}$$

### 2.3.7 In Vitro Dissolution Testing

The *in vitro* dissolution system consisted of a USP II apparatus (Sotax®, Thun, Switzerland) at a temperature of 37 °C and at a stirring rate of 100 rpm. Dissolution media (500 ml) was composed of phosphate buffer (pH 6.8) supplemented with 0.5% sodium lauryl sulfate. 2 mL of medium was sampled and replaced with fresh media at intervals of 5 min, 15 min, 30 min, 45 min, 60 min, 75 min and 90 min. An equivalent of 81.50 mg of CBD was used for all MS formulations as well as all ASD formulations. Considering CD-CBD formulations produced by FD and SD, an equivalent of 64.25 mg of CBD was used due to practical concerns in order to use maximum two capsules (000). After the dissolution testing, all samples were filtered with a PTFE filter (0.45 µm) and diluted adequately to avoid any CBD recrystallization with the dissolution medium before being analyzed by HPLC. The tests were run in triplicate and the results obtained are the mean and standard deviations of three determinations.

### *2.3.8 Stability measurement*

Stability of each formulation was evaluated by analyzing samples two months after production in terms of crystallinity by DSC (see section 2.4) and drug quantification (see section 2.5).

## *2.4 Results*

### *2.4.1 Experimental strategy*

CBD have been treated through five well-known techniques in order to develop amorphous formulations allowing the enhancement of oral availability of the drug. As summarized on [Figure 21](#), two solvent evaporation methods, two impregnation methods and one melting method have been compared. Moreover, different classical excipients for respective techniques were used to stabilize the amorphous form.

CDs were used to solubilize the maximum amount of CBD prior to solvent evaporation processes. Both FD and SD methods are common for promoting amorphous formulations and CD will help to stabilize the CBD amorphous form [26]. Then, impregnation of CBD within MS was also tested under basic ambient conditions or using CO<sub>2</sub>-subcritical fluids (Subcritic-CO<sub>2</sub>) as previously used in our laboratory [21]. Finally, thermoplastic polymers were selected in order to stabilize the amorphous form of CBD following its melting by HME [27]. Through this experimental strategy, a wide variety of amorphization methods and of excipients will be tested and compared. This will highlight the different process options available for the development of an oral CBD form having an appropriate bioavailability.

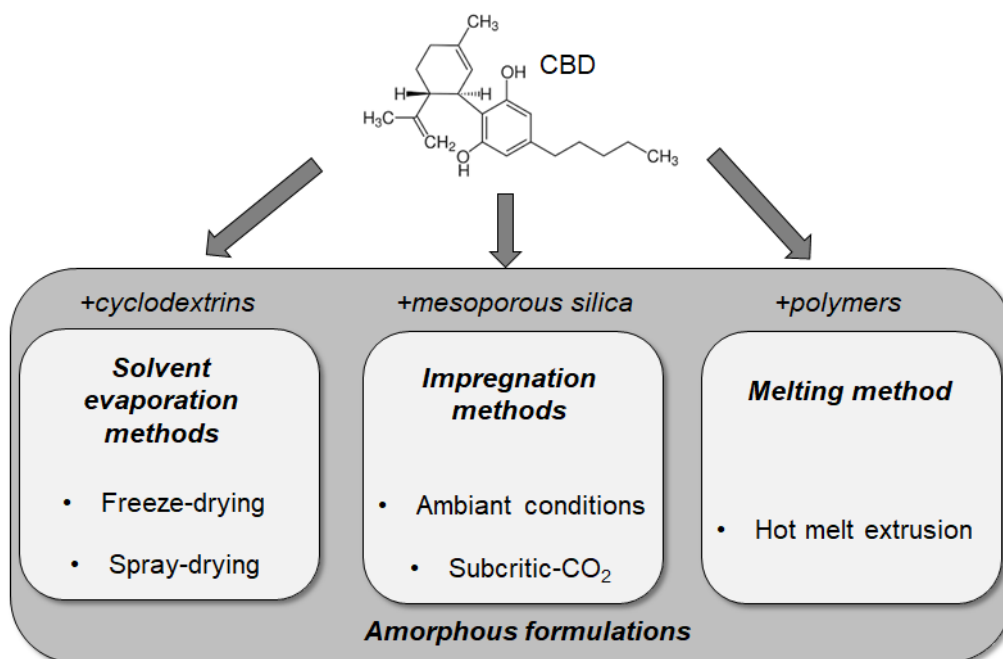


Figure 21: Experimental strategy. CBD have been treated using five techniques in order to develop amorphous formulations. Two solvent evaporation methods, two impregnation methods and one melting method were compared. Different excipients were used to stabilize the amorphous form as CDs, MS and thermoplastic polymers.

#### 2.4.2 Evaluation of amorphous CBD-drug loading with different excipients following different treatments

First, CD-CBD inclusion complexes were studied. Complexation of poorly water-soluble drug with CDs is one of the most common strategies to enhance drug solubility [28]. Moreover, CD have also been used to stabilize the amorphous form of a hydrophobic API [22,26]. The first step was to evaluate the effect of the type of CD on the property of CBD drug. Then, two downstream processes (FD and SD) were used to convert solutions to solid forms and CD should be able to stabilize the amorphous form of CBD over a long period of time.

Three different substituted CDs (CH3 $\beta$ CD, the HP $\beta$ CD and the HP $\gamma$ CD) were selected based on literature. Indeed, Manila et al. have tested the interest of CH3 $\beta$ CD and HP $\beta$ CD on increasing CBD aqueous solubility and showed a high potential for CH3 $\beta$ CD [6,29]. Moreover, some authors have performed systematic complex characterization of CBD with the three natives CD;  $\alpha$ CD,  $\beta$ CD and  $\gamma$ CD [30]. They have revealed that the highest increase of CBD solubility was obtained with the  $\gamma$ CD (5.3 mg/ml), probably due to its volume cavity.

Using the approach of Higuchi and Connors, phase-solubility studies were performed at increasing concentrations of the three CD. **Figure 22** shows that the solubility of CBD increased linearly with the concentrations of HP $\beta$ CD and HP $\gamma$ CD which corresponds to the AL type profile (formation of 1:1 inclusion complexes). On the contrary, the phase-solubility profile of CBD with CH3 $\beta$ CD was an Ap-type which corresponds to the formation of 1:1 inclusion complex. With CH3 $\beta$ CD concentration up to 150 mM, it seems that inclusion complex followed a higher stoichiometry. This observation was in line with studies of Manilla [6]. At concentration of 200 mM of HP $\gamma$ CD, HP $\beta$ CD and CH3 $\beta$ CD, the solubilized CBD concentration were of 0.9, 4.9 and 25.5 mg/ml, respectively. The solubility of pure CBD is 0.0627  $\mu$ g/ml in milliQ water while at 200 mM of HP $\gamma$ CD, HP $\beta$ CD and CH3 $\beta$ CD, it increased by 14354, 78,149 and 406699 – fold, respectively. Obviously, CH3 $\beta$ CD have been selected for the production of ASD of CBD through FD and SD processes.

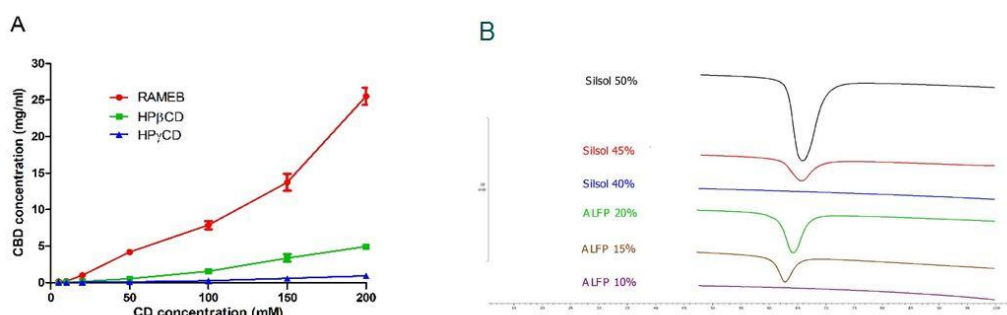


**Figure 22.** (A) The phase-solubility diagrams of CBD in aqueous solution of CH3 $\beta$ CD (RAMEB), HP $\beta$ CD and HP $\gamma$ CD obtained after 24 hours at 37 °C. (B) CBD crystallinity of CBD-MS formulations treated by subcritical carbon dioxide (50 °C and 60 bar). Considering respectively the use of MS-Silsol and MS-ALFP, crystallinity was detected with 50% and 45% of CBD, and 20% and 15% of CBD.

With regards to the use of MS, the first step was also to determine the highest loading capacity of amorphous CBD. For MS-Silsol with a pore size of 6.6 nm, formulations produced using subcritical conditions (50 °C and 60 bar) containing 50% and 45% of CBD showed crystallinity. The 40% formulations did not show endothermic peaks reflecting total stabilization of amorphous CBD within the mesopores. Considering the use of MS-ALFP with pore size of 2.5 nm, formulations containing 20% and 15% of CBD showed crystallinity while no endothermic peaks could be observed with formulations containing 10% of CBD (**Fig. 22.B**). Those results were also observed using room pressure impregnation method.

The maximal loading of amorphous CBD in polymeric matrix using HME has not been studied. Indeed, one disadvantage of this technique is the minimum amount of powder that must be used per batch production. Given that 30 g of physical mixture (PM) were used for each production and due to the cost of the CBD and the difficulty of supply for regulatory reasons, the amount of powder used in the physical mixture was set at 5%. This parameter could be optimized in further study.

The amorphization of CBD was proven on each powders as it is a key property of our study. The three different drug amorphization strategies were compared to raw CBD (**Fig. 23**). DSC analysis was done directly after the production and after two months of storage (section 3.8).

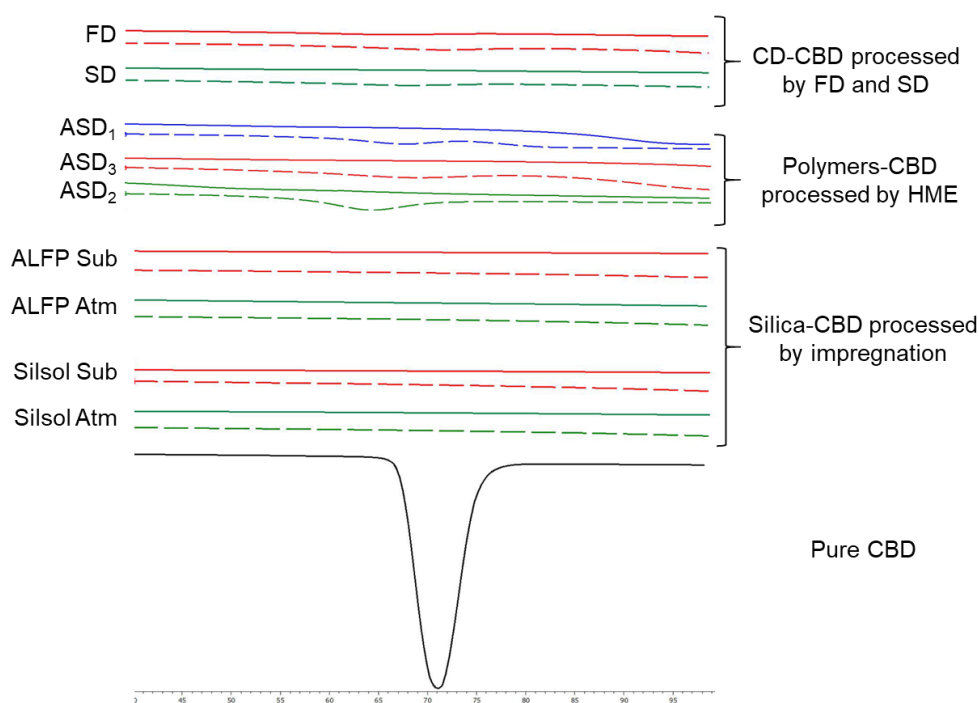


*Figure 23. The amorphization of CBD evaluated by DSC directly after production (straight line) or 2 months later (dotted line). Powders of CD-CBD complexes were produced by FD (FD-red) and spray-drying (SD-green). Powders of polymers-CBD were produced by HME (ASD<sub>1</sub>-blue, ASD<sub>2</sub>-green and ASD<sub>3</sub>-red). Powders of silica-CBD were produced by impregnation methods under ambient conditions (Atm-green) and by the use of CO<sub>2</sub>-subcritical fluids (Sub-red). Two MS were used as Silsol and ALFP.*

In summary, all formulations tested in this study were built with a percentage of CBD that provides 100% of amorphous drug. In the CBD-CD formulations, 8.3% of CBD were loaded, 40% of CBD in the CBD-Silsol formulations and 10% of CBD in the CBD-ALFP formulations were loaded and 5% of CBD in the CBD-polymer formulations.

### 2.4.3 Comparison of processes drug recovery and CBD homogeneity into powders

Following each powder method production, the homogeneity of the powder was evaluated and the CBD recovery quantified by using the following relation:

$$\text{Recovery (\%)} = \frac{\% \text{ of CBD after treatment}}{\% \text{ of CBD before treatment}} \times 100$$

**Figure 24** shows the drug recovery obtained from three individual samplings of each powder produced. For the MS, the use of pressurized carbon dioxide allowed homogeneity and a process recovery within the limits we have set at 90% - 110% with both MS-Silsol and MS-ALFP. A difference was found when using the ambient pressure impregnation method where the use of MS-ALFP provided formulations with acceptable homogeneity but process recovery outside the fixed limits. This could be explained by the moisture in the uncontrolled oven during the impregnation process. In fact, the MS-ALFP is traditionally used as moisture adsorption excipient. The impregnation step can adsorb water and prevents the CBD from fully penetrating the pores. Besides, the use of MS-Silsol at atmospheric pressure results in formulations with homogeneity and process recovery values within the limits.

As shown in **Figure 24**, HME was able to achieve ASD with appropriate CBD homogeneity and recovery. Indeed, the extrusion parameters during the process provided an optimal mixing of CBD within the polymer without any drug degradation.

For CD formulations, we observed a recovery of CBD after the FD process greater than 100% which can be explained by this static method. These assays remain within our acceptance limits. On the contrary, a recovery of 78% was obtained for the powders produced by SD process. This can be explained by the inlet temperature in the drying chamber set at 100°C while the melting temperature of CBD is about 70 °C (see **Fig. 23** – pure CBD). This temperature was used in order to obtain an acceptable process yield in terms of the amount of powder collected at the end. Indeed, if the temperature is not high enough, a sticky powder is produced which significantly impacts performance of the process [25].

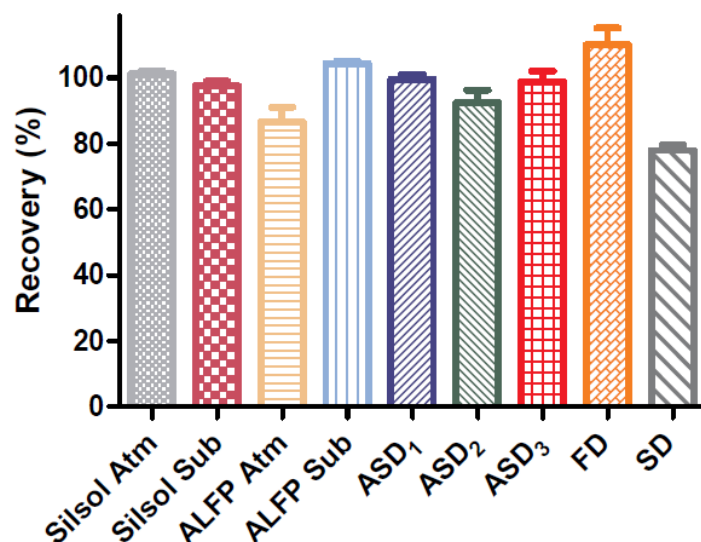


Figure 24. Evaluation of process recovery and homogeneity of CBD within powders produced by different methods with distinct excipients. Silsol Atm, Silsol Sub, ALFP Atm and ALFP Sub correspond to powder of MS either Silsol or ALFP and CBD produced by impregnation under ambient conditions and using Subcritical CO<sub>2</sub>, respectively. ASD<sub>1</sub>, ASD<sub>2</sub> and ASD<sub>3</sub> correspond to milled extrudates of CBD and KVA64, SOL or K12PF, respectively, produced by HME. FD and SD correspond to powder of RAMEB and CBD produced by FD and spray-drying (SD), respectively.

#### 2.4.4 In Vitro Dissolution Tests

As the drug amorphization was demonstrated for each production method and associated excipients, we evaluated the impact of these amorphous formulations by conducting dissolutions tests. **Figure 25** shows dissolution kinetics of powders containing CBD and produced by different methods with specific excipients.

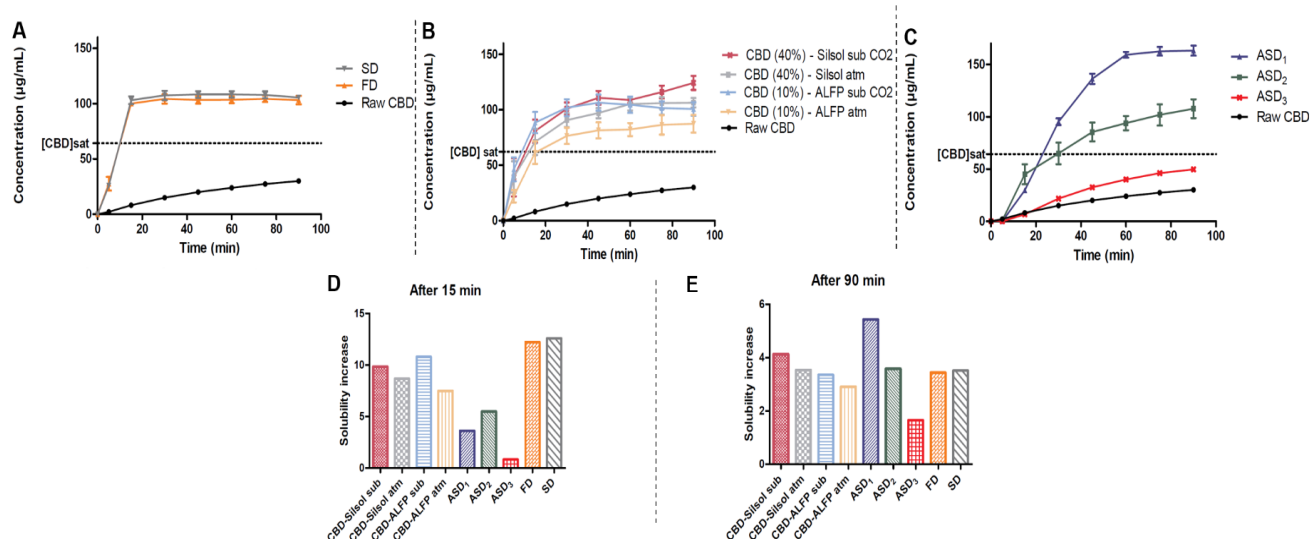


Figure 25. Release of CBD in the dissolution media from different powders containing amorphous CBD. (A) FD and SD correspond respectively, to powder of RAMEB and CBD produced by FD (FD-orange) and spray-drying (SD-grey). (B) Silsol atm, Silsol sub, ALFP atm and ALFP sub correspond to powder of MS either Silsol or ALFP and CBD produced by impregnation at ambient conditions (atm) and using Subcritical CO<sub>2</sub> (sub), respectively. (C) ASD<sub>1</sub>, ASD<sub>2</sub> and ASD<sub>3</sub> correspond to milled extrudates of CBD and KVA64, SOL or K12PF, respectively, produced by HME. (D) Comparison of CBD solubility after 15 min and after 90 min (E) of dissolution test in function of formulations.

Each formulation, excepted for ASD<sub>3</sub>, allowed a significant increase of the dissolution rate as well as an increase of the kinetic CBD solubility which was measured at  $64.24 \pm 6.76 \mu\text{g/mL}$  in the phosphate buffer pH 6.8 + 0.5% SLS medium.

We noticed that the three types of strategies allowed different dissolution profiles although all formulations provided amorphous CBD. Indeed, the dissolution rate of the formulations produced with polymers was slower than the formulations containing CDs or MS. This could be explained by the hydration that can occur when polymers come into contact with water. The resulting hydrogel layer regulates the penetration of the medium into the drug-complex polymer. The drug release occurs by diffusion, erosion or both [31–33]. Moreover, it is obvious that the dissolution is dependent on the nature of the excipient. K12PF is a pure polyvinylpyrrolidone-based polymer traditionally used as solubilizers and crystallization inhibitors in injectable formulations [34]. The solubilizing property of PVP is the formation of water-soluble complexes with numerous API [35]. The formulation produced with K12PF was the one that does not provide a significant increase of dissolution rate of the CBD. Our hypothesis is that such water



complexes couldn't be produced because of the inappropriate structure of the CBD. Further specific investigations have to be conducted.

KVA64 is a polyvinylpyrrolidone-based polymer coupled with poly(vinyl acetate) entities and ASD formed with it provided the highest aqueous solubility [34]. KVA64 provided aqueous solubility 3-folds higher than K12PF after 90 min. This could be attributed to the amphiphilic structure of KVA64. Indeed, in addition to the hydrophilic PVP group, KVA64 is composed of a lipophilic group, the vinyl acetate. This lipophilic part interacts with the CBD while the hydrophilic part allows the complex to stay water-soluble.

SOL is polyethylene glycol grafted with a copolymer of poly(vinyl caprolactone) and poly(vinyl acetate) [36]. This polymer also has an amphiphilic structure so one would have expected it to act like KVA64. However, [Figure 25.C](#) shows that KVA64 better enhances the aqueous solubility. This difference could be due to the strong gelling effect of the SOL<sup>®</sup> described by Hughey [37].

Considering the use of MS, trends showed that the use of MS-Silsol provided faster dissolution rate and higher aqueous solubility than the use of MS-ALFP. This is explained by the lower pore size of MS-ALFP. Indeed, the smaller pore size made it more difficult for water to penetrate into the mesostructure and delayed the release of CBD with ultimately a lower CBD concentration. However, it should be noted that the two production methods (sub CO<sub>2</sub> or atm) provided none statistically different formulations.

Considering the use of CDs, a maximum concentration of dissolved CBD approximately of 100 µg/mL was obtained after 15 minutes and maintained during at least two hours. The production process, whether FD or SD, has no influence in terms of dissolution profiles. In order to prove that the amorphization of CBD occurred during evaporation processes, we performed the same experiments with physical mixture of RAMEB and CBD. First of all, thermal analysis did not show an endothermic peak which was logical since DSC assay is also used to prove the complexation of an API with CD [38]. Therefore, after 90 min of dissolution testing with the physical mixture of RAMEB and CBD, 47.23 µg/ml of CBD were dissolved compared to 24.85 µg/ml, 105.59 µg/ml and 103.30 µg/ml for pure CBD, SD and FD formulations, respectively. This demonstrates the interest of using solvent evaporation methods to induce the amorphization of the drug whereas a simple blend does not allow this behavior.

To summarize, all formulation found their advantage in the stabilizing of the amorphous form of CBD which is more soluble than its crystalline form. It was also noted that KVA64 provided the highest solubility enhancement action. The solubility increasing fold after

15 min shows that the use of polymers provided delayed CBD release ([Figure 25-D](#)) but this delay was counterbalanced by the highest fold increase for the KVA64 after 90 minutes ([Figure 25-E](#)). The use of sodium lauryl sulfate (SLS) increases the aqueous solubility of CBD and was used to detect pure CBD in solution by analytical techniques. Nevertheless, because all formulations were solubilized in the same medium, SLS do not interfere with the increasing solubility comparison.

It is important to note that CBD is highly degraded in acidic conditions (data not shown). Further formulations should include for example enteric coating to provide maximum of stability.

#### *2.4.5 Stability of the CBD over Time*

We showed by DSC analysis that after at least 2 months of storage, the CBD was still in its amorphous form ([Fig. 23](#)). In addition, we quantified the drug two months after its production for each powder. [Figure 26](#) shows that except MS-ALFP formulations, all formulations produced in this study showed adequate stability for at least two months (see [Fig. 24](#) for comparison).

The use of MS-ALFP resulted in a very poor stability of CBD over time. This was explained by the adsorption of water up to 11% of water content in some MS-ALFP formulations (data not shown).

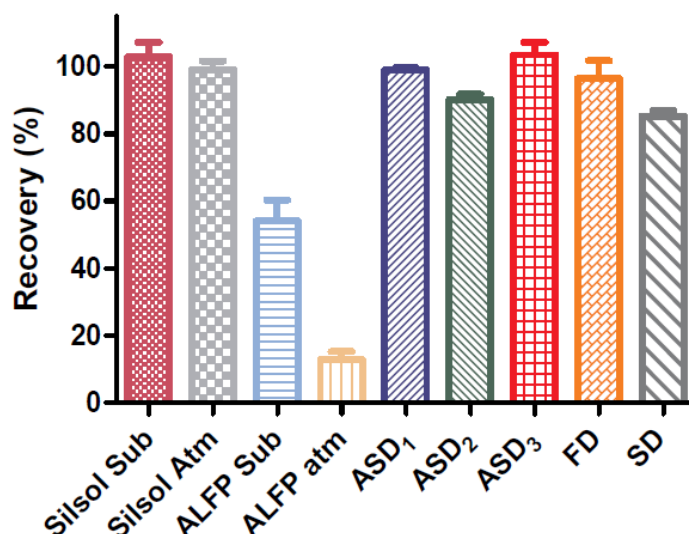


Figure 26. Quantification of CBD contained in different powders, 2 months after production. Silsol Atm, Silsol Sub, ALFP Atm and ALFP Sub correspond to powder of MS either Silsol or ALFP and CBD produced by impregnation at ambient conditions and using Subcritical CO<sub>2</sub>, respectively. ASD<sub>1</sub>, ASD<sub>2</sub> and ASD<sub>3</sub> correspond to milled extrudates of CBD and KVA64, SOL or K12PF, respectively, produced by HME. FD and SD correspond to powder of RAMEB and CBD produced by FD and spray-drying (SD), respectively.

#### 2.4.6 Critical strategy comparison summary

The three strategies are suitable to increase the aqueous solubility of CBD. However, each strategy must be confronted with the status of the excipients and with the main technique used for its production. In fact, an inexpensive and well-documented conventional excipient will be preferred to a new excipient for which a setback of its use needs to be investigated. The highest drug loading capacity has been demonstrated by the use of the MS-Silsol, with a loading up to 40% (m/m) of CBD. Furthermore, the impregnation methods are easy to implement and do not take time but the use of mesoporous carrier and high pressure equipment suffer from a lack of use in the pharmaceutical industry [18,39,40]. Scale-up processes have to be further investigated in order to produce these very promising forms on a large scale. Besides, the use of CDs as well as water-soluble polymers benefit from a large-scale use with in particular a large number of medicine containing this type of excipients [24,41–43]. It would therefore be more interesting from an industrial point of view to choose one of these two strategies.

## 2.5 Conclusion

This study highlighted different strategies developed to increase the aqueous solubility of CBD. Different processes as HME, impregnation with subcritical CO<sub>2</sub>, FD and spray-drying were used to promote amorphization which helps solubilisation of the drug. ASDs were produced using various excipients such as water-soluble polymers, MS or CDs in order. Our study proves the interest of using the amorphous CBD to increase its dissolution rate as well as its water solubility. We demonstrated that MS, CDs and polymers (K12PF, KVA64 and SOL) were suitable excipients to stabilize this promising form for at least two months. While the use of MS allowed a high drug loading up to 40% (w/w) of CBD, only 5 to 10% of drug loading could be used for formulations composed of CDs and polymers. As explained very recently by Sihorkar et al. CDs complexation provides an interesting means to solubilize drugs and to stabilize amorphous forms but with a low or moderate dose drugs due to the stoichiometric molar ratio required for inclusion complexation to take place between the drug and CDs [44]. The drug loading capacity of polymer processes by HME would be optimized for further experiments. With respect to dissolution rate, the ASD formed between the drug and KVA64 appears to be the most promising. In a scale-up point of view, HME is widely used in the industry and may facilitate a large-scale production of solubility-enhanced formulations of CBD. To conclude, we have opened many doors to obtain multiple tracks for the production of stable solid dosage form of CBD.

## 2.6 Acknowledgements

The authors wish to acknowledge FEDER funds for the support in SOLPHARE project (884148-329407).

## 2.7 References

- [1] M. Machado Bergamaschi, R. Helena Costa Queiroz, A. Waldo Zuairi, J. Alexandre S. Crippa, Safety and Side Effects of Cannabidiol, a Cannabis sativa Constituent, *Curr. Drug Saf.* 6 (2011) 237–249. <https://doi.org/10.2174/157488611798280924>.
- [2] O. Devinsky, M.R. Cilio, H. Cross, J. Fernandez-Ruiz, J. French, C. Hill, R. Katz, V. Di Marzo, D. Jutras-Aswad, W.G. Notcutt, J. Martinez-Orgado, P.J. Robson, B.G. Rohrback, E. Thiele, B. Whalley, D. Friedman, Epilepsy and Other Neuropsychiatric Disorders, *Epilepsia*. 55 (2014) 791–802. <https://doi.org/10.1111/epi.12631>.Cannabidiol.
- [3] S.A. Millar, N.L. Stone, A.S. Yates, S.E. O'Sullivan, A systematic review on the pharmacokinetics of cannabidiol in humans, *Front. Pharmacol.* 9 (2018). <https://doi.org/10.3389/fphar.2018.01365>.
- [4] G. Newswire, G.W. Pharmaceuticals, G. Biosciences, EPIDIOLEX (cannabidiol) Oral Solution – the First FDA-approved Plant-derived Cannabinoid Medicine – Now Available by Prescription in the U.S. | The Daily Marijuana Observer, (2018) 1–3. <https://mjobserver.com/united-states/epidiolex-cannabidiol-oral-solution-the-first-fda-approved-plant-derived-cannabinoid-medicine-now-available-by-prescription-in-the-u-s/>.
- [5] A.A. Izzo, F. Borrelli, R. Capasso, V. Di Marzo, R. Mechoulam, Non-psychotropic plant cannabinoids: new therapeutic opportunities from an ancient herb, *Trends Pharmacol. Sci.* 30 (2009) 515–527. <https://doi.org/10.1016/j.tips.2009.07.006>.
- [6] P.J. J. Mannila, T. Järvinen, K. Järvinen, Precipitation Complexation Method Produces Cannabidiol/b-Cyclodextrin Inclusion Complex Suitable for Sublingual Administration of Cannabidiol, *J. Pharm. Sci.* 101 (2007) 312–319. <https://doi.org/10.1002/jps>.
- [7] G.H. & K. McArdle, Drug loading and characterization of porous silicon materials, in: *Med. Uses Cannabis Cannabinoids*, 2004: pp. 205–228.
- [8] S. Baghel, H. Cathcart, N.J. O'Reilly, Polymeric Amorphous Solid Dispersions: A Review of Amorphization, Crystallization, Stabilization, Solid-State Characterization, and Aqueous Solubilization of Biopharmaceutical Classification System Class II Drugs, *J. Pharm. Sci.* 105 (2016) 2527–2544. <https://doi.org/10.1016/j.xphs.2015.10.008>.
- [9] A. Singh, Z.A. Worku, G. Van Den Mooter, Oral formulation strategies to improve solubility of poorly water-soluble drugs, *Expert Opin. Drug Deliv.* 8 (2011) 1361–1378. <https://doi.org/10.1517/17425247.2011.606808>.
- [10] D.D. Sun, T.C.R. Ju, P.I. Lee, Enhanced kinetic solubility profiles of indomethacin amorphous solid dispersions in poly(2-hydroxyethyl methacrylate) hydrogels, *Eur. J. Pharm. Biopharm.* 81 (2012) 149–158. <https://doi.org/10.1016/j.ejpb.2011.12.016>.
- [11] R. Laitinen, K. Loßmann, C.J. Strachan, H. Grohgan, T. Rades, Emerging trends in the stabilization of amorphous drugs, *Int. J. Pharm.* 453 (2013) 65–79. <https://doi.org/10.1016/j.ijpharm.2012.04.066>.
- [12] S. Metre, S. Mukesh, S.K. Samal, M. Chand, A.T. Sangamwar, Enhanced Biopharmaceutical

- Performance of Rivaroxaban through Polymeric Amorphous Solid Dispersion, *Mol. Pharm.* 15 (2018) 652–668. <https://doi.org/10.1021/acs.molpharmaceut.7b01027>.
- [13] O. Jennotte, N. Koch, A. Lechanteur, B. Evrard, Three-dimensional printing technology as a promising tool in bioavailability enhancement of poorly water-soluble molecules: A review, *Int. J. Pharm.* 580 (2020) 119200. <https://doi.org/10.1016/j.ijpharm.2020.119200>.
- [14] G. Van Den Mooter, The use of amorphous solid dispersions: A formulation strategy to overcome poor solubility and dissolution rate, *Drug Discov. Today Technol.* 9 (2012) e79–e85. <https://doi.org/10.1016/j.ddtec.2011.10.002>.
- [15] S. Chaudhari, A. Gupte, Mesoporous Silica as a Carrier for Amorphous Solid Dispersion, *Br. J. Pharm. Res.* 16 (2017) 1–19. <https://doi.org/10.9734/bjpr/2017/33553>.
- [16] A. Maleki, H. Kettiger, A. Schoubben, J.M. Rosenholm, V. Ambroggi, M. Hamidi, Mesoporous silica materials: From physico-chemical properties to enhanced dissolution of poorly water-soluble drugs, *J. Control. Release.* 262 (2017) 329–347. <https://doi.org/10.1016/j.jconrel.2017.07.047>.
- [17] X. Ma, H. Feng, C. Liang, X. Liu, F. Zeng, Y. Wang, Mesoporous silica as micro/nano-carrier: From passive to active cargo delivery, a mini review, *J. Mater. Sci. Technol.* 33 (2017) 1067–1074. <https://doi.org/10.1016/j.jmst.2017.06.007>.
- [18] C.A. McCarthy, R.J. Ahern, R. Dontireddy, K.B. Ryan, A.M. Crean, Mesoporous silica formulation strategies for drug dissolution enhancement: A review, *Expert Opin. Drug Deliv.* 13 (2016) 93–108. <https://doi.org/10.1517/17425247.2016.1100165>.
- [19] A. Gignone, L. Manna, S. Ronchetti, M. Banchemo, B. Onida, Incorporation of clotrimazole in Ordered Mesoporous Silica by supercritical CO<sub>2</sub>, *Microporous Mesoporous Mater.* 200 (2014) 291–296. <https://doi.org/10.1016/j.micromeso.2014.05.031>.
- [20] J.R. V. Lehto, Drug loading and characterization of porous silicon materials, in: *Porous Silicon Biomed. Appl.*, 2014: pp. 337–355.
- [21] N. Koch, O. Jennotte, B. Grignard, A. Lechanteur, B. Evrard, Impregnation of mesoporous silica with poor aqueous soluble molecule using pressurized carbon dioxide: is the solubility in the supercritical and subcritical phase a critical parameter?, *Eur. J. Pharm. Sci.* (2020) 105332. <https://doi.org/https://doi.org/10.1016/j.ejps.2020.105332>.
- [22] D.M. J. Hong, C. Shah, Effect of Cyclodextrin Derivation and Amorphous State of Complex on Accelerated Degradation of Ziprasidone, *J. Pharm. Sci.* 100 (2011) 2703–2716. <https://doi.org/10.1002/jps>.
- [23] P. Saokham, C. Muankaew, P. Jansook, T. Loftsson, Solubility of cyclodextrins and drug/cyclodextrin complexes, *Molecules.* 23 (2018) 1–15. <https://doi.org/10.3390/molecules23051161>.
- [24] E.M.M. Del Valle, Cyclodextrins and their uses: A review, *Process Biochem.* 39 (2004) 1033–1046. [https://doi.org/10.1016/S0032-9592\(03\)00258-9](https://doi.org/10.1016/S0032-9592(03)00258-9).

- [25] A. Lechanteur, B. Evrard, Influence of composition and spray-drying process parameters on carrier-free DPI properties and behaviors in the lung: A review, *Pharmaceutics*. 12 (2020). <https://doi.org/10.3390/pharmaceutics12010055>.
- [26] M. Skiba, M. Lahiani-Skiba, N. Milon, F. Bounoure, H. Fessi, Preparation and characterization of amorphous solid dispersions of nimesulide in cyclodextrin copolymers, *J. Nanosci. Nanotechnol.* 14 (2014) 2772–2779. <https://doi.org/10.1166/jnn.2014.8587>.
- [27] J. Thiry, P. Lebrun, C. Vinassa, M. Adam, L. Netchacovitch, E. Ziemons, P. Hubert, F. Krier, B. Evrard, Continuous production of itraconazole-based solid dispersions by hot melt extrusion: Preformulation, optimization and design space determination, *Int. J. Pharm.* 515 (2016) 114–124. <https://doi.org/10.1016/j.ijpharm.2016.10.003>.
- [28] K.T. Savjani, A.K. Gajjar, J.K. Savjani, Drug Solubility: Importance and Enhancement Techniques, *ISRN Pharm.* 2012 (2012) 1–10. <https://doi.org/10.5402/2012/195727>.
- [29] J. Mannila, T. Järvinen, K. Järvinen, M. Tarvainen, P. Jarho, Effects of RM- $\beta$ -CD on sublingual bioavailability of  $\Delta$ 9-tetrahydrocannabinol in rabbits, *Eur. J. Pharm. Sci.* 26 (2005) 71–77. <https://doi.org/10.1016/j.ejps.2005.04.020>.
- [30] P. Lv, D. Zhang, M. Guo, J. Liu, X. Chen, R. Guo, Y. Xu, Q. Zhang, Y. Liu, H. Guo, M. Yang, Structural analysis and cytotoxicity of host-guest inclusion complexes of cannabidiol with three native cyclodextrins, *J. Drug Deliv. Sci. Technol.* 51 (2019) 337–344. <https://doi.org/10.1016/j.jddst.2019.03.015>.
- [31] P.I. Lee, N. a Peppas, the glassy polymer during this process. *Ouano, Solutions*. 6 (1987) 207–215.
- [32] B. Narasimhan, N.A. Peppas, Molecular analysis of drug delivery systems controlled by dissolution of the polymer carrier, *J. Pharm. Sci.* 86 (1997) 297–304. <https://doi.org/10.1021/js960372z>.
- [33] P. Colombo, R. Bettini, P. Santi, N.A. Peppas, Swellable matrices for controlled drug delivery: Gel-layer behaviour, mechanisms and optimal performance, *Pharm. Sci. Technol. Today*. 3 (2000) 198–204. [https://doi.org/10.1016/S1461-5347\(00\)00269-8](https://doi.org/10.1016/S1461-5347(00)00269-8).
- [34] S.R. J. Pratik, T. Rupesh, A brief review on Kollidon, *J. Drug Deliv. Ther.* 9 (2019) 493–500. <https://doi.org/10.22270/jddt.v9i2.2539>.
- [35] V. Bühler, Kollidon® - Polyvinylpyrrolidone excipients for the pharmaceutical industry BASF, 2008. <https://doi.org/10.4315/0362-028X.JFP-13-344>.
- [36] R.N. Shamma, M. Basha, Soluplus®: A novel polymeric solubilizer for optimization of Carvedilol solid dispersions: Formulation design and effect of method of preparation, *Powder Technol.* 237 (2013) 406–414. <https://doi.org/10.1016/j.powtec.2012.12.038>.
- [37] J.R. Hughey, J.M. Keen, D.A. Miller, K. Kolter, N. Langley, J.W. McGinity, The use of inorganic salts to improve the dissolution characteristics of tablets containing Soluplus®-based solid dispersions, *Eur. J. Pharm. Sci.* 48 (2013) 758–766. <https://doi.org/10.1016/j.ejps.2013.01.004>.

- [38] S.F. and S.P. P. Mura, F. Maestrelli, M. Cirri, DIFFERENTIAL SCANNING CALORIMETRY AS AN ANALYTICAL TOOL IN THE STUDY OF DRUG–CYCLODEXTRIN INTERACTIONS, *J. Of Thermal Anal. Calorim.* 73 (2003) 635–646. [https://doi.org/10.1016/0040-6031\(85\)87041-6](https://doi.org/10.1016/0040-6031(85)87041-6).
- [39] M. Vallet-Regí, M. Colilla, I. Izquierdo-Barba, M. Manzano, Mesoporous silica nanoparticles for drug delivery: Current insights, *Molecules.* 23 (2018) 1–19. <https://doi.org/10.3390/molecules23010047>.
- [40] E. Weidner, Impregnation via supercritical CO<sub>2</sub>—What we know and what we need to know, *J. Supercrit. Fluids.* 134 (2018) 220–227. <https://doi.org/10.1016/j.supflu.2017.12.024>.
- [41] R. V. Tiwari, H. Patil, M.A. Repka, Contribution of hot-melt extrusion technology to advance drug delivery in the 21st century, *Expert Opin. Drug Deliv.* 13 (2016) 451–464. <https://doi.org/10.1517/17425247.2016.1126246>.
- [42] M. Maniruzzaman, A. Nokhodchi, Continuous manufacturing via hot-melt extrusion and scale up: regulatory matters, *Drug Discov. Today.* 22 (2017) 340–351. <https://doi.org/10.1016/j.drudis.2016.11.007>.
- [43] G. Crini, S. Fourmentin, É. Fenyvesi, G. Torri, M. Fourmentin, N. Morin-Crini, Cyclodextrins, from molecules to applications, *Environ. Chem. Lett.* 16 (2018) 1361–1375. <https://doi.org/10.1007/s10311-018-0763-2>.
- [44] V. Sihorkar, T. Dürig, The role of polymers and excipients in developing amorphous solid dispersions: An industrial perspective, 2020. <https://doi.org/10.1016/b978-0-12-821222-6.00005-1>.



## Chapter II. PRODUCTION AND SHAPING OF ASDs BY HOT-MELT EXTRUSION AND CAPSULE FILLING

### 1. Context and purpose of the study

As shown in chapter I, HME is a suitable technique to manufacture ASDs of CBD with an increased aqueous solubility and a stability of at least two months in terms of amorphous state and drug content. However, no immediate release formulation has been obtained.

To form an ASD with suitable dissolution performances, the API and the polymeric matrix should show an affinity for each other. Therefore, a screening of three polymers was performed to select the one that allowed the highest dissolution rate of CBD. EPO (methacrylate copolymer), Parteck® MXP (PVA) and KVA64 (vinylpyrrolidone-vinyl acetate copolymer) were chosen as hydrophilic matrices for the ASDs as they already proven their ability to form immediate release formulations of BCS II molecules produced by HME [1–3].

The purpose of this work was to study the impact of process parameters and excipients on CBD dissolution in order to optimize an extruded oral solid form allowing an immediate release of the drug. Moreover, quality of the produced extrudates, milled and formulated into capsules, was assessed based on hard capsule monograph of European Pharmacopoeia (Eur. Ph.). The dissolution studies were performed in an acidic medium because it was stated in the literature that CBD needs to be solubilized in the upper intestine to be absorbed optimally [4]. An immediate dissolution of this API under stomach conditions is therefore sought.

Extrusion parameters, especially temperature and screw speed, are known to have an influence on the physicochemical state of the drug in the matrix, leading to specific dissolution rates [5]. In this work, 10% CBD and the selected polymer were extruded at three temperatures (120, 140 and 160 °C) and two screw speeds (50 and 100 rpm) to evaluate on CBD dissolution rate. This CBD proportion was considered as an appropriate compromise between the cost of the drug and the ability of manufacturing oral dosage forms with a dose comprised in therapeutic dosage range already tested in clinical trials [6]. The effect of a recrystallization inhibitor, Eudragit® NM30D (ENM, 30% aqueous dispersion of ethyl acrylate and methyl methacrylate copolymer), was studied for the formulation which showed a recrystallization during the dissolution test.

The results of this study are described in the research paper entitled: “Development of ASDs of CBD: influence of the carrier, the HME parameters and the use of a crystallization inhibitor” published in the Journal of Drug Delivery Science and Technology.

To complete the study, quality control according to the tests of the Eur. Ph. concerning the hard capsules and a stability study following ICH Q1A (R2) guidelines were performed on capsules filled with the optimized ASD [7]. As explained in [Appendix II.1](#), capsules met the Eur. Ph. requirements, confirming the ability of capsule filling technique to shape ASDs with suitable quality and reproducibility. Moreover, CBD remained amorphous during six months, demonstrating the physical state stabilizing properties of EPO ([Appendix II.2](#)).

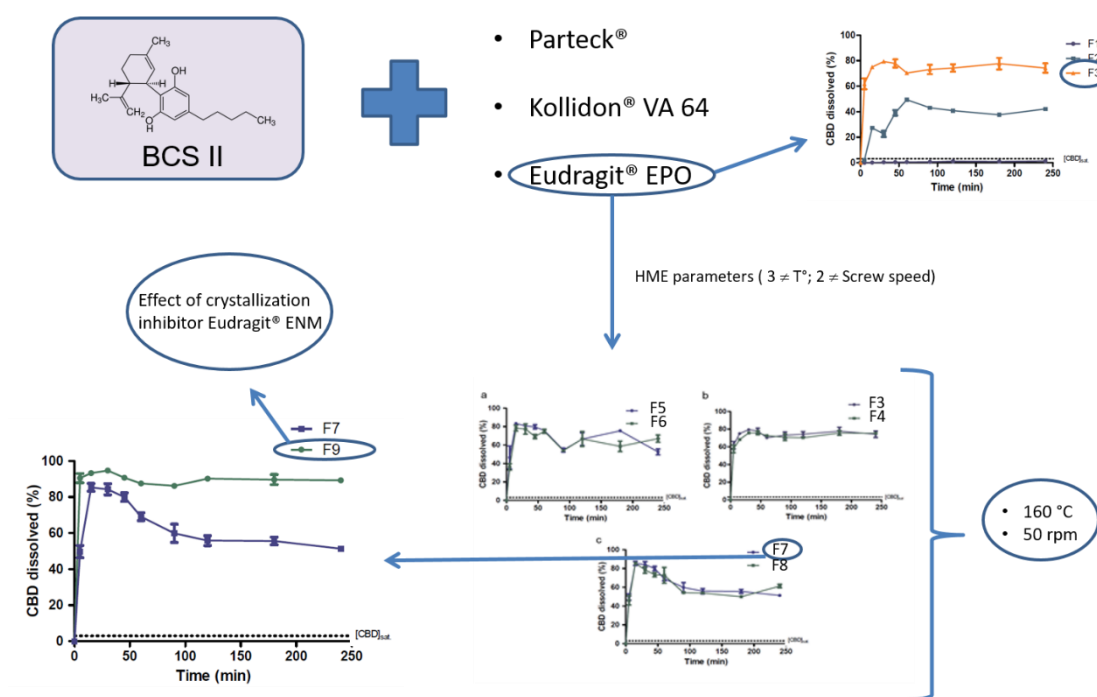
- [1] W. De Jaeghere, T. De Beer, J. Van Bocxlaer, J.P. Remon, C. Vervaet, Hot-melt extrusion of polyvinyl alcohol for oral immediate release applications, *Int. J. Pharm.* 492 (2015) 1–9. <https://doi.org/10.1016/j.ijpharm.2015.07.009>.
- [2] L. Dierickx, B. Van Snick, T. Monteyne, T. De Beer, J.P. Remon, C. Vervaet, Co-extruded solid solutions as immediate release fixed-dose combinations, *Eur. J. Pharm. Biopharm.* 88 (2014) 502–509. <https://doi.org/10.1016/j.ejpb.2014.06.010>.
- [3] W. Fan, X. Zhang, W. Zhu, X. Zhang, L. Di, Preparation of curcumin-eudragit® EPO solid dispersions with gradient temperature through Hot-Melt extrusion, *Molecules.* 26 (2021). <https://doi.org/10.3390/molecules26164964>.
- [4] D. Izgelov, M. Freidman, A. Hoffman, Investigation of cannabidiol gastro retentive tablets based on regional absorption of cannabinoids in rats, *Eur. J. Pharm. Biopharm.* 152 (2020) 229–235. <https://doi.org/10.1016/j.ejpb.2020.05.010>.
- [5] H. Liu, P. Wang, X. Zhang, F. Shen, C.G. Gogos, Effects of extrusion process parameters on the dissolution behavior of indomethacin in Eudragit® E PO solid dispersions, *Int. J. Pharm.* 383 (2010) 161–169. <https://doi.org/10.1016/j.ijpharm.2009.09.003>.
- [6] S.A. Millar, N.L. Stone, A.S. Yates, S.E. O'Sullivan, A systematic review on the pharmacokinetics of cannabidiol in humans, *Front. Pharmacol.* 9 (2018). <https://doi.org/10.3389/fphar.2018.01365>.
- [7] ICH, International Conference on Harmonization (ICH). Guidance for industry: Q1A(R2) STABILITY TESTING OF NEW DRUG SUBSTANCES AND PRODUCTS, *Ich Harmon. Tripart. Guidel.* 4 (2003) 24.

## 2. Publication

### **“DEVELOPMENT OF AMORPHOUS SOLID DISPERSIONS OF CANNABIDIOL: INFLUENCE OF THE CARRIER, THE HOT-MELT EXTRUSION PARAMETERS AND THE USE OF A CRYSTALLIZATION INHIBITOR”**

**Olivier Jennotte**, Nathan Koch, Anna Lechanteur, Brigitte Evrard

**University of Liège**, Laboratory of Pharmaceutical Technology and Biopharmacy,  
Center for Interdisciplinary Research on Medicines, Avenue Hippocrate B36 (+2) 4000  
Liège



J. Drug Deliv. Sci. Technol. 71, 103372

<https://doi.org/10.1016/j.jddst.2022.103372>

## 2.1 Abstract

HME has been widely used to manufacture ASD to enhance water solubility of molecules. In this study, the influence of the polymer, the extrusion parameters and the use of a crystallization inhibitor were investigated for the production of ASDs.

Three polymers, namely KVA64, Parteck® MXP and EPO, were first investigated to manufacture ASDs with CBD as a model poor water-soluble drug. Selected mixtures were extruded at three temperatures and two screw speeds. ENM, was added to the formulation which had the most appropriated dissolution behavior in order to highlight the prevention of the recrystallization.

Dissolution tests first showed a difference between polymers regarding the dissolution of CBD. EPO allowed the highest and the quickest dissolution of CBD (80 % after 30 min), so it was selected for the rest of the study. The dissolution tests on the ASD produced with different extrusion parameters showed that the temperature had an influence on the CBD concentration upkeep during the test.

Finally, it was observed that ENM was able to maintain the elevated CBD concentration during at least four hours, while the same formulation without this inhibitor was subjected to a drop of CBD concentration.

This study showed the importance of first, the choice of polymers for the manufacture of ASDs containing CBD. Secondly, the influence of the extrusion temperature on the upkeep of the CBD concentration was highlighted. Finally, it was shown that the use of a crystallization inhibitor prevents the CBD recrystallization during at least four hours of dissolution.

**Keywords:** Amorphous solid dispersion, Cannabidiol, Aqueous solubility enhancement, Crystallization inhibitor

## 2.2 Introduction

CBD is one of the major phytocannabinoids found in *Cannabis sativa* [1]. Unlike the well-known THC, CBD has no psychoactive effect and does not induce any dependence, which explains its interest in medicine [2,3]. A plethora of pharmaceutical properties are attributed to CBD, such as antioxidant [4], anti-inflammatory [4,5], antimicrobial [6] or anxiolytic [7]. However, there are only two approved medicines on the market, namely Epidiolex® which is an oral solution of pure CBD used to treat severe, orphan epilepsy [8] and Sativex®, an oro-mucosal spray of CBD and THC used to treat the multiple sclerosis-related spasticity [9]. To date no oral solid dosage form of CBD, which would be more stable than the two cited liquid forms, are marketed. The low choice of the CBD marketed medicines is probably linked with one of the major drawbacks of CBD concerning oral formulations which is its low bioavailability. It is estimated to be about 6% and is mainly due to a low aqueous solubility which categorizes this drug, like more than 50% of the newly designed API, in class II of BCS developed by Amidon et al. [10–13]. This poor aqueous solubility, assignable to the complexity of the molecules structure, prevents the *in vivo* dissolution and absorption of the drug and lowers its bioavailability. Therefore, it is a real challenge in the pharmaceutical field to improve the aqueous solubility and the dissolution rate of BCS II molecules.

Several techniques are described in the literature to improve the solubility and/or dissolution rate of BCS II molecules. Among them can be cited: particle size reduction [14], complexation with CDs [15], salt formation [16], impregnation of matrices with API [12], but also the formation of stabilized amorphous drugs, which is one of the most explored techniques for the bioavailability enhancement [17].

The amorphization of crystalline molecules is the transition from a low energy state (crystalline form), in which the molecule is stable, to a high-energy state (amorphous form), in which the molecule is less stable [18]. The molecular disorder of the amorphous compounds generally increases their kinetic solubility, in comparison to their crystalline form(s) [19]. However, the amorphous form suffers from some inconveniences. First, the amorphous API are more hygroscopic than in their crystalline form, which increases the risk of degradation by hydrolysis or oxidation [20]. Secondly, the introduction of an amorphous API in an aqueous medium can induce its crystallization and precipitation, more or less rapid, via a solid-to-solid transition. Indeed, the amorphous state is metastable and tends to go back to a more stable state [21]. Finally, there is a risk of recrystallization during storage, which makes the marketing of these API difficult without additives [22,23].

To overcome these drawbacks, the amorphous API can be stabilized in a carrier, generally a polymer, in which the crystallization is controlled [24]. This binary system, called ASD, has been widely used to enhance the aqueous solubility and therefore the bioavailability of BCS II molecules [25–28]. Moreover, a crystallization inhibitor can be added to the formulation. Studies have been conducted on HPMC [29,30], PVP [29,31], HPMCAS [30,32,33] and methacrylate copolymers [31,34]. These studies highlighted the ability of these polymers to raise the energy threshold required for nucleation and crystallization and lower the mobility of the molecules. These mechanisms inhibit the drug crystallization during dissolution tests, maintaining the supersaturation state [35]. There are many techniques used to produce ASD, such as spray-drying [36], supercritical fluid impregnation [37], rapid high energy thermal manufacturing process, KinetiSol® Dispersing [38] or HME [39].

HME is the process of dragging raw material, mostly polymers, API and eventual additives, along a barrel which contains rotating screw(s) under elevated temperatures. The final product goes out of the barrel through a die which will shape the extrudate. This technique offers many advantages such as no use of organic solvents, low numbers of processing steps and the possibility of a continuous operation [40,41]. HME has been widely used, both by the pharmaceutical industry and academia, to enhance the aqueous solubility and the dissolution rate of BCS II drugs by manufacturing ASD [42–44]. Several extrusion parameters, such as the temperature and the residence time have an influence, not only on the process, but also on the final product properties [45,46]. For example, Pawar et al. extruded amorphous polymeric systems with efavirenz, a poor water-soluble drug, using different temperatures and screw speeds. It was shown that the dissolution rate of the drug was better when it was extruded at higher extrusion temperatures and optimum screw speed [47]. Another criterion to take into account when developing ASDs is the selection of the polymer as it has an impact of the process, the drug solubility, stability and the downstream processes such as 3D printing [48].

The goal of this work was first to produce an optimal formulation of CBD with enhanced aqueous solubility and dissolution rate, using the HME. Secondly, the influence of a crystallization inhibitor on the upkeep of the supersaturation was evaluated.

To do so, three polymers, namely KVA64, Parteck® MXP (PVA) and EPO were tested and compared as carriers for the production of ASD of CBD. Physical mixtures of CBD and each of these three polymers were first extruded to obtain ASD. Then, the strands were milled and the amorphous state of the CBD and its dissolution behavior from the obtained powders were evaluated. The best polymer concerning the aqueous solubility and dissolution rate enhancement of CBD was selected to study the effect of different

extrusion parameters on the dissolution behavior of CBD. ENM was added to the formulation which had the most appropriate dissolution profile (a high dissolution of CBD followed by recrystallization) in order to maintain a supersaturation state during the *in vitro* dissolution tests and show the utility of ENM.

Finally, the stability of the ASD under three different temperature conditions was evaluated.

## 2.3 Material and methods

### 2.3.1 Materials

CBD was purchased from THC Pharm (Frankfurt, Germany). Parateck® MXP EMPROVE® ESSENTIAL (polyvinyl alcohol,  $T_g$ : 54 °C, water-soluble, EMD Millipore Corporation, USA) EPO (amino alkyl methacrylate copolymer,  $T_g$ : 50 °C, soluble in water at pH<5, Evonik, Germany) and KVA64 (vinylpyrrolidone-vinyl acetate copolymer,  $T_g$ : 101 °C, water-soluble, BASF, Germany) were used as matrix formers. ENM (30% aqueous dispersion of ethylacrylate and methyl methacrylate copolymer, Evonik, Germany) was used as a crystallization inhibitor. Milli-Q water was produced with a Purist UV (RePhile Bioscience). Acetonitrile was HPLC grade and purchased from J.T. Baker (Gliwice, Poland).

### 2.3.2 Solubility Measurement

The solubility measurement of pure CBD, F1, F2 and F3 in a simulated gastric medium was assessed via the shake-flask method [49,50]. The exact composition of the gastric medium is described in Table 4. An excess amount of each compound was dispersed in 10.0 mL of medium and shaken for 24 h at 100 rpm and  $37 \pm 0.5$  °C. Samples were analyzed via HPLC. These solubility measurements were carried out in triplicate in order to determine the saturation concentration of CBD with and without polymers in the gastric medium, which was chosen as the dissolution medium.

Table 4 - Composition of simulated gastric juice [50]

Gastric juice (pH $1.3 \pm 0.1$ )	
2752 mg NaCl	20 mg glucuronic acid
306 mg $\text{NaH}_2\text{PO}_4 \cdot \text{H}_2\text{O}$	85 mg urea
824 mg KCl	330 mg glucosamine hydrochloride
302 mg $\text{CaCl}_2$	1 g BSA
306 mg $\text{NH}_4\text{Cl}$	2.5 g pepsin
6.5 mL 37% HCl	3 g mucin
650 mg glucose	Milli-Q water ad 1 L



### 2.3.3 Production of the Amorphous Solid Dispersions Using Hot-Melt Extrusion

ASDs of CBD and each of the three polymers were produced by HME. Before the extrusion, CBD was mixed with each polymer in proportion 1:9 using a mortar and a pestle to obtain homogenous physical mixtures. The physical mixtures were then extruded using a Pharma 11 twin-screw extruder (Thermo Scientific, Germany) with a screw configuration containing 2 kneading zones and the obtained strands were then milled with a Fredrive-Lab equipped with a Hammerwitt head (Frewitt, Switzerland). The size of the grid was 0.35 mm and the speed of the blades was set at 7000 rpm.

In addition, physical mixtures composed of CBD and the most suitable polymer for its aqueous solubility enhancement were extruded at three different temperatures and two different screw speeds to study the potential influence of the process parameters on the dissolution behavior of the different formulations.

The formulation which showed the most appropriate dissolution behavior was extruded with ENM, a recrystallization inhibitor, in order to evaluate the ability of this polymer to maintain the concentration of CBD in a supersaturated state during the *in vitro* dissolution tests. All the extrusion parameters are gathered in [Table 5](#). Each formulation was extruded in triplicates.

Table 5 – Formulations composition and extrusion parameters

Formulations	CBD (%)	KVA64 (%)	PVA (%)	EPO (%)	ENM (%)	Screw speed (rpm)	Extrusion T° (°C)
F1	10	90	0	0	0	50	140
F2	10	0	90	0	0	50	200
F3	10	0	0	90	0	50	140
F4	10	0	0	90	0	100	140
F5	10	0	0	90	0	50	120
F6	10	0	0	90	0	100	120
F7	10	0	0	90	0	50	160
F8	10	0	0	90	0	100	160
F9	10	0	0	82.5	7.5	50	160

### 2.3.4 Characterization of the ASD

#### 2.3.4.1 HPLC

A validated reverse phase HPLC analytical method was developed for the quantification of CBD. The HPLC (Agilent® 1100, Santa Clara, USA) was equipped with OpenLab

CDS LC ChemStation version C.01.05 and a diode-array detector. A Zorbax® C18 300 SB analytical column with particles of 3.5 µm (150 mm × 4.6 mm ID) was used with a mobile phase composed of a mixture of water and acetonitrile (38/62 % (v/v)). The flow rate was set at 1.0 mL/min and the column temperature was set at 30 °C. The injection volume was 20.0 µL, the chromatographic run time was 10 min and the detection of CBD was made at a wavelength of 240 nm.

#### 2.3.4.2 Differential Scanning Calorimetry

DSC apparatus (Mettler-Toledo DSC1/700) was used in order to check the physical state of CBD in the physical mixtures and in the extrudates after the milling. 5 to 10 mg of samples were accurately weighed and sealed in an aluminum pan. One heating ramp ranging from 25 to 100 °C was applied at a rate of 20 °C/min and the results were analyzed using the STARe software.

#### 2.3.4.3 X-Ray Powder Diffraction (XRPD)

To assess crystallinity, X-ray diffractograms of pure CBD, pure polymers and the different milled extrudates were collected using a Bruker D8 TWIN-TWIN diffractometer in Bragg-Brentano configuration (Cu K $\alpha$  radiation, variable divergence slit V6, sample rotation 15 rpm) with a Lynxeye XET detector in 1D mode (192 channels) and a total scan time of 15 or 30 min for a 0.02° step size.

#### 2.3.4.4 Drug Recovery

The drug content of the milled extrudates was evaluated directly after the milling. Known amounts of the powder were dissolved in acetonitrile and analyzed by HPLC.

#### 2.3.5 *In vitro* Dissolution Tests

The *in vitro* dissolution profile of pure CBD and of the milled extrudates was evaluated using a USP II paddle method apparatus AT7 (Sotax®, Switzerland). Since there is no standard oral dose of CBD listed in the literature, a dose of 65 mg was chosen to perform the dissolution tests. This amount allowed the conduction of the dissolution tests under non-sink conditions in order to obtain a potential supersaturation of CBD in the dissolution medium. One size 000 gelatin capsule was filled with each formulation or with the pure drug and placed in baths containing 500 mL of simulated gastric juice, heated at 37 ± 0.5 °C and stirred at 100 rpm. Aliquot samples of 2.0 mL were withdrawn at 5, 15, 30, 45, 60, 90, 120, 180 and 240 min. An equal volume of the gastric medium was replaced after each withdrawal. Samples were then analyzed by HPLC. The dissolution tests were carried out in triplicates.

### *2.3.6 Influence of Time and Temperature on Drug Content and Physical State of CBD*

The drug content and the physical state of EPO-CBD (F3 to F9) was studied for three months. The milled extrudates of each formulation were packaged in amber sealed bottles and placed at three different temperatures (4, 25 and 37 °C). These three temperatures were chosen within the limits of the equipment available in the laboratory to mimic the temperature of a fridge (4°C), the room T° (25°C) and a higher temperature (37°C). This study will allow to evaluate the influence of time and temperature on the drug content and the physical state of the formulations, prior to ICH stability studies. Samples of 5 to 10 mg were taken at 1, 2 and 3 months and the amorphous state and the drug content were tested.

## *2.4 Results and Discussion*

### *2.4.1 Solubility Measurement*

The solubility measurement of CBD, F1, F2 and F3 in the simulated gastric medium was carried out to further estimate CBD potential aqueous solubility and the dissolution rate enhancement by the ASD. CBD was practically insoluble in the gastric medium with a maximal solubility of  $3.30 \pm 0.43$  µg/mL. Concerning the three ASD, the measured CBD concentrations after 24 h were  $5.08 \pm 5.21$  µg/mL,  $113.24 \pm 6.88$  µg/mL and  $182.17 \pm 3.75$  µg/mL for F1, F2 and F3, respectively.

### *2.4.2 Drug Recovery*

The drug content uniformity in the milled extrudates was evaluated by HPLC analysis. The data presented in [Figure. 27](#) show that the percentage of CBD was not affected by the extrusion process parameters, nor by the composition of the formulation. Indeed, the CBD recovery for every formulation was between 91 and 106%.

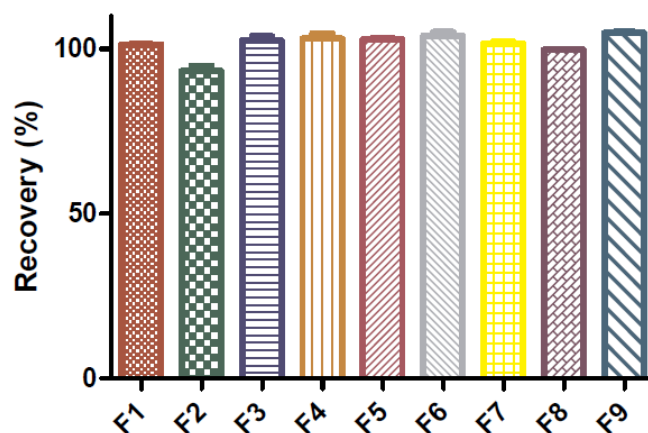


Figure 27 – CBD recovery in the different formulations ( $n=3$ ,  $\pm SD$ ).

#### 2.4.3 X-Ray Powder Diffraction

XRPD was used to study the physical state of CBD in the milled extrudates. The diffractogram of CBD shows sharp peaks, characteristic of crystallinity. These sharp peaks disappeared completely from the diffractograms of milled extrudates composed of CBD and KVA64 and from those composed of CBD and EPO, confirming the complete amorphization of CBD in these two polymers (Fig. 28a and 28c). Fig. 28b shows residual sharp peaks in the milled extrudates with CBD and PVA, showing the inability of PVA to amorphize the totality of CBD with an extrusion  $T^\circ$  of 200 °C.

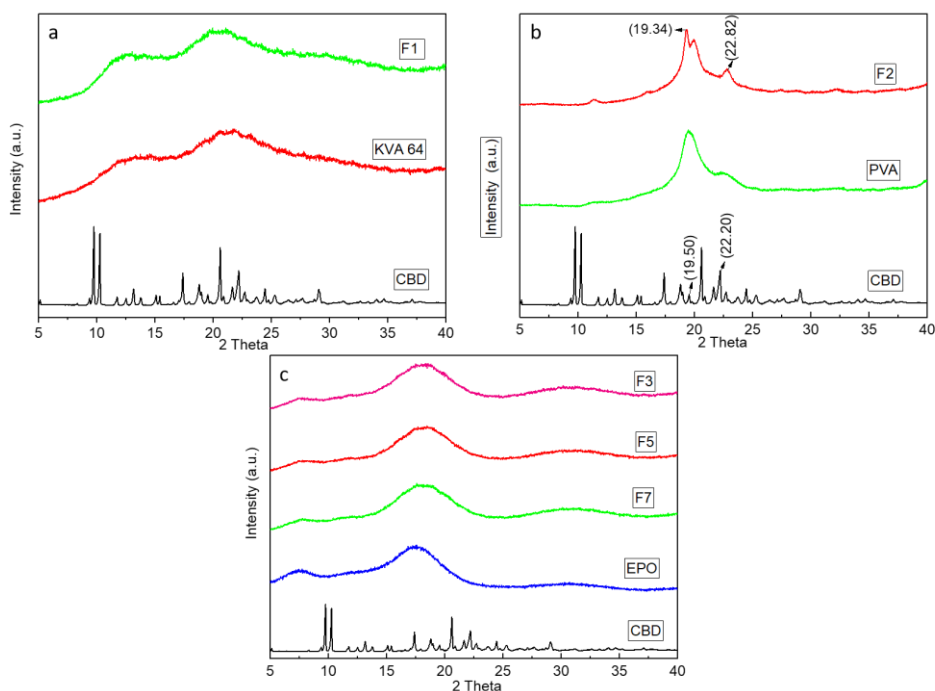


Figure 28 - Diffractograms of pure CBD, pure KVA64 and the milled extrudate composed of CBD/KVA64 (F1), (a), pure PVA and the milled extrudate composed of CBD/PVA, F2), (b) and pure EPO and the milled extrudates composed of CBD/EPO extruded at 140 °C (F3), 120 °C (F5) and 160 °C (F7), (c).

#### 2.4.4 Differential Scanning Calorimetry Studies

A drug in the amorphous state usually dissolves better than when it is in its crystalline form. DSC studies were performed in order to evaluate the physical state of CBD in the different formulations. The thermograms for pure CBD, pure polymers, physical mixtures and extrudates processed with different extrusion parameters are shown in **Figure 29**. The blue curves, which correspond to the physical mixtures of the different formulations, show an endothermic peak in a range of 66 - 76 °C which corresponds to the melting temperature of CBD (red curves). This melting peak shows 9.89 % of CBD in its crystal form when associated with KVA64 (which corresponds to approximately 100 % of the amount of CBD in the formulation), 8.23 % with PVA, 1 % with EPO and 1.7 % with EPO/ENM. According to the DSC results, KVA64 showed no ability to reduce the crystallinity of CBD in the physical mixture. It could be due to the high  $T_g$  of this polymer. EPO and PVA both have a  $T_g$  below the  $T_m$  of CBD which could easily dissolved in the plasticized polymers during the DSC analysis. However, this screening has highlighted a difference in the residual crystallinity of CBD in these two polymers, suggesting that EPO is more suitable to produce ASD of CBD. On the contrary, the curves of the milled extrudates (black) had no endothermic peak, showing the amorphous state of CBD in every formulation. The difference in the measurement of

CBD crystallinity in milled extrudates containing the PVA is due to the greater sensitivity of XRPD compared to DSC for measuring crystallinity. The CBD crystallinity in these extrudates should be negligible, since nothing is detected by DSC.

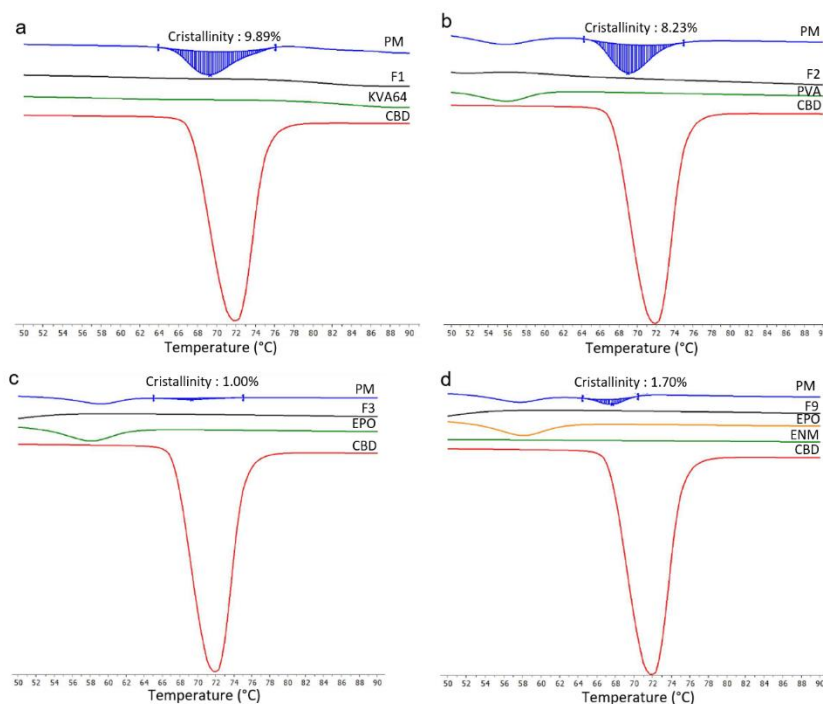


Figure 29 - DSC curves of CBD, KVA64 (a), PVA (b), EPO (c), ENM (d) and their respective physical mixtures (PM) and milled extrudates (F1, F2, F3 and F9).

#### 2.4.5 Polymer Selection

The *in vitro* dissolution tests were conducted with equivalent of 65 mg of CBD, pure or contained in the ASD under non-sink conditions. Figure 30 shows the dissolution profiles of the ASD of CBD and KVA64 (F1), PVA (F2) and EPO (F3). DSC studies proved that CBD was in its amorphous state in all of these three formulations. However, its release was different from each polymer. F1 did not reach a supersaturated concentration after four hours of dissolution testing. This could be due to the dissolution mechanism of this polymer in the gastric medium. Indeed, while KVA64 has already shown its ability to enhance the dissolution of CBD in a buffer with intestinal pH, other authors have shown that, at acidic pH and at certain proportions, KVA64 could dissolve from the exterior of the mass powder, leaving a hydrophobic layer of amorphous drug, preventing the drug release by acting as an enteric coating (Koch et al., 2020; Tres et al., 2016). Despite PVA aqueous solubility, F2 showed a maximum of dissolution of only 50 % of CBD after 60 min. This low dissolution enhancement could be explained by a partial miscibility between CBD and PVA [52]. The high solubility of EPO in acidic pH

(up to pH 5) allowed F3 to provide a faster and greater dissolution of CBD, with a dissolution of approximately 80 % of CBD after 30 min, which is 35-fold increase compared to the pure CBD at this time.

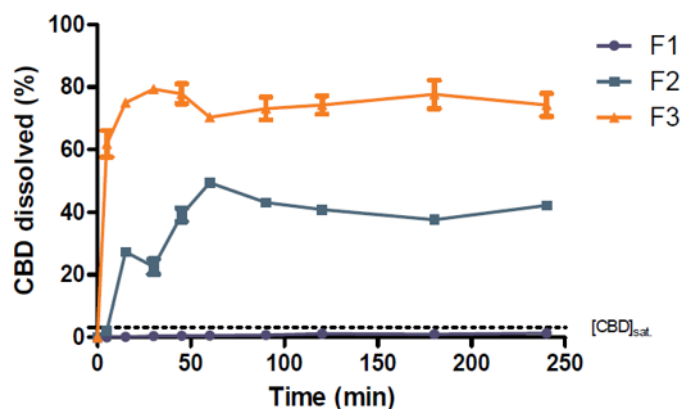


Figure 30 - Dissolution profile of F1 (CBD/KVA64), F2 (CBD/PVA) and F3 (CBD/EPO) in the simulated gastric medium ( $n=3$ ,  $\pm SD$ ).

#### 2.4.6 State of CBD within EPO Depending on Process Temperature

*In vitro* dissolution tests are useful to characterize the state of a drug in a polymer since differences in terms of drug release provide evidence of formation of molecularly dispersed drug [53]. Indeed, depending on whether the molecule is in an "agglomerated" state or totally dispersed in the polymer, the critical nucleation size will be reached more or less easily and therefore recrystallization during the dissolution test will be done more or less quickly. Based on the faculty of EPO to rapidly dissolve CBD, this polymer was selected to study any eventual influence of the process parameters on the CBD release. Three extrusion temperatures (120, 140 and 160 °C) and two screw speeds (50 and 100 rpm) were used to produce six formulations. These two parameters are known to influence the physical properties of the final product [40]. Figure 31 shows the release profile of the ASD extruded at 120 °C (a), 140 °C (b) and 160 °C (c). It was observed that, on the one hand, the speed of the screws did not have a significant influence on the release profile of the different formulations. On the other hand, the temperature seemed to impact the dissolution behavior of the ASD, and more precisely, on the upkeep of the concentration of CBD. Each CBD-EPO formulation showed an initial burst effect, allowing the release of  $\pm 80$  % of CBD within the first 15 min. This effect is not always a release mechanism to avoid, but it has to be controlled because it favors the recrystallization of the drug, called "spring effect" in which the concentration of the drug drops, which lowers the area under the curve of the dissolution profile [54]. The high concentration of CBD was maintained during the dissolution test of the

formulations extruded at 140 °C but it dropped after about one hour for the formulations extruded at 120 and 160 °C. The supersaturated degree (Ds, Eq. 6) was calculated for every formulation at the maximum of dissolution and at the end of the test and the difference between these two values was made to evaluate the recrystallization of CBD (related to a diminution of its concentration) in a function of time.

$$Ds = Ct/C_{saturation}$$

Eq. 6

Ds<sub>t</sub> is the supersaturated degree at time t, C, the concentration (µg/mL) and t, the time (min).

The more elevated was ΔDs, the more the difference between the CBD concentration at its maximum and at the end of the test was high, and so the recrystallization. As observed on Table 6, the formulations extruded at 140 °C (F3 and F4) had almost no recrystallization while the diminution of the CBD concentration was higher for the formulations extruded at 120 °C (F5 and F6) and 160 °C (F7 and F8).

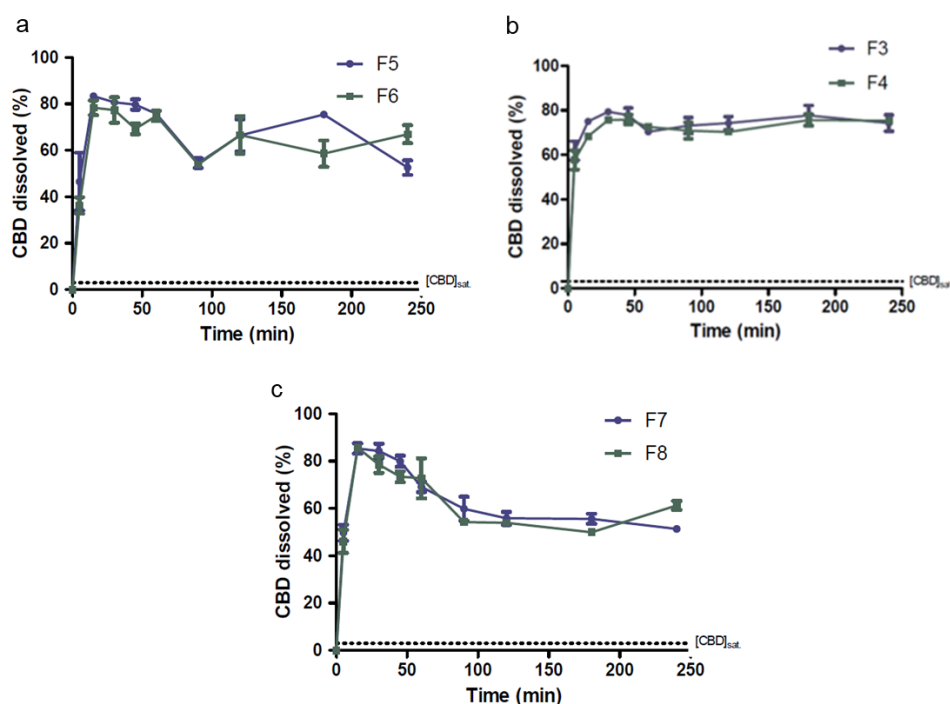


Figure 31 – Dissolution profile of the formulations F3 (50 rpm – 140 °C), F4 (100 rpm – 140 °C), F5 (50 rpm – 120 °C), F6 (100 rpm – 120 °C), F7 (50 rpm – 160 °C) and F8 (100 rpm – 160 °C) ( $n=3 \pm SD$ ).



Table 6 -  $D_s$  at the maximum of dissolution ( $D_{s_{max}}$ ),  $D_s$  at the end of the dissolution test ( $D_{s_{240\ min}}$ ) and  $\Delta D_s$  for formulations F3 to F9

Formulation	$D_{s_{max}}$	$D_{s_{240\ min}}$	$\Delta D_s$
F3	15.62	14.63	0.99
F4	14.90	14.84	0.06
F5	16.42	10.35	6.07
F6	15.43	13.19	2.24
F7	16.81	10.09	6.72
F8	16.87	12.08	4.79
F9	17.83	17.59	0.24

Our results are in accordance with another study. Liu et al. have extruded indomethacin with EPO at different temperatures. Differences in terms of dissolution profile have been obtained. Indeed, the recrystallization is governed by the nucleation and nuclei growth phenomena. While there is a critical nucleation size, the degree of dispersion of the drug within the polymer influences the recrystallization. We hypothesize that the extrusion at 140 °C provided finely dispersed CBD within the polymer, on the contrary of the extrusion at 120 °C and 160 °C in which agglomerates of amorphous CBD could reach more easily the critical nucleation size. As these states have an influence on the dissolution behavior, they could explain the upkeep of the CBD concentration during the whole dissolution test for F3 and the drop of CBD concentration for F5 and F7.

#### 2.4.7 Influence of the Crystallization Inhibitor

F7 is characterized by the most “spring-effect like” dissolution profile. It was thus selected to test the ability of ENM to avoid the drop of CBD concentration and obtain a plateau during the four hours of dissolution testing.

Figure 32 shows that ENM had a significant impact on the upkeep of the CBD concentration in the simulated gastric medium during the entire dissolution test. Indeed, while the percentage of solubilized CBD from F7 dropped from 85 % at 15 min to 53 % after 240 min corresponding to a  $\Delta D_s$  of 6.72, this percentage was maintained above 85 % during the four hours of dissolution testing for the formulation containing ENM (F9), with a  $\Delta D_s$  of 0.24, showing the faculty of this water insoluble polymer to delay the recrystallization of CBD in the dissolution medium. The dissolution tests show that ENM may avoid nucleation process. It is coherent with a previous work from Nollenberger et al., which managed to inhibit the recrystallization of felodipin from a supersaturated solution by using a water insoluble polymer, Eudragit® NE. Nevertheless, if drug-

polymer interactions are intuitively one of the main hypothesis responsible for this crystallization protection, no evidence could be highlighted.

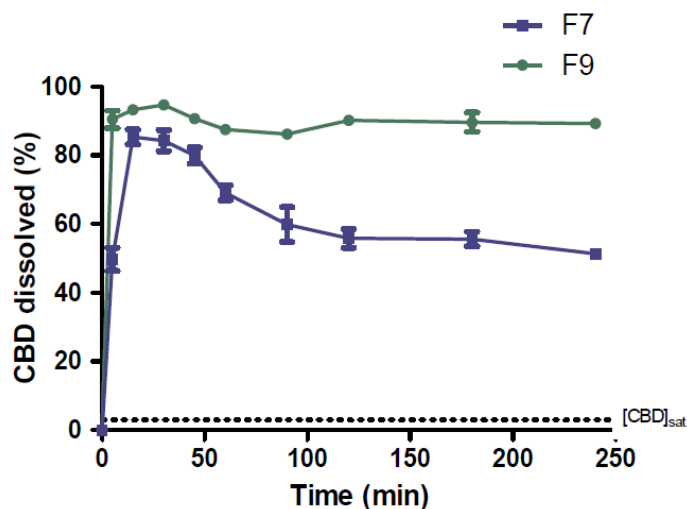


Figure 32 - Dissolution profile of F7 (50 rpm – 160 °C, without ENM) and F9 (50 rpm – 160 °C, with ENM) (n=3,  $\pm$ SD).

#### 2.4.8 Influence of Time and Temperature on Drug Content and Physical State of CBD

The drug content and the physical state of samples of the formulations F3 to F9, placed at three different temperatures (4, 25 and 37 °C), were evaluated after one, two and three months.

DSC studies showed no thermal event in each formulation, which means that the amorphous state of CBD was maintained during at least three months, no matter the extrusion parameters.

Figure 33 shows the evolution of the CBD content in the formulations stored under the three temperatures. The limit not to be exceeded was set at 90 % of the initial drug content. Under this limit, the formulation was considered as unstable. It can be seen that CBD content was higher than 90% of the initial drug content at 4 and 25 °C during at least three months while it dropped under 90% after only one month at 37 °C. These results suggest that the formulations can be stored between at least 4 and 25 °C even if stability studies based on ICH guidelines should be conducted on these nine formulations.

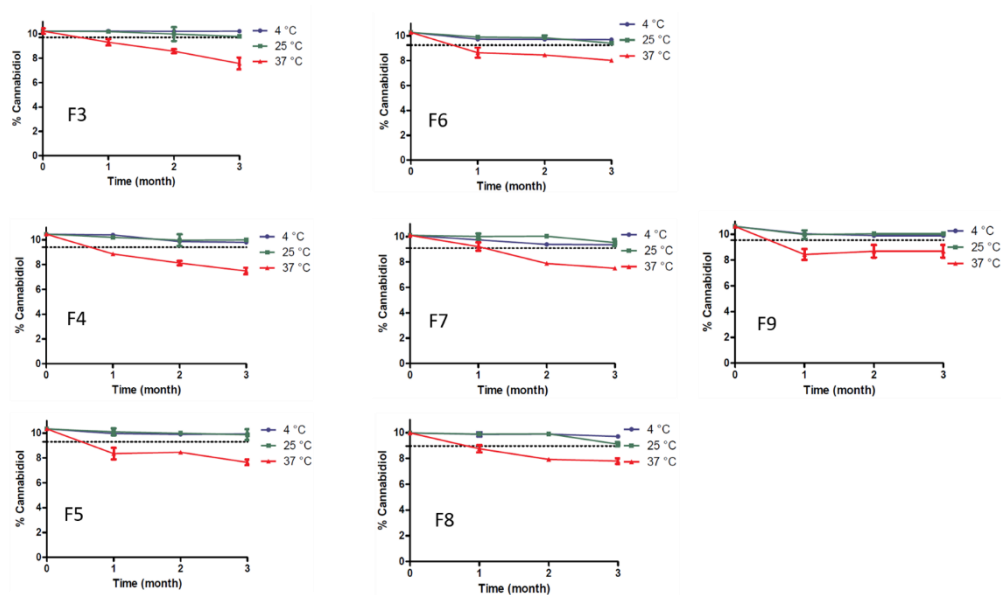


Figure 33 - CBD content in F3 (50 rpm – 140 °C), F4 (100 rpm – 140 °C), F5 (50 rpm – 120 °C), F6 (100 rpm – 120 °C), F7 (50 rpm – 160 °C), F8 (100 rpm – 160 °C) and F9 (50 rpm – 160 °C) as a function of time (month). The dotted line shows the 90 % of the initial drug content.

## 2.5 Conclusion

In this study, ASD of CBD and three different polymers were successfully produced using HME. Despite the amorphization of CBD extruded with each polymer, its aqueous solubility and dissolution rate were polymer dependent. Indeed, EPO allowed a higher aqueous solubility and dissolution rate enhancement than PVA and KVA64. For this reason, EPO was used to study the influence of the extrusion temperature and the screw speed. The screw speed did not show any influence on the release profile of CBD while the extrusion temperature shown an influence on the upkeep of the CBD concentration during the dissolution test. An extrusion temperature of 140 °C prevented the recrystallization of the dissolved CBD while the dissolution profile of the ASD extruded at 120 and 160 °C suffer from a drop of CBD concentration, probably due to CBD recrystallization. To evaluate the ability of ENM to avoid this recrystallization, this neutral polymer was added to F7 and the blend was extruded at 50 rpm and 160 °C. The ASD with ENM (F9) showed no recrystallization during the dissolution test, highlighting ENM crystallization inhibitor property.

This study showed the importance in the choice of the polymeric matrix, the eventual additives and the extrusion parameters for the production of ASD of CBD with an enhanced aqueous solubility and dissolution rate.

## 2.6 Acknowledgments

This work was supported by FEDER funds (SOLPHARE project, 884148-329407). The authors would like to thank Julie Laloy from the Department of Pharmacy at UNamur for providing us with the gastric medium.

## 2.7 References

- [1] S.A. Millar, R.F. Maguire, A.S. Yates, S.E. O'sullivan, Towards better delivery of cannabidiol (Cbd), *Pharmaceuticals*. 13 (2020) 1–15. <https://doi.org/10.3390/ph13090219>.
- [2] C. Scuderi, D. De Filippis, T. Iuvone, A. Blasio, A. Steardo, Cannabidiol in Medicine: A Review of its Therapeutic Potential in CNS Disorders, *Phyther. Res.* 23 (2008) 597–602. <https://doi.org/10.1002/ptr>.
- [3] J. Corroon, J.A. Phillips, A Cross-Sectional Study of Cannabidiol Users, *Cannabis Cannabinoid Res.* 3 (2018) 152–161. <https://doi.org/10.1089/can.2018.0006>.
- [4] R.S. Borges, J. Batista, R.B. Viana, A.C. Baetas, E. Orestes, M.A. Andrade, K.M. Honório, A.B.F. Da Silva, Understanding the molecular aspects of tetrahydrocannabinol and cannabidiol as antioxidants, *Molecules*. 18 (2013) 12663–12674. <https://doi.org/10.3390/molecules181012663>.
- [5] B. Costa, M. Colleoni, S. Conti, D. Parolaro, C. Franke, A.E. Trovato, G. Giagnoni, Oral anti-inflammatory activity of cannabidiol, a non-psychoactive constituent of cannabis, in acute carrageenan-induced inflammation in the rat paw, *Naunyn. Schmiedeberg's Arch. Pharmacol.* 369 (2004) 294–299. <https://doi.org/10.1007/s00210-004-0871-3>.
- [6] M.A.T. Blaskovich, A.M. Kavanagh, A.G. Elliott, B. Zhang, S. Ramu, M. Amado, G.J. Lowe, A.O. Hinton, D.M.T. Pham, J. Zuegg, N. Beare, D. Quach, M.D. Sharp, J. Pogliano, A.P. Rogers, D. Lyras, L. Tan, N.P. West, D.W. Crawford, M.L. Peterson, M. Callahan, M. Thurn, The antimicrobial potential of cannabidiol, *Commun. Biol.* 4 (2021). <https://doi.org/10.1038/s42003-020-01530-y>.
- [7] V. Almeida, R. Levin, F.F. Peres, S.T. Niigaki, M.B. Calzavara, A.W. Zuardi, J.E. Hallak, J.A. Crippa, V.C. Abílio, Cannabidiol exhibits anxiolytic but not antipsychotic property evaluated in the social interaction test, *Prog. Neuro-Psychopharmacology Biol. Psychiatry*. 41 (2013) 30–35. <https://doi.org/10.1016/j.pnpbp.2012.10.024>.
- [8] S.A. Millar, N.L. Stone, A.S. Yates, S.E. O'Sullivan, A systematic review on the pharmacokinetics of cannabidiol in humans, *Front. Pharmacol.* 9 (2018). <https://doi.org/10.3389/fphar.2018.01365>.
- [9] S. Giacoppo, P. Bramanti, E. Mazzone, Sativex in the management of multiple sclerosis-related spasticity: An overview of the last decade of clinical evaluation, *Mult. Scler. Relat. Disord.* 17 (2017) 22–31. <https://doi.org/10.1016/j.msard.2017.06.015>.
- [10] G.L. Amidon, H. Lennernäs, V.P. Shah, J.R. Crison, A Theoretical Basis for a Biopharmaceutic Drug Classification: The Correlation of in Vitro Drug Product Dissolution and in Vivo Bioavailability, *Pharm. Res. An Off. J. Am. Assoc. Pharm. Sci.* 12 (1995) 413–420. <https://doi.org/10.1023/A:1016212804288>.
- [11] S. Kalepu, V. Nekkanti, Insoluble drug delivery strategies: Review of recent advances and business prospects, *Acta Pharm. Sin. B.* 5 (2015) 442–453. <https://doi.org/10.1016/j.apsb.2015.07.003>.
- [12] N. Koch, O. Jennotte, Y. Gasparini, F. Vandenbroucke, A. Lechanteur, B. Evrard, Cannabidiol aqueous solubility enhancement: Comparison of three amorphous formulations strategies using different type of polymers, *Int. J. Pharm.* 589 (2020) 119812. <https://doi.org/10.1016/j.ijpharm.2020.119812>.
- [13] E. Perucca, M. Bialer, Critical Aspects Affecting Cannabidiol Oral Bioavailability and Metabolic

- Elimination, and Related Clinical Implications, *CNS Drugs*. 34 (2020) 795–800. <https://doi.org/10.1007/s40263-020-00741-5>.
- [14] J. Hecq, M. Deleers, D. Fanara, H. Vranckx, K. Amighi, Preparation and characterization of nanocrystals for solubility and dissolution rate enhancement of nifedipine, *Int. J. Pharm.* 299 (2005) 167–177. <https://doi.org/10.1016/j.ijpharm.2005.05.014>.
- [15] S. Rawat, S.K. Jain, Solubility enhancement of celecoxib using  $\beta$ -cyclodextrin inclusion complexes, *Eur. J. Pharm. Biopharm.* 57 (2004) 263–267. <https://doi.org/10.1016/j.ejpb.2003.10.020>.
- [16] A.T.M. Serajuddin, Salt formation to improve drug solubility, *Adv. Drug Deliv. Rev.* 59 (2007) 603–616. <https://doi.org/10.1016/j.addr.2007.05.010>.
- [17] X. Pan, T. Julian, L. Augsburger, Increasing the dissolution rate of a low-solubility drug through a crystalline-amorphous transition: A case study with indomethacin, *Drug Dev. Ind. Pharm.* 34 (2008) 221–231. <https://doi.org/10.1080/03639040701580606>.
- [18] B.C. Hancock, Disordered drug delivery: Destiny, dynamics and the Deborah number, *Pharm. J.* 267 (2001) 520. <https://doi.org/10.1211/0022357021778989>.
- [19] D. Novakovic, A. Isomäki, B. Pleunis, S.J. Fraser-Miller, L. Peltonen, T. Laaksonen, C.J. Strachan, Understanding Dissolution and Crystallization with Imaging: A Surface Point of View, *Mol. Pharm.* 15 (2018) 5361–5373. <https://doi.org/10.1021/acs.molpharmaceut.8b00840>.
- [20] P.J. Skrdla, P.D. Floyd, P.C. Dell'Orco, Predicting the solubility enhancement of amorphous drugs and related phenomena using basic thermodynamic principles and semi-empirical kinetic models, *Int. J. Pharm.* 567 (2019) 118465. <https://doi.org/10.1016/j.ijpharm.2019.118465>.
- [21] D.E. Alonzo, G.G.Z. Zhang, D. Zhou, Y. Gao, L.S. Taylor, Understanding the Behavior of Amorphous Pharmaceutical Systems during Dissolution, *Pharm. Res.* 27 (2010) 608–618. <https://doi.org/10.1007/s11095-009-0021-1>.
- [22] P. Mistry, K.K. Amponsah-efah, R. Suryanarayanan, Rapid Assessment of the Physical Stability of Amorphous Solid Dispersions, *Cryst. Growth Des.* 17 (2017) 2478–2485. <https://doi.org/10.1021/acs.cgd.6b01901>.
- [23] S.A. Raina, B.V.A.N. Eerdenbrugh, D.E. Alonzo, H. Mo, G.G.Z. Zhang, Y.I. Gao, L.S. Taylor, Trends in the Precipitation and Crystallization Behavior of Supersaturated Aqueous Solutions of Poorly Water-Soluble Drugs Assessed Using Synchrotron Radiation, *Pharm. Drug Deliv. Pharm. Technol. Trends*. 104 (2015) 1981–1992. <https://doi.org/10.1002/jps.24423>.
- [24] G. Van Den Mooter, The use of amorphous solid dispersions: A formulation strategy to overcome poor solubility and dissolution rate, *Drug Discov. Today Technol.* 9 (2012) e79–e85. <https://doi.org/10.1016/j.ddtec.2011.10.002>.
- [25] J. Thiry, M.G.M. Kok, L. Collard, A. Frère, F. Krier, M. Fillet, B. Evrard, Bioavailability enhancement of itraconazole-based solid dispersions produced by hot melt extrusion in the framework of the Three Rs rule, *Eur. J. Pharm. Sci.* 99 (2017) 1–8. <https://doi.org/10.1016/j.ejps.2016.12.001>.
- [26] D.D. Sun, T.C.R. Ju, P.I. Lee, Enhanced kinetic solubility profiles of indomethacin amorphous solid dispersions in poly(2-hydroxyethyl methacrylate) hydrogels, *Eur. J. Pharm. Biopharm.* 81 (2012) 149–158. <https://doi.org/10.1016/j.ejpb.2011.12.016>.

- [27] H. Konno, T. Handa, D.E. Alonzo, L.S. Taylor, Effect of polymer type on the dissolution profile of amorphous solid dispersions containing felodipine, *Eur. J. Pharm. Biopharm.* 70 (2008) 493–499. <https://doi.org/10.1016/j.ejpb.2008.05.023>.
- [28] A.A. Ambike, K.R. Mahadik, A. Paradkar, Spray-Dried Amorphous Solid Dispersions of Simvastatin, a Low T<sub>g</sub> Drug: In Vitro and in Vivo Evaluations, *Pharm. Res.* 22 (2005) 990–998. <https://doi.org/10.1007/s11095-005-4594-z>.
- [29] R.B. Chavan, R. Thipparaboina, D. Kumar, N.R. Shastri, Evaluation of the inhibitory potential of HPMC, PVP and HPC polymers on nucleation and crystal growth, *RSC Adv.* 6 (2016) 77569–77576. <https://doi.org/10.1039/c6ra19746a>.
- [30] F. Tajarobi, A. Larsson, H. Matic, S. Abrahmsén-Alami, The influence of crystallization inhibition of HPMC and HPMCAS on model substance dissolution and release in swellable matrix tablets, *Eur. J. Pharm. Biopharm.* 78 (2011) 125–133. <https://doi.org/10.1016/j.ejpb.2010.11.020>.
- [31] O.A. Abu-Diak, D.S. Jones, G.P. Andrews, An investigation into the dissolution properties of celecoxib melt extrudates: Understanding the role of polymer type and concentration in stabilizing supersaturated drug concentrations, *Mol. Pharm.* 8 (2011) 1362–1371. <https://doi.org/10.1021/mp200157b>.
- [32] H. Konno, L.S. Taylor, Ability of different polymers to inhibit the crystallization of amorphous felodipine in the presence of moisture, *Pharm. Res.* 25 (2008) 969–978. <https://doi.org/10.1007/s11095-007-9331-3>.
- [33] K. Ueda, K. Higashi, K. Yamamoto, K. Moribe, The effect of HPMCAS functional groups on drug crystallization from the supersaturated state and dissolution improvement, *Int. J. Pharm.* 464 (2014) 205–213. <https://doi.org/10.1016/j.ijpharm.2014.01.005>.
- [34] B.S. Nollenberger K., Gryczke A., Meier CH., Dressman J., Schmidt M.U., Pair Distribution Function X-Ray Analysis Explains Dissolution Characteristics of Felodipine Melt Extrusion Products, *J. Pharm. Sci.* 98 (2008) 1476–1486. <https://doi.org/10.1002/jps>.
- [35] S. Sarabu, V.R. Kallakunta, S. Bandari, A. Batra, V. Bi, T. Durig, F. Zhang, M.A. Repka, Hypromellose acetate succinate based amorphous solid dispersions via hot melt extrusion: Effect of drug physicochemical properties, *Carbohydr. Polym.* 233 (2020) 115828. <https://doi.org/10.1016/j.carbpol.2020.115828>.
- [36] A. Singh, G. Van Den Mooter, Spray drying formulation of amorphous solid dispersions ☆, *Adv. Drug Deliv. Rev.* 100 (2016) 27–50. <https://doi.org/10.1016/j.addr.2015.12.010>.
- [37] C. Potter, Y. Tian, G. Walker, C. McCoy, P. Hornsby, C. Donnelly, D.S. Jones, G.P. Andrews, Novel Supercritical Carbon Dioxide Impregnation Technique for the Production of Amorphous Solid Drug Dispersions: A Comparison to Hot Melt Extrusion, (2015). <https://doi.org/10.1021/mp500644h>.
- [38] J.C. Dinunzio, C. Brough, D.A. Miller, R.O. Williams, J.W. McGinity, European Journal of Pharmaceutical Sciences Applications of KinetiSol® Dispersing for the production of plasticizer free amorphous solid dispersions, *Eur. J. Pharm. Sci.* 40 (2010) 179–187. <https://doi.org/10.1016/j.ejps.2010.03.002>.
- [39] J. Thiry, F. Krier, S. Ratwatte, J. Thomassin, C. Jerome, B. Evrard, European Journal of

- Pharmaceutical Sciences Hot-melt extrusion as a continuous manufacturing process to form ternary cyclodextrin inclusion complexes, *Eur. J. Pharm. Sci.* 96 (2017) 590–597. <https://doi.org/10.1016/j.ejps.2016.09.032>.
- [40] J. Thiry, F. Krier, B. Evrard, A review of pharmaceutical extrusion : Critical process parameters and, *Int. J. Pharm.* 479 (2015) 227–240. <https://doi.org/10.1016/j.ijpharm.2014.12.036>.
- [41] A.K. Vynckier, L. Dierickx, J. Voorspoels, Y. Gonnissen, J.P. Remon, C. Vervaet, Hot-melt co-extrusion: Requirements, challenges and opportunities for pharmaceutical applications, *J. Pharm. Pharmacol.* 66 (2014) 167–179. <https://doi.org/10.1111/jphp.12091>.
- [42] A.M. Agrawal, M.S. Dudhedia, E. Zimny, Hot Melt Extrusion: Development of an Amorphous Solid Dispersion for an Insoluble Drug from Mini-scale to Clinical Scale, *AAPS PharmSciTech.* 17 (2016) 133–147. <https://doi.org/10.1208/s12249-015-0425-7>.
- [43] J. Thiry, P. Lebrun, C. Vinassa, M. Adam, L. Netchacovitch, E. Ziemons, P. Hubert, F. Krier, B. Evrard, Continuous production of itraconazole-based solid dispersions by hot melt extrusion : Preformulation , optimization and design space determination, *Int. J. Pharm.* 515 (2016) 114–124. <https://doi.org/10.1016/j.ijpharm.2016.10.003>.
- [44] Y. Tian, E. Jacobs, D.S. Jones, C.P. McCoy, H. Wu, G.P. Andrews, The design and development of high drug loading amorphous solid dispersion for hot-melt extrusion platform, *Int. J. Pharm.* 586 (2020) 119545. <https://doi.org/10.1016/j.ijpharm.2020.119545>.
- [45] Y. Shibata, M. Fujii, Y. Sugamura, R. Yoshikawa, S. Fujimoto, S. Nakanishi, Y. Motosugi, N. Koizumi, M. Yamada, K. Ouchi, Y. Watanabe, The preparation of a solid dispersion powder of indomethacin with crospovidone using a twin-screw extruder or kneader, *Int. J. Pharm.* 365 (2009) 53–60. <https://doi.org/10.1016/j.ijpharm.2008.08.023>.
- [46] H. Liu, P. Wang, X. Zhang, F. Shen, C.G. Gogos, Effects of extrusion process parameters on the dissolution behavior of indomethacin in Eudragit® E PO solid dispersions, *Int. J. Pharm.* 383 (2010) 161–169. <https://doi.org/10.1016/j.ijpharm.2009.09.003>.
- [47] J. Pawar, D. Suryawanshi, K. Moravkar, R. Aware, V. Shetty, Study the influence of formulation process parameters on solubility and dissolution enhancement of efavirenz solid solutions prepared by hot-melt extrusion : a QbD methodology, (2018).
- [48] F. Qian, J. Huang, M.A. Hussain, Drug-polymer solubility and miscibility: Stability consideration and practical challenges in amorphous solid dispersion development, *J. Pharm. Sci.* 99 (2010) 2941–2947. <https://doi.org/10.1002/jps.22074>.
- [49] A. Pestieau, F. Krier, A. Brouwers, B. Streel, B. Evrard, Selection of a discriminant and biorelevant in vitro dissolution test for the development of fenofibrate self-emulsifying lipid-based formulations, *Elsevier B.V.*, 2016. <https://doi.org/10.1016/j.ejps.2016.04.038>.
- [50] C.H.M. Versantvoort, A.G. Oomen, E. Van De Kamp, C.J.M. Rempelberg, A.J.A.M. Sips, Applicability of an in vitro digestion model in assessing the bioaccessibility of mycotoxins from food, *Food Chem. Toxicol.* 43 (2005) 31–40. <https://doi.org/10.1016/j.fct.2004.08.007>.
- [51] F. Tres, K. Treacher, J. Booth, L.P. Hughes, S.A.C. Wren, J.W. Aylott, J.C. Burley, Indomethacin-Kollidon VA64 Extrudates: A Mechanistic Study of pH-Dependent Controlled Release, (2016). <https://doi.org/10.1021/acs.molpharmaceut.5b00979>.



- [52] C. Wei, N.G. Solanki, J.M. Vasoya, A. V. Shah, A.T.M. Serajuddin, Development of 3D Printed Tablets by Fused Deposition Modeling Using Polyvinyl Alcohol as Polymeric Matrix for Rapid Drug Release, *J. Pharm. Sci.* 109 (2020) 1558–1572. <https://doi.org/10.1016/j.xphs.2020.01.015>.
- [53] C. Leuner, J. Dressman, Improving drug solubility for oral delivery using solid dispersions, *Eur. J. Pharm. Biopharm.* 50 (2000) 47–60. [https://doi.org/10.1016/S0939-6411\(00\)00076-X](https://doi.org/10.1016/S0939-6411(00)00076-X).
- [54] D.D. Bavishi, C.H. Borkhataria, Spring and parachute: How cocrystals enhance solubility, *Prog. Cryst. Growth Charact. Mater.* 62 (2016) 1–8. <https://doi.org/10.1016/j.pcrysgrow.2016.07.001>.

### Chapter III. USE OF FUSED-DEPOSITION MODELING 3D PRINTING COUPLED WITH HOT- MELT EXTRUSION FOR THE PRODUCTION OF IMMEDIATE RELEASE SOLID FORMS

#### 1. Context and purpose of the study

The first manufacturing/shaping method that was used to produce oral solid forms with CBD immediate release was HME followed by milling of the extrudates and capsule filling. Different polymers and extrusion parameters were tested, resulting in the selection of extrusion temperature/speed of 140 °C/50 rpm and EPO as polymeric carrier, based on their impact on CBD dissolution.

3D printing was the second strategy used to develop oral solid forms of CBD with an immediate release. The main benefits of 3D printing technology lie in the production of small batches of medicines, with the possibility of tailored dosages, sizes, release characteristics and shapes impossible to manufacture by conventional techniques such as capsule filling or tableting. Among the various 3D printing techniques, FDM is the most studied to shape ASDs due to its time-saving and cheap process, small equipment size and accuracy [1].

In this work, FDM coupled with HME was studied for the production of printed tablets containing an ASD of CBD and EPO allowing an immediate release of the drug and compliance to the Eur. Ph. requirements.

However, EPO is not printable on its own because of its brittleness [2]. PEO, a water-soluble polyethylene oxide, was chosen to plasticize the filament in order to prevent its breakage by the feeding gears of FDM printer. Different EPO/PEO ratios were blended with 10% of CBD, extruded and tested in term of dissolution in order to select the one which allowed the highest CBD dissolution rate.

The selected formulation was printed into different shapes, 3 cylinders with different percentages of infill and 3 capsule-like printed tablets with different surfaces. It is now well-known that the geometry of printed tablets has an influence on the dissolution rate [3]. In this study the pharmacotechnical properties of the different shapes were evaluated, based on the monograph of uncoated tablets of the Eur. Ph., as there is no official requirements concerning printed forms yet [4].

Then, the printed geometry that allowed an immediate release of CBD and a compliance to the Eur. Ph. was printed with different sizes to evaluate FDM ability to manufacture printed forms with different dosages without altering their mechanical and dissolution performances. This part of the study demonstrates the interest of FDM in personalized

medicine. The results are described in the article named: "Formulation and quality consideration of cannabidiol printed tablets produced by fused deposition modeling" submitted to the Journal of Drug Delivery Science and Technology.

To complete the study, a stability study following ICH Q1A (R2) guidelines was performed P1 and its corresponding extruded filament in order to assess the remaining of CBD amorphous state over time. As it can be observed in [Appendix III.1](#), CBD remained amorphous in both filament and P1. It can be conclude that EPO and PEO have appropriate stabilizing properties for CBD and that the second heating of the material during the FDM step, had no influence on CBD physical state.

Moreover, the ability of P1 to enhance CBD bioavailability was assessed. Pharmacokinetic profile of P1 showed a bioavailability of 3.8 fold higher than pure CBD ([Appendix III.3](#)).

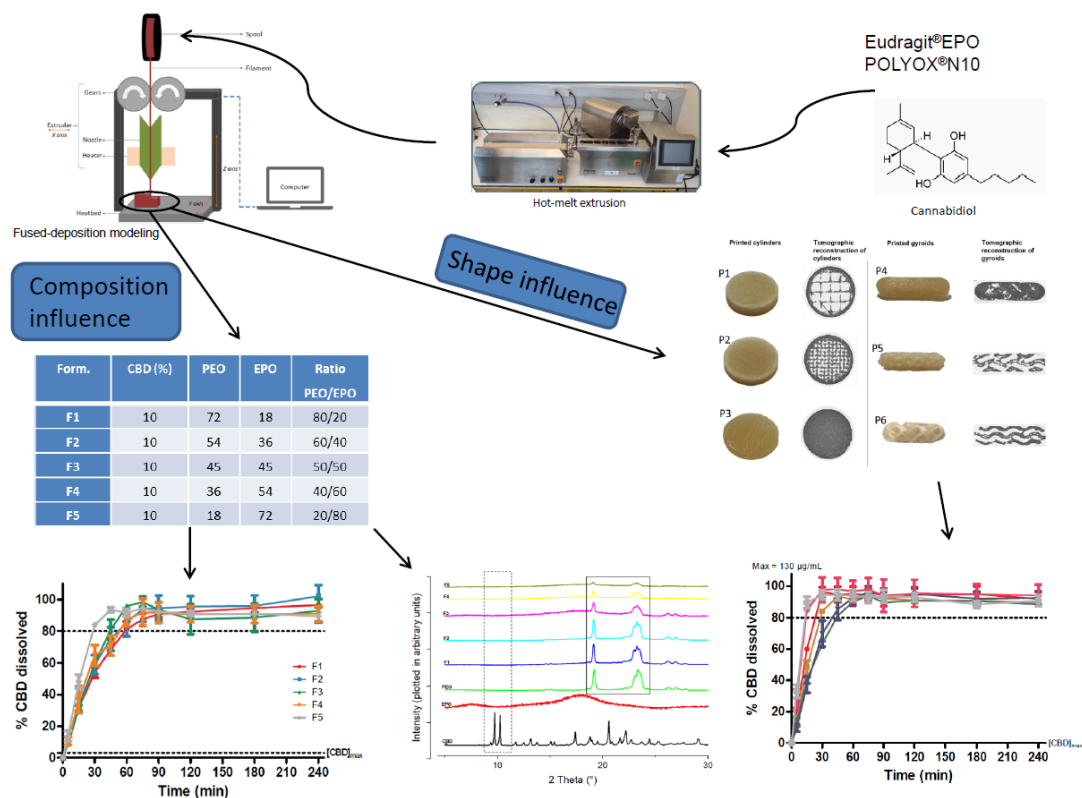
- [1] T.N.A.T. Rahim, A.M. Abdullah, H. Md Akil, Recent Developments in Fused Deposition Modeling-Based 3D Printing of Polymers and Their Composites, *Polym. Rev.* 59 (2019) 589–624. <https://doi.org/10.1080/15583724.2019.1597883>.
- [2] Y. Yang, H. Wang, X. Xu, G. Yang, Strategies and mechanisms to improve the printability of pharmaceutical polymers Eudragit® EPO and Soluplus®, *Int. J. Pharm.* 599 (2021) 120410. <https://doi.org/10.1016/j.ijpharm.2021.120410>.
- [3] A. Goyanes, P. Robles Martinez, A. Buanz, A.W. Basit, S. Gaisford, Effect of geometry on drug release from 3D printed tablets, *Int. J. Pharm.* 494 (2015) 657–663. <https://doi.org/10.1016/j.ijpharm.2015.04.069>.
- [4] S. Mohapatra, R.K. Kar, P.K. Biswal, S. Bindhani, Approaches of 3D printing in current drug delivery, *Sensors Int.* 3 (2022) 100146. <https://doi.org/10.1016/j.sintl.2021.100146>.
- [5] X. Lin, Y. Hu, L. Liu, L. Su, N. Li, J. Yu, B. Tang, Z. Yang, Physical Stability of Amorphous Solid Dispersions: a Physicochemical Perspective with Thermodynamic, Kinetic and Environmental Aspects, *Pharm. Res.* 35 (2018). <https://doi.org/10.1007/s11095-018-2408-3>.
- [6] ICH, International Conference on Harmonization (ICH). Guidance for industry: Q1A(R2) STABILITY TESTING OF NEW DRUG SUBSTANCES AND PRODUCTS, *Ich Harmon. Tripart. Guidel.* 4 (2003) 24.

## 2. Publication

### **Formulation and Quality Consideration of Cannabidiol Printed Tablets Produced by Fused-Deposition Modeling**

Olivier Jennotte, Nathan Koch, Anna Lechanteur, Brigitte Evrard

Laboratory of Pharmaceutical Technology and Biopharmacy, Department of Pharmacy, Center for Interdisciplinary Research on Medicines (CIRM), University of Liege, 4000 Liege, Belgium.



Submitted to the Journal of Drug Delivery Science and Technology

## 2.1 Abstract

Due to differences in genetics, weight, height, metabolism, health condition, age and tendency for compliance from patient to patient, there is a need for medicines with adaptable drug combinations, dosages and release rates to treat each individual adequately. However, the tailoring of drug dosage release is a major challenge for personalized medicine. FDM has already proven its usefulness in the individualization of the medicine by its ability to manufacture solid dosage forms with various geometries with adjustable size and percentage of infill. Among the concerned drugs, CBD is a promising molecule with poor aqueous solubility. Therefore, this work aimed to explore the development of a solid oral form of CBD, a BCS II model drug, printed by FDM. We have focused our research on the influence of the composition and the morphology of the formulation and on the reproducibility of the process as well as on its pharmaco-technical performances. Since still no guidelines regarding the evaluation of the performances or the quality control of the final 3D printed product exist, the control of the final products was according to the Eur. Ph. uncoated tablets monograph. First, we extruded and printed CBD filaments with various percentage ratio of EPO and PEO in order to select the most appropriate composition in terms of dissolution rate. We observed that the fastest dissolution was allowed by the formulation with the highest ratio of EPO. Secondly, the selected composition was printed in six different shapes, three cylinders with different percentages of infill and three capsule-like forms, to study the influence of the printed design on dissolution rate and processability. The highest dissolution rate was obtained with a capsule-like shape but the time to print it was 3-folds higher than the time to print cylinders. Therefore, the cylinder with the highest dissolution rate was selected for the last part of the study which focused on the dosage adaptability. Cylinders with three different strengths were studied in terms of pharmaco-technical performances and dissolution speed. It appeared that the dissolution rates after 15 minutes of the test were dose-dependent but after 30 minutes, the dissolution profiles became similar. This study has proven that challenges inherent to the manufacture of customized dosage forms can be overcome by FDM 3D printing.

**Keywords:** Cannabidiol, fused-deposition modeling, personalized medicine, amorphous solid dispersions.

## 2.2 Introduction

CBD is a promising non-psychoactive cannabinoid that shows several clinical outcomes. Commercially, this molecule is used in Epidiolex® (Greenwich Biosciences, Inc), a FDA-approved drug to treat Lennox-Gastaut and Dravet syndromes, which are childhood-onset epilepsy [1]. These two syndromes are difficult to treat and the dosage of Epidiolex® can reach a maximum of 10 mg/kg twice a day [2]. In addition to these indications, CBD has been studied for the treatment of different health problems, such as opioids use disorder, social anxiety, schizophrenia or cancers with a wide range of dosages varying from less than 1mg/kg/day to 50 mg/kg/day [3–5]. For example, Hurd *et al.* recently performed a clinical trial to assess the efficacy of CBD to inhibit the drug cue-induced craving and anxiety in drug-abstinent individuals with heroin use disorder [6]. Oral solutions of 400 or 800 mg of CBD or a placebo were administrated to 42 subjects one daily for three consecutive days. The behavior of the subjects was then observed for two weeks. This trial showed a considerable reduction of both craving and anxiety induced by drug cues for the patients to whom the CBD was administrated compared to the patients on placebo. Moreover, there were no serious adverse effect reported.

Moreover, some authors conducted a systematic review of clinical studies performed on CBD [7]. It first appeared that the tested CBD formulations were mainly administrated in the form of an oily solution, formulated in capsule or not. However, lipid formulations suffer from some drawbacks such as the sensitivity to oxidation or the compatibility with the capsule when encapsulation is considered [8]. The development of an oral solid dosage form of CBD would therefore be interesting for future investigations on its therapeutic effects. Secondly, among the trials that demonstrated positive effects of CBD on the treatment studied, the authors observed that the dosage of CBD can induce the variation of its therapeutic effect. Although clinical studies need to be conducted on a larger number of subjects, this suggests that in the future, clinicians will need to be able to formulate CBD drugs with adjustable dosage in order to be able to treat patients in the most effective way. In addition to these variable dosage challenges, the low bioavailability of CBD must be considered. Indeed, CBD is part of BCS class II. BCS II molecules show poor aqueous solubility (0.01µg/mL) and a high hepatic first pass metabolism which result in an estimated bioavailability of 6% [9]. Moreover, CBD absorption is erratic, leading to high variation of plasmatic concentrations in clinical population [10–12]. It is therefore crucial to develop strategies that improve CBD oral bioavailability with solid oral formulations which are preferred by patients and more stable than the liquid formulations.

Several techniques are used to improve the solubility of BCS II molecules, such as dissolution of the drug in lipid media, complexation into CDs, the impregnation of MS or the formation of ASDs, especially by HME and spray-drying [13–15]. Compared to the spray-drying technique, HME has the advantage of working without the use of expansive and polluting solvents.

In a previous study, twin screw HME has already been used to increase the aqueous solubility of CBD [16]. This technique involves the heating of a mixture between an API and one or more polymers along two screws, inside a barrel, until obtaining a filament in the shape of a spaghetti or a film, depending on the shape of the die. The filament can further, among others processes, be pelletized and filled into capsules, used directly as implant, be milled and compressed or shaped by 3D printing [17–20].

Since the FDA-approval of the first 3D printed dosage form Spritam® manufactured using the drop-on-powder deposition (Aprecia Pharmaceuticals), the application of 3D printing has been extensively studied in the pharmaceutical field. 3D printing represents a great potential in drug formulation due to its flexibility, its ability to produce very complex structures, amorphous forms, dosage forms with multiple drugs without incompatibilities and on-demand manufacturing [21]. In addition, 3D printing makes it possible to move away from the one-size-fits-all manufacturing approach applied by conventional manufacturing techniques. Due to differences in genetics, weight, height, metabolism, health condition, age and tendency for compliance from patient to patient, there is a need for drugs with adaptable drug combinations, dosages and release rates to treat each individual adequately [20,22]. Therefore, the faculty of 3D printing to convert a great number of digital patterns into solid drug dosage forms with different dose or drug release makes 3D printing a great tool in personalized medicine. In this regard, FDM has already offered solutions to many challenges. This technique consists of driving a filament by two wheels into a print head in which it is melted. The molten filament is deposited, layer by layer, on a platform until obtaining a 3D object, previously designed on a computer [23]. FDM has been reported for the print multiple layered tablets, each layer with a different drug to reduce the risk of a missing dose by the patient [24]. In another study, attractive shapes were printed by FDM to increase the compliance of young patients [25]. Another example is the use of FDM to manufacture pulsatile delivery system to treat patients suffering from conditions that require complex release profile [26]. Moreover, it's a low cost and simple method and it does not imply the use of organic solvents. These advantages could one day widespread decentralized drug manufacture by FDM, such as in hospitals or public pharmacies in which its advantages regarding the personalized medicine could be fully exploited. However despite the myriad of studies on the benefits of the 3D printing technique, there are still



no guidelines regarding the evaluation of the performances or the quality control of the final 3D printed product [27]. Currently, the FDA recommends following the same production and control guidelines as conventional manufacturing techniques [28].

Therefore, this work aims to explore the development of a solid oral form of CBD with an immediate release printed by FDM. We have focused our research on the influence of the composition and the morphology of the formulation on the reproducibility of the process as well as on its pharmaco-technical performances according to the Eur. Ph. uncoated tablets monograph.

This study is divided into three parts. First, different combinations of two polymers mixed with CBD were extruded and printed in order to select the most suitable for the production of CBD printed tablets with an immediate release. FDA defines immediate release formulations as formulations which allow a dissolution of at least 80% of an API in 30 min [29]. This type of formulation should increase the CBD bioavailability. Indeed, Izgelov claimed that, due to its lipid nature, absorption of CBD mainly occurs in the upper part of the intestine, explaining the advantage of the dissolution of the drug in the stomach [30]. In this regard, immediate release formulations were chosen as they should dissolve early in the GIT, making dissolved CBD available to be absorbed early in the intestine. Secondly, the selected formulation was extruded and printed in six different designs and the influence of the morphology was evaluated in terms of reproducibility and pharmaco-technical performances. Finally, the dosage adaptability allowed by the FDM was studied. In this regard, three different dosages of CBD were characterized and compared.

## 2.3 Material and methods

### 2.3.1 Materials

CBD was purchased from THC Pharm (Frankfurt, Germany). EPO (amino alkyl methacrylate copolymer,  $T_g$ : 50 °C, soluble in water at pH<5, gifted by Evonik, Germany) was used as matrix former. Poly ethylene oxide (PEO, POLYOX® WSR N10, MW 100000, gifted by Colorcon, UK), a semi-crystalline polymer ( $T_g$  = -67 °C and  $T_m$  = 65-70 °C) was used for its plasticizing effect.

### 2.3.2 Thermogravimetric Analysis (TGA)

TGA analysis were performed on CBD, EPO and PEO using Mettler-Toledo® TGA2 (Schwerzenbach, Swiss) controlled by the STARe System software version 12.10. Samples between 7 and 13 mg were added to an aluminum pan without lid. The % mass

loss of CBD was measured during a heating ramp ranging from 25 to 500 °C at a rate of 20 °C/min. The experiments were conducted under nitrogen gas flow of 80 mL/min.

### 2.3.3 Drug Loaded Filaments Preparation

Five EPO/PEO ratios, added with 10% of CBD, were used to produce filaments by HME in order to select the optimal formulation (**Table 7**). The physical mixtures were prepared using a mortar and a pestle and extruded using a Pharma 11 twin-screw extruder (ThermoFisher Scientific, Germany) with a screw configuration containing two kneading zones at 140 °C and 50 rpm. Two devices were set up in the extrusion line in order to modulate the filament diameter. The first one is a melt pump 12/3 (Advanced Futur Polymer, France), heated at 140 °C, connected between the barrel and the die. This pump is composed of two toothed wheels which decreased the pulsation output of the filament at the die. The second device is an air-cooled conveyor belt (ThermoFisher Scientific, Germany) which pulled the filament more or less quickly in order to decrease or increase the diameter of the filament. A digital caliper was used to measure the diameter during extrusion and the target value was 1.75 mm.

**Table 7** - HME formulations

Formulation	CBD (%)	PEO	EPO	Ratio PEO/EPO
F1	10	72	18	80/20
F2	10	54	36	60/40
F3	10	45	45	50/50
F4	10	36	54	40/60
F5	10	18	72	20/80

### 2.3.4 Design and Printing of the Formulations

Formulations F1 to F5 were printed into cylinder referred as P2 on **Figure 36**. The formulation which allowed the greatest increase of CBD aqueous solubility was then printed using the six design templates in order to evaluate which properties were influenced by the morphology of the printed tablets. The six designs of oral forms were created online using TinkerCAD (<https://tinkercad.com/>) for the cylindrical shapes and Shapeways (<https://shapeways.com/>) for the gyroidal shapes (**Fig. 36**). The term gyroid has been chosen to describe the capsule-like shapes with or without villi. The obtained .stl files were converted to gcode files using the software Ultimaker Cura, version 4.11.0 (Ultimaker, The Netherlands).

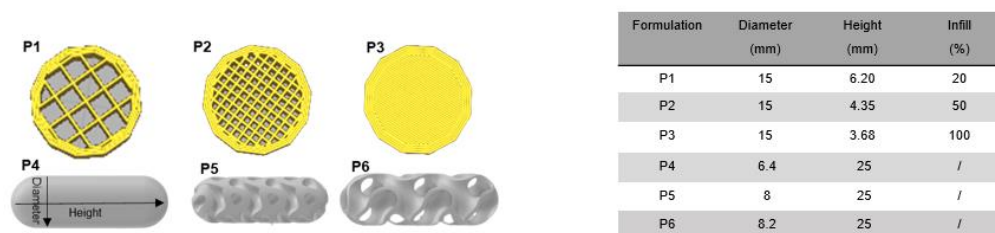


Figure 36 - Representation of the six designs (left) and theoretical morphological characteristics and % of infill for each design (right).

The dimensions of each design were adjusted in order to achieve a target mass of 650 mg per printed tablet which corresponds to an equivalent of 65 mg of CBD. This dosage was chosen in order to be within the dose range tested in the different studies found in the literature [7]. The printed tablets were produced with a 3D Original Prusa i3 MK3 printer (Prusa, Prague, Czech Republic) equipped with a 0.4 mm nozzle. As the melted formulations were sticky, a heating-resistant scotch tape was placed on it in order to remove the product easily from the heated platform. The printing temperature and bed temperature were set at 180 °C and 25 °C, respectively. The printing speed was 40 mm/s for the cylinders and 28 mm/s for the gyroids.

### 2.3.5 X-ray Diffraction

In order to evaluate the physical state of CBD once printed, disks (23.12 mm diameter x 1.00 mm height) made of drug loaded mixtures of EPO and PEO were printed and analyzed. X-ray diffractograms were collected using a Bruker D8 TWIN-TWIN diffractometer in Bragg-Brentano configuration (Cu Kalpha radiation, variable divergence slit V6, sample rotation 15 rpm) with a Lynxeye XET detector in 1D mode (192 channels) and a total scan time of 15 or 30 min for a 0.02° step size.

### 2.3.6 Drug Content of Filaments and Printed Tablets

Since the formulations are exposed to high temperatures during both stages of their production, the drug content was measured after the HME and after the printing steps. Samples of 20-30 mg were cut from the filaments and the printed tablets and dissolved in acetonitrile prior to HPLC analysis. A validated reverse phase HPLC analytical method, described in a previous work, was used [31]. The HPLC equipment consisted of an Agilent® 1100 (Santa Clara, USA) with OpenLab CDS IC ChemStation version C.01.05 as the software. The mobile phase was composed of water/acetonitrile (38/62% (v/v)) and the column was Zorbax® C18 300 SB with particles of 3.5 µm (150 mm x 4.6 mm ID). The flow rate was set at 1.0 mL/min and the temperature was kept at 30 °C. The injection volume was 20.0 µL, the chromatographic run time was 10 min and the

detection of CBD was made at a wavelength of 240 nm. The measurements were carried out in triplicate.

#### *2.3.7 Computerized Tomography Scan*

In order to measure their volume and surface area, the printed tablets were analyzed with a computerized tomography scan, Skyscan 1172/G (Bruker, Billerica, Massachusetts, United States). The voltage of the x-ray source was 100 kV, and a 0.5 mm aluminum filter was used to harden the x-rays (RX). The magnification was set for a pixel size of 19.91  $\mu\text{m}$ , taking into account 4x4 binning at the detector. The exposure time of an x-ray was 300 ms, for a total of 1,200 360° radios per acquisition. Reconstruction was performed on NRecon software (v. 1.7.3.1), using ring artifact correction (level 5) and 20% beam hardening correction. The processing was carried out on the Avizo software (v. 9.2) supplemented with calculation modules and scripts which were coded. The reconstructions first went through a median filter using an 18-neighborhood, then a thresholding was performed (threshold identified by the Otsu method). The larger 6-connected component has been extracted, and the cavities (all 26-connected components of the background except the largest) have been plugged. The technique of marching cubes was used to triangulate the interface of the solid with the exterior, then a Gaussian smoothing (2 iterations with a lambda of 0.6) was applied before measuring the area.

#### *2.3.8 Characterization of the Printed Tablets Properties*

As there is no monograph dedicated to the printed products yet, they were characterized with tests based on the monograph dedicated to the uncoated tablets of the Eur. Ph. Edition 11.2.

##### *Friability Test*

Ten printed tablets of each design were randomly taken, dusted, weighed and placed in the drum of a Friabilator USP F2 Sotax® (Aesch, Switzerland). After 100 rotations of the drum, the printed tablets were dusted, weighed again and the target mass loss was less than 1% (Monograph 2.9.7. Eur. Ph. Edition 11.2).

*Tensile Strength (TS)*

The tensile strength of each designed printed tablet was determined in triplicate using the breaking force (F) measured by a crushing strength tester Pharmatron MT-50 Sotax® (Aesch, Switzerland) and following [Equations 8](#) and [9](#) [32]:

$$TS = \frac{2F}{\pi Dt} \text{ for cylinders } \text{Eq. 8}$$

$$TS = \frac{2}{3} \left( \frac{10F}{\pi D^2 \left( 2.84 \frac{t}{D} - 0.126 \frac{t}{W} + 3.15 \frac{W}{D} + 0.01 \right)} \right) \text{ for gyroids } \text{Eq.9}$$

Where:

D is the diameter

t is the overall thickness

W is the wall height

The measure of the tensile strength was preferred to the simple measurement of the hardness, described in the tablet monograph, in order to normalize the hardness according to the shape of the printed tablet.

*Mass Variation*

Ten printed tablets of each design were individually weighted and the Acceptance Value (AV) was calculated using [Equation 7](#) (Monograph 2.9.40. Eur. Ph. Edition 11.2):

*Uniformity of Mass (Monograph 2.9.5 Eur. Ph. Edition 11.2)*

Ten printed tablets of each design were weighed and the average mass was determined. The test was considered as conform if not more than two of the individual masses deviate from the average mass by more than 5% of deviation and none deviate by more than twice that percentage.

*In Vitro Drug Release Studies*

The dissolution tests were carried out using the USP II paddle method apparatus AT7 (Sotax®, Switzerland). The first set of dissolution tests involved formulations containing different EPO/PEO ratios in a cylinder shape with 50% infill (P2), while the second set involved the best formulation printed in six different shapes (P1-P6). Crystalline CBD and the tested formulations were placed in a sinker containing 500 mL of HCl 0.1 M. The stirring speed was 100 rpm and the temperature was maintained at 37 °C during 4h. Aliquot samples of 2.0 mL were withdrawn at 5, 15, 30, 45, 60, 90, 120, 180 and 240 min. An equal volume of the gastric medium was replaced after each withdrawal. Samples were then analyzed by HPLC. The dissolution tests were carried out in triplicates.

### 2.3.9 Statistical Analysis

One-way ANOVA with a Tukey post-test was used thanks to GraphPad Prism 5.0 software to analyze the results. Differences in results of were considered significant with \* $p \leq 0.05$  and \*\*  $p \leq 0.01$ .

## 2.4 Results and discussion

### 2.4.1 *Impact of the Polymers Ratio on the Dissolution Speed*

#### 2.4.1.1 Filaments extrusion and Printed Tablets Production

The filament diameter is a crucial parameter to control before the printing. Indeed, it influences the traction of the filament by the two driving wheels of the printer as well as the mass and the dimensions of the final printed tablet. Achieving an accurate and consistent filament diameter is challenging and the production process of this filament sometimes needs to be modified. For example, the temperature, feed rate or screw speed can be changed to vary the diameter of the filament [33]. Extra equipment can also be added to the process, such as the use of a filament maker which is composed of an extruder that melts the material and extrudes it through a die, producing a filament that is pulled around a spool [34]. An optical sensor allows a very precise adjustment of the filament diameter. In this work, the diameter of the extruded filaments of F1, F2, F3, F4 and F5 measured at 20 different sections, was relatively constant with a range between 1.69 and 1.80 mm. This proved the suitability of the melt pump with the addition of a conveyor belt to precisely control the diameter.

Another essential parameter to obtain a printable formulation is the flexibility of the filament. EPO was chosen as a polymeric matrix for the increase of the aqueous solubility, in an acid medium, of CBD following a previous study [16]. Due to its ability to dissolve rapidly in the stomach, EPO is suitable for the production of immediate release formulations [35]. However, its brittleness makes it not printable without being plasticized so it was mixed with PEO for the production of the filaments [36]. Indeed, too brittle filaments could break between the two gears of the printer. PEO has already demonstrated its ability to increase the printability of EPO by plasticizing it [37]. All the formulations could be extruded, with a torque decreasing proportionally with the increase in the proportion of PEO, highlighting its plasticizing effect [38]. The resulting filaments were smooth, translucent, suggesting a complete dissolution of CBD in the polymers blend, and slightly yellow, due to the natural color of CBD [39].

Moreover, all the formulations could be printed, even those containing large proportions of EPO confirming the increase in flexibility of this polymer, even with low percentages of PEO.

#### 2.4.1.2 Drug Recovery

The HME and the FDM processes both involving relatively high temperatures thus the drug recovery was evaluated after HME and after the 3D printing of the five formulations (F1-F5). Since the final forms produced by FDM 3D printing are intended for hospital or

public pharmacies whereas the filament will be produced as a raw material, the limits of the CBD content have been set between 90 and 110% for printed tablets and 95-105% for the filaments.

The results on [Figure 37](#) show that the drug recovery, whether in the filaments or in the printed tablet, was between the defined limits, with a minimum and maximum of  $98.5 \pm 0.5\%$  and  $102.5 \pm 0.7\%$ , respectively. Moreover, there were no significant differences before and after the printing, for each formulation. These results are in accordance with the TGA analysis ([Appendix III.2](#)), as the extrusion and printing temperatures ( $140\text{ }^{\circ}\text{C}$  and  $180\text{ }^{\circ}\text{C}$ , respectively) did not exceed the degradation temperature of the CBD ( $220\text{ }^{\circ}\text{C}$ ).

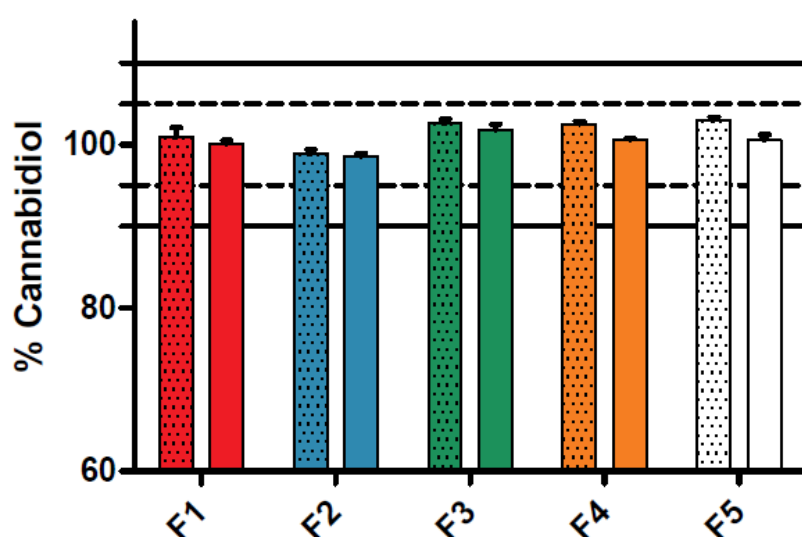


*Figure 37 – CBD recovery of the filaments (dashed columns) and the printed tablets (empty columns) of F1, F2, F3, F4 and F5. The defined limits of the drug recovery in the filaments are represented by the dotted lines at 95 and 105% and by the continuous lines at 90 and 110% for the drug recovery in the printed tablets.*

#### 2.4.1.3 In Vitro Dissolution Tests

The dissolution in an acidic medium of formulations F1, F2, F3, F4 and F5 was first carried out in order to choose the formulation which allowed the fastest dissolution of CBD. The curves on [Figure 38.a](#) show that each formulation improved the solubility of CBD compared to raw CBD. This improvement is explained first by the maintenance of the CBD in its amorphous form by the two polymers in the printed tablets, confirmed by the absence of the characteristic peaks of the crystalline CBD around  $10^{\circ}$  on the diffractogram patterns of F1, F2, F3, F4 and F5 printed disks ([Fig. 39](#)). The solubility of the CBD is also improved by the property of EPO to create micelles which can solubilize poor water-soluble molecules [40]. However, only F5 conducted to an immediate



release of the CBD, with  $83.91 \pm 2.15\%$  dissolved after 30 min which is significantly different from the other four formulations (Fig. 38.b). Indeed, F1, F2, F3 and F4 respectively dissolve  $54.03 \pm 4.64\%$ ,  $58.85 \pm 8.57\%$ ,  $59.69 \pm 1.92\%$  and  $65.85 \pm 9.19\%$ . This could be explained by the PEO/EPO ratio. PEO is well-known to form, on contact with aqueous media, a hydrogel which can slow the liberation of the drug [35,41]. This gelling effect leads to the conclusion that the more PEO there is, the slower the CBD will dissolve.

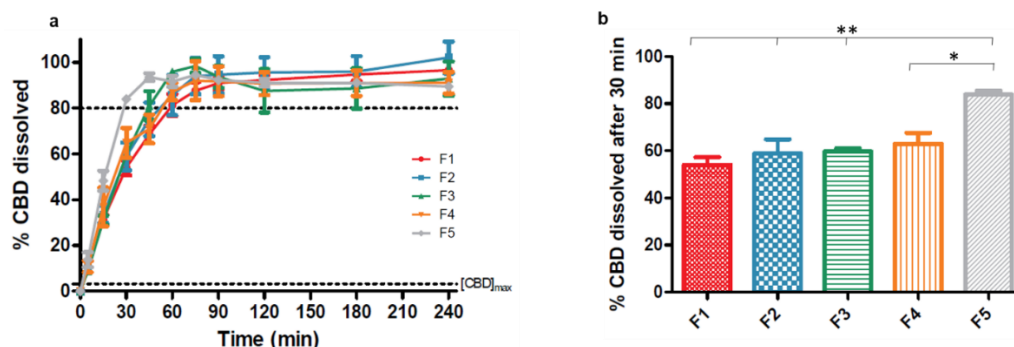


Figure 38 – Dissolution profile of F1 (red), F2 (blue), F3 (green), F4 (orange) and F5 (gray) in HCl 0.1 M (a) and focus on the percentage of dissolved CBD after 30 min depending on the EPO/PEO ratio (b).

The formulation F5 (PEO/EPO (20/80)) was selected to study the pharmaceutical quality of the six designs of printed tablets due to its ability to immediately release the CBD.

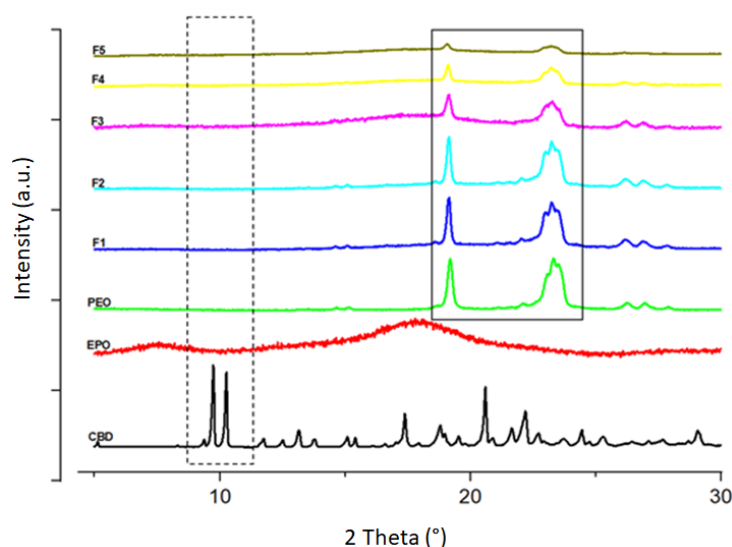


Figure 39 - XRD patterns of crystalline CBD (black), raw EPO (red), raw PEO (light green) and the printed disks composed of F1 (dark blue), F2 (light blue), F3 (purple), F4 (yellow) and F5 (dark green). The diffractogram of EPO shows a halo confirming the amorphous state of this polymer. The dotted frame shows the absence of the characteristic peaks of crystalline CBD at about 10° in each formulation, which means that CBD is completely amorphous in all printed disks. The continuous line frame highlights the semi-crystalline character of PEO which shows characteristic peaks at about 19° and 24°. These peaks are also present in the printed disks, suggesting rapid recrystallization of PEO.

#### 2.4.2 Impact of the morphology on the reproducibility and the pharmaco-technical performances

Cylinders and capsule-like forms (called gyroid in this study) are the most used shapes for the production of drugs. In that regard, these shapes were chosen to study the impact of the morphology on the reproducibility of the printed tablets manufacture, their mechanical properties and their *in vitro* dissolution performance. Each design could be printed by the printer, but with different durations (Fig. 40 and Table 8). Indeed, the cylinders were printed about three times faster than gyroids. It could be explained by the more complex structure of the gyroids compared to the one of the cylinders. One of the ways to print complex shapes accurately is to reduce the printing speed [42].

The diameter and height of the 10 printed tablets of each design were measured and the deviation from the dimensions of the digital model is shown in Table 8. All the printed tablets had a deviation of the diameter from  $-1 \pm 0.15\%$  to  $1 \pm 0.51\%$  compared to the digital model. Regarding the height, the printed tablets had a deviation ranging from  $-1.44 \pm 0.23\%$  to  $-0.33 \pm 0.71\%$ . These narrow ranges are similar to other studies [43,44]. As described above, the mass of the printed product depends on the uniformity of the diameter of the filament fed into the printer. The *mass variation* and *uniformity of mass* tests ensure that the mass of all the printed tablets produced is within the limits defined

by the Eur. Ph. **Figure 41** represents the mean mass measured on ten printed tablets of each design and the AV for each design. Results show a deviation of the mass of the printed tablets compared to the target mass (650 mg) going from -18.43 mg for P5 to +24.99 mg for P1. Numerous ranges of mass deviation from the mass target are found in the literature [45,46]. The deviation from this study is among the largest. This can be explained by the relatively large size of the printed tablets. Indeed, the mass of the printed shapes is mainly influenced by the consistency of the diameter of the previously extruded filament. The larger the printed tablets, the more the inconsistency of the filament will be reflected in the mass deviation. Concerning the mass uniformity, the AV of P4, P5 and P6 (gyroids) tend to be higher than the ones of P1, P2 and P3 (cylinders). This is probably another consequence of the complexity of the gyroid structure. However, all the designs were in accordance with the mass variation test, as every AV was below 15.00, and with mass uniformity test, as deviations of respectively -7.69% and +6.36% for the most under and over weighted tablet were observed. Moreover, no more than two printed tablets per formulation deviated from more than 5% of the average mass. The test was therefore compliant and proved the ability of the FDM to produce printed tablets with adequate reproducibility.

The results concerning the printed tablets dimensions and the mass variation and uniformity highlight the good reproducibility of the printed tablets manufacture by the 3D Original Prusa i3 MK3 printer, no matter the design to print.

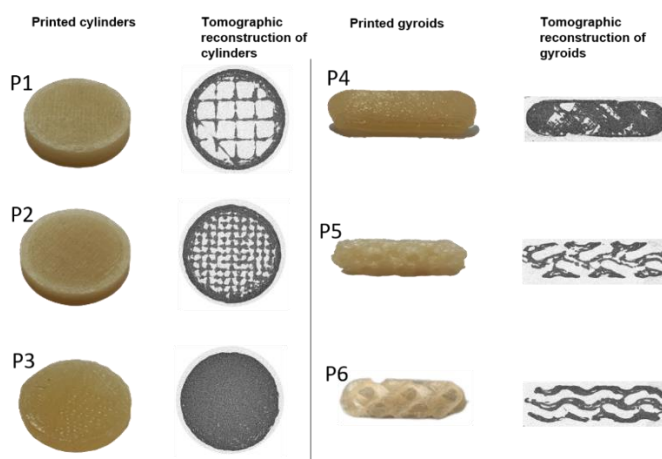


*Figure 40 - Pictures of the printed tablets and their respective tomographic reconstruction performed by Computerized Tomography Scan.*

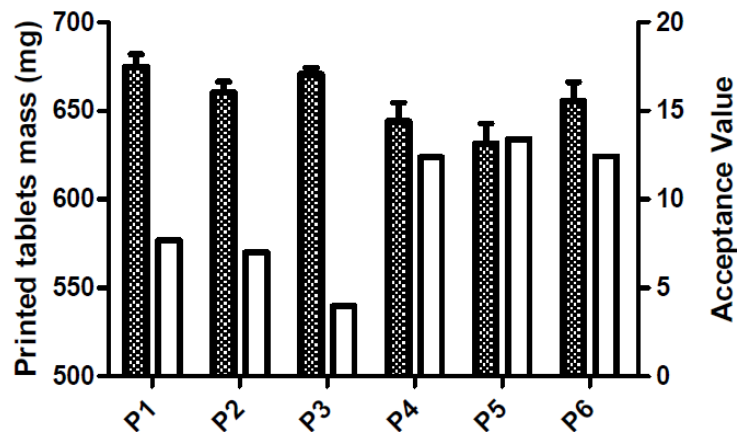


Figure 41 - Mass of the printed tablet of the 6 designs (mean and SD,  $n = 10$ ) represented by the dashed columns and the AV for each design represented by the empty columns (measured on ten printed tablets).

In addition to the reproducibility, the morphology of the final printed form influences its mechanical properties [47,48]. The *friability* and the *tensile strength* are two important parameters concerning the study of the integrity of oral solid dosage forms during the production, transport and handling by the patient. The results on Table 8 show that the mass loss during the friability test was  $<1\%$  for each formulation and met the Eur. Ph. recommendation. Compared to the standard techniques for the manufacturing of oral solid forms such as tableting, or other 3D printing techniques like powder-based 3D printing, FDM allows the production of products with a poor friability without additional steps or excipients (Chang et al., 2021; Infanger et al., 2019; Lakshman et al., 2011).

Table 8 - Characterization of the printed tablets

	Diameter <sup>a</sup> (%) (n=10)	Height <sup>a</sup> (%) (n=10)	Surface Area (mm <sup>2</sup> )	Surface Area to volume ratio	Friability (%)*	Tensile Strength (MPa) (n=3)	Printing Time (min)
P1	99.00±0.15	99.67±0.71	1129.1	1.86	0.25	1.80±0.01	±5
P2	100.53±0.13	99.54±0.09	908.3	1.53	0.11	2.43±0.04	±5
P3	101.00±0.17	98.91±0.17	792.8	1.34	0.24	4.32±0.27	±5
P4	100.47±0.14	98.56±0.16	626.6	1.03	0.14	4.63±0.07	±14
P5	101.00±0.51	98.72±0.34	2528.8	4.09	0.21	0.58±0.01	±14
P6	99.39±0.17	98.56±0.23	2914.6	4.83	0.85	0.25±0.02	±14

a% = printed model/digital model (measured in triplicate). \* = measured on ten printed tablets.

Finally, dissolution tests were conducted to study the impact of the morphology on the release of the CBD in HCl 0.1 M. Figure 42.b shows that the dissolution profiles during

the first 30 min of the test are different. P1, P2, P5 and P6 allowed an immediate release of CBD (>80%). P5 and P6 even exceeded 80% dissolution of CBD in less than 15 min which is equivalent to more than 52 mg of CBD. This is, to the best of our knowledge, the dissolution of the highest dose of a poor soluble API from a printed tablet at this time. Indeed, formulations manufactured by FDM show generally a slower release than the ones manufactures by conventional techniques [49]. This may be caused by the rigid structures formed after the successive melting and solidification by cooling of the polymeric product conducting to a slow erosion-based dissolution of the product. Alhijaj *et al.* investigated the polymeric blend of EPO/polysorbate 80/PEG 4000/Polyethylene oxide to print formulations with an immediate release of felodipin [50]. The immediate release was obtained as 84.3% of the drug dissolved in 30 min, but it represents only about 5 mg of the drug. Similarly, Sadia *et al.* printed blends of EPO/TEC/TCP/drug using four different drugs including the poorly water-soluble prednisolone [36]. The *in vitro* dissolution tests showed 85% of dissolved drug in 30 min, equal to about 25 mg of prednisolone. In a more recent study, Crisan *et al.* aimed at printing immediate release forms containing high doses of diclofenac sodium. They managed to release up to about 70 mg of API in 10 min in a pH 6.8 buffer. However, even is diclofenac sodium is classified in BCS II in acidic media, it is highly soluble in this pH 6.8 buffer [51,52].

On the other hand, P3 and P4 released CBD less quickly as it took them 45 min to reach 80% of dissolution, so they did not meet the FDA criteria for immediate release oral dosage forms. These differences can be explained first by the higher tensile strength of P3 and P4, reflecting a more compact and resistant structure, slower to dissolve. The slower dissolution can also be explained by the surface-to-volume (SA/V) ratio of the printed tablet ([Table 8](#)). The higher this ratio, the faster the dissolution [53,54]. The results shown in [Figure 42.d](#) are consistent with these studies. Indeed, the greater the SA/V, the less time it takes to dissolve 80% of the CBD.

The dissolution tests showed that, for a constant weight, the gyroids allow a faster dissolution of the CBD as these designs had a higher SA/V ratio. However, the shape of the printed tablets had no influence on the increase of the CBD aqueous solubility. Indeed, [Figure 42.c](#) shows that all the dissolution profiles are similar once the maximum of dissolution is reached. This can be explained by the same composition of all the printed tablets.

The data of the dissolution tests conducted in this study show that FDM 3D printing allows the manufacturing of oral solid dosage forms with adjustable dissolution speed and rate, which is very interesting for drugs with different therapeutic uses such as CBD.

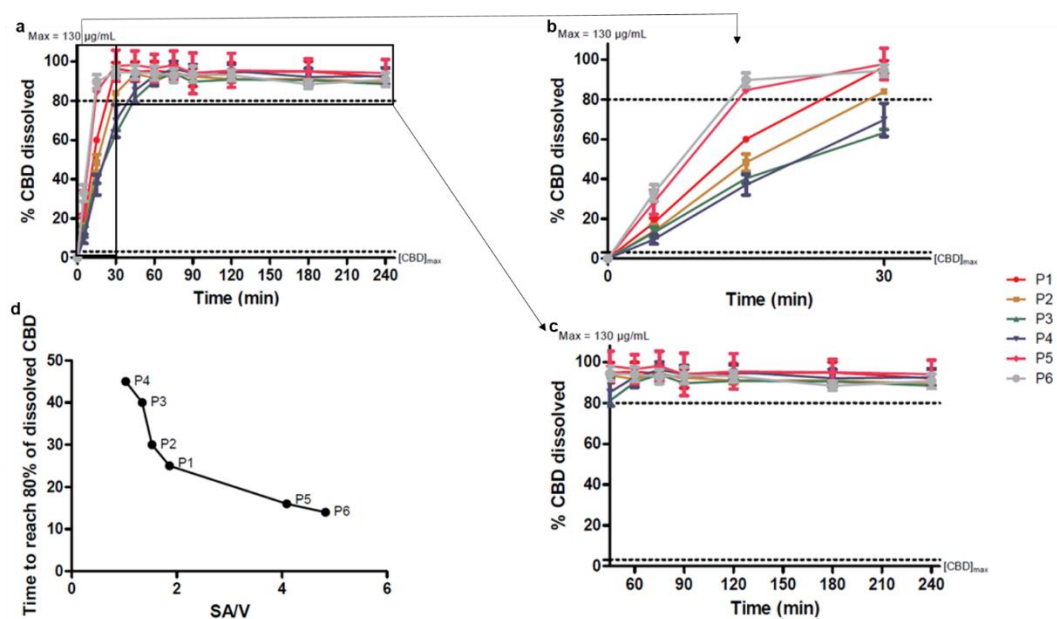


Figure 42 – Dissolution profile of P1 (red), P2 (yellow), P3 (green), P4 (blue), P5 (pink) and P6 (gray) during the whole test (A), between the beginning and 45 min of the test (B) and between 45 and the end of the test (C).

Among the printed tablets that allow an immediate release of CBD (P1, P2, P5 and P6), even if P5 and P6 achieve 80% release significantly faster than the others (P value  $\leq 0.01$ ), P1 was chosen for the rest of the study because its production is three times faster than P5 and P6.

#### 2.4.3 Evaluation of the dosage adaptability

This section was intended to support the hypothesis that by manufacturing printed tablets with the same shape and infill but with different dosages, the requirements of the Eur. Ph. and the reproducibility described above would still be fulfilled. The dimensions of cylinders with 20% infill based on the design of P1 were adjusted to obtain printed tablets containing 32.5 or 97.5 mg of CBD which are 50% and 150% of the target mass of P1, respectively. The characterization of the printed cylinders with different dosages are gathered on [Table 9](#). The diameter of the printed tablets containing 32.5 and 97.5 mg of CBD were similar to the one of the printed cylinder with 65 mg of CBD with a deviation of  $-0.3 \pm 0.05\%$  and  $-1.88 \pm 0.2\%$ , respectively. The same goes for the height, with a deviation of  $+0.04 \pm 0.17\%$  for the cylinders containing 32.5 mg of CBD and  $-1.98 \pm 0.31\%$  for the cylinders with 97.5 mg of CBD. The deviation of the average mass of the printed tablets compared to the target mass was smaller for the cylinders with 32.5 mg of CBD (+7.20 mg) than for the cylinders with 97.5 mg of CBD (-30.02 mg). This could be due to the proportional effect of the inconstancy of the filament diameter

and the size of the printed shape, as explained above. However, both dosages allowed a mass uniformity in accordance with the Eur. Ph., as the AVs were below 15.00. No significant changes were expected in the mechanical properties by modifying the printed tablets dimensions and dosage as the manufacturing process remains the same. Friability test compliance was unaffected by these changes, confirming the rigid structure of the printed shapes. It goes the same for the tensile strength which was not affected as it is normalized according to the shape of the printed tablet.

*Table 9 - Characterization of the printed cylinders with 20% infill and different dosages*

Dosage (mg CBD)	Diameter <sup>a</sup> (%) n=10	Height <sup>a</sup> (%) n=10	Deviation of average mass (mg)*	SA/V ratio	Friability (%)*	AV*	Tensile Strength (MPa) n=10	Printing Time (min)
32.5	99.70± 0.05	100.0 4± 0.17	+7.20± 1.77	1.36	0.21	3.11	2.13± 0.07	±3
65	99.00± 0.15	99.67 ±0.71	+24.99± 3.05	1.86	0.25	7.69	1.80± 0.01	±5
97.5	98.12± 0.20	98.02 ±0.31	30.02± 2.87	0.98	0.26	14.53	2.00± 0.2	±7

a% = printed model/digital model (measured in triplicate). \* = measured on ten printed tablets.

The dissolution tests performed with the three dosages showed a dissolution rate proportionnal to the dosage of CBD at the start of the test ([Fig. 43](#)). Indeed, the 32.5 mg, 65 mg and 97.5 mg cylinders dissolved 43.93±2.01%, 59.98±0.29% and 77.48±3.63% after 15 min, respectively. The difference in dissolution rate is not due to SA/V. The SA/V of the three cylinders tested evolves as follows:  $SA/V_{97.5mg} < SA/V_{32.5mg} < SA/V_{65mg}$  ([Table 9](#)). In this case, the increase of the early dissolution rate could be due to the higher gradient concentration between the solid form and the aqueous medium that could lead to a faster dissolution of the formulations with a high drug load. However, after 30 min of dissolution testing, the three dosage forms reached their maximum of dissolution which was maintained until the end of the test. More than 80% of CBD was dissolved for the three formulations, translating an IR.

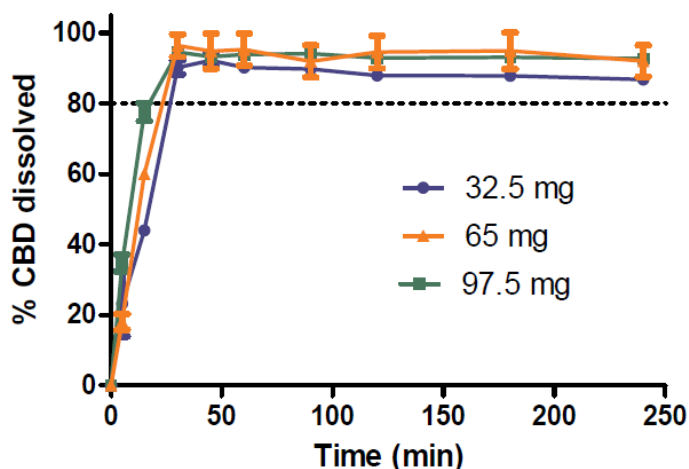


Figure 43 - Dissolution profile of the printed cylinders with 20% infill and different dosages.

These results concerning the dosage adaptability show the advantage of using FDM for the production of solid oral forms containing APIs used at various dosages depending on the treatment. Indeed, the dosage could be customized, by the simple step of modifying the digital pattern intended to be printed, without affecting the quality of the final product.

## 2.5 Conclusion

The pharmaceutical industry is paying more and more attention to personalized medicine. This study has proven that challenges inherent to the manufacture of customized dosage forms can be overcome by FDM 3D printing. Indeed, printed tablets of CBD with complex structures were successfully produced with a good reproducibility. Different dissolution rates of CBD were obtained from these printed tablets, even with a high quantity of CBD. Since there are no specific guidelines for the product manufactured by 3D printing, the quality control of these printed tablets was conducted following the monograph concerning the uncoated tablets of the Eur. Ph., as recommended by the FDA. As a result, all printed tablets were in accordance with the specifications of this monograph. In addition, the modification of the strength of these printed forms had no impact on their quality. These results are encouraging when it comes to the implementation of FDM in hospitals or public pharmacies in order to develop personalized medicine affordable by every patient.



### 2.6 Acknowledgments

The authors wish to acknowledge FEDER funds for the support in SOLPHARE FEDER project ([884148-329407](#)) and the Fonds Léon Fredericq for the support in project 2021-2022-12. The authors also wish to thank Wenda Lazzari and Astrid Couturier (Mithra CDMO) for the loan and the support of the melt pump.

## 2.7 References

- [1] M. Ryan, Cannabidiol in epilepsy: The indications and beyond, *Ment. Heal. Clin.* 10 (2020) 317–325. <https://doi.org/10.9740/mhc.2020.11.317>.
- [2] M. Mazurkiewicz-Beldzińska, M. Zawadzka, Use of cannabidiol in the treatment of epilepsy, *Neurol. Neurochir. Pol.* 56 (2022) 14–20. <https://doi.org/10.5603/PJNNS.a2022.0020>.
- [3] M.M. Bergamaschi, R. Helena Costa Queiroz, M. Hortes, N. Chagas, D. Chaves Gomes De Oliveira, B.S. De Martinis, F. Kapczinski, J. Quevedo, R. Roesler, N. Schröder, A.E. Nardi, R. Martín-Santos, J.E.C. Hallak, A.W. Zuardi, J. Alexandre, S. Crippa, Cannabidiol Reduces the Anxiety Induced by Simulated Public Speaking in Treatment-Naïve Social Phobia Patients, *Neuropsychopharmacology*. 36 (2011) 1219–1226. <https://doi.org/10.1038/npp.2011.6>.
- [4] C.G. Heider, S.A. Itenberg, J. Rao, H. Ma, X. Wu, Mechanisms of Cannabidiol (CBD) in Cancer Treatment: A Review, (2022). <https://doi.org/10.3390/biology11060817>.
- [5] P. McGuire, P. Robson, W.J. Cubala, D. Vasile, P.D. Morrison, R. Barron, A. Taylor, S. Wright, Cannabidiol (CBD) as an adjunctive therapy in schizophrenia: A multicenter randomized controlled trial, *Am. J. Psychiatry*. 175 (2018) 225–231. <https://doi.org/10.1176/appi.ajp.2017.17030325>.
- [6] Y.L. Hurd, S. Spriggs, J. Alishayev, G. Winkel, K. Gurgov, C. Kudrich, A.M. Oprescu, E. Salsitz, Cannabidiol for the Reduction of Cue-Induced Craving and Anxiety in Drug-Abstinent Individuals With Heroin Use Disorder: A Double-Blind Randomized Placebo-Controlled Trial, *Am J Psychiatry*. 176 (2019) 911–922. <https://doi.org/10.1176/appi.ajp.2019.18101191>.
- [7] S. Millar, N. Stone, Z. Bellman, A. Yates, T. England, C.A. Sophie Millar, A systematic review of cannabidiol dosing in clinical populations, *Artelo Biosci. Biotechnol. Biol. Sci. Res. Coun.* (2019). <https://doi.org/10.1111/bcp.14038>.
- [8] O.M. Feeney, M.F. Crum, C.L. McEvoy, N.L. Trevaskis, H.D. Williams, C.W. Pouton, W.N. Charman, C.A.S. Bergström, C.J.H. Porter, 50 years of oral lipid-based formulations: Provenance, progress and future perspectives, *Adv. Drug Deliv. Rev.* 101 (2016) 167–194. <https://doi.org/10.1016/j.addr.2016.04.007>.
- [9] Y. Nakano, M. Tajima, E. Sugiyama, V.H. Sato, H. Sato, Development of a Novel Nano-emulsion Formulation to Improve Intestinal Absorption of Cannabidiol, *Med. Cannabis Cannabinoids*. 2 (2019) 35–42. <https://doi.org/10.1159/000497361>.
- [10] N.N.B. Williams, T.R. Ewell, K.S.S. Abbotts, K.J. Harms, K.A. Woelfel, G.P. Dooley, T.L. Weir, C. Bell, Comparison of five oral cannabidiol preparations in adult humans: Pharmacokinetics, body composition, and heart rate variability, *Pharmaceutics*. 14 (2021) 1–14. <https://doi.org/10.3390/ph14010035>.
- [11] J.M. Hobbs, A.R. Vazquez, N.D. Remijan, R.E. Trotter, T. V McMillan, K.E. Freedman, Y. Wei, K.A. Woelfel, O.R. Arnold, L.M. Wolfe, S.A. Johnson, T.L. Weir, C.A. Sarah Johnson, Evaluation of pharmacokinetics and acute anti-inflammatory potential of two oral cannabidiol preparations in healthy adults, (2020). <https://doi.org/10.1002/ptr.6651>.
- [12] K.F. Boehnke, · Winfried Häuser, M.-A. Fitzcharles, Cannabidiol (CBD) in Rheumatic Diseases (Musculoskeletal Pain), *Curr. Rheumatol. Rep.* 24 (2022) 238–246. <https://doi.org/10.1007/s11926->

022-01077-3.

- [13] B.N. Tran, Q. Van Pham, B.T. Tran, G. Thien Le, A.H. Dao, T.H. Tran, C.N. Nguyen, Supercritical CO<sub>2</sub> impregnation approach for enhancing dissolution of fenofibrate by adsorption onto high-surface area carriers, *J. Supercrit. Fluids.* 184 (2022) 105584. <https://doi.org/10.1016/j.supflu.2022.105584>.
- [14] J. Petitprez, · François-Xavier Legrand, · Catherine Tams, · J D Pipkin, V. Antle, M. Kfoury, S. Fourmentin, Huge solubility increase of poorly water-soluble pharmaceuticals by sulfobutylether- $\beta$ -cyclodextrin complexation in a low-melting mixture, *Environ. Chem. Lett.* 20 (2022) 1561–1568. <https://doi.org/10.1007/s10311-022-01415-y>.
- [15] A. Singh, G. Van den Mooter, Spray drying formulation of amorphous solid dispersions, *Adv. Drug Deliv. Rev.* 100 (2016) 27–50. <https://doi.org/10.1016/j.addr.2015.12.010>.
- [16] O. Jennotte, N. Koch, A. Lechanteur, B. Evrard, Development of amorphous solid dispersions of cannabidiol: Influence of the carrier, the hot-melt extrusion parameters and the use of a crystallization inhibitor, *J. Drug Deliv. Sci. Technol.* 71 (2022) 103372. <https://doi.org/10.1016/j.jddst.2022.103372>.
- [17] I. Koutsamanis, M. Spoerk, F. Arbeiter, S. Eder, E. Roblegg, Development of Porous Polyurethane Implants Manufactured via Hot-Melt Extrusion, *Polymers (Basel)*. 12 (2020). <https://doi.org/10.3390/polym12122950>.
- [18] A. Butreddy, S. Sarabu, S. Bandari, A. Batra, K. Lawal, N.N. Chen, V. Bi, T. Durig, M.A. Repka, Influence of Plasdone™ S630 Ultra-an Improved Copovidone on the Processability and Oxidative Degradation of Quetiapine Fumarate Amorphous Solid Dispersions Prepared via Hot-Melt Extrusion Technique, *AAPS PharmSciTech.* 22 (2021) 196. <https://doi.org/10.1208/s12249-021-02069-9>.
- [19] N.N. Mohammed, S. Majumdar, A. Singh, W. Deng, N.S. Murthy, E. Pinto, D. Tewari, T. Durig, M.A. Repka, Klucel™ EF and ELF polymers for immediate-release oral dosage forms prepared by melt extrusion technology, *AAPS PharmSciTech.* 13 (2012) 1158–1169. <https://doi.org/10.1208/s12249-012-9834-z>.
- [20] N. Dumpa, A. Butreddy, H. Wang, N. Komanduri, S. Bandari, M.A. Repka, 3D printing in personalized drug delivery: An overview of hot-melt extrusion-based fused deposition modeling, *Int. J. Pharm.* 600 (2021) 120501. <https://doi.org/10.1016/j.ijpharm.2021.120501>.
- [21] N. Samiei, Recent trends on applications of 3D printing technology on the design and manufacture of pharmaceutical oral formulation: a mini review, *Beni-Suef Univ. J. Basic Appl. Sci.* 9 (2020). <https://doi.org/10.1186/s43088-020-00040-4>.
- [22] J. Quodbach, M. Bogdahn, J. Breitreutz, R. Chamberlain, K. Eggenreich, A.G. Elia, N. Gottschalk, G. Gunkel-Grabole, L. Hoffmann, D. Kapote, T. Kipping, S. Klinken, F. Loose, T. Marquetant, H. Windolf, S. Geißler, T. Spitz, Quality of FDM 3D Printed Medicines for Pediatrics: Considerations for Formulation Development, Filament Extrusion, Printing Process and Printer Design, *Ther. Innov. Regul. Sci.* 56 (2022) 910–928. <https://doi.org/10.1007/s43441-021-00354-0>.
- [23] A. Goyanes, F. Fina, A. Martorana, D. Sedough, S. Gaisford, A.W. Basit, Development of modified release 3D printed tablets (printlets) with pharmaceutical excipients using additive manufacturing, *Int. J. Pharm.* 527 (2017) 21–30. <https://doi.org/10.1016/j.ijpharm.2017.05.021>.
- [24] M. Sadia, A. Isreb, I. Abbadi, M. Isreb, D. Aziz, A. Selo, P. Timmins, M.A. Alhnan, From 'fixed dose combinations' to 'a dynamic dose combiner': 3D printed bi-layer antihypertensive tablets, *Eur. J.*

- Pharm. Sci. 123 (2018) 484–494. <https://doi.org/10.1016/j.ejps.2018.07.045>.
- [25] N. Scoutaris, S.A. Ross, D. Douroumis, 3D Printed B Starmix ^ Drug Loaded Dosage Forms for Paediatric Applications, (2018) 1–11.
- [26] S.J. Trenfield, A. Awad, C.M. Madla, G.B. Hatton, J. Firth, A. Goyanes, S. Gaisford, A.W. Basit, Shaping the future: recent advances of 3D printing in drug delivery and healthcare, *Expert Opin. Drug Deliv.* 16 (2019) 1081–1094. <https://doi.org/10.1080/17425247.2019.1660318>.
- [27] S. Mohapatra, R.K. Kar, P.K. Biswal, S. Bindhani, Approaches of 3D printing in current drug delivery, *Sensors Int.* 3 (2022) 100146. <https://doi.org/10.1016/j.sintl.2021.100146>.
- [28] J. Norman, R.D. Madurawe, C.M.V. Moore, M.A. Khan, A. Khairuzzaman, A new chapter in pharmaceutical manufacturing: 3D-printed drug products, *Adv. Drug Deliv. Rev.* 108 (2017) 39–50. <https://doi.org/10.1016/j.addr.2016.03.001>.
- [29] FDA, Dissolution Testing and Acceptance Criteria for Immediate-Release Solid Oral Dosage Form Drug Products Containing High Solubility Drug Substances Guidance for Industry, 8 (2018). [http://www.fda.gov/Drugs/GuidanceComplianceRegulatoryInformation/Guidances/default.htm%0Afile:///C:/Users/ASUS/Desktop/Rujukan PhD/Drug Release/1074043 FNL\\_clean.pdf](http://www.fda.gov/Drugs/GuidanceComplianceRegulatoryInformation/Guidances/default.htm%0Afile:///C:/Users/ASUS/Desktop/Rujukan PhD/Drug Release/1074043 FNL_clean.pdf).
- [30] D. Izgelov, M. Freidman, A. Hoffman, Investigation of cannabidiol gastro retentive tablets based on regional absorption of cannabinoids in rats, *Eur. J. Pharm. Biopharm.* 152 (2020) 229–235. <https://doi.org/10.1016/j.ejpb.2020.05.010>.
- [31] N. Koch, O. Jennotte, Y. Gasparrini, F. Vandenbroucke, A. Lechanteur, B. Evrard, Cannabidiol aqueous solubility enhancement: Comparison of three amorphous formulations strategies using different type of polymers, *Int. J. Pharm.* 589 (2020) 119812. <https://doi.org/10.1016/j.ijpharm.2020.119812>.
- [32] K.G. Pitt, M.G. Heasley, Determination of the tensile strength of elongated tablets, *Powder Technol.* 238 (2013) 169–175. <https://doi.org/10.1016/j.powtec.2011.12.060>.
- [33] J. Aho, J.P. Bøtker, N. Genina, M. Edinger, L. Arnfast, Roadmap to 3D-Printed Oral Pharmaceutical Dosage Forms : Feedstock Filament Properties and Characterization for Fused Deposition Modeling, *J. Pharm. Sci.* 108 (2019) 26–35. <https://doi.org/10.1016/j.xphs.2018.11.012>.
- [34] C. Parulski, O. Jennotte, A. Lechanteur, B. Evrard, Challenges of fused deposition modeling 3D printing in pharmaceutical applications: Where are we now?, *Adv. Drug Deliv. Rev.* 175 (2021). <https://doi.org/10.1016/j.addr.2021.05.020>.
- [35] H.E. Gültekin, S. Tort, F. Acartürk, Fabrication of Three Dimensional Printed Tablets in Flexible Doses: A Comprehensive Study from Design to Evaluation, *SSRN Electron. J.* 74 (2022) 103538. <https://doi.org/10.2139/ssrn.4028237>.
- [36] M. Sadia, A. So, B. Arafat, A. Isreb, W. Ahmed, Adaptation of pharmaceutical excipients to FDM 3D printing for the fabrication of patient-tailored immediate release tablets, *Int. J. Pharm.* 513 (2016) 659–668. <https://doi.org/10.1016/j.ijpharm.2016.09.050>.
- [37] S. Henry, L. De Wever, V. Vanhoorne, T. De Beer, C. Vervaet, Influence of print settings on the critical quality attributes of extrusion-based 3d-printed caplets: A quality-by-design approach, *Pharmaceutics*. 13 (2021). <https://doi.org/10.3390/PHARMACEUTICS13122068>.

- [38] M.M. Crowley, F. Zhang, M.A. Repka, S. Thumma, S.B. Upadhye, S.K. Battu, J.W. McGinity, C. Martin, Pharmaceutical applications of hot-melt extrusion: Part I, *Drug Dev. Ind. Pharm.* 33 (2007) 909–926. <https://doi.org/10.1080/03639040701498759>.
- [39] J. Macedo, A. Samaro, V. Vanhoorne, C. Vervae, J.F. Pinto, Processability of poly(vinyl alcohol) Based Filaments With Paracetamol Prepared by Hot-Melt Extrusion for Additive Manufacturing, *J. Pharm. Sci.* 109 (2020) 3636–3644. <https://doi.org/10.1016/j.xphs.2020.09.016>.
- [40] X. Lin, L. Su, N. Li, Y. Hu, G. Tang, L. Liu, H. Li, Z. Yang, Understanding the mechanism of dissolution enhancement for poorly water-soluble drugs by solid dispersions containing Eudragit® E PO, *J. Drug Deliv. Sci. Technol.* 48 (2018) 328–337. <https://doi.org/10.1016/j.jddst.2018.10.008>.
- [41] S. Shojaee, P. Emami, A. Mahmood, Y. Rowaiye, A. Dukulay, W. Kaialy, I. Cumming, A. Nokhodchi, An Investigation on the Effect of Polyethylene Oxide Concentration and Particle Size in Modulating Theophylline Release from Tablet Matrices, *AAPS PharmSciTech.* 16 (2015) 1281–1289. <https://doi.org/10.1208/s12249-015-0295-z>.
- [42] T.S. Tamir, G. Xiong, Q. Fang, X. Dong, Z. Shen, F.Y. Wang, A feedback-based print quality improving strategy for FDM 3D printing: an optimal design approach, *Int. J. Adv. Manuf. Technol.* 120 (2022) 2777–2791. <https://doi.org/10.1007/s00170-021-08332-4>.
- [43] S. Obeid, M. Madžarević, M. Krkobabić, S. Ibrić, Predicting drug release from diazepam FDM printed tablets using deep learning approach: Influence of process parameters and tablet surface/volume ratio, *Int. J. Pharm.* 601 (2021). <https://doi.org/10.1016/j.ijpharm.2021.120507>.
- [44] C. Wei, N.G. Solanki, J.M. Vasoya, A. V. Shah, A.T.M. Serajuddin, Development of 3D Printed Tablets by Fused Deposition Modeling Using Polyvinyl Alcohol as Polymeric Matrix for Rapid Drug Release, *J. Pharm. Sci.* 109 (2020) 1558–1572. <https://doi.org/10.1016/j.xphs.2020.01.015>.
- [45] C. Parulski, E. Gresse, O. Jennotte, A. Felten, E. Ziemons, A. Lechanteur, B. Evrard, Fused deposition modeling 3D printing of solid oral dosage forms containing amorphous solid dispersions: How to elucidate drug dissolution mechanisms through surface spectral analysis techniques?, *Int. J. Pharm.* 626 (2022). <https://doi.org/10.1016/j.ijpharm.2022.122157>.
- [46] J. Skowrya, K. Pietrzak, M.A. Alhnan, Fabrication of extended-release patient-tailored prednisolone tablets via fused deposition modelling (FDM) 3D printing, *Eur. J. Pharm. Sci.* 68 (2015) 11–17. <https://doi.org/10.1016/j.ejps.2014.11.009>.
- [47] P.K. Nukala, S. Palekar, N. Solanki, Y. Fu, M. Patki, A.A. Shohatee, L. Trombetta, K. Patel, Investigating the application of FDM 3D printing pattern in preparation of patient-tailored dosage forms, *J. 3D Print. Med.* 3 (2019) 23–37. <https://doi.org/10.2217/3dp-2018-0028>.
- [48] M. Fanous, M. Bitar, S. Gold, A. Sobczuk, S. Hirsch, J. Ogorka, G. Imanidis, Development of immediate release 3D-printed dosage forms for a poorly water-soluble drug by fused deposition modeling: Study of morphology, solid state and dissolution, *Int. J. Pharm.* 599 (2021) 120417. <https://doi.org/10.1016/j.ijpharm.2021.120417>.
- [49] W. Kempin, V. Domsta, G. Grathoff, I. Brecht, B. Semmling, S. Tillmann, W. Weitschies, A. Seidlitz, Immediate Release 3D-Printed Tablets Produced Via Fused Deposition Modeling of a Thermo-Sensitive Drug, (2018).
- [50] M. Alhijaj, P. Belton, S. Qi, An investigation into the use of polymer blends to improve the printability

of and regulate drug release from pharmaceutical solid dispersions prepared via fused deposition modeling (FDM) 3D printing, *Eur. J. Pharm. Biopharm.* 108 (2016) 111–125. <https://doi.org/10.1016/j.ejpb.2016.08.016>.

- [51] A.G. Crişan, S. Iurian, A. Porfire, L.M. Rus, C. Bogdan, T. Casian, R.C. Lucacel, A. Turza, S. Porav, I. Tomuţă, QbD guided development of immediate release FDM-3D printed tablets with customizable API doses, *Int. J. Pharm.* 613 (2022). <https://doi.org/10.1016/j.ijpharm.2021.121411>.
- [52] G. Kibria, M.A. Roni, M.S. Absar, R.U. Jalil, Effect of plasticizer on release kinetics of diclofenac sodium pellets coated with eudragit RS 30 D, *AAPS PharmSciTech.* 9 (2008) 1240–1246. <https://doi.org/10.1208/s12249-008-9163-4>.
- [53] A. Goyanes, P. Robles Martinez, A. Buanz, A.W. Basit, S. Gaisford, Effect of geometry on drug release from 3D printed tablets, *Int. J. Pharm.* 494 (2015) 657–663. <https://doi.org/10.1016/j.ijpharm.2015.04.069>.
- [54] S. Obeid, M. Madžarević, M. Krkobabić, S. Ibrić, Predicting drug release from diazepam FDM printed tablets using deep learning approach: Influence of process parameters and tablet surface/volume ratio, *Int. J. Pharm.* 601 (2021). <https://doi.org/10.1016/j.ijpharm.2021.120507>.

## Chapter IV. FEASIBILITY STUDY OF THE USE OF A HOMEMADE 3D POWDER PRINTER FOR THE PRODUCTION OF SOLID FORMS WITH IMMEDIATE RELEASE OF CANNABIDIOL

### 1. Context and purpose of the study

Printed tablets composed of an ASD of CBD with an immediate release were successfully manufactured by FDM coupled with HME, as previously described. However, development of filaments intended to be printed by FDM is challenging, expensive and time consuming [1]. Indeed, the filament must have specific mechanical properties as well as a constant diameter. Diameter control is often done using equipment in addition to the hot-melt extruder, especially a conveyor belt, but melt pump of filament maker may also be used.

DPE has recently been studied in the pharmaceutical field. This 3D printing technology can be useful in overcoming FDM limitations. Indeed, DPE does not require the manufacture of a filament since it allows to print directly from a powder mixture [2]. Therefore, the goal of this study was to assess the ability of a direct powder extruder which has been developed by our partner SIRRI, to print immediate-release solid forms of CBD while complying with Eur. Ph. requirements for uncoated tablets.

The previous study demonstrated the feasibility of increasing CBD aqueous solubility and dissolution rate from printed oral dosage forms formulated with EPO and PEO. Due to flow issue encountered with EPO, we had to work with milled Eudragit® E100 (E100) to obtain a powder with flow characteristic compatible with DPE [3]. SOL, another amorphous polymer with good flow properties, was also tested to manufacture printed tablets.

Extrudability studies of different polymers-CBD blends were performed in order to select the formulations to be printed for the fabrication of cylindrical oral dosage forms.

These printer cylinders were evaluated in terms of mechanical and dissolution performances.

The results of this work are described in the article to be submitted entitled: "Feasibility study of the use of a homemade direct powder extrusion printer to manufacture printed tablets with an immediate release of a BCS II molecule".

To complete the study, XRD analysis were performed on each printed tablet stored at  $25 \pm 2$  °C with of  $60 \pm 5\%$  RH during two months, in order to assess the stability of CBD's amorphous state over time. As shown in [Appendix III.1](#), CBD remained

amorphous in all printed tablets, demonstrating the formulations' ability to stabilize the amorphous state of CBD.



- [1] C. Parulski, O. Jennotte, A. Lechanteur, B. Evrard, Challenges of fused deposition modeling 3D printing in pharmaceutical applications: Where are we now?, *Adv. Drug Deliv. Rev.* 175 (2021). <https://doi.org/10.1016/j.addr.2021.05.020>.
- [2] B.M. Boyle, P.T. Xiong, T.E. Mensch, T.J. Werder, G.M. Miyake, 3D printing using powder melt extrusion, *Addit. Manuf.* 29 (2019) 100811. <https://doi.org/10.1016/j.addma.2019.100811>.
- [3] A. Samaro, B. Shaqour, N.M. Goudarzi, M. Ghijs, L. Cardon, M.N. Boone, B. Verleije, K. Beyers, V. Vanhoorne, P. Cos, C. Vervaet, Can filaments, pellets and powder be used as feedstock to produce highly drug-loaded ethylene-vinyl acetate 3D printed tablets using extrusion-based additive manufacturing?, *Int. J. Pharm.* 607 (2021). <https://doi.org/10.1016/j.ijpharm.2021.120922>.

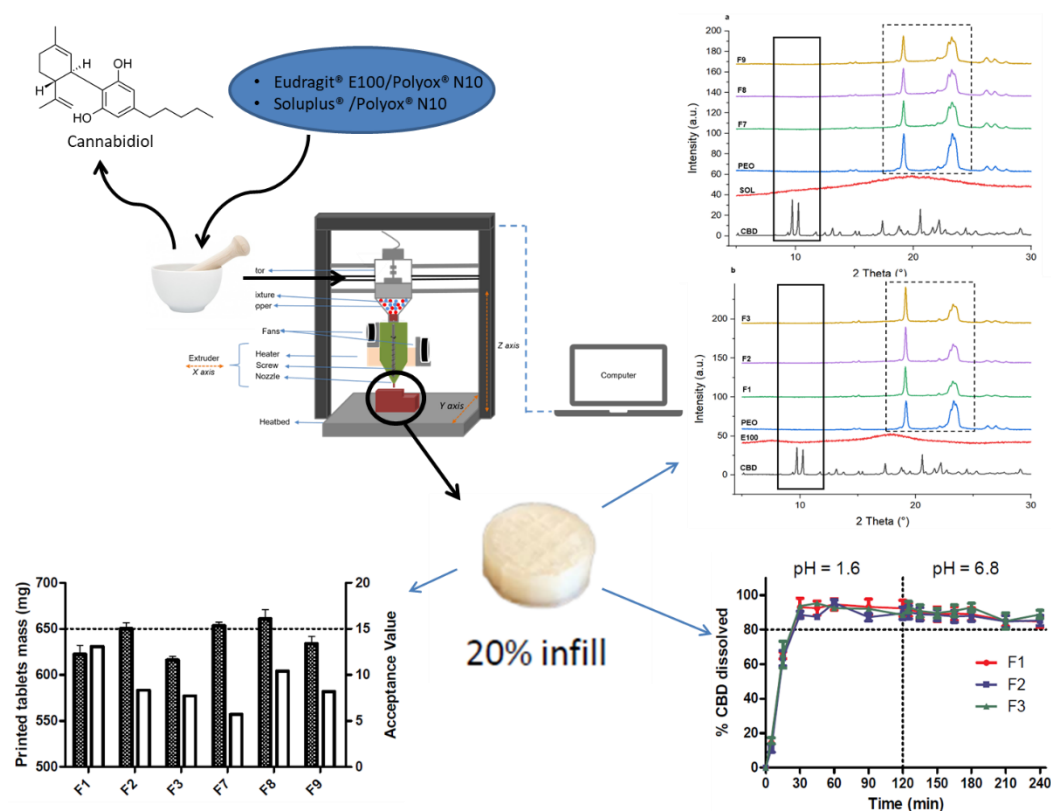
## 2. Publication

### ***Feasibility Study of the Use of a Homemade Direct Powder Extrusion Printer to Manufacture Printed Tablets With an Immediate Release of a BCS II Molecule***

Olivier Jennotte<sup>1</sup>, Nathan Koch<sup>1</sup>, Anna Lechanteur<sup>1</sup>, Rosoux François<sup>2</sup>, Emmerechts Carl<sup>2</sup>, Beeckman Eric<sup>2</sup>, Brigitte Evrard<sup>1</sup>

<sup>1</sup>Laboratory of Pharmaceutical Technology and Biopharmacy, Department of Pharmacy, Center for Interdisciplinary Research on Medicines (CIRM), University of Liege, 4000 Liege, Belgium.

<sup>2</sup>SIRRIS, Collective Centre of the Belgium Technology Industry, 4102, Liege Science Park, Belgium.



To be submitted.

### 2.1. Abstract

Among the various 3D printing techniques, FDM is the most studied in pharmaceutical research. However, it requires the fabrication of filaments with suitable mechanical properties using HME, which can be laborious and time-consuming. DPE has emerged as a single-step printing technique that can overcome FDM limits as it enables the direct printing of powder blends without the need of filaments. This study demonstrated the manufacturing of cylindrical-shaped printed tablets containing CBD, a BCS II molecule, with an immediate release. Different blends of PEO/E100 and PEO/SOL, each with 10% of CBD, were printed and tested according to the Eur. Ph. for uncoated tablets. Each printed cylinder met the Eur. Ph. specifications for friability, mass variation and mass uniformity. However, only the E100-based formulations enabled a CBD immediate release, as formulations containing SOL formed a gel once in contact with the dissolution medium, reducing the drug dissolution rate. To the best of our knowledge, this is the first time that an immediate release of a BCS II molecule is obtained by DPE, showing the promising future of this innovative technique for the formulation of these molecules with a poor solubility.

## 2.2. Introduction

3D printing is an additive manufacturing technique able to convert a CAD model into a physical object by a layer by layer deposition of material [1]. This technique stands out from traditional drug product manufacturing techniques in many ways. It allows to manufacture complex geometries [2], different dosage forms [3,4], drug products combining several incompatible APIs [5], complex drug delivery devices [6,7] and also original and unique shapes that increase patients' compliance [8].

Among the various 3D printing techniques, FDM is the most studied in pharmaceutical research due to its time-saving and cheap process, small size and accuracy [9]. The FDM process involves the extrusion of a filament made of thermoplastic polymers and one or more APIs, followed by layer-by-layer deposition of the molten material until the final printed shape is achieved. It allows the manufacture of solid dosage forms with tailored doses [10], release [11] or shape [12] or different drugs [13], which proves its usefulness for personalized medicine [14,15]. However, this technique has some drawbacks. Prior to printing, the filament must generally be prepared by HME that involves temperatures above  $T_g$  of polymers, which is not suitable for thermosensitive APIs. Moreover, filaments for FDM printing are challenging to obtain. Indeed, they must have specific mechanical properties, i.e., suitable brittleness and flexibility. In most cases, a certain amount of plasticizer has to be added to the formulation to adjust filament flexibility, which is not desired for the physical state stability of the drug. The filament diameter is another parameter to control. It must be homogeneous and can vary between 1.75 and 3.00 mm depending on the printer model used [16]. Filament diameter control often requires the use of expensive additional equipment such as a conveyor belt, a melt pump or a filament maker [17]. Another method for filament loading is the immersion of a filament in a solution that contains the drug which penetrates into the filament by passive diffusion. This immersion method is suitable for thermosensitive drugs, but the drug loading is limited, generally to maximum 3% [18].

DPE may be useful to circumvent FDM drawbacks. This technique was first developed for the plastics industry [19]. It was recently implemented in the pharmaceutical field by Goyanes and his team who successfully manufactured ITZ printed tablets with different grades of HPC [20]. The process implies the feeding of a powder mixture into the printer hopper, heating and extrusion followed by the deposition, layer by layer of the molten material according to the previously digitally designed geometry. This one-step direct printing of powder avoids the need of filament manufacture by HME which significantly reduces process time and waste. The thermal-stress underwent by the API is also reduced since the DPE induces only one heating step, while there are two during FDM process, making DPE as a good alternative for the printing of thermosensitive drugs.

Additionally, DPE can overcome the limitations encountered in HME regarding high drug loading. Indeed, the formulation of high drug loaded filaments usually requires additional excipients in order to obtain not too-brittle or too-flexible filament, which is not the necessary for DPE [21]. This technique has already proven its potential to print objects with various applications. For example, Goyanes *et al.* used different grades of HPC to manufacture printed tablets with a sustained release of ITZ [20]. In another study, the ability of DPE to manufacture mini printed tablets with a high drug loading (25%) was demonstrated. The small size on the mini printed tablet allowed it to fit in a zero-size capsule in order to be combined with other mini printed tablets, or other API, for treatment of disease requiring polymedication within a single dosage form [21]. Later, Malebari *et al.* investigated DPE for the printing of a combination of lopinavir/ritonavir in a pediatric dosage with HPMC and PEG in order to circumvent drug precipitation problem at intestinal pH observed with the administration of marketed drug Kaletra® [22]. Printed tablets were characterized by a zero-order sustained release drug during *in vitro* dissolution tests, which is promising for treating children with HIV. DPE also offers the possibility to print blends containing CDs as reported by Pistone *et al.* [23]. Indeed, authors successfully printed mixtures composed of niclosamide, HP $\beta$ CD and PEG 6000. After *in vitro* dissolution tests, the solubility increase ability of HP $\beta$ CD for poorly soluble drugs was highlighted.

Immediate release dosage forms, defined as forms allowing a drug dissolution of 80% within 30 minutes, were also printed using DPE, although the studied drugs belonged to BCS class I, having a high aqueous solubility [24–26]. To the best of our knowledge, no BCS II drugs with an immediate release has been successfully printed by DPE.

Therefore, the aim of this work was to print solid dosage forms allowing an immediate release of a BCS II drug, namely CBD. This drug was chosen as a BCS II model drug for two reasons. Firstly, because this molecule has a low oral bioavailability, partly due to its low aqueous solubility (0.1  $\mu$ g/mL in water) [27]. Secondly, CBD is being studied for many therapeutic properties, such as opioids use disorder, social anxiety, schizophrenia or cancers with a wide range of dosages varying from less than 1mg/kg/day to 50 mg/kg/day [28–30]. The majority of clinical studies for this promising drug are performed with liquid formulations, probably because it is the fastest and least expensive way to perform CBD dosage titrations. Indeed, conventional manufacturing methods such as tableting often hinder the rapid progress through pre-clinical studies, due to being dose inflexible, high cost and causing high waste [31,32]. DPE process could reduce time, cost and waste of these trials, given that it is sufficient to feed the exact amount of powder mixture with a specific drug loading needed for the study.

Moreover, formulations printed by DPE are solid forms, generally better accepted by the patients in comparison to liquid formulations [33,34].

A powder-based homemade printer was used to produce the printed tablets. CBD was previously mixed with E100 or SOL, known for their ability to increase solubility of poorly soluble drugs, and PEO as a plasticizer, before being printed. The obtained printed tablets were evaluated in terms of immediate release and tested according to the Eur. Ph. monograph for uncoated tablets, as to this day there is no official guidelines regarding the evaluation of the performances or the quality control of a final 3D printed product yet [35].

This study represents the first attempt to produce printed tablets containing a BCS II molecule with an immediate release, using a DPE process. It is expected to prove the interest and the robustness of this new 3D-printing technique for on-demand formulations. In the context of actual medicines shortages, DPE could provide a point-of-care rapid solution.

## 2.3. Material and methods

### 2.3.1 Materials

CBD was purchased from THC Pharm (Frankfurt, Germany). E100 (amino alkyl methacrylate copolymer,  $T_g$ : 50 °C, soluble in water at pH<5, gifted by Evonik, Germany) were used as matrix former. Poly ethylene oxide (PEO, MW 100000, gifted by Colorcon, UK), a semi-crystalline polymer ( $T_g$  = -67 °C and  $T_m$  = 65-70 °C) was used for its plasticizing effect. SOL (Polyvinyl caprolactam–polyvinyl acetate–polyethylene glycol graft copolymer,  $T_g$  = 67 °C) was kindly received from BASF Chemical Co. (Ludwigshafen, Germany).

### 2.3.2 Powder Flow Measurement

Powder mixtures must have an appropriate flow to be printed by DPE. Therefore, bulk and tapped density were measured according to the Ph. Eur. procedure 2.9.36 and the protocol was based on Lechanteur et al work [36]. Briefly, a 10 mL cylinder was used and filled with the formulation. The bulk density was directly read in the cylinder. The tapped density was obtained with a tap density tester TD1 Sotax® (Aesch, Switzerland). The volume was read after 1250 taps. The values were determined as the mean of three replicates.

The Hausner's index and Carr's index were calculated with [Eq. 1](#) and [2](#):

$$\text{Hausner's Index} = \frac{\text{Bulk Density}}{\text{Tapped Density}} \quad \text{Eq.1}$$

$$\text{Carr's Index} = \frac{\text{Bulk Density} - \text{Tapped Density}}{\text{Bulk Density}} \times 100 \quad \text{Eq.2}$$

Powder flowability can vary from very, very poor to excellent depending on the different index values (*Monograph 2.9.36-2, Eur. Ph. Edition 11.2*).

### 2.3.3 Direct Powder Extrusion 3D Printing

In the present study, a homemade modified powder-based 3D printer was used ([Fig. 44](#)). The process is similar to conventional FDM printing but the printing is conducted directly from a powder mixture instead of a filament. It can be divided into three major steps. First, the powder mixture is loaded in a hopper which can hold up to 9 mL. The second step relies on the principle of a vertical hot-melt extruder. The mixture falls from the hopper and goes by gravity along a rotating Archimedes screw contained in a heated barrel until being extruded through a 0.4 mm nozzle. That implies that the powder must have a good flow and a low viscosity at melting. However, kneading and heating powers of DPE are weaker than a classical extruder as DPE is composed by only one small-

size screw without kneading elements, reducing DPE capacity to process highly viscous materials. Therefore, extrudability studies should be conducted in order to assess the printability of a powder blend. Indeed, powder with poor flowability would not fall along the screw and molten material that are too viscous would clog the nozzle.

For extrudable powder mixtures, the last step is the deposition of the molten material, layer by layer on a heated bed, until the final form is obtained.

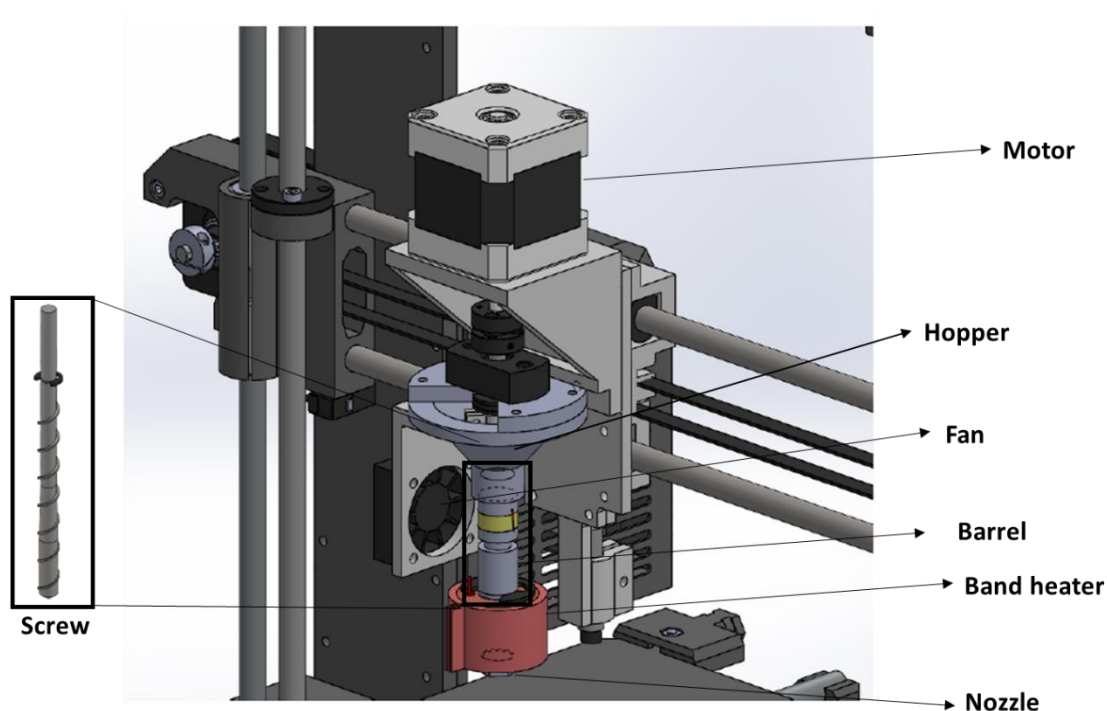


*Figure 44 - Design of the printhead of the homemade modified powder-based 3D printer. The screw is enclosed in a barrel, heated by a band heater. A fan is directed between the barrel and a loading hopper to control the temperature profile along the extruder so that the powder mixture does not melt in an early way and can go by gravity along the screw until being melted and extruded by a 0.4 mm nozzle.*

E100 or SOL were used as polymeric carriers for the manufacturing of ASDs. As these two polymers are not printable on their own because of their brittleness, PEO was added to each formulation as a plasticizer.

As explained above, DPE printer must be able to extrude the powder mixture through the nozzle in order to deposit it layer by layer to obtain the desired printed object. Therefore, extrudability studies were performed on different E100/PEO and SOL/PEO ratios, each combined with 10% of CBD ([Table 10](#)).

Prior to mixing, every component was sieved through a 0.4 mm mesh sieve to provide a better size uniformity between the different powders. The powder mixtures were performed using a mortar and a pestle until no aggregated particles were observed.



Extrudability tests were performed as follow: each powder mixture was introduced in the printer loading hopper and the screw was rotated for 180 seconds at 16 rpm and a temperature of 155 °C. After this time, obtained filaments were measured. The longer the filament, the more extrudable the powder mixture.

*Table 10 - Composition of powder mixtures*

<b>Formulations</b>	<b>CBD (%)</b>	<b>PEO (%)</b>	<b>E100 (%)</b>	<b>SOL (%)</b>
<b>F1</b>	10	72	18	0
<b>F2</b>	10	67.5	22.5	0
<b>F3</b>	10	63	27	0
<b>F4</b>	10	58.5	31.5	0
<b>F5</b>	10	54	36	0
<b>F6</b>	10	49.5	40.5	0
<b>F7</b>	10	72	0	18
<b>F8</b>	10	67.5	0	22.5
<b>F9</b>	10	63	0	27
<b>F10</b>	10	58.5	0	31.5
<b>F11</b>	10	54	0	36
<b>F12</b>	10	49.5	0	40.5

The different powder mixtures were printed with the following parameters: printing speed 20 mm/s, layer height 0.1 mm, heated bed T° 25 °C and printing T° 155 °C. The printhead was disassembled and cleaned after the printing of each formulation in order to prevent the cross-mixing between them. Once printed, the dimensions of the cylinders were taken using a digital caliper to evaluate the printer precision.

The printed tablets were designed as cylindrical objects (diameter = 15 mm, height = 6.2 mm) using Tinkercad™ free online software (Autodesk, CA, USA). Cylinder dimensions and infill (20%) were set to obtain printed forms of 650 mg per printed tablet which corresponds to an equivalent of 65 mg of CBD. This dosage was chosen in order to be within the dose range tested in the different studies found in the literature [31]. The obtained .stl files were converted to gcode files using the software Ultimaker Cura, version 4.11.0 (Ultimaker, The Netherlands).

#### 2.3.4 Drug Content of Printed Tablets

Since the formulations are exposed to high temperatures during their production, the drug content was measured after printing. Samples of 20-30 mg were cut from the printed tablets and dissolved in acetonitrile prior to HPLC analysis. A validated reverse phase HPLC analytical method, described in a previous work, was used (Koch et al., 2020). The HPLC equipment consisted of an Agilent® 1100 (Santa Clara, USA) with OpenLab CDS IC ChemStation version C.01.05 as the software. The mobile phase was composed of water/acetonitrile (38/62% (v/v)) and the column was Zorbax® C18 300 SB with particles of 3.5 µm (150 mm x 4.6 mm ID). The flow rate was set at 1.0 mL/min and the temperature was kept at 30 °C. The injection volume was 20.0 µL, the chromatographic run time was 10 min and the detection of CBD was made at a wavelength of 240 nm. The measurements were carried out in triplicate.

#### 2.3.5 Characterization of Printed Tablets

As there is still no monograph concerning the printed forms in the Eur. Ph., the printed cylinders were characterized with tests according to the monograph for uncoated tablets of the Eur. Ph. Edition 11.2.

##### *Friability Test (Monograph 2.9.7 Eur. Ph. Edition 11.2)*

Ten printed tablets of each formulation were dusted, weighed and placed in the drum of a Friabilator USP F2 Sotax® (Aesch, Switzerland). After 100 rotations of the drum, the printed tablets were dusted, weighed again and the target mass loss was less than 1% (Monograph 2.9.7. Eur. Ph. Edition 11.2).

##### *Tensile Strength*

The tensile strength of printed tablets of each formulation was determined in triplicate using the breaking force (F) measured by a crushing strength tester Pharmatron MT-50 Sotax® (Aesch, Switzerland) and with the following equation:

$$TS = \frac{2F}{\pi Dt}$$

Where:

D is the diameter

t is the overall thickness

*Mass Variation (Monograph 2.9.40 Eur. Ph. Edition 11.2)*

Ten printed tablets of each formulation were individually weighted and the AV) was calculated using the following equation (Monograph 2.9.40. Eur. Ph. Edition 11.2):

$$AV = | M - X | + 2.4s$$

Where:

M is a reference value which depends on X

X is the mean of the individual content, expressed as a percentage of the theoretical value of CBD

s is the sample standard deviation

The target AV was lower than 15.00.

*Uniformity of Mass (Monograph 2.9.5 Eur. Ph. Edition 11.2)*

Ten printed tablets of each formulation were weighed and the average mass was determined. The test was considered as conform if not more than two of the individual masses deviate from the average mass by more than 5% of deviation and none deviate by more than twice that percentage.

*X-ray Diffraction*

In order to evaluate the physical state of CBD once printed, disks (23.12 mm diameter x 1.00 mm height) made of the printable powder mixtures of were printed and analyzed. X-ray diffractograms were collected using a Bruker D8 TWIN-TWIN diffractometer in Bragg-Brentano configuration (Cu Kalpha radiation, variable divergence slit V6, sample rotation 15 rpm) with a Lynxeye XET detector in 1D mode (192 channels) and a total scan time of 15 or 30 min for a 0.02° step size.

*2.3.6 Dissolution Tests*

The in vitro dissolution experiments were conducted using USP II paddle method apparatus AT7 (Sotax®, Switzerland). One printed tablet of each formulation was placed in a sinker containing 500 mL of HCl 0.1 N at pH 1.6 for two hours followed by two hours with an addition of Na<sub>3</sub>PO<sub>4</sub> 0.2 M. The pH was adjusted to 6.8 with addition of HCl 1 N or NaOH 2 N within a time interval of less than 5 minutes. The stirring speed was 100 rpm and the temperature was maintained at 37°C. The samples were analyzed by HPLC-UV and replaced by fresh medium (2.9.3. Ph. Eur. Ed. 11.2). Every formulation was analyzed in triplicate.

### *2.3.7 Dynamic Light Scattering*

Solutions composed of the polymers and/or CBD in acidic and neutral media were characterized by Dynamic Light Scattering (DLS) using a Malvern Zetasizer® (Nano ZS, Malvern Instrument, UK) at 25 °C with a fixed angle of 90° (n=3) in order to measure their particle size during dissolution.

## 2.4 Results and discussion

### 2.4.1 Powder Flow Measurement

The flowability of each powder formulation has been measured since it influences the filling of the hopper. As shown in [Table 11](#), flowability of the powders varies from fair to excellent by decreasing the percentage of PEO. These measurements show that the used powder in this study possess appreciable flowability, which is necessary to assure appropriate material extrusion.

*Table 11 - Carr's and Hausner's indexes and resulting flowability for each formulation*

Formulations	Carr's Index	Hausner' s Index	Flowability
F1	10.00	1.11	Excellent
F2	11.11	1.13	Good
F3	12.22	1.14	Good
F4	13.33	1.15	Good
F5	16.67	1.20	Fair
F6	17.78	1.22	Fair
F7	8.89	1.10	Excellent
F8	10.00	1.11	Excellent
F9	12.22	1.14	Good
F10	14.44	1.17	Good
F11	17.78	1.22	Fair
F12	17.78	1.22	Fair

### 2.4.2 3D Printing of Powder Mixtures

Prior to the printing step, powder mixtures containing increasing proportions of E100/PEO or SOL/PEO each combined with 10% of CBD were tested to determine if they were extrudable within the modified printer head (Table1). Every formulation was extrudable, except for F5 and F6 which clogged the nozzle, probably because of a too high viscosity. Filament lengths obtained after extrusion of the other formulations are gathered in [Table 12](#). Mixtures containing SOL could be extruded with a maximum of 40.5% SOL while mixtures containing E100 could be extruded with a maximum of 31.5% E100. The filament length decreased with the increase of the E100 or SOL proportion. This highlighted the strong influence of the composition of the formulation on the extrudability. Indeed, small reductions in the proportions of PEO led to large reductions

in the amount of extruded material. As the flowing was good for every formulation, the difference of extrudability would be due to E100 and SOL viscosity at the printing temperature. Indeed, these two polymers have already been reported as having a relatively high viscosity when melted, with a higher viscosity of E100 compared to SOL [37].

*Table 12 - Length of filament obtained for each formulation after extrudability studies*

Formulation	F1	F2	F3	F4	F5	F6	F7	F8	F9	F10	F11	F12
Filament length (cm)	36	30	22	7	0	0	47	39	31	10	5	3

The modified powder-based printer was used to print the extrudable powder mixtures (F1 to F4 and F7 to F12). All mixtures could be printed, except for F4, F10, F11 and F12 which resulted in an incomplete shape compared to the digital model. This is explained by the poor extrudability of these mixtures, as observed by the little amounts of material extruded during the extrudability study. For these formulations, the printing speed should be decreased in order to match the nozzle throughput, but the printing time per tablet would be too long so these formulations were withdrawn.

The time from loading the powder until obtaining the final cylinder was about 6 minutes which is in the time range of different printed tablets produced by FDM [38]. Moreover, the losses are negligible compared to those generated by more conventional 3D printing techniques such as FDM. Indeed, FDM implies an additional HME step for the filament production that generates material loss. This makes 3D direct powder extrusion a promising technique for the production of small batches intended for clinical studies or personalized medicine, for example.

#### 2.4.3 Characterization of Printed Tablets

The diameter and height of the 10 printed tablets of each design were measured and the deviation from the dimensions of the digital model is shown in [Table 13](#). All the printed tablets had a deviation of the diameter from  $-5.00 \pm 2.17\%$  to  $1.47 \pm 0.14\%$  compared to the digital model. Regarding the height, the printed tablets had a deviation ranging from  $-3.44 \pm 1.23\%$  to  $-0.34 \pm 0.17$ . These low deviations dimensions of the printed cylinders compared to the digital model highlights the precision of this homemade direct powder extruder.

The monograph concerning uncoated tablets of the Eur. Ph. was used to characterize the printed tablets as there is no existing monograph for the printed formulations. Since powder mixtures are exposed to high temperatures during the printing process, the drug recovery measurement is important, as these temperatures can degrade the API.

Results of CBD recovery are shown on [Table 13](#) and suggest that there is no drug degradation in formulations, as CBD recovery is ranging from  $95.77 \pm 0.66\%$  to  $99.20 \pm 2.33$ . Drug recoveries are in accordance with TGA analysis ([Appendix IV.2](#)) as printing temperatures did not exceed the degradation temperature of CBD ( $220\text{ }^{\circ}\text{C}$ ), E100 ( $289\text{ }^{\circ}\text{C}$ ), PEO ( $389\text{ }^{\circ}\text{C}$ ) and SOL ( $290\text{ }^{\circ}\text{C}$ ). These results indicated that the processing conditions did not significantly impact the CBD chemical stability in the printed tablets. The *friability* and the *tensile strength* are two important parameters concerning the study of the integrity of oral solid dosage forms during the production, transport and handling by the patient. Moreover, these two parameters especially the tensile strength have an influence of the dissolution of the dosage forms. Indeed, a printed tablet with a high tensile strength will dissolve slower than one with a low tensile strength as the structure is harder to disintegrate. The results on Table 4 show that the mass loss during the friability test was  $<1\%$  for each formulation and met the Eur. Ph. specifications. Compared to the standard techniques for the manufacturing of oral solid dosage forms such as tableting, or other 3D printing techniques like drop-on-powder 3D printing, DPE allows the production of products with a poor friability without additional steps or excipients [39]. There is no requirement concerning the tensile strength and the values were comparable to another study focused on DPE [20].

*Table 13 - Characterization of printed tablets*

Formulations	CBD Recovery (%)	Diameter <sup>a</sup> (%) (n=10)	Height <sup>a</sup> (%) (n=10)	Friability* (%)	Tensile Strength
<b>F1</b>	$96.75 \pm 1.05$	$97.00 \pm 1.15$	$98.57 \pm 1.71$	0.25	$0.97 \pm 0.23$
<b>F2</b>	$98.12 \pm 3.02$	$96.51 \pm 0.75$	$98.54 \pm 0.39$	0.17	$1.01 \pm 0.17$
<b>F3</b>	$95.77 \pm 0.66$	$95.00 \pm 2.17$	$99.66 \pm 0.17$	0.22	$0.99 \pm 0.11$
<b>F7</b>	$97.15 \pm 1.33$	$101.47 \pm 0.14$	$97.66 \pm 1.16$	0.02	$0.85 \pm 0.37$
<b>F8</b>	$99.20 \pm 2.33$	$101.00 \pm 0.51$	$98.02 \pm 0.74$	0.09	$0.91 \pm 0.03$
<b>F9</b>	$96.00 \pm 1.58$	$98.79 \pm 0.87$	$96.56 \pm 1.23$	0.12	$0.87 \pm 0.21$

a% = printed model/digital model (measured in triplicate). \* = measured on ten printed tablets.

Both *mass variation* and *uniformity of mass* tests were performed to ensure that the mass of all the produced printed tablets was within limits defined by the Eur. Ph. [Figure 45](#) represents the mean mass measured on ten printed tablets of each formulation and the AV for each formulation. As it can be observed, printed tablets mean masses differ between each formulation, going from 616.28 mg to 660.99 mg. Such deviations have already been reported in the literature [20,23,40].

However, every formulation was in accordance with the mass variation test as every AV was below 15.00. Concerning the uniformity of mass test, the average mass of ten printed tablets of each formulation was calculated.

In order to be in compliance Eur. Ph. requirements of the uniformity of mass test, no printed tablet must have a deviation from the average mass superior to 10% and no more than two printed tablets of each formulation must deviate from more than 5%. The results of our study showed deviations of respectively -9.21% and +6.84% for the most under and over weighted tablet. Moreover, no more than two printed tablets per formulation deviated from more than 5% of the average mass. The test was therefore compliant and proved the ability of the DPE to produce printed tablets with adequate reproducibility.

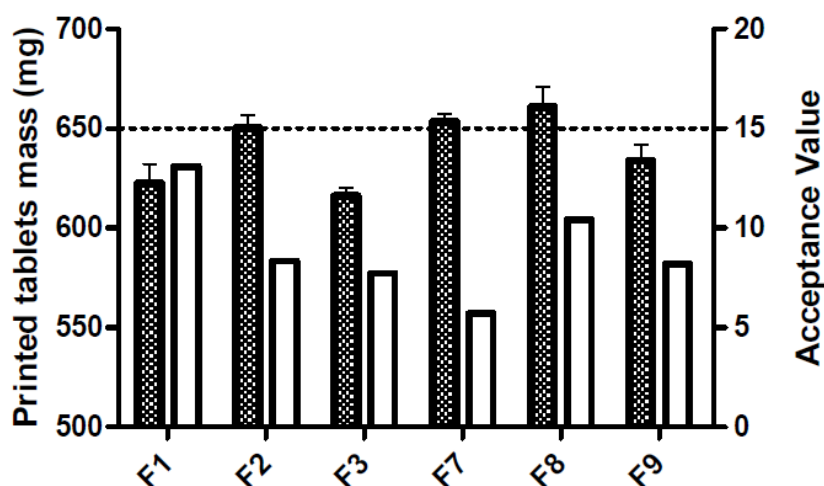


Figure 45 - Mass of the printed tablet of the 6 formulations (mean and SD,  $n = 10$ ) represented by the dashed columns and the AV for each formulation represented by the empty columns (measured on ten printed tablets). The target mass is represented by the dashed line.

X-ray diffraction was used to study the physical state of CBD, polymers and printed tablets. CBD and PEO showed sharp peaks confirming their crystalline or semi-crystalline nature, respectively (Fig. 46). The pattern of E100 showed a wide halo, characteristic of amorphous compounds. The characteristic peaks around ten of CBD were not found on formulation patterns, indicating a total amorphization of the drug during the printing process. DPE does not always induce a drug total amorphization as formulations remain only a few minutes at high temperature while conventional methods to transform a drug in its amorphous state generally involve a dissolution of the drug in specific solvent or prolonged contact of the drug at high temperatures [20,22,24,41,42]. This implies that our homemade printed is suitable for the production of amorphous formulations of CBD.



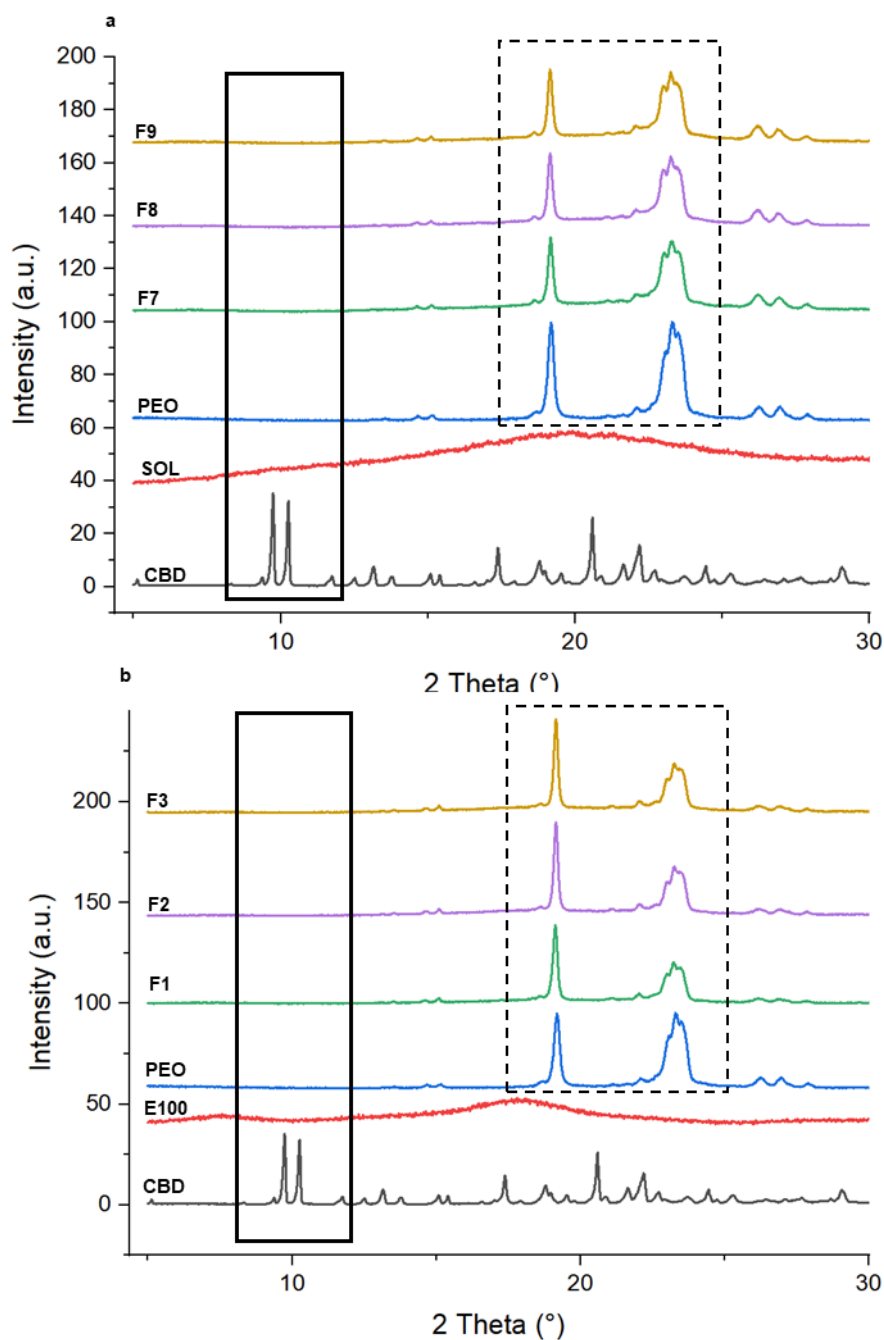
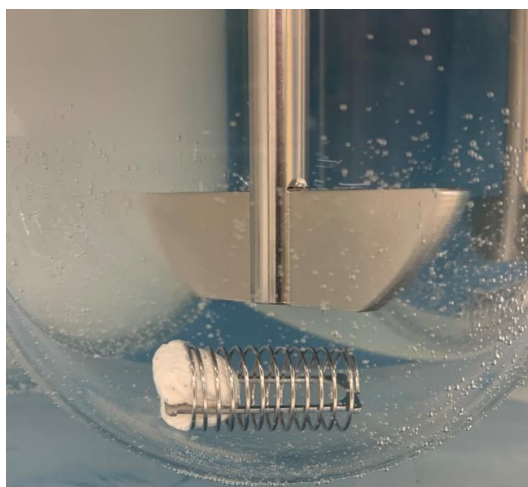


Figure 46 - XRD patterns of crystalline CBD, E100, SOL, PEO and the printed disks composed of F1, F2, F3, F7, F8 and F9. The diffractograms of E100 and SOL show a halo confirming the amorphous state of these polymers. The dotted frame shows the absence of the characteristic peaks of crystalline CBD at about 10° in each formulation, which means that CBD is completely amorphous in all printed disks. The continuous line frame highlights the semi-crystalline character of PEO which shows characteristic peaks at about 19° and 24°. These peaks are also present in the printed disks, suggesting rapid recrystallization of PEO.

#### 2.4.4 In Vitro Dissolution Tests

Dissolution tests were performed in acidic conditions at pH 1.6 during two hours followed by two hours at pH 6.8. This was done to evaluate the ability of tested formulations to dissolve CBD and maintain a supersaturated solution in both acidic and neutral pH. These dissolutions tests were conducted based on a study that highlighted the tendency of CBD to be better absorbed in the upper intestine (at pH 6.8) leading to the need to dissolve a maximum of CBD in stomach conditions (at pH 1.6) [43].

Formulations containing SOL and PEO (F7, F8 and F9) did not allow an increase of CBD solubility during the four hours of dissolution test (data not shown). Indeed, a gel was formed at the layer surface of the printed tablets once in contact with the dissolution medium (**Fig. 47**). This gel behavior has already been described in the literature for both SOL and PEO [44,45]. These polymers have a strong affinity for water. Once in contact, the strength of the water-polymer bonds surpasses that of the polymer-polymer bonds, allowing water to penetrate between the polymer chains, causing swelling and the formation of a gel layer. This layer slows the erosion of both polymer and drug. Addition of salts or disintegrants have already been studied in ASDs with SOL to break the gel network and increase the drug dissolution rate [46].



*Figure 47 - Gel mass formed by F7 once in contact with the acidic dissolution medium.*

On the other hand, formulations containing E100 and PEO (F1, F2 and F3) allowed an immediate release of CBD (**Fig. 48**). Indeed,  $88.58\% \pm 2.67$ ,  $92.97\% \pm 7.47$  and  $93.63\% \pm 2.24$  of CBD was released after 30 minutes from F1, F2 and F3, respectively. This high dissolution rate suggested that E100 broke the gel layer formed by PEO. Indeed, this polymer possesses amino functions which are ionized at pH less than 5, allowing a fast dissolution. Moreover, the supersaturated solution was maintained at both pH. This

concentration upkeep was not expected as the amino functions of E100 are not ionized when pH is above 5, making this polymer not soluble.

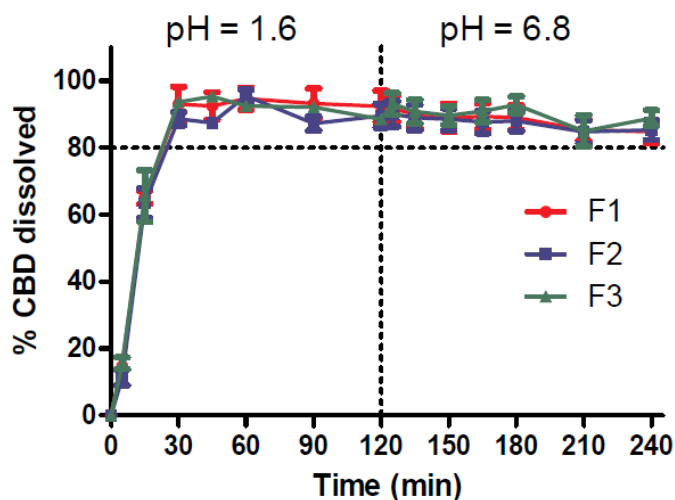


Figure 48 - Dissolution profile of formulations containing E100.

This maintain of CBD concentration in both media could be explained by the mechanism of dissolution of E100. Authors have demonstrated that EPO, which has the same composition as E100, makes it possible to dissolve poorly water-soluble molecules, in addition of maintaining the amorphous state of these molecules, by forming micelles in an acidic medium [47]. We have verified this hypothesis by DLS analysis as showed in [Figure 49](#). The dissolution of E100 alone in the acidic dissolution medium composed of HCl 0.1 N at a pH value of 1.6, a major population is measured at about 10 nm which is in the range of classic micelles which is 5-100 nm, (Fig. 6.a) [48]. After pH adjustment at a value of 6.8, no major population could be observed suggesting a micelles disorganization (Fig. 6.b). However, the dissolution of E100 and PEO in neutral medium at pH value of 6.8 seemed to stabilize the micelles formed by E100 (Fig. 6.c). This was also observed with the dissolution of one of the printed tablets composed with these two polymers (F3, Fig. 6.d and 6.e). Single particles population at about 500 nm was observed in both acidic and neutral media. The particles size difference between the solutions composed of E100 and PEO and the solutions composed of F3 is explained by the solubilization of into the core of E100/PEO particles [47].

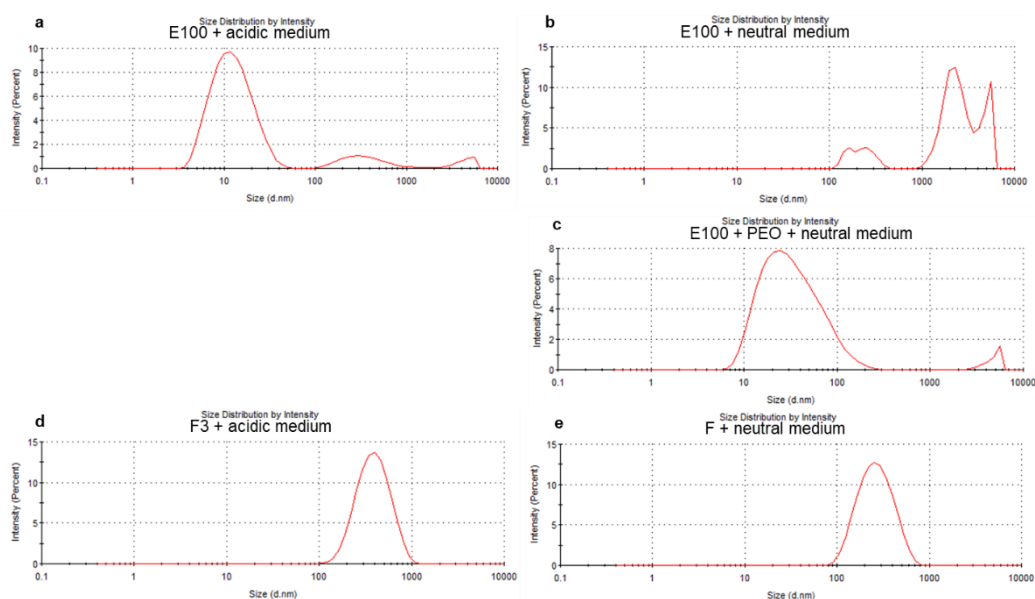


Figure 49 – Particle size distribution of a. E100 dissolved in acidic medium at pH 1.6, b. E100 dissolved in neutral medium at pH 6.8, c. E100 and PEO dissolved in neutral medium at pH 6.8, d. F3 composed of CBD/PEO/E100 (10/63/27) dissolved in acidic medium at pH 1.6 and e. F3 dissolved in neutral medium at pH 6.8.

## 2.5 Conclusion

For the first time, printed tablets containing an ASD allowing an immediate release (80% in 30 minutes) of a BCS II molecule were manufactured by direct powder extrusion 3D printing. The printing was done directly from powder mixtures without the need of developing a printable filament, reducing time, cost and difficulty of the printing process. The printed tablets were composed either of E100/PEO or SOL/PEO, at different ratios, in combination with 10% of CBD. Only the formulations containing E100 allowed an increase of aqueous solubility and dissolution rate of CBD, confirming the importance of polymer screening.

In addition to the improved performance of the aqueous solubility of CBD, printed tablets complied with the tests of the monograph concerning uncoated tablets of the Eur. Ph. The results obtained in this study highlighted the ability of direct powder extrusion for the production and shaping of ASDs with an immediate release and a suitable quality. This may be promising for the on-demand manufacture of small batches by community pharmacies, hospitals or to conduct clinical trials since the time and waste of the process is greatly reduced compared to conventional manufacturing techniques.

### 2.6 Acknowledgments

The authors wish to acknowledge FEDER funds for the support in SOLPHARE FEDER project ([884148-329407](#)) and the Fonds Léon Fredericq for the support in project 2021-2022-12. The authors also wish to thank Wenda Lazzari and Astrid Couturier (Mithra CDMO) for the loan and the support of the melt pump.

## 2.7 References

1. Omari S, Ashour EA, Elkanayati R, Alyahya M, Almutairi M, Repka MA. Formulation development of loratadine immediate- release tablets using hot-melt extrusion and 3D printing technology. *J Drug Deliv Sci Technol* [Internet]. Elsevier B.V.; 2022;74:103505. Available from: <https://doi.org/10.1016/j.jddst.2022.103505>
2. Lamichhane S, Park JB, Sohn DH, Lee S. Customized novel design of 3D printed pregabalin tablets for intra-gastric floating and controlled release using fused deposition modeling. *Pharmaceutics*. 2019;11.
3. Jiang H, Fu J, Li M, Wang S, Zhuang B, Sun H, et al. 3D-Printed Wearable Personalized Orthodontic Retainers for Sustained Release of Clonidine Hydrochloride. *AAPS PharmSciTech*. AAPS PharmSciTech; 2019;20:1–10.
4. Trenfield SJ, Awad A, Madla CM, Hatton GB, Firth J, Goyanes A, et al. Shaping the future: recent advances of 3D printing in drug delivery and healthcare. *Expert Opin Drug Deliv* [Internet]. Taylor & Francis; 2019;16:1081–94. Available from: <https://doi.org/10.1080/17425247.2019.1660318>
5. Gioumouxouzis CI, Baklavaridis A, Katsamenis OL, Markopoulou CK, Bouropoulos N, Tzetzis D, et al. A 3D printed bilayer oral solid dosage form combining metformin for prolonged and glimepiride for immediate drug delivery. *Eur J Pharm Sci* [Internet]. Elsevier; 2018;120:40–52. Available from: <https://doi.org/10.1016/j.ejps.2018.04.020>
6. Dumpa N, Butreddy A, Wang H, Komanduri N, Bandari S, Repka MA. 3D printing in personalized drug delivery: An overview of hot-melt extrusion-based fused deposition modeling. *Int J Pharm* [Internet]. Elsevier B.V.; 2021;600:120501. Available from: <https://doi.org/10.1016/j.ijpharm.2021.120501>
7. Beg S, Almalki WH, Malik A, Farhan M, Aatif M, Rahman Z, et al. 3D printing for drug delivery and biomedical applications. *Drug Discov Today* [Internet]. Elsevier Ltd; 2020;25:1668–81. Available from: <https://doi.org/10.1016/j.drudis.2020.07.007>
8. Vaz VM, Kumar L. 3D Printing as a Promising Tool in Personalized Medicine. *AAPS PharmSciTech*. AAPS PharmSciTech; 2021;22.
9. Rahim TNAT, Abdullah AM, Md Akil H. Recent Developments in Fused Deposition Modeling-Based 3D Printing of Polymers and Their Composites. *Polym Rev* [Internet]. Taylor & Francis; 2019;59:589–624. Available from: <https://doi.org/10.1080/15583724.2019.1597883>
10. Crişan AG, Iurian S, Porfire A, Rus LM, Bogdan C, Casian T, et al. QbD guided development of immediate release FDM-3D printed tablets with customizable API doses. *Int J Pharm*. 2022;613.
11. Shi K, Slavage JP, Maniruzzaman M, Nokhodchi A. Role of release modifiers to modulate drug release from fused deposition modelling (FDM) 3D printed tablets. *Int J Pharm* [Internet]. Elsevier B.V.; 2021;597:120315. Available from: <https://doi.org/10.1016/j.ijpharm.2021.120315>
12. Goyanes A, Robles P, Buanz A, Basit AW, Gaisford S. Effect of geometry on drug release from 3D printed tablets. *Int J Pharm* [Internet]. Elsevier B.V.; 2015;494:657–63. Available from: <http://dx.doi.org/10.1016/j.ijpharm.2015.04.069>
13. Pereira BC, Isreb A, Forbes RT, Dores F, Habashy R. ‘ Temporary Plasticiser ’: A novel solution to fabricate 3D printed patient- centred cardiovascular ‘ Polypill ’ architectures. *Eur J Pharm Biopharm* [Internet]. Elsevier; 2019;135:94–103. Available from: <https://doi.org/10.1016/j.ejpb.2018.12.009>

14. Khalid GM, Billa N. Solid Dispersion Formulations by FDM 3D Printing—A Review. *Pharmaceutics*. 2022;14.
15. Sandler N, Preis M. Printed Drug-Delivery Systems for Improved Patient Treatment. *Trends Pharmacol Sci* [Internet]. Elsevier Ltd; 2016;37:1070–80. Available from: <http://dx.doi.org/10.1016/j.tips.2016.10.002>
16. Jennotte O, Koch N, Lechanteur A, Evrard B. Three-dimensional printing technology as a promising tool in bioavailability enhancement of poorly water-soluble molecules: A review. *Int J Pharm* [Internet]. Elsevier B.V.; 2020;580:119200. Available from: <https://doi.org/10.1016/j.ijpharm.2020.119200>
17. Parulski C, Jennotte O, Lechanteur A, Evrard B. Challenges of fused deposition modeling 3D printing in pharmaceutical applications: Where are we now? *Adv Drug Deliv Rev*. 2021;175.
18. Fernández-García R, Prada M, Bolás-Fernández F, Ballesteros MP, Serrano DR. Oral Fixed-Dose Combination Pharmaceutical Products: Industrial Manufacturing Versus Personalized 3D Printing. *Pharm. Res.* Springer; 2020.
19. Liu X, Chi B, Jiao Z, Tan J, Liu F, Yang W. A large-scale double-stage-screw 3D printer for fused deposition of plastic pellets. *J Appl Polym Sci*. 2017;134:1–9.
20. Goyanes A, Allahham N, Trenfield SJ, Stoyanov E, Gaisford S, Basit AW. Direct powder extrusion 3D printing: Fabrication of drug products using a novel single-step process. *Int J Pharm*. 2019;567.
21. Sánchez-Guiraes SA, Jurado N, Kara A, Lalatsa A, Serrano DR. Understanding direct powder extrusion for fabrication of 3d printed personalised medicines: A case study for nifedipine minitables. *Pharmaceutics*. 2021;13.
22. Malebari AM, Kara A, Khayyat AN, Mohammad KA, Serrano DR. Development of Advanced 3D-Printed Solid Dosage Pediatric Formulations for HIV Treatment. *Pharmaceutics*. 2022;15:1–15.
23. Pistone M, Racaniello GF, Arduino I, Laquintana V, Lopalco A, Cutrignelli A, et al. Direct cyclodextrin-based powder extrusion 3D printing for one-step production of the BCS class II model drug niclosamide. *Drug Deliv Transl Res* [Internet]. Springer US; 2022;12:1895–910. Available from: <https://doi.org/10.1007/s13346-022-01124-7>
24. Fanous M, Gold S, Muller S, Hirsch S, Ogorka J, Imanidis G. Simplification of fused deposition modeling 3D-printing paradigm: Feasibility of 1-step direct powder printing for immediate release dosage form production. *Int J Pharm* [Internet]. Elsevier; 2020;578:119124. Available from: <https://doi.org/10.1016/j.ijpharm.2020.119124>
25. Mendibil X, Tena G, Duque A, Uranga N, Campanero MÁ, Alonso J. Direct powder extrusion of paracetamol loaded mixtures for 3d printed pharmaceuticals for personalized medicine via low temperature thermal processing. *Pharmaceutics*. 2021;13.
26. FDA. Dissolution Testing and Acceptance Criteria for Immediate-Release Solid Oral Dosage Form Drug Products Containing High Solubility Drug Substances Guidance for Industry. 2018;8. Available from: [http://www.fda.gov/Drugs/GuidanceComplianceRegulatoryInformation/Guidances/default.htm%0Afile:///C:/Users/ASUS/Desktop/Rujukan PhD/Drug Release/1074043 FNL\\_clean.pdf](http://www.fda.gov/Drugs/GuidanceComplianceRegulatoryInformation/Guidances/default.htm%0Afile:///C:/Users/ASUS/Desktop/Rujukan PhD/Drug Release/1074043 FNL_clean.pdf)
27. Koch N, Jennotte O, Gasparrini Y, Vandenbroucke F, Lechanteur A, Evrard B. Cannabidiol aqueous solubility enhancement: Comparison of three amorphous formulations strategies using different type of polymers. *Int J Pharm* [Internet]. Elsevier; 2020;589:119812. Available from:

<https://doi.org/10.1016/j.ijpharm.2020.119812>

28. Bergamaschi MM, Helena Costa Queiroz R, Hortes M, Chagas N, Chaves Gomes De Oliveira D, De Martinis BS, et al. Cannabidiol Reduces the Anxiety Induced by Simulated Public Speaking in Treatment-Naïve Social Phobia Patients. *Neuropsychopharmacology* [Internet]. 2011;36:1219–26. Available from: [www.neuropsychopharmacology.org](http://www.neuropsychopharmacology.org)

29. Heider CG, Itenberg SA, Rao J, Ma H, Wu X. Mechanisms of Cannabidiol (CBD) in Cancer Treatment: A Review. 2022; Available from: <https://doi.org/10.3390/biology11060817>

30. McGuire P, Robson P, Cubala WJ, Vasile D, Morrison PD, Barron R, et al. Cannabidiol (CBD) as an adjunctive therapy in schizophrenia: A multicenter randomized controlled trial. *Am J Psychiatry*. 2018;175:225–31.

31. Millar S, Stone N, Bellman Z, Yates A, England T, Sophie Millar CA. A systematic review of cannabidiol dosing in clinical populations. *Artelo Biosci Biotechnol Biol Sci Res Counc*. 2019;

32. Seoane-Viaño I, Trenfield SJ, Basit AW, Goyanes A. Translating 3D printed pharmaceuticals: From hype to real-world clinical applications. *Adv Drug Deliv Rev* [Internet]. The Authors; 2021;174:553–75. Available from: <https://doi.org/10.1016/j.addr.2021.05.003>

33. Vasconcelos T, Sarmiento B, Costa P. Solid dispersions as strategy to improve oral bioavailability of poor water soluble drugs. *Drug Discov Today*. 2007;12:1068–75.

34. Morishita M, Peppas NA. Is the oral route possible for peptide and protein drug delivery? *Drug Discov Today*. 2006;11:905–10.

35. Mohapatra S, Kar RK, Biswal PK, Bindhani S. Approaches of 3D printing in current drug delivery. *Sensors Int* [Internet]. The Authors; 2022;3:100146. Available from: <https://doi.org/10.1016/j.sintl.2021.100146>

36. Lechanteur A, Plougouven E, Orozco L, Lumay G, Vandewalle N, Evrard B. Engineered-inhaled particles : Influence of carbohydrates excipients nature on powder properties and behavior. 2022;613.

37. Alhijaj M, Belton P, Qi S. An investigation into the use of polymer blends to improve the printability of and regulate drug release from pharmaceutical solid dispersions prepared via fused deposition modeling (FDM) 3D printing. *Eur J Pharm Biopharm*. Elsevier B.V.; 2016;108:111–25.

38. Pires FQ, Alves-silva I, Pinho LAG, Chaker JA. Predictive models of FDM 3D printing using experimental design based on pharmaceutical requirements for tablet production. *Int J Pharm* [Internet]. Elsevier; 2020;588:119728. Available from: <https://doi.org/10.1016/j.ijpharm.2020.119728>

39. Infanger S, Haemmerli A, Iliev S, Baier A, Stoyanov E, Quodbach J. Powder bed 3D-printing of highly loaded drug delivery devices with hydroxypropyl cellulose as solid binder. *Int J Pharm* [Internet]. Elsevier; 2019;555:198–206. Available from: <https://doi.org/10.1016/j.ijpharm.2018.11.048>

40. Viidik L, Vesala J, Laitinen R, Korhonen O, Ketolainen J, Aruväli J, et al. Preparation and characterization of hot-melt extruded polycaprolactone-based filaments intended for 3D-printing of tablets. *Eur J Pharm Sci*. 2021;158.

41. Kim DH, Kim YW, Tin YY, Soe MTP, Ko BH, Park SJ, et al. Recent technologies for amorphization of poorly water-soluble drugs. *Pharmaceutics*. 2021;13.

42. Boniatti J, Januskaite P, da Fonseca LB, Viçosa AL, Amendoeira FC, Tuleu C, et al. Direct powder



extrusion 3d printing of praziquantel to overcome neglected disease formulation challenges in paediatric populations. *Pharmaceutics*. 2021;13.

43. Izgelov D, Freidman M, Hoffman A. Investigation of cannabidiol gastro retentive tablets based on regional absorption of cannabinoids in rats. *Eur J Pharm Biopharm* [Internet]. Elsevier; 2020;152:229–35. Available from: <https://doi.org/10.1016/j.ejpb.2020.05.010>

44. Hughey JR, Keen JM, Miller DA, Kolter K, Langley N, McGinity JW. The use of inorganic salts to improve the dissolution characteristics of tablets containing Soluplus®-based solid dispersions. *Eur J Pharm Sci* [Internet]. 2013;48:758–66. Available from: <http://dx.doi.org/10.1016/j.ejps.2013.01.004>

45. Maggi L, Segale L, Torre ML, Ochoa Machiste E, Conte U. Dissolution behaviour of hydrophilic matrix tablets containing two different polyethylene oxides (PEOs) for the controlled release of a water-soluble drug. Dimensionality study. *Biomaterials*. 2002;23:1113–9.

46. Thiry J, Lebrun P, Vinassa C, Adam M, Netchacovitch L, Ziemons E, et al. Continuous production of itraconazole-based solid dispersions by hot melt extrusion: Preformulation, optimization and design space determination. *Int J Pharm* [Internet]. Elsevier B.V.; 2016;515:114–24. Available from: <http://dx.doi.org/10.1016/j.ijpharm.2016.10.003>

47. Lin X, Su L, Li N, Hu Y, Tang G, Liu L, et al. Understanding the mechanism of dissolution enhancement for poorly water-soluble drugs by solid dispersions containing Eudragit® E PO. *J Drug Deliv Sci Technol*. 2018;48:328–37.

48. Hari SK, Gauba A, Shrivastava N, Tripathi RM, Jain SK, Pandey AK. Polymeric micelles and cancer therapy: an ingenious multimodal tumor-targeted drug delivery system. *Drug Deliv Transl Res* [Internet]. Springer US; 2023;13:135–63. Available from: <https://doi.org/10.1007/s13346-022-01197-4>



# DISCUSSION

---



## Discussion

Since the combination of computational chemistry and HTS for the research of new therapeutic molecules pharmaceutical industry has been concerned with great issue regarding poorly soluble drugs. Indeed, identified potential drug candidates show complex chemical structures and high molecular weights, resulting in 75 – 90% of drug products in development having a poor water solubility. Among this range, 40% are considered as practically insoluble ( $< 100 \mu\text{g/mL}$ ) [1]. This solubility issue has an impact on clinical trials, as over the 90% of tested drugs that fail during phase I, II or III, 15% are poorly soluble in water [2]. In order to be administrated to patients and produce their therapeutic effects, these active molecules must be formulated so that their solubility is increased. That is why the formulation step is a great challenge for manufacturers.

A variety of solubility-enhancing strategies have been studied over the last few decades to enable oral delivery of poorly soluble molecules. Among them, the formation of ASD has been of particular interest for pharmaceutical industry, leading to commercial successes such as Kaletra<sup>®</sup>, Sporanox<sup>®</sup>, Crestor<sup>®</sup> or Noxafil<sup>®</sup> [3–5]. This success is due to several reasons such as the increase of both aqueous solubility and dissolution rate of the API without decreasing its gastric or intestinal permeability. Moreover, it is important to mention that patients are generally more compliant to solid forms rather than liquid forms leading manufacturers to develop ASDs [6,7].

The most used manufacturing methods of amorphous formulations can be categorized into two classes: fusion-based methods and solvent-based methods [8,9]. The choice of the method is of paramount importance as it has an impact on the finished product properties in terms of physical and chemical stability as well as *in vitro* and *in vivo* performances [10]. Therefore, the first part of the work consisted in the comparison of three strategies for the production of amorphous formulations in order to select the most appropriate to increase CBD aqueous solubility. The first investigated strategy was divided into two solvent-based methods which were spray-drying and FD of complexes composed of CBD and CH<sub>3</sub>- $\beta$ -CD, HP $\beta$ CD or HP $\gamma$ CD. The increase of CBD aqueous solubility by a complexation with randomly methylated- $\beta$ -CD and  $\beta$ -CD have already been highlighted by Mannila *et al.* [11]. Moreover, two companies, Medexus Pharmaceuticals and Vireo Health LLC have investigated the complexation of CBD with randomly methylated- $\beta$ -CD, dimethyl-  $\beta$ -CD and trimethyl- $\beta$ -CD or with a sulfoalkyl ether CD, respectively [12]. However, data concerning delivery route or pharmacokinetic are not available. The second strategy was another solvent-based method, namely impregnation of MS at ambient pressure or at subcritical carbon dioxide pressure. The third strategy was the production of ASDs by HME, a melting-based method. This

technique has already been used to increase CBD aqueous solubility and dissolution rate, although only buccal formulations were investigated. Taha and colleagues produced polymeric buccal films containing CBD by HME. Films which were composed of PEO, HPC (Klucel™) and/or SOL, allowed an increase of CBD aqueous solubility compared to the pure drug, but only films composed of PEO resulted in an immediate release of CBD [13]. In another study, FDM coupled with HME were used to produce orodispersible films containing small amount of CBD (from 0.12 mg to 5.07 mg) and PEO [14]. *In vitro* dissolution tests showed a total release of the drug within 30 minutes. This study demonstrated that all three strategies resulted in the amorphization of CBD, which was sustained for at least two months. Additionally, all amorphous formulations produced increased the aqueous solubility of CBD in comparison to its crystalline form. The formulation that yielded the greatest improvement in solubility was an ASD consisting of a vinylpyrrolidone-vinyl acetate copolymer (KVA64) and CBD produced by HME. Due to its ability to produce amorphous formulations with a substantial increase in CBD solubility, as well as being a solvent-free and cost-effective process, HME was chosen to develop oral solid dosage forms of CBD with immediate release.

Further, an optimization of the HME process was conducted by varying the formulation composition, extrusion temperature and screw speed. The selection of the polymer matrix to obtain an ASD is highly API-dependent. Indeed, solubility or miscibility of the drug into the polymer has an influence on the stability of the amorphous state as well as on formulation dissolution performances [15]. As reported above, ASDs of CBD have already been produced by HME with PEO, HPC and SOL, but only PEO allowed a CBD immediate release. This polymer is known to form a gel in contact with water, slowing drug dissolution rate. This immediate release obtained during the aforementioned study was certainly achieved due to the low dose of CBD as well as the thin thickness of the buccal films, reducing the gelling effect. Therefore, the present study aimed to screen three polymers devoid of gel effect, namely KVA64, Parteck® MXP which is a polymer of PVA, and EPO, a methacrylate polymer. KVA64 was chosen for its ability to increase CBD solubility, as described in the first part of this work. PVA has already been used for the manufacture of BCS II drug immediate release by HME [16]. EPO was selected as it allows fast release and micelles formation [17]. ASD composed of 10% CBD and each of these three polymers were produced by HME before being milled and filled into capsules. This CBD proportion allowed the manufacture oral dosage forms with a dose comprised in therapeutic dosage range already tested in clinical trials [18]. Further, CBD physical state was evaluated in the ASDs and dissolution tests were performed. Results showed that every polymer stabilized CBD in its amorphous state, but EPO was

selected for the rest of the study, as it was the only polymer allowing an immediate release of CBD.

Extrusion parameters also have an impact on drug physicochemical state in the polymeric matrix, leading to specific dissolution rate [19]. A screening study of the dissolution behavior of EPO-CBD formulations extruded at different temperatures and different screw speeds was conducted. The extrusion at 140 °C and 50 rpm allowed the production of a formulation that showed a dissolution profile characterized by an immediate release and an upkeep of the supersaturated CBD solution during at least four hours while formulations extruded at other conditions showed a CBD recrystallization during the dissolution test. 140 °C/50 rpm were the selected extrusion parameters for the rest of this research thesis. Capsules were filled with the formulation extruded with these parameters and the compliance to the Eur. Ph. monograph concerning hard capsules as well as CBD physical stability were assessed. The required assays, namely mass variation and uniformity of mass matched monograph specifications, demonstrating the appropriate flow of the produced milled extrudates, suitable for a uniform capsule filling. Moreover, CBD remained amorphous during six months, demonstrating the stabilizing properties of EPO.

In a perspective of extruding other active molecules which would recrystallize during dissolution test no matter the extrusion parameters used, the effect of adding a recrystallization inhibitor to the formulation was evaluated. It has been demonstrated in the literature that some polymers, mostly cellulose derivatives, can act as crystallization inhibitor to suppress or delay precipitation from a supersaturated state [20,21]. In this study, 7.5% of ENM was added to the formulation extruded at 160 °C/50 rpm. It appeared that the supersaturated state of the formulation containing ENM was maintained during the entire dissolution test, showing the ability of this polymer to prevent the amorphous molecules of CBD to nucleate and recrystallize.

The second part of this work thesis was the evaluation of the impact that the shaping method can have on ASD. Besides the traditional downstream method for ASD such as capsule filling described above, these formulations can be shaped by innovative methods like 3D printing. Therefore FDM 3D printing coupled with HME was assessed to produce ASD with an immediate release of CBD and a compliant to Eur. Ph. requirements. The process involves melting and mixing of a drug-polymer mixture and the extrusion of it into a filament that is fed into a FDM printer [22]. Then, molten filament is deposited through a nozzle on a build plate, layer-by-layer, to form a 3D object.

Numerous polymers have been tested to print drugs by FMD, mostly cellulose derivatives, PVP, PVP/VA, polyvinyl caprolactam-polyvinyl acetate-polyethylen glycol graft copolymer or methacrylate copolymer [22–25]. In some cases a drug-polymer

binary mixture is used, but polymers are generally used in association with other polymers or excipients in order to have suitable properties to be extruded and printed. Indeed, the mixture must be thermoplastic with a degradation temperature ( $T_{deg}$ ) high enough to withstand the extrusion and printing temperatures. Moreover, the extruded filament should neither be too brittle nor too flexible to be loaded into the printer. Plasticizers such as TEC, triacetin, various grades of polyethylene oxides, polysorbate 80 or glycerol, often need to be added to meet these properties [26–28]. Another parameter that must be controlled in order to obtain a feedable filament is its diameter. A too thin or too thick filament will not be pulled by the wheels of the printer. Moreover, inconsistent diameter induces non-uniform melt deposition by the printer which could result in printed forms with an inadequate mass [29].

EPO was the selected polymer in the previous chapter. Formulations containing EPO have already been printed by FDM, highlighting the taste masking properties of this polymer, but also and especially its solubility increasing properties. For example, Wang *et al.* used FDM to print filament composed of caffeine, HPC and HPMC, with or without EPO. In comparison with the other formulations, the ones that contained EPO showed a better taste masking in simulated salivary fluid and a higher dissolution rate in simulated gastric fluid, demonstrating the taste masking and solubility increase properties of EPO [30]. However, this polymer is not printable on its own because of its brittleness and has to be blended with plasticizers to acquire appropriate flexibility to be fed into the printer. In this matter, several plasticizers have already been tested in combination with EPO, such as polysorbate 80, TEC, PEG 4000 or PEO. However, these plasticizers had to be used in combination or with the addition of a filler to give the adequate flexibility to EPO, with the exception of PEO which has already allowed the printing of a filament composed of pramipexole, EPO and PEO [23,25,31]. As a minimum of excipients is desired to reduce the risk of eventual undesired drug-excipient interactions, PEO was selected to plasticize EPO.

Therefore, different ratios of EPO and PEO with 10% of CBD were tested in order to select the combination with the highest dissolution rate of CBD. The dissolution profiles showed that the lower the proportion of PEO, the faster the dissolution of CBD. Indeed, the formulation which contained the lower proportion of PEO allowed a significantly higher CBD dissolution than the other formulations. This was explained by PEO propensity to form a hydrogel in contact with aqueous fluids which slows down the release of API [32,33]. The fast EPO dissolution in acidic medium would break this hydrogel and allow the API release [34].

Besides composition, geometry of printed tablets may also have modulate API dissolution rate [35,36]. In this study, formulation with the lowest PEO proportion was



chosen to print six different designs and evaluate the printed tablets in terms of dissolution rate and the compliance with Eur. Ph. requirements, i.e. friability, mass variation, uniformity of mass and dissolution. Three cylinders with different percentages of infill and three capsule-like shapes called gyroids with different surface areas were successfully printed, each with a targeted mass of 650 mg. All the printed tablets were compliant with the monograph concerning uncoated tablets of the Eur. Ph. This monograph was chosen due to the non-existence of pharmaceutical guidelines concerning 3D printed forms.

After dissolution testing, it was shown that the dissolution rate increased proportionally with printed tablets SA/V ratio. This confirmed the influence of this ratio already described in the literature. For example, Goyanes *et al.* printed formulations composed of paracetamol and PVA into different geometries with different SA/V ratio [36]. Authors observed a faster dissolution of shapes having the highest ratio. Each printed tablet provided a CBD immediate release, except for two. Indeed, cylinder with 100% of infill and gyroid with the smallest surface area dissolved less than 80% of CBD after 30 minutes. It was also observed that gyroids dissolved CBD faster than cylinders due to a higher SA/V ratio. However, cylinder with 20% of infill was considered more suitable for pharmaceutical production as it allowed a CBD immediate release and was manufactured three times faster than gyroids.

Further, cylinder with 20% of infill was printed with different sizes to evaluate FDM ability to manufacture printed forms with different dosages without altering their mechanical and dissolution performances. The printed cylinders were compliant with each test of the monograph. Concerning the dissolution, it was shown that the dissolution rate was proportional to the dosage of CBD after 15 minutes, and then became similar for all three cylinder sizes. It was hypothesized that the early dissolution rate could be due to the higher gradient concentration between the solid form and the aqueous medium that could lead to a faster dissolution of the formulations with a high drug load. However, every cylinder provided a CBD immediate release.

Finally, the physical stability of CBD within printed cylinders with 20% of infill and a mass of 650 mg was assessed. It appeared that CBD remained amorphous during six months, demonstrating the stabilizing properties of both EPO and PEO, despite the two heating steps of the process.

The results of this work proved that FDM 3D printed coupled with HME is a suitable method for manufacturing oral solid dosage forms that allow a CBD immediate release as well as a compliance with the Eur. Ph.

The many complications inherent in the manufacture of a printable filament, i.e. the need for a constant and appropriate diameter and for specific mechanical properties, led to

the emergence of DPE technique in the pharmaceutical field. This technique appears to be a promising solution to circumvent the limitations encountered in FDM. Indeed DPE does not require laborious filament manufacturing by HME and may speed up printed tablets formulation. The process is defined by heating a powder mixture before its ejection through a nozzle and its deposition, layer by layer, on a build platform until obtaining a final 3D printed object. The ejection can be generated by the action of an Archimedes screw or by compressed air [37,38]. To be printable, material must have a suitable viscosity as a too-viscous molten material would clog the printer nozzle. Powder blends flow is another important parameter, especially for screw powder extruder head, since powder goes along the screw by effect of gravity at the start of the process. Concerning pneumatic ejection, the powder blend filled in the barrel must be compressed to minimize air space in the mixture which could result in an inconsistent material ejection [39].

In the context of this study, a homemade printer based on classical FDM printer but with a single-screw powder extruder head, was used for manufacturing CBD printed tablets. It has been previously demonstrated that a mixture of PEO and EPO was suitable for manufacturing CBD printed tablets. Therefore, these two polymers were used to assess DPE as a production and shaping method of ASDs containing CBD with an immediate release. However, EPO is a powder characterized by a poor flow due to its small particule size (about 10  $\mu\text{m}$ ). E100 is the same polymer than EPO, but formulated into pellets with a size of about 4 mm. These pellets were milled and granules with a size of about 180  $\mu\text{m}$  were obtained and used instead of EPO as it had a better flow. SOL, another amorphous polymer, soluble at every pH and having a good flow, was also studied as a matrix former for ASDs production. To the best of our knowledge, neither E100, SOL nor PEO have already been investigated using DPE with a screw head. EPO and SOL have already been printed by direct pneumatic extrusion in order to increase dutasteride dissolution rate. However, drug immediate release could not be obtained. Author hypothesized that this was due to strong drug-polymer interactions, preventing formulation from fast dissolution [39]. After testing different ratios of E100/PEO and SOL/PEO, each with 10% CBD, it appeared that a minimum of 63% PEO was needed to plasticize both E100 and SOL in order to be printed. The difference with formulations composed of CBD/EPO/PEO printed by FDM, for which a minimum of only 18% PEO was needed to plasticize, can be explained by the process. As described in Chapter III, FDM printing involves two heating steps, with eventual kneading zones, which achieve better mixing of all compounds and incorporate the plasticizer between the polymer chains, leading to a better chain mobility. DPE printer has less mixing power since it consists of only one screw, heated to a single temperature and without kneading zone.

The printable formulations were printed into cylinders with 20% infill. Time of the entire production process was considerably reduced in comparison with FDM process as no filament production was needed. Dissolution tests were conducted under stomach conditions at pH 1.6 during two hours followed by a pH adjustment at 6.8 to mimic upper intestine conditions. These conditions were based on a study that highlighted the tendency of CBD to be better absorbed in the upper intestine leading to the need to dissolve a maximum of CBD in stomach conditions. Dissolution profiles showed that printed tablets containing SOL did not increase the solubility of CBD during four hours of testing explained by the gelling behavior of both SOL and PEO. On the contrary it was shown by others that printed formulations containing SOL and PEO increased the solubility of felodipine [23]. This highlights the great influence of the nature of the API in the choice of the polymer matrix.

Printed tablets containing E100 allowed a CBD immediate release with an upkeep of the supersaturation during the entire dissolution test. The absence of recrystallization of CBD in the neutral medium while E100 is insoluble at pH above 5 was explained by DLS analysis. Indeed, particles formed by E100 in the acid medium seemed to be stabilized by PEO at pH 6.8, allowing CBD to remain solubilized.

Printed tablets produced with appropriate quality, reproducibility, as well as CBD immediate release were successfully manufactured by DPE. This confirms that this 3D printing stands as a credible technology to overcome limits inherent to FDM. However, equipment improvement is necessary in order to avoid other issues such as the too low mixing potential.

This research thesis described the production of solid oral forms composed of ASDs of CBD by different techniques. These forms provided an immediate release of the API and were compliant with Eur. Ph. requirements. Although the objective has been achieved using each technique, each has advantages and disadvantages. Differences between ASDs processing by these three techniques (summarized in [Fig. 50](#)) will be discussed in terms of impact of formulation, processing temperature and shear, drug dissolution, use in the industry, hospital or community pharmacy and impact on the environment.

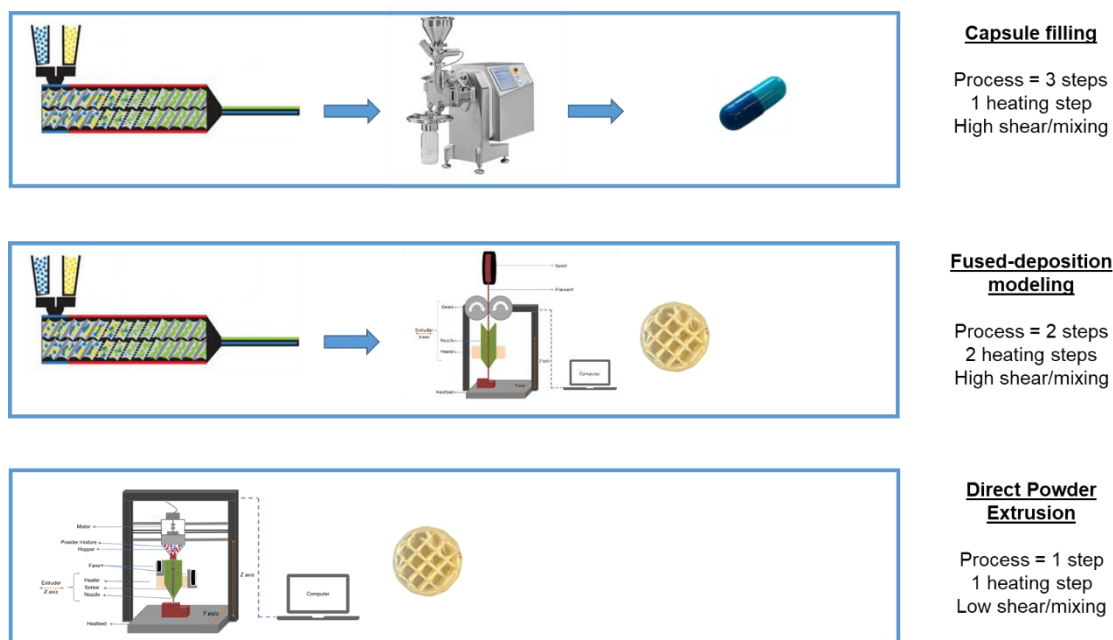


*Figure 50 - Summary of the three studied ASDs processing technologies, namely capsule filling, FDM and direct powder extrusion.*

### Choice of a Suitable Formulation

ASD is the dispersion of amorphous drug in a matrix, mostly a polymer. Various polymeric matrices have been studied and examined to prepare ASD as well described in the literature [5,40,41]. The rational selection of a polymer depends on a number of factors such as the physico-chemical properties of the API, the process or the expected release profile.

#### *Process*

ASD manufacturing by melting methods implies a process temperature above  $T_g$  and below  $T_{deg}$  of each component. Therefore, chosen polymer must have a  $T_g$  sufficiently lower from  $T_{deg}$  of the drug and eventual other excipients to avoid any degradation. This is a problem for thermosensitive drugs which have a  $T_{deg}$  close to the  $T_g$  of the polymers generally used in HME and 3DP. Plasticizer can be added to the formulation to reduce polymer  $T_g$  thus reducing the process temperature [42]. The viscosity of melted material is also reduced by the addition of plasticizers. Viscosity is a critical parameter to adjust for each of the three studied processing technologies. Indeed, a too high viscosity would induce a high torque during extrusion which could damage the equipment or prevent it from working [43].

Plasticizers can also increase material flexibility which is crucial for FDM. Currently, FDM printing faces a lack of polymers with the appropriate properties [44]. Indeed, with

some exceptions like PLA, HPMC and HPMCAS with low viscosities, polymers still need to be plasticized to be successfully driven by FDM printer wheels [45]. DPE does not require filament, so flexibility is not a major issue, but viscosity is. Indeed, the powder mixture is only heated for a limited time. Compounds that are too viscous once melted could block the nozzle if not fluidized quickly.

EPO was the polymeric carrier that allowed to produce solid oral dosages forms with CBD immediate release through this work thesis. Due to its low  $T_g$  and thermal stability, this polymer is extrudable on its own and no plasticizers were needed for capsule filling process. ASD with an immediate release produced by HME with EPO as the only excipient was already reported in the literature. Indeed, Pinho *et al.* extruded a formulation composed of theobromine and EPO [46]. *In vitro* dissolution test on the milled extrudates showed more than 80% of drug dissolution within 10 minutes.

However, as already described, the extrudability of a polymer does not necessarily ensure its printability. Indeed, EPO was too brittle to be printed by FDM and too viscous to be printed by DPE, so PEO was added to plasticized formulations processed by these two printing techniques.

### *Drug release*

Another determinant criterion for the formulation choice is the desired drug release. Indeed, even if ASDs are mostly produced to obtain an immediate drug release, they can also induce sustained, delayed or controlled release depending on chosen polymeric matrix and excipients. As reported in the literature, insoluble polymers such as ethylcellulose or Eudragit® RS can be used as polymer matrix former for the production of ASDs, resulting in a sustained release of the drug [47]. In another work, authors were able to produce ASDs of carbamazepine with an immediate, delayed or controlled release, weather polymeric matrix was composed of HPMC, Eudragit® L100-55 or cellulose acetate, respectively [48].

Through this work, whatever the processing technology used, an immediate release was obtained. However formulation had to be adjusted differently for each technique. EPO-based ASDs filled in capsule allowed an immediate release without addition of other excipients, but the burst release of the drug resulted in rapid recrystallization of the drug. This phenomenon is explained by the spring and parachute concept [49]. Spring represents the burst release followed by rapid drug recrystallization caused by the short-lived metastable drug state. This metastable state can be maintained for a certain period of time by addition of a crystallization inhibitor called parachute. Several crystallization inhibitors have been described in the literature such as HPMC, HPMC phthalate, HPC or PVP [50–52]. Acrylic polymers have also been used as crystallization

inhibitors. Indeed, Nollenberger *et al.* produced ASD composed of felodipine and EPO. The dissolution tests showed a drug recrystallization after its rapid release during the first five minutes of the test. The drop of felodipine concentration was prevented by the addition of 5% of Eudragit® NE, a copolymer based on ethyl acrylate and methyl methacrylate, to the formulation [53].

In this work, a similar polymer, namely Eudragit® NM30D (ENM), was added to the formulation in order to maintain CBD supersaturation.

ASDs printed by both FDM and DPE had to be plasticized by PEO to have an appropriate flexibility or viscosity to be produced. A fast early dissolution was also observed but no recrystallization was observed, explained by the stabilization by PEO of micelles formed by the dissolution of EPO which kept CBD in solution.

To summarize, formulation composition is one of the most critical parameter for ASD manufacturing and shaping, as it has an influence on formulation processability, but also on the drug release.

### Process Temperature and Shear

In the context of ASDs production, the purpose of heating and shearing is to break drug crystal lattice and increase molecular mobility, resulting in drug amorphization. This is followed by rapid cooling of the molten material, which solidifies in a one-phase amorphous system [54]. Depending on the used melting processing technology, materials are subjected to different conditions, particularly heat and shear. Concerning the capsule filling and FDM, the conversion of the crystalline state into an amorphous state occurs rather during the HME stage whereas it occurs during the printing stage when using the DPE. HME, depending on screw design and speed, is recognized for having a high amorphous converting power due to high temperature input, shear and residence time [55,56]. On the other hand, current DPE equipment involve shorter residence times under high temperatures and lower shear forces, reducing the amorphous converting power of this technique. Indeed, DPE does not always induce a drug total amorphization as reported in several studies [57–59]. For example, Fanous *et al.* used a direct powder extruder to print formulations composed of HPC and caffeine. After XRD analysis, authors observed an incomplete amorphization of the drug [57]. However, even if heat and shear are essential for drug amorphization, these parameters can trigger chemical degradation of API or excipients [60].

Concerning the temperature, it significantly affects degradation kinetics predicted by the Arrhenius equation [61]. Thermal induced chemical degradation has been widely reported to occur during HME process [62–64]. An optimization of screw design,

residence time or formulation is often needed when extrusion of thermosensitive drugs is considered [65]. This kind of degradation is even more likely to occur when FDM is considered, as material is subjected to two thermal stresses [58]. In this regard, DPE would be more suitable than capsule filling and FDM for ASD manufacturing containing thermosensitive drugs as it involves only one heating step during a short period of time. *Shear forces* can generate energy which can result in degradation of shear-sensitive materials [10]. This was studied by Li *et al.* who analyzed shear effect on starch with various plasticizer content during HME [66]. First, thermal degradation was assumed to be minimal with extrusion temperature that was used in the study. However, authors observed degradation on starch molecular structure. This was attributed to the shear stress, as degradation increased proportionally with plasticizer content because of greater mechanical energy. These results were similar to those report in another study [67].

Twin-screw HME is characterized by high shear, especially when kneading elements are involved. Moreover, capsule filling process implies extrudates milling which increases risk of shear-sensitive drug degradation. On another hand, current DPE equipment are characterized by a single screw without kneading elements. This results in a lower shear degradation risk for drug products manufactured by DPE than by capsule filling or FDM processes.

Nevertheless, drugs with high melting point require a combination of high temperature and shear to break the strong crystal lattice. This can be provided by HME but difficult to achieve when using DPE [68].

In conclusion, high temperature and shear are both a need and a degradation risk for ASDs manufacturing and API and excipients properties must be considered to choose an appropriate processing technology.

Another factor that can be influenced by the temperature and shear forces is the drug physical state. As described above, the methods involving HME allow a better mixing of the different compounds than the DPE. This could lead to the presence of nuclei, which are intermediates to recrystallization, after the production of ASD by DPE. Current techniques make it difficult to detect these possible nuclei, which can affect recrystallization [69,70]. However, the three processing technologies allowed the maintenance of the amorphous state of the CBD for at least six months (for capsules and FDM printed tablets) and at least two months for the DPE printed tablets (data on a longer term no available yet). This suggests that the mixing power of these techniques is sufficient to disperse the CBD molecularly in the polymeric matrix and/or that this matrix was viscous enough to prevent the nuclei from growing and recrystallizing.

Milling step is also known as a potential trigger for drug recrystallization [71]. However, ASD filled into capsules remained amorphous after this step confirming the physical stability of this formulation.

### Impact of Process Technology on Drug Dissolution

**Appendix V** shows the dissolution profile of the optimal ASD produced by each of the process technology as well as the percentage of CBD dissolved after 5 and 15 minutes. Unsurprisingly, ASD in capsule allowed a significantly faster dissolution of CBD than the printed forms after 5 and 15 minutes, explained by the greater contact surface with the dissolution medium of the ground extrudates. These differences of dissolution rate indicate the importance of ASD shaping method choice, as for a similar composition, the higher the surface, the faster the drug release. However, an equilibrium is observed between each formulation after 30 minutes. This equilibrium is due to the rapid dissolution of EPO even from the strong structures resulting from the melting and cooling of the printed materials.

In addition to the surface of the final product, the process mixing ability also have an influence on drug dissolution. Studies have shown that the more intense the mixing, the more drug-polymer interactions there are and the more the dissolution performance is improved [72–74]. These interactions allow the polymer to remain intimately connected to the drug when in contact with dissolution medium, preventing drug recrystallization. Indeed, without these interactions, the polymer would rapidly dissolve, leaving rich regions of drug alone, increasing the risk of recrystallization. With two screws and two kneading zones, the extrusion step for capsule filling and FDM provided a high level of mixing compared to DPE. However, the dissolution rate of printed tablets made by FDM and DPE was not significantly different. In addition, the EPO/PEO ratio was superior in the formulation produced by FDM than in that produced by DPE. However, it was observed that the more this ratio increased, the faster CBD was dissolved (Chapter III - Results). A faster dissolution was therefore expected for the printed tablets produced by FDM. This suggests a different distribution of the different components depending on the technique used. Investigation of CBD repartition between both polymers as well as the repartition of both polymers in the 3D space of the printed tablet should be performed with surface techniques such as time-of-flight secondary ion mass spectrometry (TOF-SIMS). Indeed, Parulski *et al.* already demonstrated TOF-SIMS ability to explain the difference of dissolution rate of different ASDs of ITZ by highlighting a difference of repartition of the API between polymers that constituted the matrix of each formulation [75].



### Impact on the Environment

One of the main advantages of melting technologies for ASDs manufacturing is to be solvent free, which avoids additional cost, low patient compliance and additional drying step. Moreover, residual organic solvents that have non therapeutic benefits but being hazardous for patients and environment are also avoided [76]. However, heating at high temperatures implies consequent energy input, especially for HME which requires higher energy input compared to other techniques [76].

Another factor to take into account regarding the environment is the production of waste. Each process step generates waste and the more steps involved, the more waste. Therefore, processing technologies with a minimum of steps are sought. In this regard, DPE would generate less waste than FDM and even less than capsule filling.

### Production Scale

#### *Industrial scale*

Marketed ASDs produced by melting methods, especially HME, are mostly shaped into tablets, but also filled into capsules [40,77]. Commercially pharmaceutical grade extruders are available at different scales with extrusion capacity going from 0.01 to 1000 kg per hour, depending on the design and formulation [76]. Extrudates are then crushed or pelletized and constitute an intermediate material before capsule filling or tableting. Capsule filling and tableting are fast production processes as up to 200,000 capsules and up to 1.6 million tablets could be produced per hour [44].

On the other hand, current FDM and DPE equipment cannot compete against such high production rates. Indeed, based on the results obtained in chapters III and IV, maximum throughput of both FDM and DPE would be 12 printed tablets per hour. Depending on printed tablets dimensions, shorter printing times are reported in the literature, but it rarely exceed 50 per hour [78–80]. Without the customization of large-sized that are able of dealing with mass production, 3D printing will stay at research stage and its many potential therapeutic applications will never be exploited [81].

In addition to larger equipment sizes, scaling up could be facilitated by making equipment compatible with CM. It is a scheme where the materials and product are continuously fed into and discharged from the system throughout the process duration. CM has been attracting increasing attention within the pharmaceutical industry because it could lead to significant decreases in production costs while improving product quality with less batch-to-batch variations [82,83]. The three stages of the capsule filling process are compatible with CM. It would therefore be possible to combine them to have a continuous production line.

CM with a 3D printing technique has already been considered. Indeed, a direct powder extrusion-based technique has recently been invented by Triastek (China) and is called MED technology [84]. MED™ printer is GMP graded and can work with up to 32 printing-nozzles in order to continuously convert powder into a molten and deposit it layer-by-layer to produce objects. A production throughput of 30,000 printed tablets per day by this printer has been reported.

To ensure drug product quality, Process Analytical Technology (PAT) tools are generally implemented to CM processes [85]. These technologies are non-destructive and provide continuous material control during drug product manufacturing [86]. Various spectroscopic techniques such as Raman, near infrared or Fourier transformed infrared have been explored as PAT tools for HME. For example, Krier *et al.* produced implants composed of celecoxib and ethylvinyl-acetate by co-extrusion [87]. Filament diameter and the quantity of API were controlled in-line with a laser measurement, NIR and Raman spectroscopy, respectively. PAT tools have also been investigated for 3D printing techniques. For example, MED™ printer is equipped with NIR for the measurement of mixture homogeneity and a photographic monitoring system to identify the physical properties of the tablets. Another example of printer equipped with PAT tool is M3DIMAKER GMP printer developed by FabRx (London, UK). The equipment is designed to prepare small batches 3D printed drugs using three different types of printheads, i.e. FDM-, DPE- or semisolid extrusion-head [88]. This printer is fitted with a camera to monitor in-line quality of the 3D printed products.

These in-line techniques should be implemented to future industrial-scale 3D equipment as they can improve the understanding of the process and guaranty the quality of the end product.

Another aspect that needs consideration for scaling-up 3D printing technologies is the development of guidelines to ensure safety, efficacy, quality and stability of printed drug products. Versatility and rapid evolving 3D printing technologies represent an obstacle for the regulatory authorities to establish guidelines given the stringent requirements of the pharmaceutical sector [89].

Still, there are positive factors regarding the future of FDM and DPE in pharmaceutical industry. Indeed, the human cost is lower compared to traditional manufacturing techniques as the number of steps to produce printed forms are generally smaller than to produce tablets or capsules [90]. Moreover, 3D printing technology is able to produce a prototype in a short period of time and test its acceptability before launching to the market. This enables the possibility to improve and customize prototypes more rapidly, which would considerably reduce time and cost of a drug product development [90].

However, one of the main interests of 3D printing is to manufacture drug products that cannot be manufactured by conventional manufacturing techniques, not to substitute traditional drugs. In that regard, FDM and DPE rather have a closer future in hospitals or community pharmacies.

### *Hospitals and community pharmacies scale*

Since these entities produce medicines “on-demand” rather than in masses, the difference in production cadence between capsule filling and 3D printing should be minimal. Manual capsule filling have been used for more than a century to manufacture oral drug products as magistral preparations [91]. Capsules are generally manufactured by batches, using a capsule filler. In this case, excipients such as flow regulator and filler are often needed for a homogeneous filling of every capsule. The filling of one capsule at a time could be considered to dispense the use of additional excipients, but it would be time-consuming and would require accurate and expensive scales, especially for small dosages. One of the limits of capsules is the difficulty of elaborating modified release in order to meet specific need for patients’ treatment.

FDM and DPE are cheap, easy to carry and relatively simple to operate and could be considered as appropriate techniques for personalized medicine. Indeed, as already explained, these printing techniques are able to produce medicines with different releases, original geometries to improve patients’ compliance, or different sizes to match patients’ weight.

Moreover, the automation and accuracy of the printers could make the printing of drug products safer.

Concerning the manufacturing and shaping of ASDs, implementation in hospitals or community pharmacies could be done in partnership with industry, at least for FDM and capsule filling [92]. Amorphous drug extrudates with homogeneous drug repartition could be manufactured, as filaments or as milled powder, by a pharmaceutical industry and sold to hospitals or local pharmacies as intermediate materials. These materials could further be filled into capsules or printed depending on patients’ needs or desire. A major limit of this process is the physical stability of the ASD. Indeed, it is known that amorphous compounds tend to recrystallized over time, depending on the stabilizer and storage conditions [93]. This stability issue could be circumvented by the use of the DPE. Indeed, the drug amorphization and its shaping take place during the same step, avoiding the need for intermediate amorphous material storage.

DPE stands as the more appropriate technique to manufacture ASDs at hospital or community pharmacy scale. Indeed, all stages of the preparation, namely the mixing of raw materials and printing can be done on site without using an intermediate product,

reducing costs and stability issue. This work thesis demonstrated the process feasibility with CBD as a BCS II model drug. However, amorphization of molecules having a higher melting point should be investigated to demonstrate the versatility of DPE. Finally, even if a GMP printer is already available, its price (EUR ~80,000) seems hardly affordable for hospitals and even more for community pharmacies [94]. This highlights the need for the design of cheaper GMP printers.

## References

- [1] T. Takagi, C. Ramachandran, M. Bermejo, A Provisional Biopharmaceutical Classification of the Top 200 Oral Drug Products in the United States, Great Britain, Spain, and Japan, *Mol. Pharm.* 3 (2006) 631–643.
- [2] D. Sun, W. Gao, H. Hu, S. Zhou, Why 90% of clinical drug development fails and how to improve it?, *Acta Pharm. Sin. B.* 12 (2022) 3049–3062. <https://doi.org/10.1016/j.apsb.2022.02.002>.
- [3] J.S. LaFontaine, J.W. McGinity, R.O. Williams, Challenges and Strategies in Thermal Processing of Amorphous Solid Dispersions: A Review, *AAPS PharmSciTech.* 17 (2016) 43–55. <https://doi.org/10.1208/s12249-015-0393-y>.
- [4] C. Brough, R.O. Williams, Amorphous solid dispersions and nano-crystal technologies for poorly water-soluble drug delivery, *Int. J. Pharm.* 453 (2013) 157–166. <https://doi.org/10.1016/j.ijpharm.2013.05.061>.
- [5] T. Vasconcelos, S. Marques, J. das Neves, B. Sarmiento, Amorphous solid dispersions: Rational selection of a manufacturing process, *Adv. Drug Deliv. Rev.* 100 (2016) 85–101. <https://doi.org/10.1016/j.addr.2016.01.012>.
- [6] T. Vasconcelos, B. Sarmiento, P. Costa, Solid dispersions as strategy to improve oral bioavailability of poor water soluble drugs, *Drug Discov. Today.* 12 (2007) 1068–1075. <https://doi.org/10.1016/j.drudis.2007.09.005>.
- [7] M. Morishita, N.A. Peppas, Is the oral route possible for peptide and protein drug delivery?, *Drug Discov. Today.* 11 (2006) 905–910. <https://doi.org/10.1016/j.drudis.2006.08.005>.
- [8] S. V. Bhujbal, B. Mitra, U. Jain, Y. Gong, A. Agrawal, S. Karki, L.S. Taylor, S. Kumar, Q. (Tony) Zhou, Pharmaceutical amorphous solid dispersion: A review of manufacturing strategies, *Acta Pharm. Sin. B.* 11 (2021) 2505–2536. <https://doi.org/10.1016/j.apsb.2021.05.014>.
- [9] N. Ito, T. Hashizuka, M. Ito, H. Suzuki, S. Noguchi, Comparison of the physical properties of disodium etidronate amorphous forms prepared by different manufacturing methods, *Int. J. Pharm.* 635 (2023) 122723. <https://doi.org/10.1016/j.ijpharm.2023.122723>.
- [10] S. Huang, R.O. Williams, Effects of the Preparation Process on the Properties of Amorphous Solid Dispersions, *AAPS PharmSciTech.* 19 (2018) 1971–1984. <https://doi.org/10.1208/s12249-017-0861-7>.
- [11] P.J. J. Mannila, T. Järvinen, K. Järvinen, Precipitation Complexation Method Produces Cannabidiol/b-Cyclodextrin Inclusion Complex Suitable for Sublingual Administration of Cannabidiol, *J. Pharm. Sci.* 101 (2007) 312–319. <https://doi.org/10.1002/jps>.
- [12] S.A. Millar, R.F. Maguire, A.S. Yates, S.E. O'sullivan, Towards better delivery of cannabidiol (Cbd), *Pharmaceuticals.* 13 (2020) 1–15. <https://doi.org/10.3390/ph13090219>.
- [13] I. Taha, M.A. Elsohly, M.M. Radwan, S.H. Omari, M.A. Repka, E.A. Ashour, Employing Hot-Melt Extrusion Technology to Enhance the Solubility of Cannabidiol ( CBD ), *Annu. Poster Sess.* 21 (2022).
- [14] G.K. Eleftheriadis, E. Kantarelis, P.K. Monou, E.G. Andriotis, N. Bouropoulos, E.K. Tzintzimis, D.

- Tzetzis, J. Rantanen, D.G. Fatouros, Automated digital design for 3D-printed individualized therapies, *Int. J. Pharm.* 599 (2021) 120437. <https://doi.org/10.1016/j.ijpharm.2021.120437>.
- [15] F. Qian, J. Huang, M.A. Hussain, Drug-polymer solubility and miscibility: Stability consideration and practical challenges in amorphous solid dispersion development, *J. Pharm. Sci.* 99 (2010) 2941–2947. <https://doi.org/10.1002/jps.22074>.
- [16] C. Wei, N.G. Solanki, J.M. Vasoya, A. V. Shah, A.T.M. Serajuddin, Development of 3D Printed Tablets by Fused Deposition Modeling Using Polyvinyl Alcohol as Polymeric Matrix for Rapid Drug Release, *J. Pharm. Sci.* 109 (2020) 1558–1572. <https://doi.org/10.1016/j.xphs.2020.01.015>.
- [17] X. Lin, L. Su, N. Li, Y. Hu, G. Tang, L. Liu, H. Li, Z. Yang, Understanding the mechanism of dissolution enhancement for poorly water-soluble drugs by solid dispersions containing Eudragit® E PO, *J. Drug Deliv. Sci. Technol.* 48 (2018) 328–337. <https://doi.org/10.1016/j.jddst.2018.10.008>.
- [18] S.A. Millar, N.L. Stone, A.S. Yates, S.E. O'Sullivan, A systematic review on the pharmacokinetics of cannabidiol in humans, *Front. Pharmacol.* 9 (2018). <https://doi.org/10.3389/fphar.2018.01365>.
- [19] J. Pawar, D. Suryawanshi, K. Moravkar, R. Aware, V. Shetty, Study the influence of formulation process parameters on solubility and dissolution enhancement of efavirenz solid solutions prepared by hot-melt extrusion : a QbD methodology, (2018).
- [20] J.L. Terebetski, B. Michniak-Kohn, Combining ibuprofen sodium with cellulosic polymers: A deep dive into mechanisms of prolonged supersaturation, *Int. J. Pharm.* 475 (2014) 536–546. <https://doi.org/10.1016/j.ijpharm.2014.09.015>.
- [21] Y.W. Li, H.M. Zhang, B.J. Cui, C.Y. Hao, H.Y. Zhu, J. Guan, D. Wang, Y. Jin, B. Feng, J.H. Cai, X.R. Qi, N.Q. Shi, "Felodipine-indomethacin" co-amorphous supersaturating drug delivery systems: "Spring-parachute" process, stability, in vivo bioavailability, and underlying molecular mechanisms, *Eur. J. Pharm. Biopharm.* 166 (2021) 111–125. <https://doi.org/10.1016/j.ejpb.2021.05.030>.
- [22] K. Vithani, A. Goyanes, V. Jannin, A.W. Basit, S. Gaisford, B.J. Boyd, An Overview of 3D Printing Technologies for Soft Materials and Potential Opportunities for Lipid-based Drug Delivery Systems, *Pharm. Res.* 36 (2019). <https://doi.org/10.1007/s11095-018-2531-1>.
- [23] M. Alhijaj, P. Belton, S. Qi, An investigation into the use of polymer blends to improve the printability of and regulate drug release from pharmaceutical solid dispersions prepared via fused deposition modeling (FDM) 3D printing, *Eur. J. Pharm. Biopharm.* 108 (2016) 111–125. <https://doi.org/10.1016/j.ejpb.2016.08.016>.
- [24] M.A. Azad, D. Olawuni, G. Kimbell, A.Z.M. Badruddoza, M.S. Hossain, T. Sultana, Polymers for extrusion-based 3D printing of pharmaceuticals: A holistic materials–process perspective, 2020. <https://doi.org/10.3390/pharmaceutics12020124>.
- [25] M. Sadia, A. So, B. Arafat, A. Isreb, W. Ahmed, Adaptation of pharmaceutical excipients to FDM 3D printing for the fabrication of patient-tailored immediate release tablets, *Int. J. Pharm.* 513 (2016) 659–668. <https://doi.org/10.1016/j.ijpharm.2016.09.050>.
- [26] G. Kollamaram, D.M. Croker, G.M. Walker, A. Goyanes, A.W. Basit, S. Gaisford, Low temperature fused deposition modeling ( FDM ) 3D printing of thermolabile drugs, *Int. J. Pharm.* 545 (2018) 144–152. <https://doi.org/10.1016/j.ijpharm.2018.04.055>.

- [27] M. Uboldi, A. Chiappa, M. Pertile, A. Piazza, S. Tagliabue, A. Foppoli, L. Palugan, A. Gazzaniga, L. Zema, A. Melocchi, Investigation on the use of fused deposition modeling for the production of IR dosage forms containing Timapiprant, *Int. J. Pharm.* X. 5 (2023) 100152. <https://doi.org/10.1016/j.ijpx.2022.100152>.
- [28] J.M. Nasereddin, N. Wellner, M. Alhijaj, P. Belton, S. Qi, Development of a Simple Mechanical Screening Method for Predicting the Feedability of a Pharmaceutical FDM 3D Printing Filament, *Pharm. Res.* 35 (2018). <https://doi.org/10.1007/s11095-018-2432-3>.
- [29] C. Parulski, O. Jennotte, A. Lechanteur, B. Evrard, Challenges of fused deposition modeling 3D printing in pharmaceutical applications: Where are we now?, *Adv. Drug Deliv. Rev.* 175 (2021). <https://doi.org/10.1016/j.addr.2021.05.020>.
- [30] H. Wang, N. Dumpa, S. Bandari, T. Durig, M.A. Repka, Fabrication of Taste-Masked Donut-Shaped Tablets Via Fused Filament Fabrication 3D Printing Paired with Hot-Melt Extrusion Techniques, *AAPS PharmSciTech.* 21 (2020) 1–11. <https://doi.org/10.1208/s12249-020-01783-0>.
- [31] H.E. Gültekin, S. Tort, F. Acartürk, An Effective Technology for the Development of Immediate Release Solid Dosage Forms Containing Low-Dose Drug: Fused Deposition Modeling 3D Printing, *Pharm. Res.* 36 (2019). <https://doi.org/10.1007/s11095-019-2655-y>.
- [32] S. Shojaee, P. Emami, A. Mahmood, Y. Rowaiye, A. Dukulay, W. Kaialy, I. Cumming, A. Nokhodchi, An Investigation on the Effect of Polyethylene Oxide Concentration and Particle Size in Modulating Theophylline Release from Tablet Matrices, *AAPS PharmSciTech.* 16 (2015) 1281–1289. <https://doi.org/10.1208/s12249-015-0295-z>.
- [33] H.E. Gültekin, S. Tort, F. Acartürk, Fabrication of Three Dimensional Printed Tablets in Flexible Doses: A Comprehensive Study from Design to Evaluation, *SSRN Electron. J.* 74 (2022) 103538. <https://doi.org/10.2139/ssrn.4028237>.
- [34] D.S. Frank, P. Prasad, L. Iuzzolino, L. Schenck, Dissolution Behavior of Weakly Basic Pharmaceuticals from Amorphous Dispersions Stabilized by a Poly(dimethylaminoethyl Methacrylate) Copolymer, *Mol. Pharm.* 19 (2022) 3304–3313. <https://doi.org/10.1021/acs.molpharmaceut.2c00456>.
- [35] M. Sadia, B. Arafat, W. Ahmed, R.T. Forbes, M.A. Alhnan, Channelled tablets: An innovative approach to accelerating drug release from 3D printed tablets, *J. Control. Release.* 269 (2018) 355–363. <https://doi.org/10.1016/j.jconrel.2017.11.022>.
- [36] A. Goyanes, P. Robles, A. Buanz, A.W. Basit, S. Gaisford, Effect of geometry on drug release from 3D printed tablets, *Int. J. Pharm.* 494 (2015) 657–663. <https://doi.org/10.1016/j.ijpharm.2015.04.069>.
- [37] B.M. Boyle, P.T. Xiong, T.E. Mensch, T.J. Werder, G.M. Miyake, 3D printing using powder melt extrusion, *Addit. Manuf.* 29 (2019) 100811. <https://doi.org/10.1016/j.addma.2019.100811>.
- [38] D. Muhindo, R. Elkanayati, P. Srinivasan, M.A. Repka, E.A. Ashour, Recent Advances in the Applications of Additive Manufacturing (3D Printing) in Drug Delivery: A Comprehensive Review, *AAPS PharmSciTech.* 24 (2023) 1–22. <https://doi.org/10.1208/s12249-023-02524-9>.
- [39] S.J. Kim, J.C. Lee, J.Y. Ko, S.H. Lee, N.A. Kim, S.H. Jeong, 3D-printed tablets using a single-step hot-melt pneumatic process for poorly soluble drugs, *Int. J. Pharm.* 595 (2021). <https://doi.org/10.1016/j.ijpharm.2021.120257>.

- [40] P. Pandi, R. Bulusu, N. Kommineni, W. Khan, M. Singh, Amorphous solid dispersions: An update for preparation, characterization, mechanism on bioavailability, stability, regulatory considerations and marketed products, *Int. J. Pharm.* 586 (2020) 119560. <https://doi.org/10.1016/j.ijpharm.2020.119560>.
- [41] S. Baghel, H. Cathcart, N.J. O'Reilly, Polymeric Amorphous Solid Dispersions: A Review of Amorphization, Crystallization, Stabilization, Solid-State Characterization, and Aqueous Solubilization of Biopharmaceutical Classification System Class II Drugs, *J. Pharm. Sci.* 105 (2016) 2527–2544. <https://doi.org/10.1016/j.xphs.2015.10.008>.
- [42] A.N. Ghebremeskel, C. Vemavarapu, M. Lodaya, Use of surfactants as plasticizers in preparing solid dispersions of poorly soluble API: Selection of polymer-surfactant combinations using solubility parameters and testing the processability, *Int. J. Pharm.* 328 (2007) 119–129. <https://doi.org/10.1016/j.ijpharm.2006.08.010>.
- [43] S.S. Gupta, N. Solanki, A.T.M. Serajuddin, Investigation of Thermal and Viscoelastic Properties of Polymers Relevant to Hot Melt Extrusion, IV: Affinisol™ HPMC HME Polymers, *AAPS PharmSciTech.* 17 (2016) 148–157. <https://doi.org/10.1208/s12249-015-0426-6>.
- [44] J. Wang, Y. Zhang, N. Heshmati, A. Raviraj, R. Thakkar, A. Nokhodchi, M. Maniruzzaman, Emerging 3D printing technologies for drug delivery devices : Current status and future perspective, *Adv. Drug Deliv. Rev.* 174 (2021) 294–316. <https://doi.org/10.1016/j.addr.2021.04.019>.
- [45] P. Xu, J. Li, A. Meda, F. Osei-Yeboah, M.L. Peterson, M. Repka, X. Zhan, Development of a quantitative method to evaluate the printability of filaments for fused deposition modeling 3D printing, *Int. J. Pharm.* (2020) 119760. <https://doi.org/10.1016/j.ijpharm.2020.119760>.
- [46] L.A.G. Pinho, S.G.B. Lima, L.F.B. Malaquias, F. de Q. Pires, L.L. Sá-Barreto, L. Cardozo-Filho, T. Gratieri, G.M. Gelfuso, M. Cunha-Filho, Improvements of theobromine pharmaceutical properties using solid dispersions prepared with newfound technologies, *Chem. Eng. Res. Des.* 132 (2018) 1193–1201. <https://doi.org/10.1016/j.cherd.2017.10.019>.
- [47] J. Maincent, R.O. Williams, Sustained-release amorphous solid dispersions, *Drug Deliv. Transl. Res.* 8 (2018) 1714–1725. <https://doi.org/10.1007/s13346-018-0494-8>.
- [48] H. Li, M. Zhang, L. Xiong, W. Feng, R.O. Williams, Bioavailability improvement of carbamazepine via oral administration of modified-release amorphous solid dispersions in rats, *Pharmaceutics*. 12 (2020) 1–16. <https://doi.org/10.3390/pharmaceutics12111023>.
- [49] D.D. Bavishi, C.H. Borkhataria, Spring and parachute: How cocrystals enhance solubility, *Prog. Cryst. Growth Charact. Mater.* 62 (2016) 1–8. <https://doi.org/10.1016/j.pcrysgrow.2016.07.001>.
- [50] K. Yamashita, T. Nakate, K. Okimoto, A. Ohike, Y. Tokunaga, R. Ibuki, K. Higaki, T. Kimura, Establishment of new preparation method for solid dispersion formulation of tacrolimus, *Int. J. Pharm.* 267 (2003) 79–91. <https://doi.org/10.1016/j.ijpharm.2003.07.010>.
- [51] N. Kohri, Y. Yamayoshi, H. Xin, K. Iseki, N. Sato, S. Todo, K. Miyazaki, Improving the Oral Bioavailability of Albendazole in Rabbits by the Solid Dispersion Technique, *J. Pharm. Pharmacol.* 51 (2010) 159–164. <https://doi.org/10.1211/0022357991772277>.
- [52] J. Vaughn, J. McConville, M. Crisp, K. Johnston, R. Williams, Supersaturation produces high bioavailability of amorphous danazol particles formed by evaporative precipitation into aqueous



- solution and spray freezing into liquid technologies, *Drug Dev. Ind. Pharm.* 32 (2006) 559–567. <https://doi.org/10.1080/03639040500529176>.
- [53] B.S. Nollenberger K., Gryczke A., Meier CH., Dressman J., Shmidt M.U., Pair Distribution Function X-Ray Analysis Explains Dissolution Characteristics of Felodipine Melt Extrusion Products, *J. Pharm. Sci.* 98 (2008) 1476–1486. <https://doi.org/10.1002/jps>.
- [54] T. Feng, P. Rodolfo, T. Carvajal, Process Induced Disorder in Crystalline Materials: Differentiating Defective Crystals from the Amorphous Form of Griseofulvin, *J. Pharm. Sci.* 97 (2007) 3207–3221. <https://doi.org/10.1002/jps>.
- [55] D.K. Tan, D.A. Davis, D.A. Miller, R.O. Williams, A. Nokhodchi, Innovations in Thermal Processing: Hot-Melt Extrusion and KinetiSol® Dispersing, *AAPS PharmSciTech.* 21 (2020). <https://doi.org/10.1208/s12249-020-01854-2>.
- [56] B. Lang, J.W. McGinity, R.O. Williams, Dissolution enhancement of itraconazole by hot-melt extrusion alone and the combination of hot-melt extrusion and rapid freezing-effect of formulation and processing variables, *Mol. Pharm.* 11 (2014) 186–196. <https://doi.org/10.1021/mp4003706>.
- [57] M. Fanous, S. Gold, S. Muller, S. Hirsch, J. Ogorka, G. Imanidis, Simplification of fused deposition modeling 3D-printing paradigm: Feasibility of 1-step direct powder printing for immediate release dosage form production, *Int. J. Pharm.* 578 (2020) 119124. <https://doi.org/10.1016/j.ijpharm.2020.119124>.
- [58] A. Goyanes, N. Allahham, S.J. Trenfield, E. Stoyanov, S. Gaisford, A.W. Basit, Direct powder extrusion 3D printing: Fabrication of drug products using a novel single-step process, *Int. J. Pharm.* 567 (2019). <https://doi.org/10.1016/j.ijpharm.2019.118471>.
- [59] J. Boniatti, P. Januskaite, L.B. da Fonseca, A.L. Viçosa, F.C. Amendoeira, C. Tuleu, A.W. Basit, A. Goyanes, M.I. Ré, Direct powder extrusion 3d printing of praziquantel to overcome neglected disease formulation challenges in paediatric populations, *Pharmaceutics.* 13 (2021). <https://doi.org/10.3390/pharmaceutics13081114>.
- [60] J. Baronsky-Probst, C. V. Möltgen, W. Kessler, R.W. Kessler, Process design and control of a twin screw hot melt extrusion for continuous pharmaceutical tamper-resistant tablet production, *Eur. J. Pharm. Sci.* 87 (2017) 14–21. <https://doi.org/10.1016/j.ejps.2015.09.010>.
- [61] F. Zaman, A.E. Beezer, J.C. Mitchell, Q. Clarkson, J. Elliot, A.F. Davis, R.J. Willson, The stability of benzoyl peroxide by isothermal microcalorimetry, *Int. J. Pharm.* 227 (2001) 133–137. [https://doi.org/10.1016/S0378-5173\(01\)00791-8](https://doi.org/10.1016/S0378-5173(01)00791-8).
- [62] S. Huang, K.P. O'Donnell, J.M. Keen, M.A. Rickard, J.W. McGinity, R.O. Williams, A New Extrudable Form of Hypromellose: AFFINISOL™ HPMC HME, *AAPS PharmSciTech.* 17 (2016) 106–119. <https://doi.org/10.1208/s12249-015-0395-9>.
- [63] M.M. Crowley, F. Zhang, J.J. Koleng, J.W. McGinity, Stability of polyethylene oxide in matrix tablets prepared by hot-melt extrusion, *Biomaterials.* 23 (2002) 4241–4248. [https://doi.org/10.1016/S0142-9612\(02\)00187-4](https://doi.org/10.1016/S0142-9612(02)00187-4).
- [64] M.A. Repka, S.K. Battu, S.B. Upadhye, S. Thumma, M.M. Crowley, F. Zhang, C. Martin, J.W. McGinity, Pharmaceutical Applications of Hot-Melt Extrusion: Part II, *Drug Dev. Ind. Pharm.* 33 (2007) 1043–1057. <https://doi.org/10.1080/03639040701525627>.

- [65] I. Ghosh, R. Vippagunta, S. Li, S. Vippagunta, Key considerations for optimization of formulation and melt-extrusion process parameters for developing thermosensitive compound, *Pharm. Dev. Technol.* 17 (2012) 502–510. <https://doi.org/10.3109/10837450.2010.550624>.
- [66] M. Li, J. Hasjim, F. Xie, P.J. Halley, R.G. Gilbert, Shear degradation of molecular, crystalline, and granular structures of starch during extrusion, *Starch/Staerke*. 66 (2014) 595–605. <https://doi.org/10.1002/star.201300201>.
- [67] A.E. McPherson, J. Jane, Extrusion of cross-linked hydroxypropylated corn starches. II. Morphological and molecular characterization, *Cereal Chem.* 77 (2000) 326–332. <https://doi.org/10.1094/CCHEM.2000.77.3.326>.
- [68] W. Fan, W. Zhu, X. Zhang, Y. Xu, L. Di, Application of the combination of ball-milling and hot-melt extrusion in the development of an amorphous solid dispersion of a poorly water-soluble drug with high melting point, *RSC Adv.* 9 (2019) 22263–22273. <https://doi.org/10.1039/c9ra00810a>.
- [69] A.N.N. Newman, G. Zografi, Critical Considerations for the Qualitative and Quantitative Determination of Process-Induced Disorder in Crystalline Solids, *J. Pharm. Sci.* (2014) 1–10. <https://doi.org/10.1002/jps.23930>.
- [70] C. Bhugra, M.J. Pikal, Role of Thermodynamic, Molecular, and Kinetic Factors in Crystallization From the Amorphous State, *J. Pharm. Sci.* 97 (2008) 1329–1349. <https://doi.org/10.1002/jps>.
- [71] P.N. Balani, W. Kiong Ng, R.B.H. Tan, S.Y. Chan, Influence of Excipients in Comilling on Mitigating Milling-Induced Amorphization or Structural Disorder of Crystalline Pharmaceutical Actives, *J. Pharm. Sci.* 99 (2009) 2462–2474. <https://doi.org/10.1002/jps>.
- [72] J.C. DiNunzio, C. Brough, J.R. Hughey, D.A. Miller, R.O. Williams, J.W. McGinity, Fusion production of solid dispersions containing a heat-sensitive active ingredient by hot melt extrusion and Kinetisol® dispersing, *Eur. J. Pharm. Biopharm.* 74 (2009) 340–351. <https://doi.org/10.1016/j.ejpb.2009.09.007>.
- [73] J.C. Dinunzio, C. Brough, D.A. Miller, R. O. Williams III, J.W. McGinity, Fusion Processing of Itraconazole Solid Dispersions by KinetiSol1 Dispersing: A Comparative Study to Hot Melt Extrusion, *J. Pharm. Sci.* 99 (2010) 1239–1253. <https://doi.org/10.1002/jps>.
- [74] J.E. Patterson, M.B. James, A.H. Forster, T. Rades, Melt extrusion and spray drying of carbamazepine and dipyridamole with polyvinylpyrrolidone/vinyl acetate copolymers, *Drug Dev. Ind. Pharm.* 34 (2008) 95–106. <https://doi.org/10.1080/03639040701484627>.
- [75] C. Parulski, E. Gresse, O. Jennotte, A. Felten, E. Ziemons, A. Lechanteur, B. Evrard, Fused deposition modeling 3D printing of solid oral dosage forms containing amorphous solid dispersions: How to elucidate drug dissolution mechanisms through surface spectral analysis techniques?, *Int. J. Pharm.* 626 (2022). <https://doi.org/10.1016/j.ijpharm.2022.122157>.
- [76] M.A. Repka, S. Shah, J. Lu, S. Maddineni, J. Morott, K. Patwardhan, N.N. Mohammed, Melt extrusion: Process to product, *Expert Opin. Drug Deliv.* 9 (2012) 105–125. <https://doi.org/10.1517/17425247.2012.642365>.
- [77] A. Butreddy, S. Bandari, M.A. Repka, Quality-by-design in hot melt extrusion based amorphous solid dispersions: An industrial perspective on product development, *Eur. J. Pharm. Sci.* 158 (2021) 105655. <https://doi.org/10.1016/j.ejps.2020.105655>.

- [78] J. Macedo, A. Samaro, V. Vanhoorne, C. Vervaet, J.F. Pinto, Processability of poly(vinyl alcohol) Based Filaments With Paracetamol Prepared by Hot-Melt Extrusion for Additive Manufacturing, *J. Pharm. Sci.* 109 (2020) 3636–3644. <https://doi.org/10.1016/j.xphs.2020.09.016>.
- [79] F.Q. Pires, I. Alves-silva, L.A.G. Pinho, J.A. Chaker, Predictive models of FDM 3D printing using experimental design based on pharmaceutical requirements for tablet production, *Int. J. Pharm.* 588 (2020) 119728. <https://doi.org/10.1016/j.ijpharm.2020.119728>.
- [80] S. Cailleaux, N.M. Sanchez-Ballester, Y.A. Gueche, B. Bataille, I. Soulairol, Fused Deposition Modeling (FDM), the new asset for the production of tailored medicines, *J. Control. Release.* 330 (2021) 821–841. <https://doi.org/10.1016/j.jconrel.2020.10.056>.
- [81] J. Norman, R.D. Madurawe, C.M.V. Moore, M.A. Khan, A. Khairuzzaman, A new chapter in pharmaceutical manufacturing: 3D-printed drug products, *Adv. Drug Deliv. Rev.* 108 (2017) 39–50. <https://doi.org/10.1016/j.addr.2016.03.001>.
- [82] S.D. Schaber, D.I. Gerogiorgis, R. Ramachandran, J.M.B. Evans, P.I. Barton, B.L. Trout, Economic analysis of integrated continuous and batch pharmaceutical manufacturing: A case study, *Ind. Eng. Chem. Res.* 50 (2011) 10083–10092. <https://doi.org/10.1021/ie2006752>.
- [83] D.K. Tan, M. Maniruzzaman, A. Nokhodchi, Advanced pharmaceutical applications of hot-melt extrusion coupled with fused deposition modelling (FDM) 3D printing for personalised drug delivery, *Pharmaceutics.* 10 (2018). <https://doi.org/10.3390/pharmaceutics10040203>.
- [84] Y. Zheng, F. Deng, B. Wang, Y. Wu, Q. Luo, X. Zuo, X. Liu, L. Cao, M. Li, H. Lu, S. Cheng, X. Li, Melt extrusion deposition (MED™) 3D printing technology – A paradigm shift in design and development of modified release drug products, *Int. J. Pharm.* 602 (2021) 120639. <https://doi.org/10.1016/j.ijpharm.2021.120639>.
- [85] M. Fonteyne, J. Vercruysse, F. De Leersnyder, B. Van Snick, C. Vervaet, J.P. Remon, T. De Beer, Process Analytical Technology for continuous manufacturing of solid-dosage forms, *TrAC - Trends Anal. Chem.* 67 (2015) 159–166. <https://doi.org/10.1016/j.trac.2015.01.011>.
- [86] S. Bandari, D. Nyavanandi, N. Dumpa, M.A. Repka, Coupling hot melt extrusion and fused deposition modeling: Critical properties for successful performance, *Adv. Drug Deliv. Rev.* 172 (2021) 52–63. <https://doi.org/10.1016/j.addr.2021.02.006>.
- [87] F. Krier, J. Mantanus, P.Y. Sacré, P.F. Chavez, J. Thiry, A. Pestieau, E. Rozet, E. Ziemons, P. Hubert, B. Evrard, PAT tools for the control of co-extrusion implants manufacturing process, *Int. J. Pharm.* 458 (2013) 15–24. <https://doi.org/10.1016/j.ijpharm.2013.09.040>.
- [88] M. Algorri, M.J. Abernathy, N.S. Cauchon, T.R. Christian, C.F. Lamm, C.M.V. Moore, Re-Envisioning Pharmaceutical Manufacturing: Increasing Agility for Global Patient Access, *J. Pharm. Sci.* 111 (2022) 593–607. <https://doi.org/10.1016/j.xphs.2021.08.032>.
- [89] A. Konta, M. García-Piña, D. Serrano, Personalised 3D Printed Medicines: Which Techniques and Polymers Are More Successful?, *Bioengineering.* 4 (2017) 79. <https://doi.org/10.3390/bioengineering4040079>.
- [90] M. Pandey, H. Choudhury, J. Lau, C. Fern, A. Teo, K. Kee, J. Kou, J. Lee, J. Jing, 3D printing for oral drug delivery : a new tool to customize drug delivery, (2020) 986–1001.

- [91] S.W. Hoag, Capsules dosage form: Formulation and manufacturing considerations, Elsevier Inc., 2017. <https://doi.org/10.1016/B978-0-12-802447-8.00027-3>.
- [92] M.R.P. Araújo, L.L. Sa-Barreto, T. Gratieri, G.M. Gelfuso, M. Cunha-Filho, The digital pharmacies era: How 3D printing technology using fused deposition modeling can become a reality, *Pharmaceutics*. 11 (2019). <https://doi.org/10.3390/pharmaceutics11030128>.
- [93] D. Jelic, Thermal Stability of Amorphous Solid Dispersions, *Molecules*. 26 (2021).
- [94] D.R. Serrano, A. Kara, I. Yuste, F.C. Luciano, B. Ongoren, B.J. Anaya, G. Molina, L. Diez, B.I. Ramirez, I.O. Ramirez, S.A. Sánchez-Guirales, R. Fernández-García, L. Bautista, H.K. Ruiz, A. Lalatsa, 3D Printing Technologies in Personalized Medicine, Nanomedicines, and Biopharmaceuticals, *Pharmaceutics*. 15 (2023). <https://doi.org/10.3390/pharmaceutics15020313>.



# CONCLUSIONS AND PERSPECTIVES

---



## CONCLUSIONS AND PERSPECTIVES

Increasing aqueous solubility and dissolution rate of the many drug candidates categorized in the BCS II class is essential in order to exploit their therapeutic potential. During this project, melt extrusion processes were selected with the purpose of producing oral solid dosage forms containing an ASD of CBD, a BCS II model drug, with an immediate release. Moreover, two innovative 3D printing techniques for shaping ASD, FDM and DPE, were used and compared to a more traditional technique, i.e. capsule filling, in terms of drug release and compliance with Eur. Ph. requirements. A summary of the findings is presented on [Fig. 51](#) and described below.

EPO was selected as the main polymer to manufacture ASD for its ability to enhance the solubility and dissolution rate of CBD. While the extrusion/capsule filling process could be performed with EPO/CBD binary mixture, formulations intended to be printed had to be adapted with PEO as a plasticizer. However, the three formulations optimized through the three shaping processes allowed for an immediate release of CBD.

Moreover, the produced oral dosage forms were compliant with Eur. Ph. specifications, demonstrating the promising future of innovative techniques such as FDM and DPE for the manufacture and shaping of ASD in order to solve the solubility issue of BCS II drug candidates, alongside already well-implemented techniques such as capsule filling.

To conclude, this work highlighted the great diversity of production and shaping techniques of ASD. Depending on the API properties but also where the final form would be produced, capsule filling, FDM or DPE will be chosen. Through this thesis, we have demonstrated pros and cons for each of them and provided some guidelines for further oral solid dosage forms of CBD.



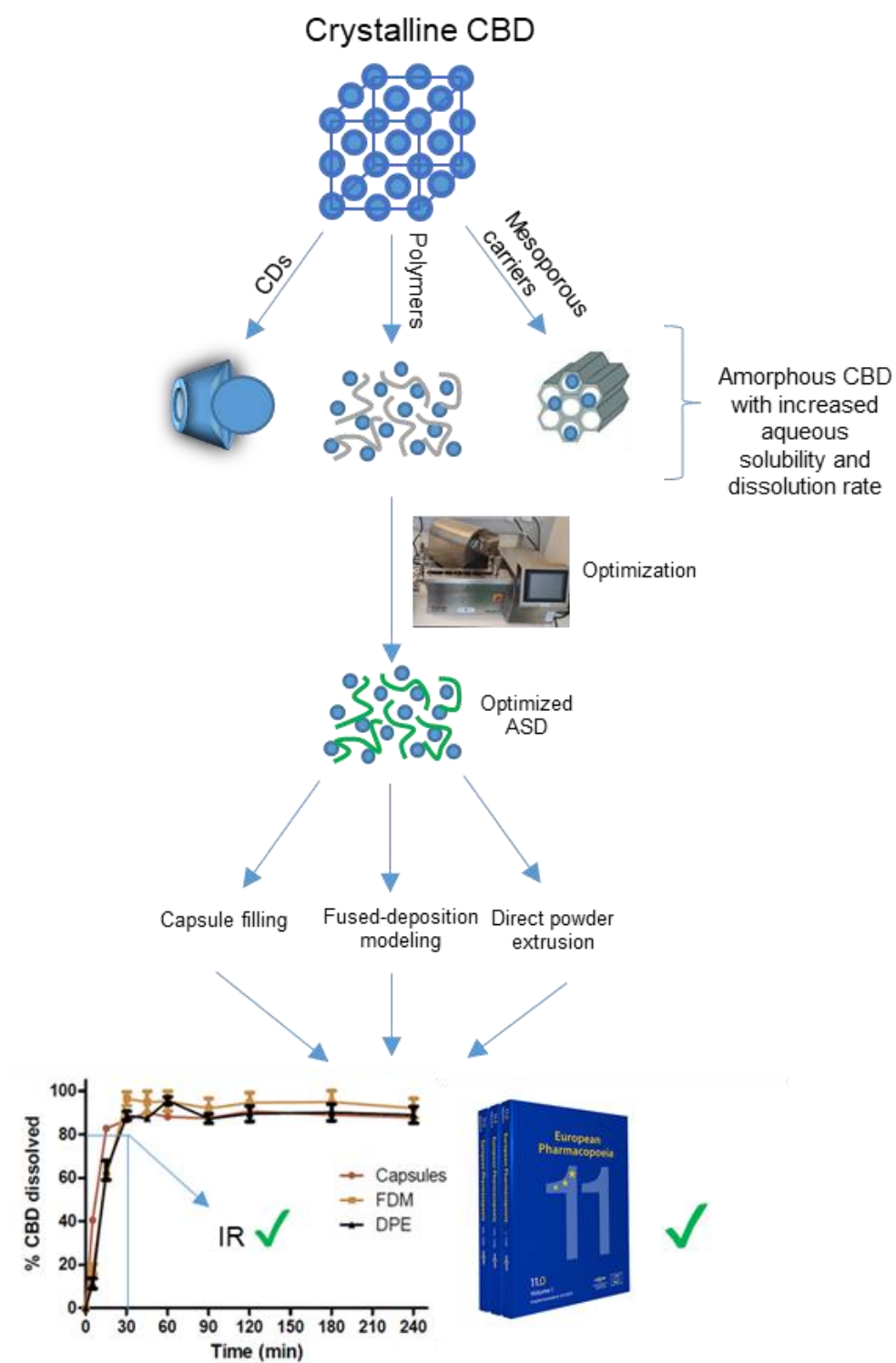


Figure 51 - Summary of the findings.

Despite the fact that additive manufacturing techniques have demonstrated great interests, many obstacles lie ahead the commercialization of drug product manufactured by FDM or DPE:

- There is a need of guidelines to ensure that 3D printed drug products have the same efficacy, safety and stability as the products conventionally manufactured. Given the versatility of raw materials and 3D printing techniques, the development of these guidelines remains a great challenge for the regulatory authorities.
- Only two GMP extrusion-based printers have been developed, which is few. The research to design equipment suitable for drug printing should be extended in order to stimulate competition between industries which should lead to the manufacturing of affordable 3D printing equipment. This would accelerate the implementation of the printing of drug products at small scale such as in hospitals or community pharmacies or at industrial scale.
- Another great advance in the field of ASD 3D printing would be the development of suitable polymers which could at once maintain the amorphous state of the drug and increase its solubility and dissolution rate, while being extrudable and printable. This would avoid laborious and time-consuming pre-formulation steps. Moreover, it would no longer be necessary to mix several excipients to make the formulation processable, which would reduce the risk of undesirable interactions.

# Summary

---

Currently, it is considered that about 75-90% of new drug candidates show poor aqueous solubility and that approximately 40% of the marketed active molecules are categorized in BCS class II. These molecules are characterized by a good permeability but also by a low and erratic oral bioavailability due to and insufficient dissolution throughout the gastro-intestinal tract. The purpose of this work was the use of different techniques to develop oral solid dosage forms containing an amorphous solid dispersion (ASD) of cannabidiol (CBD), a model BCS II drug, allowing its immediate release.

The first part was dedicated to the evaluation of three strategies to increase CBD aqueous solubility, namely solvent evaporation, mesoporous carrier impregnation and melting method. The manufacture of polymeric ASDs by hot-melt extrusion (HME) was selected as it allowed the highest increase of CBD solubility. Further, the optimization of the formulation composition and extrusion parameters was carried out. After dissolution studies of the milled extrudates filled into capsules, Eudragit® EPO (EPO)/CBD (90/10) extruded at 140 °C and 50 rpm was chosen as the optimal formulation for its ability to allow CBD immediate release. The second part concerned the evaluation of the impact that the shaping technique can have on ASD. A traditional technique, capsule filling was compared with two more recent techniques, fused-deposition modeling (FDM) and direct powder extrusion (DPE). EPO had to be blended with Polyox® N10 (PEO) to enable the manufacture of a filament with appropriate mechanical properties to be printed by FDM. The printing of different geometries was studied as it can have an influence of drug dissolution. After evaluating the printed tablets in terms of printing time, dissolution rate, reproducibility and mechanical properties, cylinder with 20% of infill was considered as optimal for manufacturing oral dosage forms with CBD immediate release. Finally, DPE was used to print different ratios PEO and Eudragit® E100 (E100) which has the same composition than EPO but with a more appropriate flow to be printed by DPE. The printed tablets dissolution was compared with different ratios of PEO and Soluplus® (SOL), which is another solubility enhancing polymer with an appropriate flow. Dissolution tests of SOL-based printed tablets showed no increase of either CBD solubility or dissolution rate, explained by the formation of a gel by both SOL and PEO in contact with the dissolution medium. On the other hand, every printed E100-based formulations enabled a CBD immediate release. Each shaping technique enabled the manufacture of immediate release oral solid dosage forms that met Eur. Ph. specifications, demonstrating the promising future of innovative techniques such as FDM and DPE for the manufacture and shaping of ASD, especially at hospital or community pharmacy scale, in order to solve the solubility issue of BCS II drug candidates, alongside already well-implemented techniques such as capsule filling.

Aujourd'hui, 75 à 90 % des molécules d'intérêt thérapeutique présentent une faible solubilité aqueuse et environ 40 % des molécules actives sur le marché sont catégorisées BCS II. Ces molécules se caractérisent par une bonne perméabilité et une biodisponibilité orale faible et erratique due à une dissolution insuffisante dans le tractus gastro-intestinal. Le but de ce travail était l'utilisation de différentes techniques pour développer des formes orales solides à libération immédiate contenant une dispersion solide amorphe (ASD) de cannabidiol (CBD), une molécule modèle BCS II. La première partie a été consacrée à l'évaluation de trois stratégies pour augmenter la solubilité du CBD ; l'évaporation de solvant, l'imprégnation de supports mésoporeux et une méthode de fusion. La fabrication d'ASD par extrusion à chaud (HME) a été sélectionnée car elle permettait la plus forte augmentation de solubilité du CBD. L'optimisation de la formulation et des paramètres d'extrusion a ensuite été réalisée. Après des études de dissolution des extrudats broyés remplis dans des capsules, Eudragit® EPO (EPO)/CBD (90/10) extrudé à 140 °C/50 tr/min a été choisi comme formulation optimale pour sa capacité à permettre la libération immédiate du CBD. La deuxième partie concernait l'évaluation de l'impact que la technique de mise en forme peut avoir sur les ASDs. Le remplissage de gélules a été comparé à deux techniques plus récentes, la modélisation par dépôt fondu (FDM) et l'extrusion directe de poudre (DPE). L'EPO devait être mélangé avec du Polyox® N10 (PEO) pour permettre la fabrication d'un filament aux propriétés mécaniques appropriées pour la FDM. L'impression de différentes géométries a été étudiée car elle peut avoir une influence sur la dissolution. Après avoir évalué les comprimés imprimés en termes de temps d'impression, taux de dissolution, reproductibilité et propriétés mécaniques, le cylindre avec 20 % de remplissage a été considéré comme optimal pour la fabrication de formes orales à libération immédiate de CBD. Enfin, le DPE a été utilisée pour imprimer différents ratios PEO et Eudragit® E100 (E100) qui a la même composition que l'EPO mais avec un écoulement plus approprié pour être la DPE. La dissolution des comprimés imprimés a été comparée à différents ratios de PEO et de Soluplus® (SOL). Les tests de dissolution des formulations à base de SOL n'ont montré aucune augmentation de solubilité du CBD étant donné la formation d'un gel par SOL et PEO en contact avec le milieu de dissolution. D'autre part, toutes les formulations imprimées à base d'E100 ont permis une libération immédiate du CBD. Chaque technique a permis la fabrication de formes solides orales à libération immédiate conformes à la Pharmacopée européenne, démontrant l'avenir prometteur de techniques innovantes telles que FDM et DPE pour la fabrication et la mise en forme d'ASD, en particulier à l'échelle hospitalière ou officinale, afin de résoudre le problème de solubilité des molécules BCS II, aux côtés de techniques traditionnelles telles que le remplissage de capsules.

# APPENDICES

---

## APPENDIX I. VALIDATION OF HPLC METHOD FOR DOSING CBD *IN VITRO*

The aim of validation is to establish that the analytical method is suitable for its intended use and consequently to prove the reliability of the results obtained within well-defined limits. Several widely recognized validation criteria should be tested in order to ensure the reliability of the developed method.

The validation criteria presented in this report are:

- ✓ Response function (calibration curve)
- ✓ Trueness
- ✓ Precision (repeatability and intermediate precision)
- ✓ Accuracy
- ✓ Linearity
- ✓ Limits of detection (LOD) and of quantitation (LOQ)
- ✓ Range

The quantification of CBD was assessed by a validated HPLC method. The HPLC equipment consisted of an Agilent 1100 (Santa Clara, USA) with OpenLab CDS LC Chemstation version C.01.05 as the software. A isocratic mobile phase composed of a mixture of water:acetonitrile (32:68; v:v) was used with a C-18 300SB Zorbax® column (4.6 x 150mm) with particle size of 3.5 µm. The flow rate was set at 1.0 mL/min and the column temperature was kept constant at 30 °C. 20 µL of the samples was injected at room temperature and the run time was set at 10 min. Detection wavelength was 220 nm.

### 1. Calibration solutions

A standard CBD solution with a concentration of 100 µg/mL is prepared in ACN by weighting 2.00 mg in a 20 mL volumetric flask. ACN is added until the beginning of the neck before ultrasonicated during 5 minutes in an ultrasonic bath. After cooling, ACN is added to achieve exactly 20mL.

Five calibrations solutions are then prepared from the standard solution by dilution with an aqueous solution of natrium phosphate buffer set at pH 6.8 added with 0.5% of SLS:

- S1 (50 µg/mL): 5 mL of standard solution completed in a 10 mL volumetric flask without aqueous medium.
- S2 (25 µg/mL): 2.5 mL of standard solution completed in a 10 mL volumetric flask without aqueous medium.

- S3 (10 µg/mL): 1 mL of standard solution completed in a 10 mL volumetric flask without aqueous medium.
- S4 (5 µg/mL): 0.5 mL of standard solution completed in a 10 mL volumetric flask without aqueous medium.
- S5 (0.5 µg/mL): 0.5 mL of standard solution completed in a 100 mL volumetric flask without aqueous medium.

## 2. Validation report

### 2.1 Experimental design

In order to validate the analytical method, two kinds of samples were prepared in an independent way: calibration standards and validations standards. The calibration standards are described in the section above.

**Table 14** reports the number of calibrations standards by concentrations level, the concentration levels envisaged and the different series that were performed. The total number of observations is 45.

*Table 14 – Calibration standards*

Series	C levels (µg/mL)	No. of repetitions
1	0.5	3
1	5	3
1	10	3
1	25	3
1	50	3
2	0.5	3
2	10	3
2	25	3
2	50	3
3	0.5	3
3	5	3
3	10	3
3	25	3
3	50	3

The validation standards are reconstituted samples within the matrix containing known concentration of the analyte of interest which are considered as true values by consensus.



**Table 15** reports the number of validation standards by concentration level, the concentration levels envisaged and the different series that were performed.

*Table 15 – Validation standards*

Series	C levels (µg/mL)	No. of independent repetitions
1	0.5	3
1	5	3
1	10	3
1	25	3
1	50	3
2	0.5	3
2	5	3
2	10	3
2	25	3
2	50	3
3	0.5	3
3	5	3
3	10	3
3	25	3
3	50	3

The total number of observations is 45.

## 2.2 Response function

The response function of an analytical method is, within the range, the existing relationship between the response (signal) and the concentration (quantity) of the analyte sample. The calibration curve is the most appropriate response function.

**Table 16** presents all selected regression models that have been sorted according to the Accuracy Index.

Table 16– Sorting of the calibration models

Model	Accuracy Index	Lower and upper limits of quantification (LOQ) (µg/mL)	Dosing range Index	Precision Index	Trueness Index
Weighted (1/X <sup>2</sup> ) linear regression	0.7871	[0.5228 , 52.27]	1.000	0.4949	0.9854

The selected calibration model is: **Weighted (1/X<sup>2</sup>) linear regression.**

The calibration curves obtained from this regression model (Table 16 and Fig. 52) are represented by the following equation:

$Y = a + bX$  where Y = Analytical response (in Unit) and X= Introduced concentration (in µg/mL).

Table 16– Regression parameters

Series	Intercept	Slope	r <sup>2</sup>	Residual d.f.	RSS
1	0.3882	74.97	0.9998	13	6781
2	0.2312	76.65	0.9999	13	752.0
3	-1.124	76.37	0.9994	13	1.6206E+04

r<sup>2</sup>= coefficient of determination; d.f.= degrees of freedom; RSS= residual sum of squares

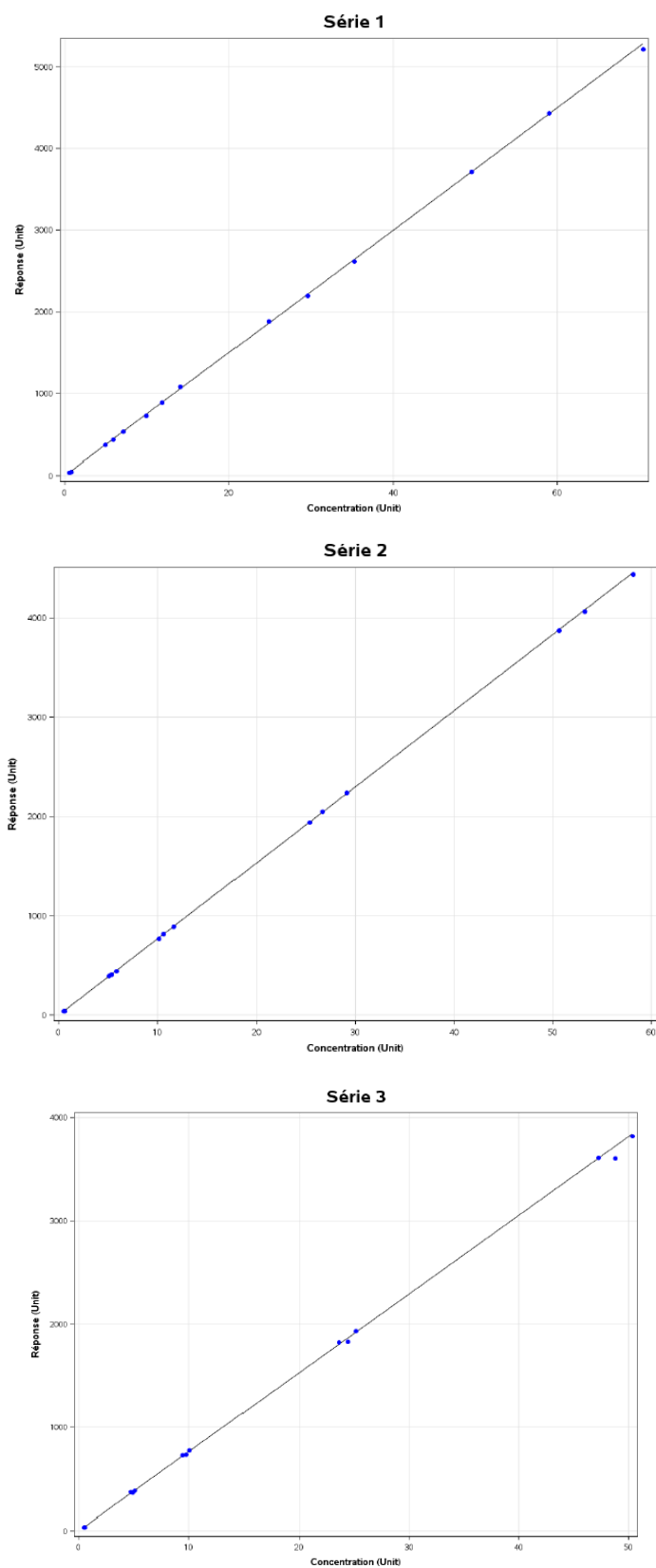


FIGURE 52 - CALIBRATION CURVES

## 2.3 Trueness

Trueness refers to the closeness of agreement between a conventionally accepted value of reference value and a mean experimental one. It gives information on systematic error. As shown in [Table 17](#), trueness is expressed in terms of absolute bias (in µg/mL), relative bias (%) or recovery (%) at each concentration level of the validation standard.

If, for a concentration level,  $\mu$  is the mean of the introduced concentrations and  $\bar{x}$  is the estimate of the mean concentration obtained from calculated concentrations then we have:

$$\text{Absolute bias} = \bar{x} - \hat{\mu}$$

$$\text{Relative bias (\%)} = 100 \times \frac{\bar{x} - \hat{\mu}}{\hat{\mu}}$$

$$\text{Recovery (\%)} = 100 \times \frac{\bar{x}}{\hat{\mu}}$$

Table 17 – Trueness

C level (µg/mL)	Mean introduced C (µg/mL)	Mean back-calculated C (µg/mL)	Absolute bias (µg)	Relative bias (%)	Recovery (%)	95 Confidence Interval of Recovery (%)
0.5	0.5228	0.5254	0.002667	0.5102	100.5	[98.56 , 102.5]
5	5.228	5.279	0.05185	0.9919	101.0	[100.2 , 101.8]
10	10.46	10.59	0.1356	1.297	101.3	[99.63 , 103.0]
25	26.14	26.45	0.2808	1.074	101.1	[100.0 , 102.1]
50	52.27	52.37	0.09974	0.1908	100.2	[99.16 , 101.2]

## 2.4 Precision

Precision is the closeness of agreement among measurements from multiple sampling of a homogenous sample under the recommended conditions. It gives some information on random errors and it can be evaluated at two levels: repeatability and intermediate precision.

As can be seen in [Table 18](#) and [Table 19](#), precision is expressed in terms of standard deviation (SD) and relative standard deviation (RSD) values for repeatability and intermediate precision.

The estimates of variance components are obtained by the iterative approach of restricted maximum likelihood (REML).

*Table 18 – Relative Intermediate Precision and Repeatability*

C level (µg/mL)	Mean introduced C (µg/mL)	Repeatability (RSD%)	Intermediate precision (RSD%)
0.5	0.5228	2.541	2.541
5	5.228	1.061	1.061
10	10.46	2.164	2.164
25	26.14	1.340	1.363
50	52.27	1.345	1.345

RSD%= Repeatability and Intermediate precision has been obtained by dividing the corresponding SD by “Mean introduced concentration”

*Table 19 – Absolute intermediate Precision and Repeatability*

C level (µg/mL)	Mean introduced C (µg/mL)	Repeatability (SD - µg/mL)	Between-series (SD - µg/mL)	Ratio of Variance component (between/within)	Intermediate precision (SD - µg/mL)
0.5	0.5228	0.01329	0	0	0.01329
5	5.228	0.05544	0	0	0.05544
10	10.46	0.2262	0	0	0.2262
25	26.14	0.3503	0.06431	0.03370	0.3503
50	52.27	0.7031	0	0	0.7031

*Table 20 – 95% Upper Confidence Limit*

C level (µg/mL)	Mean introduced C (µg/mL)	95% Upper Confidence Limit Repeatability (SD - µg/mL)	95% Upper Confidence Limit Precision (SD - µg/mL)
0.5	0.5228	0.02273	0.02273
5	5.228	0.09487	0.09487
10	10.46	0.3870	0.3870
25	26.14	0.6710	0.9940
50	52.27	1.203	1.203

In addition, the Recovery of each series as well as for all the series is reported in the [Table 21](#).

Table 21 – By series Recovery of the Samples

C level (µg/mL)	Series	Mean introduced C (µg/mL)	Back-calculated C (µg/mL)	Recovery (%)
0.5	1	0.5323	0.5233	100.1
0.5	2	0.5501	0.5238	100.2
0.5	3	0.4858	0.5291	101.2
0.5	Mean of all series	0.5228	0.5254	100.5
5	1	5.323	5.272	100.9
5	2	5.501	5.274	100.9
5	3	4.858	5.292	101.2
5	Mean of all series	5.228	5.279	101.0
10	1	10.65	10.66	102.0
10	2	11.00	40.53	100.7
10	3	9.717	10.58	101.2
10	Mean of all series	10.46	10.59	101.3
25	1	26.62	26.34	100.8
25	2	27.50	26.26	100.5
25	3	24.29	26.66	102.0
25	Mean of all series	26.14	26.42	101.1
50	1	53.22	52.73	100.9
50	2	55.01	52.13	99.72
5	3	48.58	52.26	99.97
50	Mean of all series	52.27	52.37	100.2

## 2.5 Uncertainty of measurements

The uncertainty is a parameter associated with the results of a measurement that characterizes the dispersion of the values that could reasonably be attributed to the measurand ([Table 22](#)).

Table 22 – Uncertainty

C level (µg/mL)	Mean introduced C (µg/mL)	Uncertainty of the bias (µg/mL)	Uncertainty (µg/mL)	Expanded Uncertainty (µg/mL)	Relative Expanded Uncertainty (%)
0.5	0.5228	0.04428	0.01400	0.02801	5.358
5	5.228	0.01848	0.05844	0.1169	2.236
10	10.46	0.07450	0.2384	0.4769	4.561
25	26.14	0.1225	0.3766	0.7533	2.882
50	52.27	0.2344	0.7411	1.482	2.836

## 2.6 Accuracy

Accuracy refers to the closeness of agreement between the test results and the accepted reference value, namely the conventionally true value. The Accuracy takes into account the total error, i.e. systematic and random errors, related to the test results. It is assessed from the Accuracy Profile illustrated in [Fig. 53](#).

The acceptance limits have been accepted at 7.5%, selected according to the intended use of the analytical procedure.

An accuracy profile is obtained by linking on one hand the lower bounds and on the other hand the upper bounds of the  $\beta$ -expectation tolerance intervals calculated at each concentration level. The formula for calculating these  $\beta$ -expectation tolerance intervals is:

$$bias (\%) \pm kRSD_{IP} (\%)$$

The method is considered as valid within the range for which the Accuracy Profile is within the acceptance limits. This approach gives the guarantee that each further measurement of unknown samples is included within the tolerance limits at the 5.0% level.

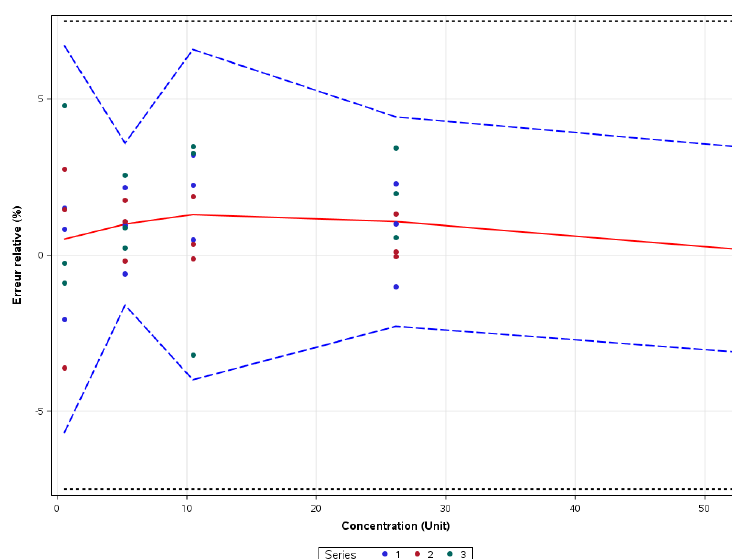


FIGURE 53 - ACCURACY PROFILE OBTAINED BY CONSIDERING WEIGHTED ( $1/X^2$ ) LINEAR REGRESSION.

The plan red line is the relative bias, the dashed lines are the b-expectations tolerance limits and the dotted lines represent the acceptance limits. The dots represent the relative error of the back-calculated concentrations and are plotted with respect to their targeted concentration.

The upper and lower  $\beta$ -expectation tolerance limits expressed in relative error are also presented in [Table 23](#) as a function of the introduced concentrations. Risk of measurements at each level are only estimated when there are at least two replicates per series ([Fig. 54](#)).



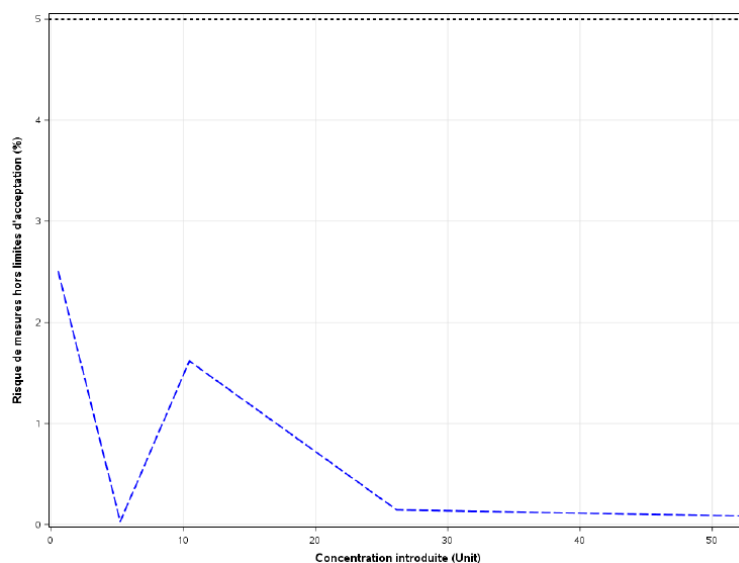


FIGURE 54 - RISK PROFILE OBTAINED BY CONSIDERING WEIGHTED ( $1/X^2$ ) LINEAR REGRESSION.

The dotted line represents the maximum risk level chosen: 5.0 %.

Table 23 - Method accuracy obtained by considering Weighted ( $1/X^2$ ) linear regression

C level (µg/mL)	Mean introduced C (µg/mL)	β-expectation tolerance limits (µg/mL)	Relative β-expectation tolerance limits (%)	Risk (%)
0.5	0.5228	[0.4929 , 0.5579]	[-5.707 , 6.728]	2.510
5	5.228	[5.144 , 5.415]	[-1.603 , 3.587]	0.02650
10	10.46	[10.04 , 11.14]	[-3.996 , 6.590]	1.616
25	26.14	[25.54 , 27.30]	[-2.283 , 4.431]	0.1430
50	52.27	[50.65 , 54.09]	[-3.100 , 3.481]	0.08416

Risk = the risk of having measurements falling outside the acceptance limits.

## 2.7 Linearity of results

The linearity of an analytical method is the ability within a definite range to obtain results directly proportional to the concentration (quantity) of the analyte in the sample.

A linear regression model (Fig. 55) is fitted on the back-calculated concentrations as a function of the introduced concentrations in order to obtain the following equation:

$$Y = 0.07714 + 1.002 X$$

where Y = Back-calculated concentrations (µg/mL) and X = Introduced concentration (µg/mL). The coefficient of determination ( $r^2$ ) is equal to 0.9996. The residual sum of squares (RSS) is equal to 5.738.

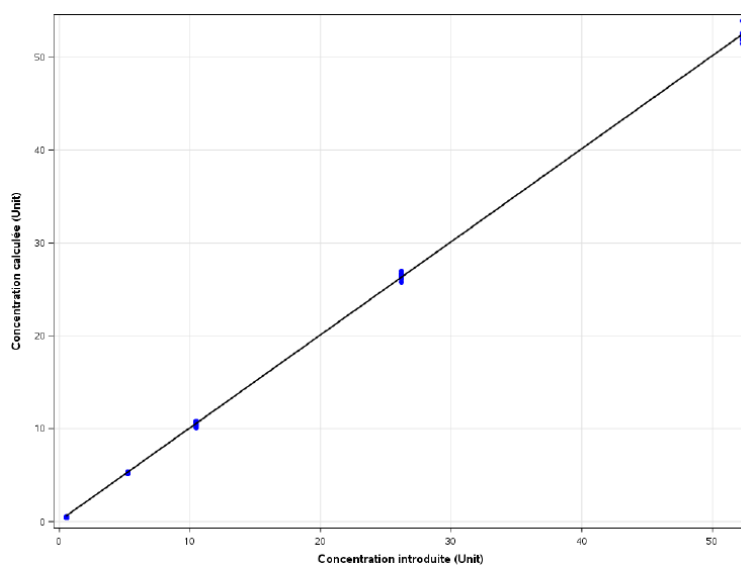


FIGURE 55 - RELATIONSHIP BETWEEN THE INTRODUCED AND THE BACK-CALCULATED CONCENTRATIONS.

In order to demonstrate method linearity, the approach based on the absolute  $\beta$ -expectation tolerance limits as illustrated in Fig. 56 can be applied.

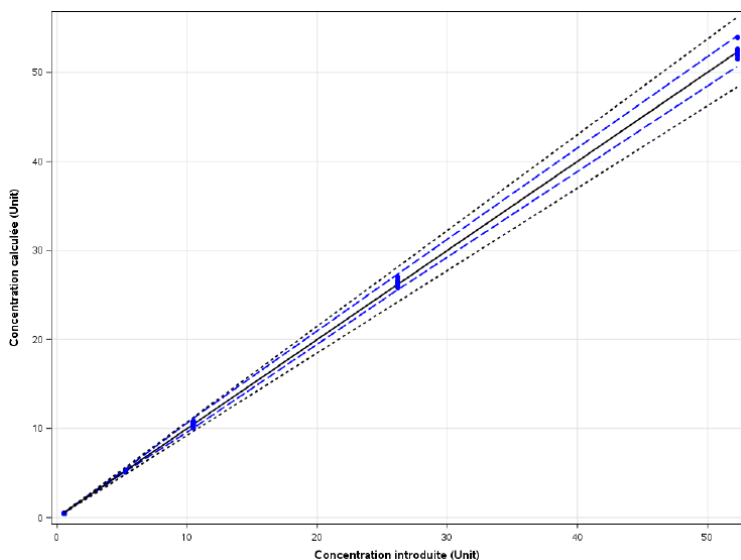


FIGURE 56 - LINEARITY GRAPH.

The plain line is the identity line:  $Y = X$ . The dashed limits on this graph correspond to the Accuracy Profile *i.e.* the  $\beta$ -expectation tolerance limits expressed in absolute values. These limits are calculated as follows:

$$\bar{x} \pm kS_{IP}$$

The dotted curves represent the acceptance limits expressed in the concentration unit. The method is considered as valid within the range for which the dashed curves are within the dotted acceptance limits.

The linearity of the model is demonstrated when the absolute  $\beta$ -expectation tolerance limits are within the absolute acceptance limits.

## 2.8 Limit of detection (LOD), limits of quantification (LOQ) and dosing range

The limit of detection is the smallest quantity of the targeted substance that can be detected, but not accurately quantified in the sample.

There actually two ways of computing the LOD

- $LOD = LOQ/3.3$
- Using Miller ET Miller (not applicable if only one level and no repetition)
- Computation by series of the Y  $LOD = \text{Intercept (0 if negative)} + 3 * \text{residual SD}$  obtained by ANOVA. Using the selected regression model, the back-calculation will give the  $X_{lod}$  for each series.
- The means of the different back-calculated  $X_{lod}$  will give the LOD of the procedure.

The application will choose the lowest value.

**LOD ( $\mu\text{g/mL}$ ) = 0.04568**

The lower limit of quantification is the smallest quantity of the targeted substance in the sample that can be assayed under experimental conditions with well-defined accuracy. the definition can also be applicable to the upper limit of quantification, which is the highest quantity of the targeted substance in the sample that can be assayed under experimental conditions with well-defined accuracy. The limits of quantification are obtained by calculation the smallest and highest concentrations beyond which the accuracy limits or b expectation limits go outside the acceptance limits.

The Dosing Range is the interval between the lower and upper limits where the procedure achieves adequate accuracy.

**Lower LOQ ( $\mu\text{g/mL}$ ) = 0.5228**

**Upper LOQ ( $\mu\text{g/mL}$ ) = 52.27**

## APPENDIX II. ADDITIONAL STUDIES ON CAPSULES

### 1. Pharmacotechnical Tests

To guarantee the quality and process reproducibility, investigations of physical characteristics was executed on capsules containing F3, composed of EPO/CBD (90/10) and extruded at 140 °C and 50 rpm. To comply with the hard capsule monograph of Eur. Ph. edition 11.2, capsules have to meet the requirements of mass variation (2.9.40) and uniformity of mass (2.9.5).

It was shown that the capsules filled with F3 were compliant with the Eur. Ph. tests concerning the hard capsules. This highlighted the ability of HME followed by extrudate milling and capsules filling to manufacture oral solid dosage forms of CBD with suitable quality and reproducibility.

### 2. Stability of CBD Physical State

Evaluating the stability of a formulation over time in terms of physical state is essential for any dosage form. This is even more essential when it comes to formulations containing one or more amorphous components. Indeed, factors such as temperature can increase the mobility of drug molecules which can nucleate to finally recrystallize. Moreover, ASDs formulated with hydrophilic polymers are likely to absorb moisture which can disrupt drug-polymer hydrogen bonds, resulting in a phase separation that can end in drug recrystallization [1].

Based on ICH Q1A (R2) guidelines, capsules were stored in closed bottles at a temperature of  $25 \pm 2$  °C with relative humidity (RH) of  $60 \pm 5\%$  RH [2]. Samples were evaluated at pre-set times (month 0, 1, 2, 3 and 6) by XRPD to evaluate the physical state of the drug and TGA (25-250 °C at 10 °C/min), to measure moisture absorption.

X-ray patterns of F3 stored at 25 °C are shown on [Figure 57](#). It can be seen that CBD remained amorphous during the whole storage period, as no characteristic peaks are found on the ASDs diffractograms over time, demonstrating the ability of EPO to maintain a system with low molecular mobility, stabilizing the amorphous state of CBD. Moreover, TGA analysis revealed an absorption of less than 1% of moisture by the ASDs stored at  $25 \pm 2$  °C with  $60 \pm 5\%$  RH. This low percentage did not have any impact on CBD amorphous state.

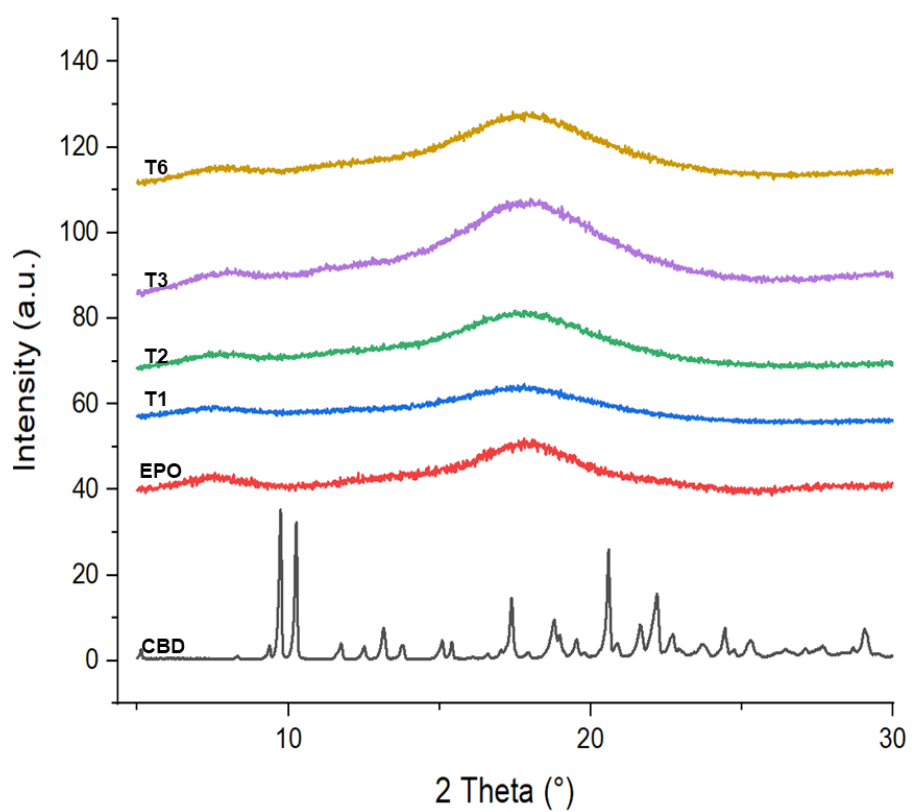


Figure 57 - XRPD patterns of crystalline CBD, raw EPO and F3 stored at  $25 \pm 2$  °C with  $60 \pm 5\%$  RH after 1, 2, 3 and 6 months (T1, T2, T3 and T6).

- [1] X. Lin, Y. Hu, L. Liu, L. Su, N. Li, J. Yu, B. Tang, Z. Yang, Physical Stability of Amorphous Solid Dispersions: a Physicochemical Perspective with Thermodynamic, Kinetic and Environmental Aspects, *Pharm. Res.* 35 (2018). <https://doi.org/10.1007/s11095-018-2408-3>.
- [2] ICH, International Conference on Harmonization (ICH). Guidance for industry: Q1A(R2) STABILITY TESTING OF NEW DRUG SUBSTANCES AND PRODUCTS, *Ich Harmon. Tripart. Guidel.* 4 (2003) 24.
- [3] E. Kosović, D. Sýkora, M. Kuchař, Stability study of cannabidiol in the form of solid powder and sunflower oil solution, *Pharmaceutics.* 13 (2021). <https://doi.org/10.3390/pharmaceutics13030412>.

## APPENDIX III. ADDITIONAL STUDIES ON FILAMENTS AND PRINTED TABLETS

### 1. Stability of CBD Physical State

The importance of evaluating ASDs stability has already been explained in [Appendix II.2](#). In addition, due to successive HME and FDM 3D printing, thermal stress may increase the risk of possible deleterious interactions between drug and polymeric matrix [1]. These interactions may cause physical instability over time.

Following ICH Q1A (R2) guidelines printed tablets P1 (cylinder 20% infill composed of CBD/PEO/EPO (10/18/72)) and corresponding extruded filament were stored in closed bottles at a temperature of  $25 \pm 2$  °C with of  $60 \pm 5\%$  RH [2]. Samples were evaluated at pre-set times (month 0, 1, 2, 3 and 6) by XRD to evaluate the physical state of the drug and TGA (25-250 °C at 10 °C/min), to measure moisture absorption.

X-ray patterns of filament and P1 are shown on [Figures 58](#) and [59](#), respectively. It can be seen that CBD remained amorphous during the whole storage period, as no characteristic peaks are found on the ASDs diffractograms over time, demonstrating the ability of EPO and PEO to maintain a system with low molecular mobility, stabilizing the amorphous state of CBD. Moreover, the TGA analysis revealed an absorption of less than 1% of moisture for both filament and P1 stored at  $25 \pm 2$  °C with  $60 \pm 5\%$  RH. This low percentage did not have any impact on CBD amorphous state.

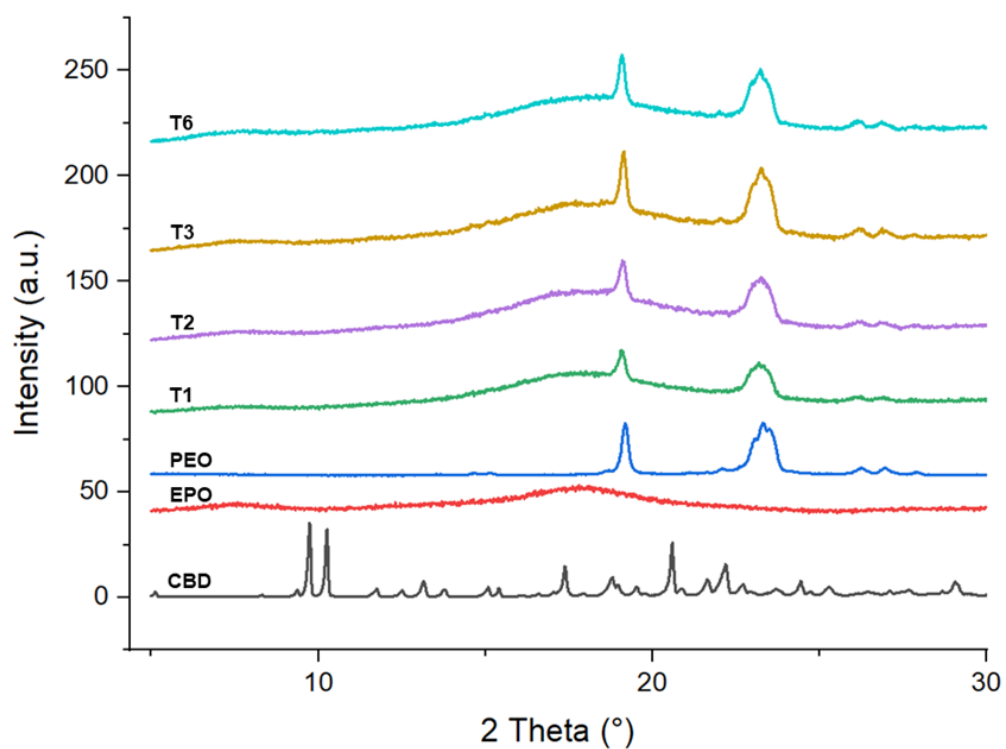


Figure 58 - XRD patterns of crystalline CBD, raw EPO, raw PEO and filament composed of CBD/PEO/EPO (10/18/72) stored at  $25 \pm 2$  °C with  $60 \pm 5\%$  RH after 1, 2, 3 and 6 months (T1, T2, T3 and T6).

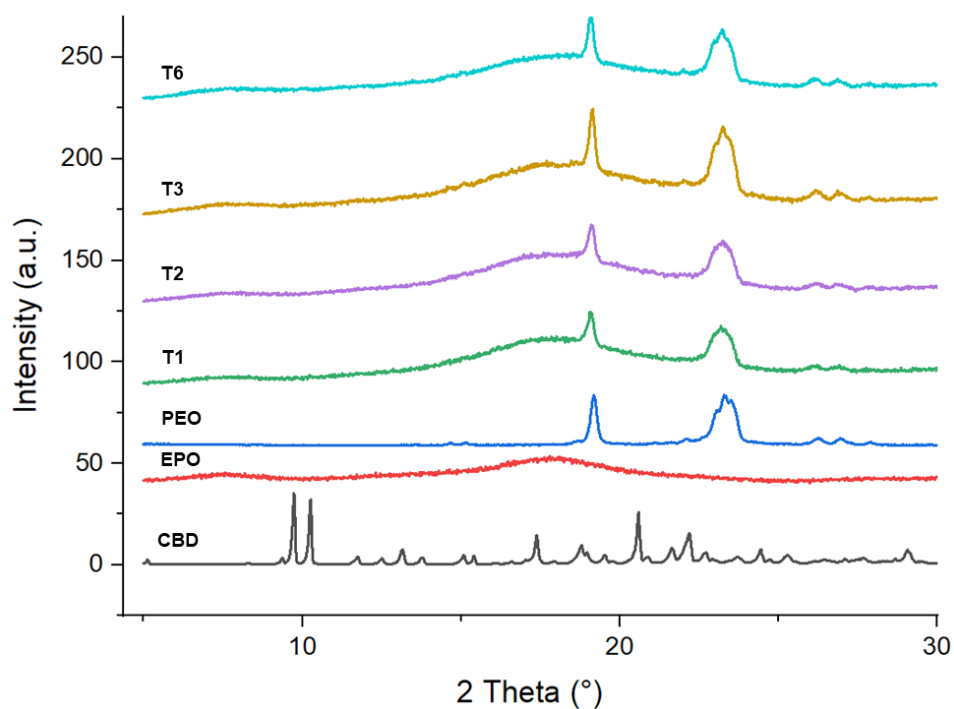


Figure 59 - XRD patterns of crystalline CBD, raw EPO, raw PEO and P1, printed cylinder with 20% infill composed of CBD/PEO/EPO (10/18/72) stored at  $25 \pm 2$  °C with  $60 \pm 5\%$  RH after 1, 2, 3 and 6 months (T1, T2, T3 and T6).



## 2. Evaluation of degradation temperature of raw materials

As shown TGA analysis, the mass loss of CBD starts at 220 °C while mass loss for EPO and PEO starts at 289 and 389 °C, respectively (**Fig. 60**).

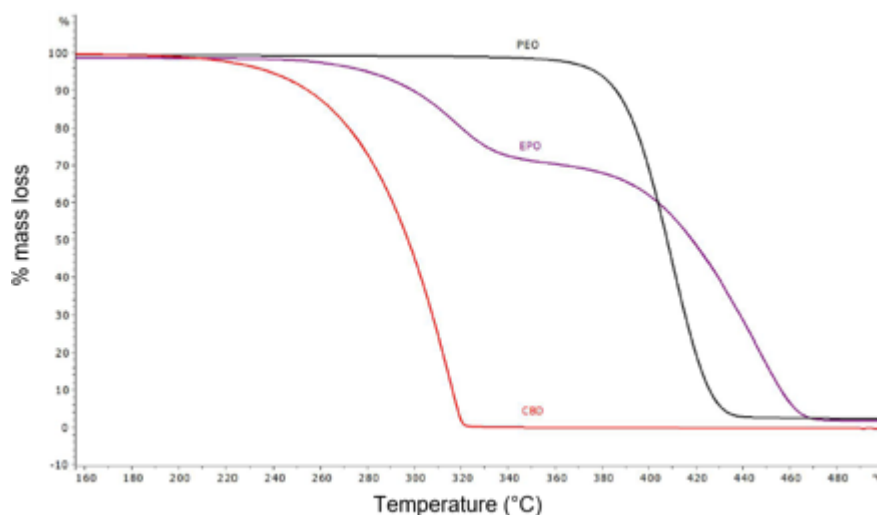


Fig. 60 - TGA curves of raw CBD, EPO and PEO.

## 3. In vivo considerations

In order to evaluate the ability of an ASD to enhanced the bioavailability of CBD, the optimized printed cylinder described in chapter III, composed of CBD/ EPO/PEO (10/72/18), has been included in a broad pharmacokinetic study performed in collaboration with Dr. Patrice Chiap (*Academic Hospital of Liège, Department of Toxicology, GLP-AEPT Unit, CIRM*). This pharmacokinetic investigation has been done by giving different CBD formulations with a CBD equivalent of 2.5 mg/kg to fasted pigs. Serum was collected from time 0 to time 24 h and CBD was extracted and quantified through validated manipulations. **Fig. 61** shows pharmacokinetic profiles of the printed tablet compared to crystalline CBD (n=5).

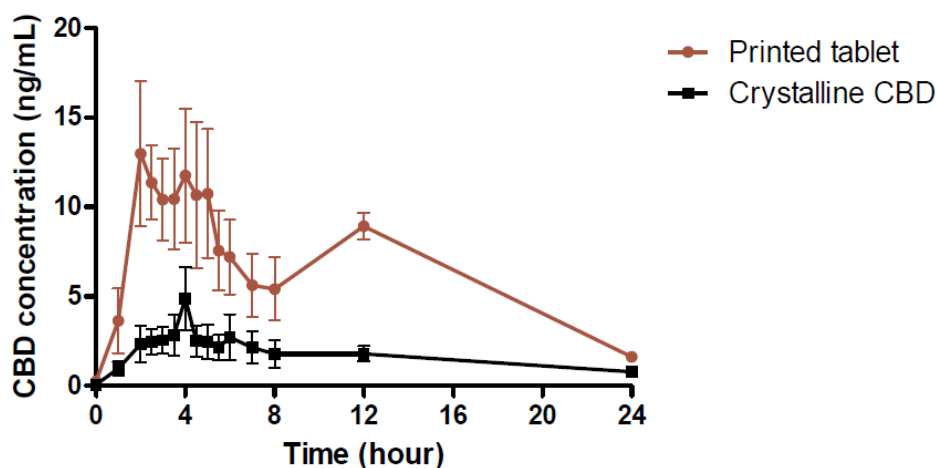


Figure 61 - Pharmacokinetic profiles of printed cylinder composed of CBD/EPO/PEO (10/72/18) and crystalline CBD given orally to pigs (CBD equivalent of 2.5 mg/kg,  $n=5$ ).

The use of ASD strategy, including the cationic polymer EPO, is interesting to increase the bioavailability of CBD when oral solid dosage form is considered. Indeed, it has been shown that the printing of ASD of CBD provided significant higher *area under the curve* (155.7 ng\*h\*mL<sup>-1</sup>) compared to the crystalline form (40.5 ng\*h\*mL<sup>-1</sup>), which represents a bioavailability enhancement of 3.8 fold. Nevertheless, as EPO is insoluble in pH above 5, the inter-variability of gastric pH in fasted conditions may reduce the impact of the formulation. This formulation increases probably better the bioavailability if given in fed conditions since gastric pH is lower and will ensure the complete solubilization of EPO [1].

## APPENDIX IV. ADDITIONAL STUDIES ON PRINTED TABLETS PRODUCED BY DPE

### 1. Stability of CBD Physical State

The CBD physical state was assessed by XRD analysis on all the printed tablets produced by DPE which compositions are listed in [Table 24](#). X-ray patterns of E100-based printed tablets and SOL-based printed tablets are shown on [Figures 62 and 63](#), respectively. It can be seen that CBD remained amorphous during the 2 months, demonstrating the polymers used to produce the printed tablets have appropriate stabilizing properties for CBD.

TABLE 24 - COMPOSITION OF PRINTED TABLETS

Formulations	CBD (%)	PEO (%)	E100 (%)	SOL (%)
F1	10	72	18	0
F2	10	67.5	22.5	0
F3	10	63	27	0
F7	10	72	0	18
F8	10	67.5	0	22.5
F9	10	63	0	27

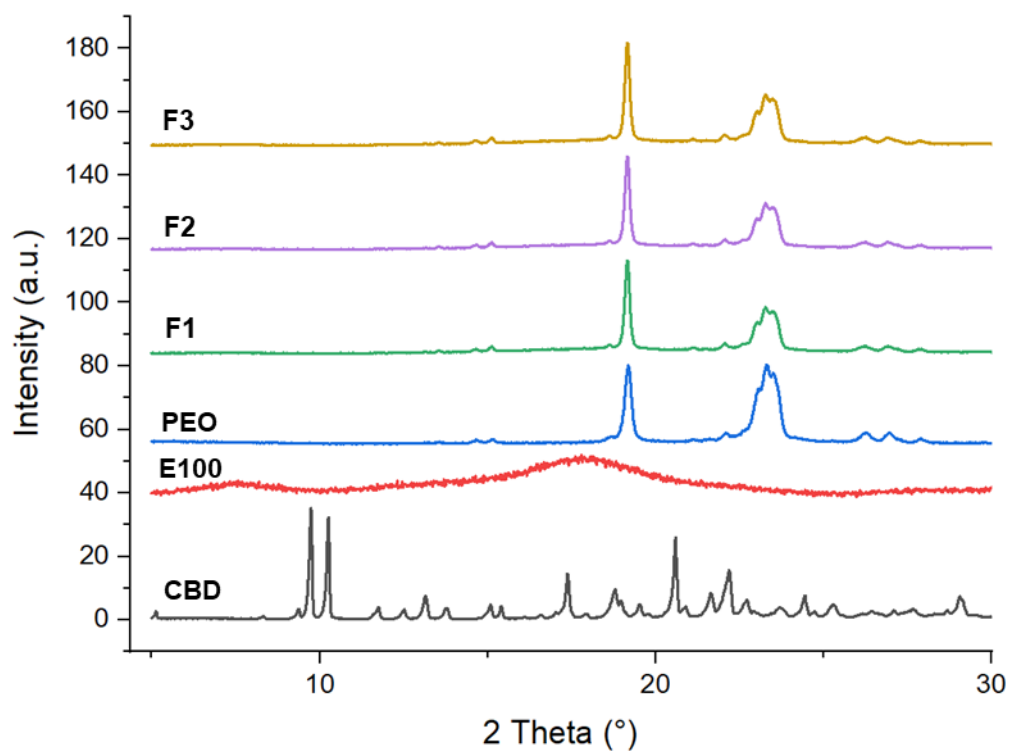


Figure 62 – XRD patterns of crystalline CBD, raw E100, raw PEO and F1, F2 and F3, stored at  $25 \pm 2^\circ\text{C}$  with  $60 \pm 5\%$  RH after 2 months.

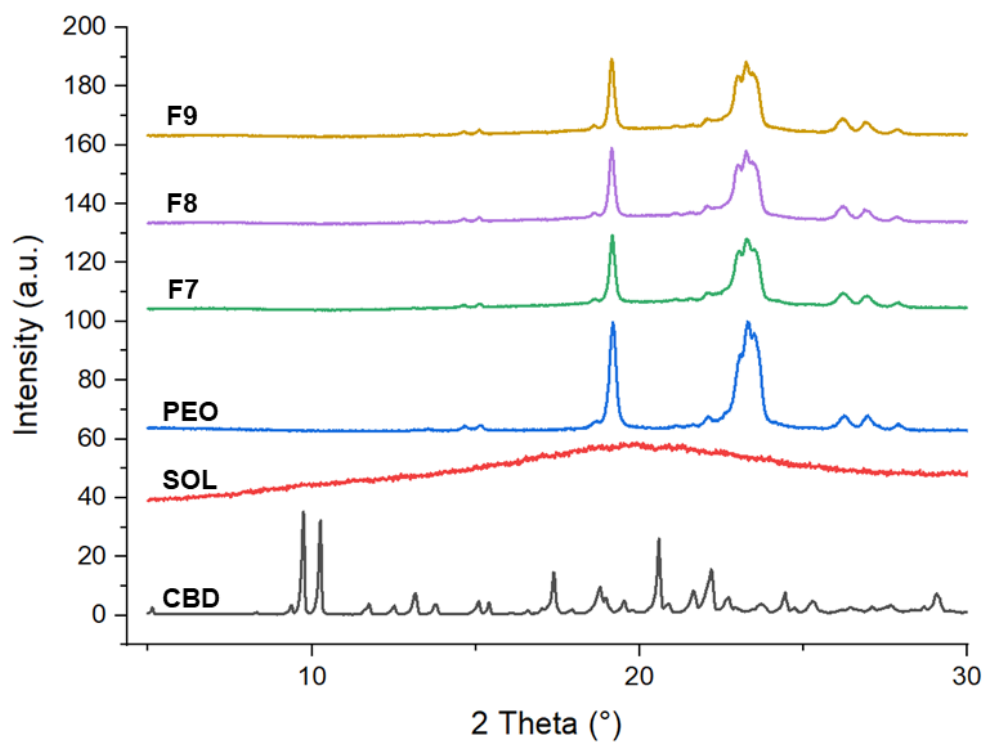


Figure 63 – XRD patterns of crystalline CBD, raw SOL, raw PEO and F7, F8 and F9, stored at  $25 \pm 2^\circ\text{C}$  with  $60 \pm 5\%$  RH after 2 months.

## 2. Evaluation of degradation temperature of raw materials

As shown TGA analysis, the mass loss of CBD starts at 220 °C while mass loss for E100, PEO and SOL starts at 289 °C, 389 °C and 290 °C, respectively. (Fig. 64).

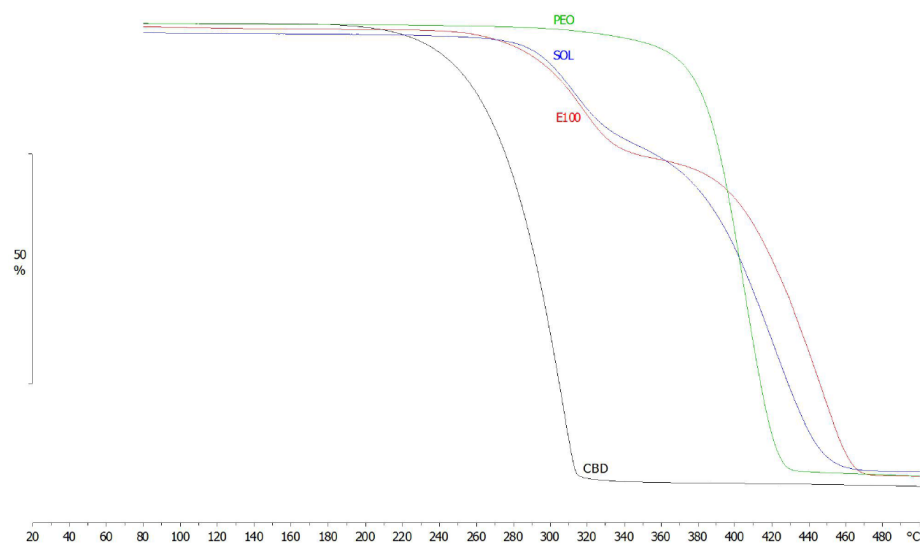


Fig. 64 - TGA curves of raw CBD, E100, SOL and PEO.

## APPENDIX V. *IN VITRO* DISSOLUTION TEST WITH ASD MANUFACTURED WITH THREE PROCESSING TECHNOLOGIES

For comparison purposes, best ASDs manufactured by capsule filling, FDM and DPE were tested in terms of *in vitro* dissolution. Tests were carried out using the USP II paddle method apparatus AT7 (Sotax®, Switzerland). Formulations were placed in a sinker containing 500 mL of HCl 0.1 M. The stirring speed was 100 rpm and the temperature was maintained at 37 °C during 4h. Aliquot samples of 2.0 mL were withdrawn at 5, 15, 30, 45, 60, 90, 120, 180 and 240 min. An equal volume of the dissolution medium was replaced after each withdrawal. Samples were then analyzed by HPLC. The dissolution tests were carried out in triplicates.

One-way ANOVA with a Tukey post-test was used thanks to GraphPad Prism 5.0 software to analyze the differences in CBD dissolution after 5 and 15 minutes. Differences in results were considered significant with \* $p \leq 0.05$ , \*\*  $p \leq 0.01$  and \*\*\*  $p \leq 0.001$ .

Unsurprisingly, ASD in capsule allowed a significantly faster dissolution of CBD than the printed forms after 5 and 15 minutes, explained by the greater contact surface with the dissolution medium of the ground extrudates ([Fig. 65](#)). Indeed, after 5 minutes, 40.47%, 18.05% and 11.33% of CBD were dissolved from capsule, FDM and DPE formulations, respectively. After 15 minutes, capsule, FDM and DPE allowed a dissolution of 82.74%, 60.00% and 63.41%, respectively. These differences of dissolution rate indicate the importance of ASD shaping method choice, as for a similar composition, the higher the surface, the faster the drug release. However, an equilibrium is observed between each formulation after 30 minutes. This equilibrium is due to the rapid dissolution of EPO even from the strong structures resulting from the melting and cooling of the printed materials.

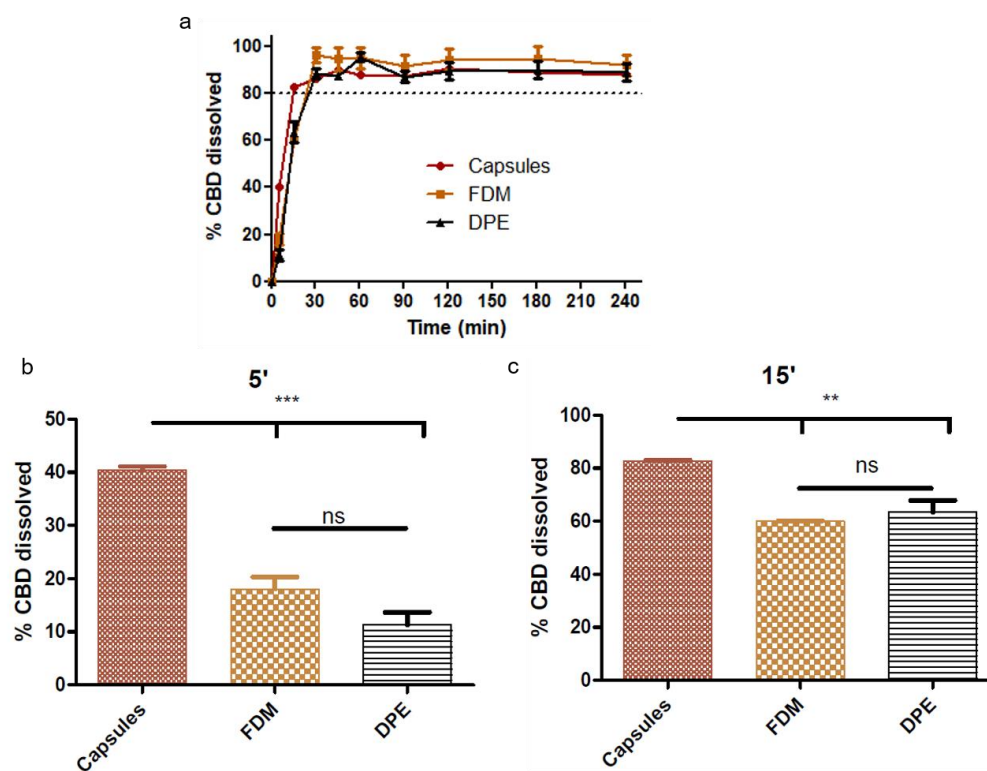


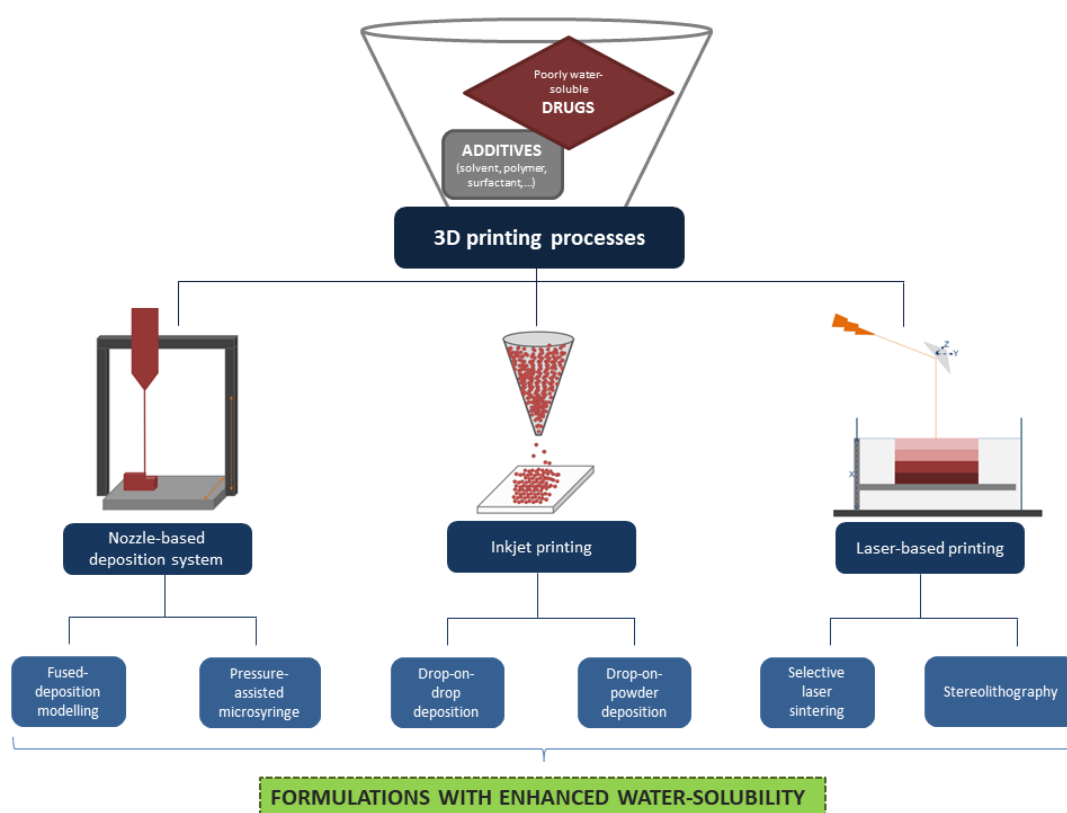
Figure 65 - a. Dissolution profile of ASD shaped by capsule filling (red), FDM (orange) and DPE (black) and percentage of CBD dissolved after 5 minutes (b) and 15 minutes (c) from the three formulations.

## APPENDIX VI. 3D PRINTING TECHNOLOGIES FOR SOLUBILITY INCREASE

### ***“Three-dimensional printing technology as a promising tool in bioavailability enhancement of poorly water-soluble molecules: a review”***

Jennotte O<sup>1</sup>., Koch N<sup>1</sup>., Lechanteur A., Evrard B.

**University of Liège**, Laboratory of Pharmaceutical Technology and Biopharmacy, Center for Interdisciplinary Research on Medicines, Avenue Hippocrate B36 (+2) 4000 Liège



O. Jennotte, N. Koch, A. Lechanteur, B. Evrard

### **Three-dimensional printing technology as a promising tool in bioavailability enhancement of poorly water-soluble molecules: A review**

Int. J. Pharm., 580 (2020), Article 119200

<https://doi.org/10.1016/j.ijpharm.2020.119200>



## 1. Introduction

One of the biggest current challenges for industries and researchers concerning the medicine development for an API is the improvement of its bioavailability. Up to 70% of the new drugs candidates have or will have aqueous solubility issues [1]. Because a drug has to be in solution to be absorbed, this phenomenon could lead to the failure of the commercialization of many high potential molecules [2]. BCS organizes the pharmaceutical compounds in four categories, depending on their aqueous solubility and their permeability through the gastrointestinal membrane. A good aqueous solubility is reached when the maximum clinical dosage of a drug is dissolved in 250 mL of an aqueous media with a pH range from 1.2 to 6.8. A great number of APIs do not respond to this specification and are classified as BCS II/IV molecules while the molecules with a sufficient solubility are gathered in the BCS I and III classes [3]. The major interest of this classification lies in the rationalization of the approach with which the bioavailability will be improved [4]. Among the strategies used to overcome the poor solubility of the BCS II/IV molecules, it can be distinguished those that modify the affinity between the compound and the solvent, and those that are dealing with more soluble solid forms [5]. CDs are commonly used to complex API to hide hydrophobic parts of a molecule and to produce complexes that have high apparent solubility. As an example, the solubility and dissolution rate of the anti-inflammatory drug celecoxib complexed with  $\beta$ -CD have been significantly enhanced [6]. The use of lipidic matrices is interesting to stimulate endogenous surfactants production [7]. More elegant formulations contain self-emulsifying excipients and produce *in situ* a micellar solution or an emulsion which considerably improves the aqueous solubility. As an example, fenofibrate, a hypolipidemic BCS II drug, has been mixed with Gelucire® 50/13 using supercritical carbon dioxide. The authors showed an increase of the aqueous solubility with an obtained supersaturation degree of  $2.28 \pm 0.14$  [8].

Concerning the drugs which have a poor dissolution rate because of high crystallinity cohesion, the use of more soluble solid forms, like polymorphs or amorphous systems, can be very useful [9]. The major drawback of this latest is the risk of recrystallization due to the unstable amorphous state. The use of ASD, mostly binary mixture of an amorphous API dispersed and stabilized in a polymeric carrier, is an ideal way to stabilize this desired but unstable state [10]. Many techniques allowing the formulation of ASD are described in the literature, such as the use of supercritical carbon dioxide in an anti-solvent mode, HME or the use of spray-drying [11–13]. When drugs have bioavailability limitations due to their slow dissolution rate, the particle size reduction is an easy way to improve the solubility. Through the Noyes-Whitney equation, it is easy

to understand that the dissolution rate increases proportionally with the specific surface [14].

Several ways to reduce the particle size are described in the literature, such as milling processes [15], rapid precipitation from a saturated supercritical solution or spray-drying [16,17].

In order to combine the multitude of aqueous solubility enhancement strategies with the current regulatory affairs and the manufacturing trends, new pharmaceutical tools have to be developed in order to facilitate formulations scale-up, to reduce the research cost and to benefit more generally to the public health. 3D printing is a recent promising answer to these latest constraints [18].

The 3D printing is a technique of additive manufacturing that produces 3D structures by depositing or binding materials layer by layer under control of computer software [19,20]. Since the first method for the 3D printing of objects, using SLA, developed by Charles Hull in the early '80s (Hull, 1986), many other methods emerged and their accessibility increased for the industrial, but also the general public [21,22]. Among them, drop-on-powder deposition, FDM and laser-based writing systems can be cited [18]. Due to its multitude of features and its flexibility, 3D printing has been applied to a great number of diverse domains like construction, biomedical, aerospace, protective structures, but also pharmacy [23]. The first publication combining 3D printing and drug delivery dates from 1996 by Benjamin M. Wu and his team [24]. Since then, the interest was growing for this kind of research, but it really exploded over the last four years. Indeed, since the FDA approval of a tablet with accelerated release manufactured by 3D printing (Spritam®, Aprelia Pharmaceuticals) in 2015, the number of publications concerning the "3D printing and drug delivery" has increased more than three times.

The different methods for 3D printing offer a large panel of advantages for the pharmaceutical field, like the personalized medicine [25], the manufacturing of multi-compartment dosage forms [26,27], complex geometries [28,29], implants [30], tablets with a high porosity [31], etc. Thanks to some of these advantages, 3D printing is an interesting approach for the formulation of drugs with an immediate release. The aim of this review is to highlight the different techniques which have been used to manufacture immediate release formulations of poorly aqueous-soluble drugs. Examples will be described for each technique.

## 2. Three-dimensional Printing Techniques

In a concern of consistency, the different terms will be first defined and detailed to classify all the reviewed techniques with a same denomination. Three main principles are used concerning the 3D printing technology: (i) inkjet systems (ii) nozzle-based

deposition systems and (iii) photo-polymerization systems [18,32] (Fig. 66). In all cases, architecture of the desired free form has first to be developed, generally by using CAD. The forms are then transformed in several slices in the appropriate file format and delivered to the software which will control the printer [33].

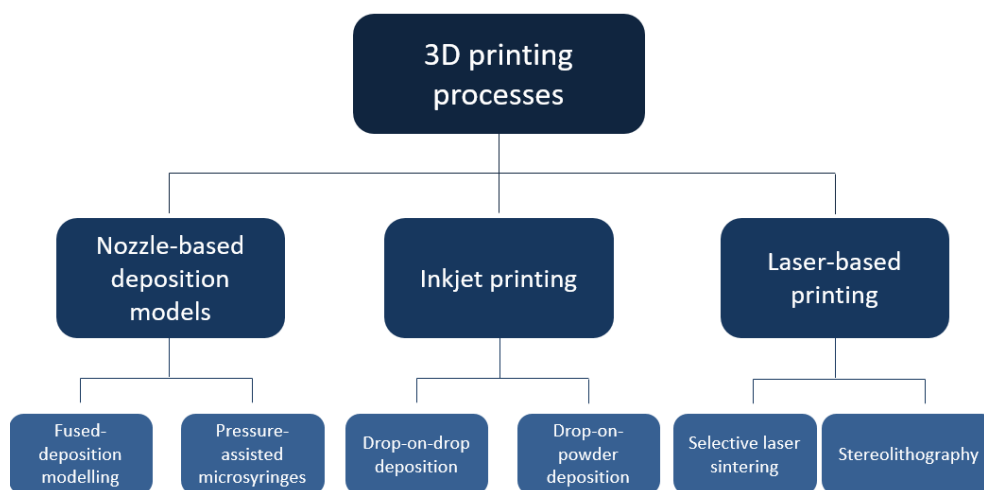


Figure 66 – 3D printing techniques.

- (i) The term “nozzle-based deposition systems” refers to the processes in which a melted or softened material – mostly a mixture of an API with a polymer – is extruded through a nozzle with desired diameter (**FDM**) [34] and other processes – often related to biological tissues engineering – in which a viscous semi-solid material is extruded from a syringe (**Pressure-assisted micro-syringes, PAM**) [35]. The nozzle (or syringe) movements are controlled by a software which guides the deposition of the extruded filaments on the plane surface and provides a layer-by-layer construction of the desired free form.
- (ii) The inkjet systems, which include a wide range of different techniques, are mostly based on the ink deposition through a thermal or piezoelectric-based nozzle on a polymer surface in a continuous or on-demand mode [36,37]. Such techniques are called **Drop-on-Powder** systems in which a binding liquid is precisely deposited on a powder bed. The overlay of multiple bonded powder bed layers provides a specific 3D structure. The ink is generally composed of a solution, suspension or emulsion of the API of interest and the powder bed is composed of polymer excipients such as different methacrylate entities, PVP derivatives or sugar and polyol like lactose or mannitol [18]. However, many authors have mixed the polymeric surface with an API and used the ink as a binder. In some cases, the

droplets are deposited one on the other without the need of polymeric support. With an optimal control of the solvent evaporation, these processes called **Drop-on-Drop** systems allow the formation of solid porous free forms [38].

- (iii) The photo-polymerization systems are based on the use of photo-active resins, which are able to polymerize in contact with UV or visible light [22]. The first laser-based liquid resins polymerization technologies developed were called **SLA** and are nowadays used especially in rapid prototyping. More recently, **SLS** has been developed to avoid the use of liquid photo-reactive substrates. This technique involves the treatment of a powder bed by a high-power laser that provides the melting of a chosen powder bed area. Again, all selected molten slices will fuse to provide a layer-by-layer architecture of the desired formulation [39,40].

As explained, 3D printing technology can be absorbed in three main principles, themselves divided in two subclasses. In the following sections, each technique is detailed and carefully illustrated with several examples in the context of drug bioavailability enhancement.

## 2.1 Nozzle-deposition models

### 2.1.1 *Fused deposition modeling*

FDM (**Fig. 67**) is a rapid prototyping technology in which a thermoplastic filament polymer, which can contain drug(s) or additive(s), is pulled by two gears through a small die diameter heated nozzle. The molten, extruded filament solidifies itself on a bed which can be heated [35]. The printed structure is previously designed thanks to a slicing software. The extruder can move within the x- and z-axes while the heat bed can move in the y-axis in order to create a 3D structure [41].

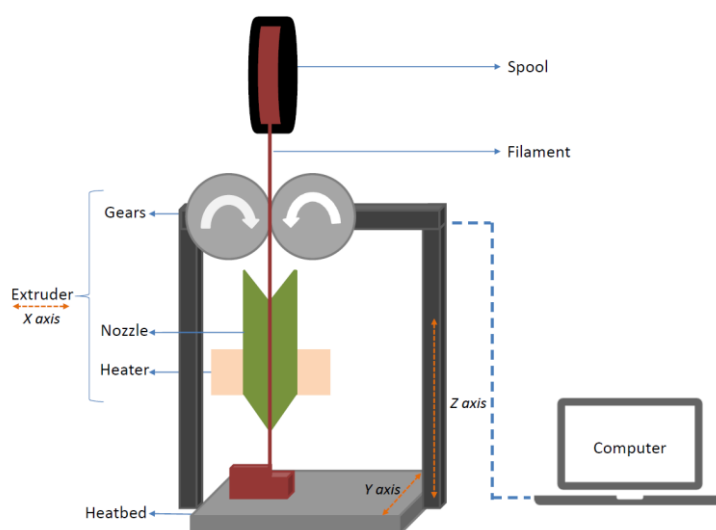


*Figure 67– Illustration of the FDM technique. A filament is delivered from a spool through an extruder composed of two gears, a nozzle and a heater. The structure is directly created from a CAD model which controls the layer-by-layer deposition of a filament extruded through the nozzle. The deposition occurs on a building platform which can be heated (heatbed).*

It is quite easy to modify the drug release from FDM 3D printed formulations, even if this technique is mostly used to manufacture sustained release formulations [42–44]. FDM is less used for the enhancement of the dissolution speed of poorly soluble drugs because, among others, of the compactness of the solidified melt, which slows the drug release. However, some authors showed that it seems possible to produce drug dosage forms with a release profile that matches the Pharmacopeia specifications for immediate release formulations, by modifying some critical parameters. These parameters are described in this chapter.

#### 2.1.1.1 Formulation and Printing Parameters

When drugs have a poor aqueous solubility due to their high crystallinity cohesion, the use of related amorphous forms provides higher aqueous solubility than crystalline forms. Indeed, amorphous forms translate no long-range order molecular structure and have more enthalpy than crystal forms. The energy required to sear molecules out of the disorganized structure is lower with amorphous form, which provides higher solubility [10].

However, amorphous forms are thermodynamically unstable due to their high internal energy. They tend to return to the crystalline state which is more stable. One of the solutions for stabilizing the amorphous state is to minimize the molecular mobility. The incorporation into a polymeric matrix is a suitable option. Such entities are called ASDs [45].

ASD allow the solvation of each individual API molecule and provide potential supersaturated concentration. This metastable state is a driving force for the nucleation and crystal growth of API in order to reach the thermodynamically stable concentration. This phenomenon, called “spring effect”, can be avoided by soluble polymers that may increase the viscosity and act as precipitation inhibitors or by drug-polymer interactions which inhibit nucleation and crystal growth. **Fig. 68** shows this behavior which is called “spring and parachute effect” [46].

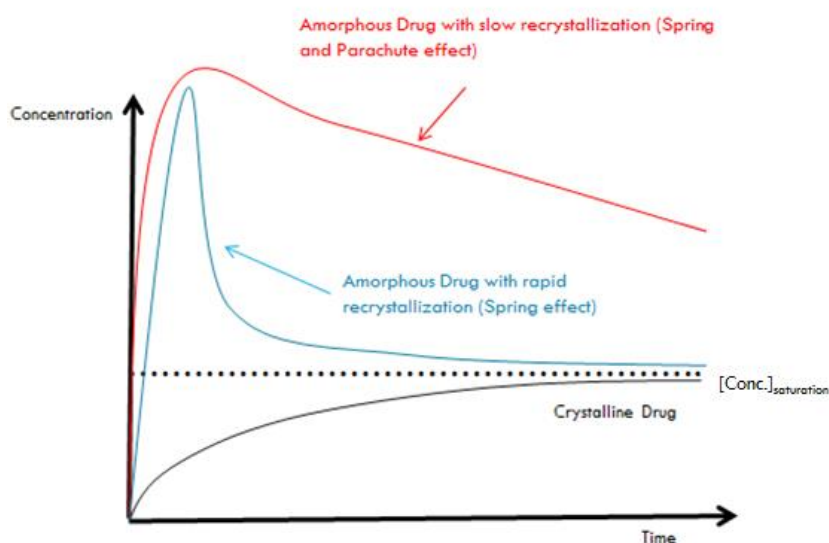


*Figure 68– Spring and parachute effect. The crystalline drug (black curve) doesn't allow to reach a supersaturated solution. The non-stabilized amorphous drug (blue curve) allows to reach a supersaturated solution, but a spring effect is observed because of the rapid recrystallization. The amorphous drug stabilized by a polymer (red curve) allows to reach a supersaturated solution which is maintained during a certain time and provides a spring with parachute effect. Adapted from [47], with permission of Elsevier.*

In order to produce an ASD, it is important to reach a molecular dispersion of API and/or additive in the polymer. Drug-polymer, polymer-polymer and additive-polymer miscibility studies have to be conducted. Indeed, the stability of ASD below polymer  $T_g$  is highly dependent on phase separation kinetics [48]. Immiscibility may lead to API recrystallization, or non-homogeneity of mechanical properties such as flexibility due to unequal repartition of the plasticizer. The miscibility involves a whole series of forces binding the drug and the polymer, each with a more or less important influence. It is important to study the strength of drug-polymer interactions, as they play a role on the ASD properties, such as its dissolution profiles or its stability [49]. Stability of ASD at temperature near  $T_g$  could be attributed to the drug-polymer bonding which makes

recrystallization more difficult [50]. Besides, drug-polymer interactions have impacts on the dissolution profiles of the filaments. As an example, improvement of indomethacin acidic solubility has been obtained by using cationic EPO, unlike with the use of other mixtures of indomethacin and non-ionic polymers, while all the compared formulations were miscible and maintained the amorphous form of indomethacin [51]. The miscibility studies can be conducted by several methods, such as the Van Krevelen and Hoftyzer's group contribution method which allows to calculate a solubility parameter, depending on cohesive forces. Solubility parameters of both API and polymers are then compared to predict the miscibility [52,53]. DSC is useful since miscible binary mixture provides one single  $T_g$  endotherm event while immiscibility can be detected by highlighting the separate  $T_g$  of mixture components [54].

Alhijaj and his team studied the possibility of using pharmaceutical approved polymer miscible blends in FDM 3D printing of oral solid dosage forms [55]. PVA, EPO and SOL were used as polymeric matrices to improve the aqueous solubility of felodipine and polysorbate 80 (Tween® 80), polyethylene oxide and PEG, which are the same polymer but with different chain lengths, were used as plasticizers. The miscibility predictions revealed that SOL and EPO are miscible with PEG/PEO and Tween® 80 while PVA is only partially miscible with Tween® 80. The mixture of PVA and Tween® 80 showed a weak stiffness that may be attributed to the discontinuity of the Tween® 80 phase in the PVA due to the low miscibility.

While a significant improvement of the dissolution of felodipine in a pH 1.2 HCl medium was observed with EPO formulation (release of 84.3% of API within 30 min) in comparison with crystalline felodipine, SOL and PVA formulations showed significantly slower drug release profiles. These facts could be explained by two principles. First, the salts strength of the medium may depress the polymer solubility of SOL and PVA [56]. Secondly, the excipients miscibility seems to have a very important role. Indeed, percentage of PEO/PEG used in EPO allows its complete dissolution in the polymer in contrary to the SOL formulations for which PEO/PEG crystallinity has been observed. This crystalline form requires wetting and hydration before the dissolution, which is not necessary when complete dissolution in the polymer is achieved and delayed the drug release [55].

One of the most appropriate techniques used for the manufacturing of ASD is the HME which is the process of converting a raw material into a product of uniform shape and density by forcing it through a die under defined conditions of heating, kneading and pressure [57]. It allows to produce filaments containing the drug dispersed or dissolved in a polymeric matrix which can be shaped using FDM 3D printing. The problem with most of the water-soluble polymers that are used in FDM ([Table 25](#)) is that they do not have the appropriate printing properties on their own.

Table 25– Most used water-soluble polymers in FDM 3D technology

Water-soluble polymer	Publications
Poly (vinyl alcohol)	[55,58–62]
Polyvinylpyrrolidone	[31,63,64]
Polyvinyl caprolactam – polyvinyl acetate – polyethylene glycol graft copolymer	[55,61,65]
Pluronic 407	[31]
Polyethylene oxide	[60,66]
Polyethylene Glycol	[31,66]
Basic Butylated Methacrylate Copolymer	[55,67]
Polyvinyl Alcohol/Polyethylene Glycol Graft Copolymer	[31,61]
Polyvinylpyrrolidone-Vinyl Acetate Copolymer	[31,63]

Therefore, the choice of the polymer is a critical parameter in the development of the FDM process for manufacturing immediate release forms. It has to keep the API in its amorphous state, allowing a better aqueous solubility. Besides, the polymer has to give appropriate printing properties to the filament, as its “printability” depends on its diameter, its thermal rheology (at printing temperature), its thermal properties (glass, fusion and degradation temperatures) and its mechanical properties (hardness and elasticity) [68,69]. All these parameters are discussed hereunder.

If the filament is not printable, additives, such as plasticizers, will have to be added to the formulation. The plasticizers will lower the  $T_g$  of the polymeric matrix, which will improve the mechanical properties and lower the temperature of extrusion/printing [70]. A plasticizer could be an additive, such as sorbitol or TEC, or the API itself, such as theophylline, as explained later in this chapter [58,59,71].

*The filament diameter* is a critical parameter for the feeding through the print head. Indeed, if the diameter exceeds the inner diameter of the hot end of the printer head, it would prevent the filament conduction. If the diameter is too thin, the filament may break because of the traction of the two printer gears [69]. The most common diameter found in the literature is 1.75 mm, but depending on the printer, it can vary between 1.75 and 3.0 mm. In order to have a consistent diameter, different techniques downstream



the HME can be used, such as a conveyor belt, a melt pump or a filament maker. The conveyor belt can be placed at the end of the extruder. A high belt speed will stretch the filament, so the diameter will grow shorter and, on the contrary, a small low speed will allow the diameter to grow higher. The melt pump is used to solve the problem of pulsating output of the twin-screw extruder, which makes difficult to maintain a constant filament diameter. This pump will maintain an accurate pulsation-free output, resulting in a constant diameter filament being extruded [72]. At last, a filament maker can be used. This kind of apparatus is equipped with an optical sensor and a dynamic puller system that work together to produce a filament spool with constant diameter [73].

*The rheological properties* of the filament are critical for the printing process, as a too high viscosity could lead to a clogging of the printer nozzle [68]. These properties can be characterized by a rotational rheometer. The viscosity depends on the formulation, but also on *the temperature*. Indeed, it is well known that the temperature impacts the viscosity of the molten material [74]. Besides, depending on the different components of the formulation, the temperature has to be sufficient to molten the material, but not too high, to avoid any degradation. Therefore, an equilibrium has to be found between a high-printing temperature where the viscosity of the melt is low but with a risk of degradation and a low printing temperature with the risk of clogging the printer nozzle because of the high viscosity. The generally used temperatures for FDM 3D printing are between 150 and 230 °C [63]. These temperatures are too high for many APIs, so the addition of a plasticizer may be necessary to reduce the extrusion and printing temperatures.

Some authors proposed a flowchart for the formulation of rapid drug release forms using HME and FDM ([Fig. 69](#)).

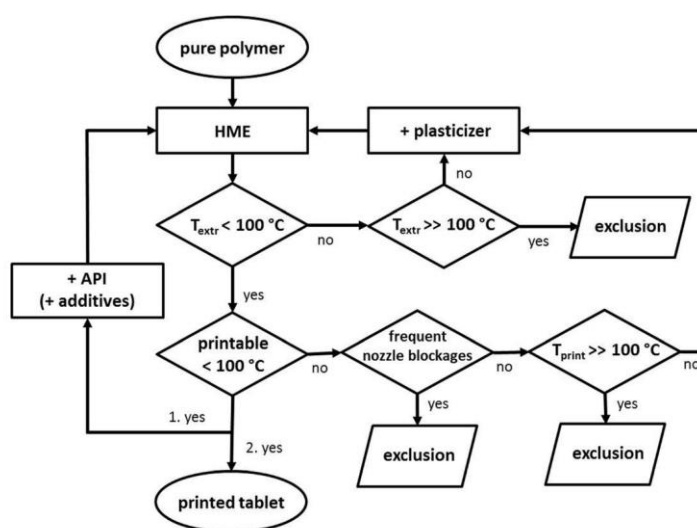


Figure 69– Flowchart for drug loaded tablet formulations;  $T_{extr}$  = temperature required for extrusion;  $T_{print}$  = temperature required for printing. Reprinted from [31], with permission of Springer Nature.

They used this flowchart for pantoprazole sodium. The targeted temperature for both HME and FDM was below 100 °C because the pantoprazole sodium has a degradation temperature at approximately 110 °C [75]. To extrude and print below this temperature, the addition of a plasticizer was recommended. Immediate release formulations of PEG 6000 + 10% of API were printed without the need of any plasticizer while immediate release formulations of PVP K12 + 10% of API were successfully printed after the addition of 15% of TEC, a plasticizer [31].

In the case of 4-aminosalicylic acid, a thermo-sensitive drug, Kollamaram *et al.* managed to produce different immediate release formulations at lower temperatures [63]. All the formulations that were tested contained KVA64 as a water-soluble polymer, PEG 1500 as a plasticizer, magnesium carbonate as a stabilizing agent and mannitol as a secondary plasticizer and a channeling agent. K12PF, another water-soluble polymer, was added to some of the formulations. The tablets were printed at 90 °C, with no degradation of the 4 – aminosalicylic acid. The complete dissolution of the drug was obtained after 20–30 min for each formulation. The release profile of the formulations which contained the K12PF was faster than the others, which led the authors to suppose that the mechanism of the drug release from these tablets was erosion.

In another study, a mixture of theophylline, Eudragit®E, an acrylate polymer and TEC as a plasticizer was extruded in order to provide printable filaments. Immediate release formulations with a caplet shape were successfully printed. However, the researchers mentioned difficulties to combine optimal HME temperature process and optimal

printing temperature process, where ideal values of printing temperature were 40 to 50 °C above the ideal HME temperature process, which was 110 to 120 °C. In this case, the ideal printing temperature would be 170 °C, which is not suitable with acrylate polymers that degrade above 166 °C. Authors found as a solution the use of high melting point compound (in this study, theophylline has a higher melting point, 273 °C, than printing temperature) that acts as a plasticizer and allows consistent flow through the printer's nozzle and a rapid solidification of the printed structure at room temperature [71].

Sadia also proved that it was possible to print immediate release oral formulations, with lower process temperatures [67]. The authors tested four different API's, 5-aminosalicylic acid, captopril, prednisolone and theophylline, to produce FDM 3D printed tablets. They used EPO as the delivery carrier and TCP as a filler. All the formulations were printed with a temperature of 135 °C. The release profile of each formulation showed a drug release of more than 85% after 30 min.

*The mechanical resilience* of the filament is another essential parameter for its feeding through the two gears of the printer without deformation, which could be due to a lack of stiffness, or breakage, when the filament is too brittle ([Fig. 70](#)).

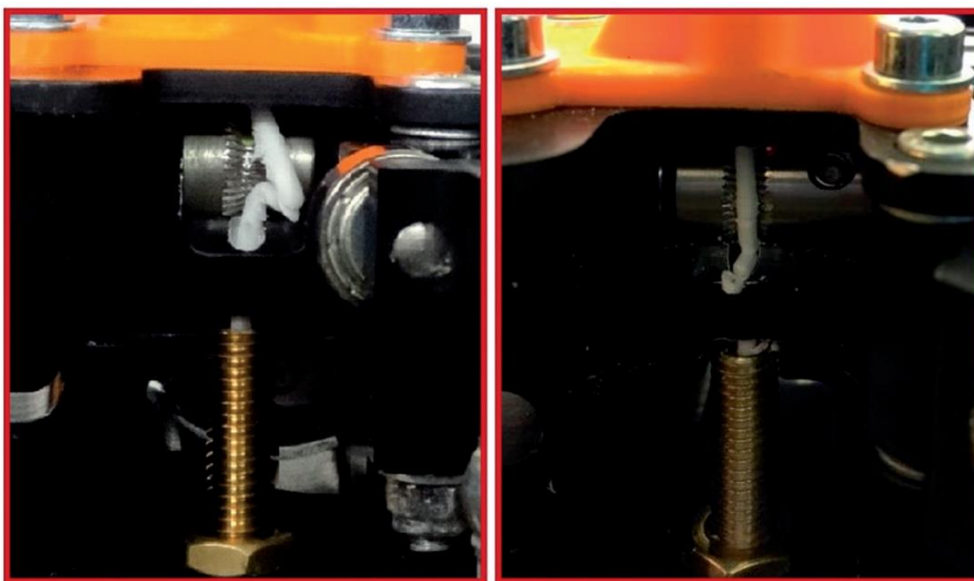


*Figure 70– Open print head with non-printable filaments. The filament on the left is too flexible (contains too much plasticizer), so it cannot be conducted through the print head. The filament on the right is too brittle (not enough plasticizer), so it breaks inside the print head, mainly because of the transversally applied pressure of the two gears. Reprinted from [69], with permission of Taylor & Francis.*

To determine this resilience, the tensile test and the three-point bend test can be effectuated on the extruded filaments, using a texture analyzer [69,76]. To fine tune the mechanical behavior of the filaments, plasticizers can be used. By modifying the percentage of plasticizers, the brittleness of the filament can be sufficiently reduced and its flexibility can be improved until obtaining a printable filament.

Melocchi studied the printability of extruded filaments based on a variety of pharmaceutical grade polymers, such as SOL, Kollicoat® IR or PVA [61]. As these polymers were not “feedable” on their own in the printer because of inappropriate mechanical properties, plasticizers had to be added before the extrusion as follow: SOL + 10% PEG 400, Kollicoat® IR + 12% glycerol and PVA + 5% glycerol. Disk-shaped structures were successfully printed with these mixtures.

In another study, authors showed that a concentration of sorbitol, used as a plasticizer, could be adjusted in a mixture with PVA in order to produce filaments with desired mechanical properties for printing. Sorbitol 10% (w/w) reduced the maximum forces during three-point test from 7.3 N to 2.2 N at a maximum distance of 3.9 mm. With 20% (w/w) of sorbitol, maximum force decreased until 0.6 N. Nevertheless, higher sorbitol concentrations provided too flexible filaments, unsuitable for printing [59].

### 2.1.1.2 Structure of the printed forms

#### *Infill*

In FDM 3D printing, the infill represents the inner support of the printed structure. An infill of 0% is characterized by a completely hollow structure while 100% of infill is characterized by a fully solid filled structure [77]. A compromise has to be found between a low percentage of infill, which presents a high porosity but a low capacity of dosage of the API, and a high percentage of infill, which allows a high dosage of the API but with lower porosity and therefore a smaller surface of contact with the aqueous media.

In a study conducted by Solanki, a 1/1 (w/w) mixture of KVA64 and Affinisol® was selected to stabilize haloperidol in its amorphous state [78]. Tablets with different percentages of infill were printed. Complete release was obtained after 45 min with 60% infilled printed tablets while the 100% infilled printed tablets completely dissolved after 3 hours. This study showed that a higher porosity, and so a higher specific surface, improve the dissolution rate. However, Kempin showed that modifying the percentage of infill doesn't always influence the dissolution time of drugs [31]. They printed PEG 6000 and PVP K12 tablets with three different percentages of infill (50%, 90% and 100%). There was no significant change in the dissolution time for the PEG 6000 printed tablets. The authors suggested that it could be due to the low viscosity of the PEG 6000 melt, which makes the PEG strands tighter, decreasing the contact area with the aqueous fluids. However, the PVP K12 printed tablets with 50% infill were completely dissolved in 3 min, which is 7 min faster than the printed tablets with 100% infill [78].

#### *Geometry of the Printed Tablet*

In addition to the porosity or the polymer that can be changed in order to modify the dissolution behavior of a printed tablet, the geometry of the printed structure also has an important impact. Following this idea, paracetamol has been extruded with PVA through single-screw extruder and the formed filaments have been used to print different geometries. A drug loading of 3.95% (w/w) has shown to provide optimal mechanical behavior while higher drug loading required the use of plasticizers to give a filament with optimal softness. Following this composition optimization, five shapes have been successfully constructed (cube, pyramid, cylinder, sphere and torus) (Fig. 71) [79].

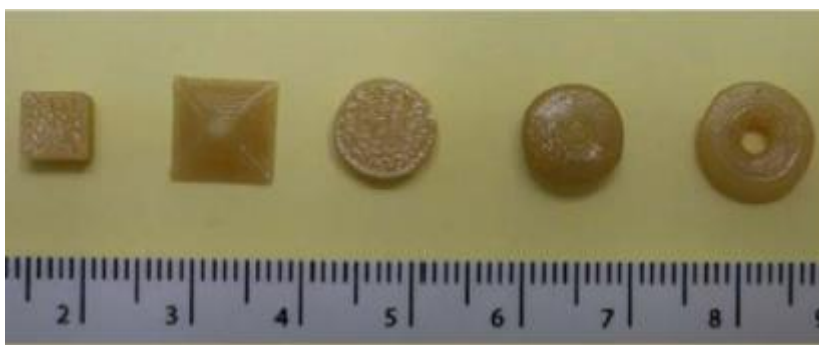
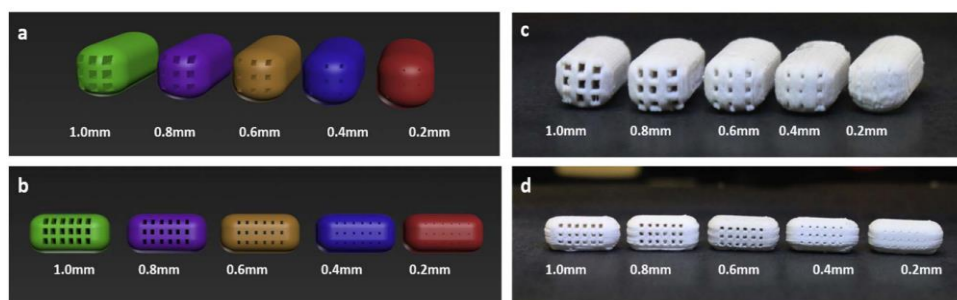


Figure 71 – Picture of different shapes of paracetamol (3.78%)-PVA formulations obtained by FDM: cube, pyramid, cylinder, sphere and torus (from left to right). Reprinted from [29], with permission of Elsevier.

Researchers showed that the fastest release rates were obtained with geometries characterized by a high SA/V ratio values. Indeed, the pyramid form had the fastest rate while the sphere had the slowest, with a similar surface area, but a different volume. When this SA/V ratio was kept constant, the results were radically different with the faster release obtained with the sphere (and cubic) forms while the pyramid forms gave the slower release. Erosion of the matrix could be an explanation. This study shown that drug release kinetic is more influenced by the ratio SA/V rather than the surface area alone, which highlighted the importance of the geometry. In this point of view, FDM is one of the most suitable techniques to provide very complex tablets form in order to optimize the desired ratio [79].

In another study, channeled tablets containing hydrochlorothiazide were also produced by FDM [80]. Five widths of channel section were tested (0.2, 0.4, 0.6, 0.8 and 1.0 mm). Besides, in order to measure the influence of the length and orientation of the channels, 9-long channels parallel to the long axis of the caplet design or 18-shorter channels at right angles to the long axis of the caplet design were applied (Fig. 72). It was shown that the printed tablet design has an influence on the *in vitro* drug release. Indeed, the short channels (0.2-0.4 mm) showed a limited improvement in the dissolution rate in comparison to the wider channels. This latter allowed a release of hydrochlorothiazide reaching a maximum, after 30 min, of 92.3% for 9-long channel designs and of 93.4% for the 18-short channel designs. As it has been written above, the dissolution rate is often directly linked to the surface area of the printed structure. Here, the release of hydrochlorothiazide is faster for the 18-short channel tablets while they have a lower surface/volume ratio in comparison to 9-long channel tablets. In this study, the release of the drug is rather depending on the length of the channels which eroded faster for the 18-short channels than for the 9-long channels.



*Figure 72 – Rendered images of caplet designs with decreasing channel size with a) 9-long channels b) 18-short channels, photographs of tablets with decreasing channel size c) 9-long channels d) 18-short channels. Reprinted from [80], with permission of Elsevier.*

**Fig. 73** shows capsule-like structure designed by Arafat and his team [81]. This design was divided into nine blocks with determined light spaces in between (0, 0.2, 0.4, 0.6, 0.8, 1.0 or 1.2 mm). The distance between the blocks was of most importance for the drug liberation. A distance of 1.0 mm between the different blocks was necessary to allow a sufficient flow of medium in the structure and to meet the Pharmacopeia criteria concerning the dissolution of immediate release formulations. In this study, the increase of the dissolution rate of the different structures is not only due to the increase of the surface/mass ratio. Indeed, the difference of the surface/mass ratio of tablets with inter-blocks spaces of more than 0.6 mm and the others is negligible. According to the authors, the reason that explains the different dissolution profiles is the structural change of the tablets during the dissolution. Wide angle laser imaging was performed during the dissolution tests in order to measure the time-to-break of the tablets. It appeared that the larger the inter-block, the faster the tablet broke, allowing a greater contact with the aqueous medium, so a faster release of the drug.

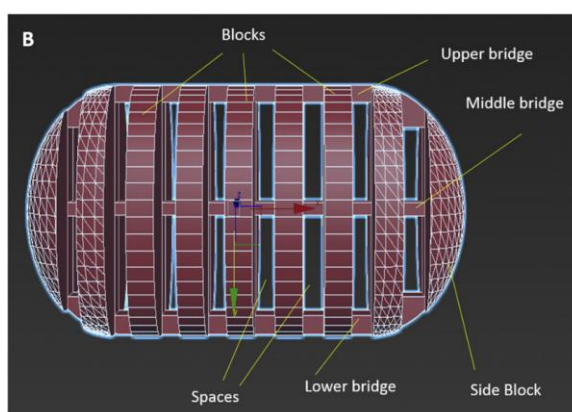


*Figure 73– Illustration of the novel design based on 9 repeating units (blocks) with determined light spaces in between (0, 0.2, 0.4, 0.6, 0.8, 1.0 or 1.2 mm). The capsule-like general shape was maintained by using curved side units. Reprinted from [81], with permission of Elsevier.*



Another complex geometry that was studied is radiator-like printed structures (Fig. 74) [82].

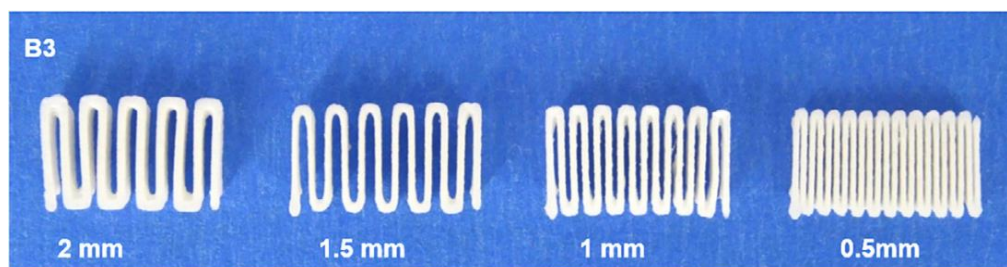


Figure 74– Radiator-like doses containing theophylline, PEG 6 K and PEO 600 K. These four designs have the same overall dimensions, but with increasing spaces (2.0, 1.5, 1.0 and 0.5 mm). Reprinted from [82], with permission of Elsevier.

PEO has already been used in FDM 3D printing in order to print immediate release formulations [55,60]. Isreb evaluated the ability of PEO 600,000 to be the backbone polymer of original FDM 3D printed structures with fast drug release [82]. PEG 6000 was used as a plasticizer in the tested formulations. Compressed PEO/PEG blends, in contact with aqueous media, tend to form a gel layer which slows the drug release down [83]. To overcome this dissolution speed reduction, the authors designed FDM 3D printed radiator-like structures with different spaces between the plates. These structures allow to have an increased surface/mass ratio. Besides, the thinness of the plates makes the formed gel layer thinner, allowing the drug to be released faster. Four different spaces were tested (0.5, 1.0, 1.5 and 2.0 mm). To be in accordance with the USP criteria for immediate release formulations, namely reaching 80% of the API dissolution in 500 mL of HCl 0.1 N in aqueous medium within 30 minutes, the space between the plates had to be 1.0 mm long minimum. The last four studies of the previous chapter proved that the dissolution rate of the printed structures is not only influenced by the surface area, but also by the geometry of the structure. Indeed, for a same surface area, different geometries can have different dissolution behavior.

This chapter highlighted one of the advantages of FDM compared to the traditional tablets manufacturing techniques such as powder compression. Indeed, elaborated geometries, impossible to make by simple compression, are easily manufactured by FDM 3D printing. This makes it possible to increase the surface of contact with the physiological fluids and so to increase the dissolution rate. But this surface area is not the only parameter that modifies the dissolution rate of printed tablets. Indeed, recent studies showed that it was not always the structures with the highest surface area that dissolved the fastest.



### 2.1.1.3 Alternatives to Hardly Swallowable Immediate Release Forms

All elaborated, complex structures described in this review article have proved their ability to form immediate release formulations, due to an increase of the surface area, a particular design or an acceleration of the polymeric erosion. However, one issue that we want to raise is that these unconventional structures would be difficult to swallow. To overcome this problem, authors tried to build orodispersible 3D forms that avoid any swallowable step.

Ehtezazi used a FDM 3D printer to produce fast dissolving oral films which have the advantage to be easily taken by the patient who presents difficulties to swallow, like the children or the elderly compared to the printed tablets [60]. Besides, they allow to avoid the hepatic first-pass metabolism if the drug is absorbed by the sublingual route [84]. The authors designed plain and mesh films, with or without taste-masking layer. The study showed that the drug release was impacted by the design of the film as well as by the presence or not of the taste-masking layer. Indeed, the films without this layer showed a faster release profile than those which contained the taste-masking layer which acts like a barrier, delaying the contact between the drug and the physiological fluids. It can also be seen that the mesh films had a faster release profile than the plain films, the surface of contact area being more important.

Following the same idea, other researchers used FDM to manufacture perforated orodispersible films with aripiprazole and compare them to orodispersible films made with standard solvent casting method. Concerning the dissolution studies, it appeared that the drug release profile was faster for the 3D printed orodispersible films, 95% of the aripiprazole was released after 15 min while 75% of the API contained in the cast films was released after the same time. The difference between the two release profiles can be explained by the higher surface area of the printed orodispersible films. Besides, the DSC measurements showed a fully amorphization of the aripiprazole in the printed orodispersible films, while it is only partially amorphous in the cast films [62].

To summarize, even if the studies about the manufacture of formulations with a sustained release profile are far more numerous than studies dealing with FDM for immediate release oral drugs, this chapter showed that more and more research are conducted to accelerate the drug release, using this technique. By modifying process parameters such as the design, the porosity or the temperature, FDM can be used to produce such oral drug dosage forms.

### 2.1.2 Pressure-Assisted Micro-Syringe Extrusion

Another approach of “nozzle-based 3D printing” is PAM. The PAM printing method is based on the extrusion of a semi-solid paste through a syringe whose movements are

controlled by the software and guided by the designed free-form (Fig. 75). A wet mass is generally transferred to syringes containing extrusion tips with precise orifice diameter.

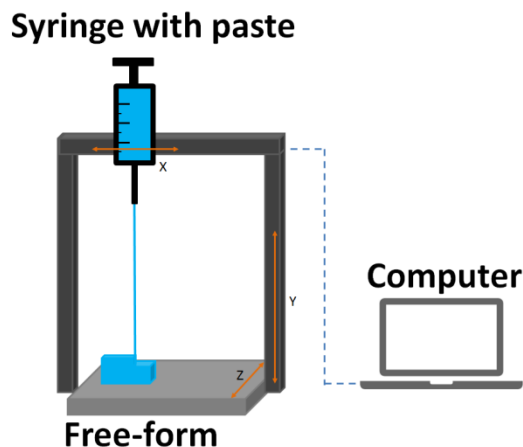


*Figure 75– Illustration of the PAM technique. A paste, generally composed of an active compound mixed with wetted polymers, is delivered through a syringe with a specific nozzle. The structure is directly created from a CAD model which controls the layer-by-layer deposition of the paste through the nozzle on a building platform.*

#### 2.1.2.1 Formulation for PAM Technique

This technique is based on the softening of materials under specific conditions that avoid drug decomposition for thermolabile materials and allow the use of generally recognized as safe (GRAS) excipients. The major difficulty of the process is to obtain an optimal viscosity of the material for its extrusion [18,85]. This parameter sees its importance especially for the passage through the orifice of the syringe. The wetting liquid has an important role in the PAM process since the first step is to obtain a wet mass. Moreover, the choice of the wetting liquid depends on the polymer and its desired rheological properties. For example, HPMC had as optimal wetting liquid a mixture of water and ethanol in proportion 90:10 (V/V). Indeed, the absence of ethanol provided highly viscous mass that could not flow through the nozzle while too much ethanol induced a too fast drying and produced a hard mass impossible to extrude [85]. PVP wetted with pure water provided optimal viscosity [86]. With the use of lipidic excipients, wetting the liquid becomes useless. Indeed, the use of matrices like Gelucire® 44/14, Gelucire® 48/16 or Kolliphor® P 188 above their low melting points provides dense and extrudable liquid formulations [87]. Therefore, the wetted liquid to use depends on the polymer and its desired rheological properties.

#### 2.1.2.2 Solubility enhancement strategies using PAM

We have noticed that PAM technique is not often used with a simple mixing of polymers and API to produce ASD allowing the enhancement of drugs solubility.

Indeed, authors used combined solubility enhancement strategies like superdisintegrants, CDs or an increased surface area to successfully improve the solubility of PAM formulations.

The antiepileptic drug carbamazepine has been complexed with HP $\beta$ CD and mixed with HPMC. Oral dispersible form has been produced by using 2.5% (w/w) of superdisintegrant Ac-Di-Sol<sup>®</sup> SD-711 (croscarmellose sodium). The fastest dissolution rate was explained by the use of CDs, but also the specific geometry that increases the surface area and the use of superdisintegrant [85]. In another study, painkiller paracetamol has been mixed with PVP K25, wetted with pure water. The use of the same superdisintegrant croscarmellose sodium provided an immediate release profile of paracetamol printed tablets, obtained by optimizing the ratio API/excipients. The free-form showed a rapid drug release, explained by the presence of disintegrant but also by the microporous structure [86]. Disintegrant sodium starch glycolate was used to formulate a dispersion composed of aspirin, hydrochlorothiazide and PVP K 30, wetted by pure water. More than 75% of the aspirin and hydrochlorothiazide were released within the first 30 min, thanks to the disintegrant [88]. Faster release profiles can be obtained with formulations containing increased concentration of soluble materials and/or increased distances among printing lines [89].

The principal advantage of this technique, especially in comparison with FDM, is the use of mild working temperature which prevents any drug degradation.

## 2.2 Laser-based printing

### 2.2.1 Stereolithography

3D printing SLA is a technology that uses a laser which produces the photopolymerization and the solidification of a liquid resin. The laser is focused on the specific area to densify. The solidification is repeated layer-by-layer in order to construct the desired free form ([Fig. 76](#)) [90].

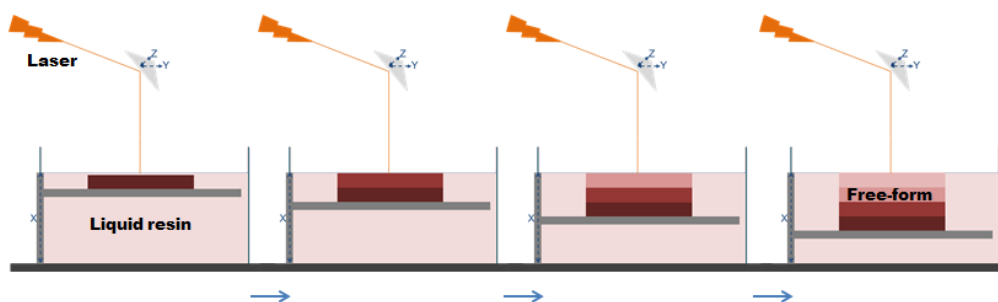


Figure 76– Principle of SLA 3D printing. A laser is focused in a vat that contains a liquid resin with a specific depth. The region in which the laser is focused polymerizes and provides a solid layer. The depth increases progressively in order to build layer-by-layer the desired free form.

### 2.2.1.1 Formulation for SLA technique

Several crosslinkable monomers have been used in order to prepare free-form dosages. In most cases, acrylate entities are used. Actually, the photopolymerization can be divided in two groups: cationic polymerization mostly used with vinyl ether, epoxides or lactones, and radical polymerization, mostly used for acrylate derivatives. Basically, a first initiating phase occurs with photo sensible initiator that provides a cation or a radical by contact of light [91]:

In general, aromatic ketones are used to provide two radical species by a homolytic cut. Once the monomers are activated, the polymerization occurs in a chain reaction like any classical polymer formation. The reactive monomers link to form a chain until the rigidity becomes too high to continue the reaction and reach the termination phase.

A suitable photoinitiator must have some properties in order to initiate the polymerization. It must hardly absorb in the wavelength range of the used laser to provide excited states with a very short life time to avoid any deactivation by oxygen and it must have the higher yield as possible [92]. Besides, monomers can be divided in two groups in function of the initiation mechanism, as mentioned above.

PEGDA is the most used polymer when SLA is considered. However, other acrylate entities could be used. For example, theophylline was treated with the photoinitiator 2-hydroxy-4-(2-hydroxyethoxy)-2-methylpropiophenone and photoactive monomers PEDGA and PEGMA. The aim of this study was to compare the two types of acrylate entities. It was observed that PEGMA provided translucent printed free form while those produced with PEGDA were opaque that could explain that PEGMA formulations provided faster dissolution rates compared to the PEGDA formulations. However, both acrylate entities were easily photopolymerized [93].

To cite a further example of initiator, diphenyl (2,4,6-trimethylbenzoyl) phosphine oxide has been used to initiate the polymerization of PEGDA in a concentration of 1% (w/v) to produce paracetamol and 4 amino salicylic acid formulations [90].

As discussed above, inkjet printing and SLA have been used in association in order to produce fast releasing gel of NSAID Naproxen and Ibuprofen. PEGDA was used with Eosin Y and mPEG amine as photoinitiator. Tablets formed with 20% of PEGDA exposed during 45 s to light have the fastest release profiles [94].

#### 2.2.1.2 Structure of the Printed Forms

Like the other 3D printing techniques, unconventional structures can be produced by SLA. Paracetamol and 4-amino salicylic acid were used as model APIs to construct a torus shape dosage form. The drugs were fast dissolved in the photoreactive solution, which was important to reach a high homogeneity. The torus shape was selected to increase the aqueous solubility by increasing the surface area. No degradation was observed during the process that may be a suitable printing process for thermolabile drugs. Moreover, the two drugs were in their amorphous forms, which is a good additional way to improve the water-solubility. The drug release was pH-independent due to the constitution of the matrices, but changes in the ratio of PEGDA:PEG 300 considerably influenced the release rates. Indeed, fast drug dissolution was obtained with a low concentration of PEGDA. Formulations containing 35% of PEGDA allowed the printing but also the complete release of paracetamol [90].

Considering the previous theophylline formulations, the highest dissolution rate was obtained with the PEGDMA perforated by 6 holes, especially due to the increase surface area [93].

Despite the promising results of those techniques, the photoactive excipients suffer from a lack of safety studies and are nowadays not approved for human consumption.

#### 2.2.2 Selective laser sintering

SLS is an alternative laser technique for which light energy is used to bind powder particles together (**Fig. 77**). The specific pattern introduced in the computer will guide the laser in order to draw the specific free forms from the powder bed. The goal is to reach a solid-state sintering obtained with a local temperature between the melting point ( $T_m$ ) of the material and  $\frac{T_m}{2}$  to obtain the maximum of porosity [95].

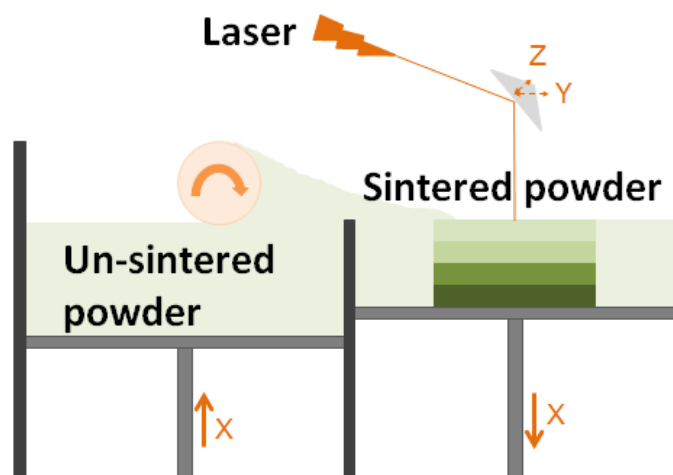


*Figure 77 – Illustration of the SLS technique. A laser is focused on a specific region and in a specific depth of the powder to sinter. A vat that contains un-sintered powder feeds the compartment containing the powder to be sintered with a rising piston and a roller. The number of solid layers of the free form is increased by the extend of the depth of the treated container.*

The first study concerning this technique in the pharmaceutical field is very recent. SLS has been employed in 2017 to construct a solid dispersion of paracetamol with Kollicoat® IR and Eudragit® L100-55. An approved pharmaceutical absorbent excipient, Candurin® Gold Sheen (3% w/w), was used to enhance the energy of absorption of the system. No degradation could be observed. Thermograms and diffractograms showed paracetamol crystallinity in the Kollicoat® but no peaks were observed with Eudragit®. As expected, Kollicoat® formulation allowed the API dissolution in the acidic media while only low releases were observed with Eudragit® formulation in the same fluid. Finally, it has been demonstrated that an increasing drug content provides less porosity and so requires more time to release the entire loading [39]. One year later, same authors have studied the possible use of SLS to produce several geometries, especially gyroid lattice. Again, paracetamol was treated with several polymers (Eudragit® L100-55, Eudragit® RL, Ethylcellulose N7 and PEO). Candurin® Gold Sheen was used. A reduction in the duration of the dissolution was observed with all formulation and is, once again, attributed to an increased surface area. PEO allowed the fastest complete release within 10 min [96].

This promising technique offers the possibility to produce extremely precise free forms without the requirement of any support.

### 3. Conclusion

The poor aqueous solubility of active ingredients is one of the most challenging issues in the pharmaceutical field. This leads to low and erratic absorption of API and may

occur numerous promising new drugs. Researchers have developed many strategies to overcome the low solubility such as the use of polymers, CDs or by reducing the particle size. The 3D printing technologies are recent methods exploding in a lot of scientific fields. They offer several advantages such as the possibility of the ultra-precise construction of complex oral dosage forms used to optimize specific surface area of medicines. Moreover, techniques like FDM are relatively cheap and could be used to produce personalized medicines. The drop-on-powder 3D printing technique allowed to produce the Spritam®, the unique FDA approved 3D printed medicine, which may be the first in a long series of innovative medicines with an immediate release. Despite this, the FDM is by far the most used technique, especially to manufacture ASDs with optimized surface area. The critical parameter is to obtain filaments with optimal flexibility and API homogeneity. A huge work of filaments optimization is still needed and essential since many commonly used polymers in the field of solubility enhancement do not allow the formation of printable filaments. This could be settled by the development of new polymers, more appropriated for 3 DP, or by varying proportions of solubility enhancers, plasticizers and API. By solving this issue, medicine could be produced as filaments that can be shaped with a precise design and a precise dosage leading the way to personalized medicine. Concerning the laser-based printing techniques, the major limitation is the lack of pharmaceutical approved excipients. Further studies have to be conducted in order to obtain safety information of photopolymerizable polymer as well as a photoinitiator in the perspective of a scale-up for human consumption. Other photoreactive monomers must also be developed in order to provide a wider range of excipients and so cope with potential API-polymer compatibility issues. Inkjet printing suffers from the need of solvents which will pose more and more problems because of the more important restrictions of residual solvent in medicines as well as environmental concern. Moreover, as inks are liquid forms, stability issues will occur more often compared to the use of dry forms. To conclude, 3D printing technologies offer the possibility to build very precise architecture which benefits the dissolution rate by optimizing the ratio SA/V but also provided all-in-one processes using known solubility enhancement strategies.





## 4. References

- [1] L. Peltonen, J. Hirvonen, Drug nanocrystals – Versatile option for formulation of poorly soluble materials, *Int. J. Pharm.* 537 (2018) 73–83. <https://doi.org/10.1016/j.ijpharm.2017.12.005>.
- [2] S. Chinta, R. Rengaswamy, Machine Learning Derived Quantitative Structure Property Relationship (QSPR) to Predict Drug Solubility in Binary Solvent Systems, *Ind. Eng. Chem. Res.* 58 (2019) 3082–3092. <https://doi.org/10.1021/acs.iecr.8b04584>.
- [3] M. Lindenberg, S. Kopp, J.B. Dressman, Classification of orally administered drugs on the World Health Organization Model list of Essential Medicines according to the biopharmaceutics classification system, *Eur. J. Pharm. Biopharm.* 58 (2004) 265–278. <https://doi.org/10.1016/j.ejpb.2004.03.001>.
- [4] A. Charalabidis, M. Sfouni, C. Bergström, P. Macheras, The Biopharmaceutics Classification System (BCS) and the Biopharmaceutics Drug Disposition Classification System (BDDCS): Beyond guidelines, *Int. J. Pharm.* 566 (2019) 264–281. <https://doi.org/10.1016/j.ijpharm.2019.05.041>.
- [5] Y. Perrie, T. Rades, *Pharmaceutics: Drug Delivery and Targeting*, 2012.
- [6] S. Rawat, S.K. Jain, Solubility enhancement of celecoxib using  $\beta$ -cyclodextrin inclusion complexes, *Eur. J. Pharm. Biopharm.* 57 (2004) 263–267. <https://doi.org/10.1016/j.ejpb.2003.10.020>.
- [7] O. Rezhdo, L. Speciner, R. Carrier, Lipid-associated oral delivery: Mechanisms and analysis of oral absorption enhancement, *J. Control. Release.* 240 (2016) 544–560. <https://doi.org/10.1016/j.jconrel.2016.07.050>.
- [8] A. Pestieau, F. Krier, P. Lebrun, A. Brouwers, B. Streel, B. Evrard, Optimization of a PGSS (particles from gas saturated solutions) process for a fenofibrate lipid-based solid dispersion formulation, *Int. J. Pharm.* 485 (2015) 295–305. <https://doi.org/10.1016/j.ijpharm.2015.03.027>.
- [9] B.C. Hancock, M. Parks, What is the true solubility advantage for amorphous pharmaceuticals?, *Pharm. Res.* 17 (2000) 397–404. <https://doi.org/10.1023/A:1007516718048>.
- [10] G. Van Den Mooter, The use of amorphous solid dispersions: A formulation strategy to overcome poor solubility and dissolution rate, *Drug Discov. Today Technol.* 9 (2012) e79–e85. <https://doi.org/10.1016/j.ddtec.2011.10.002>.
- [11] J. Thiry, P. Lebrun, C. Vinassa, M. Adam, L. Netchacovitch, E. Ziemons, P. Hubert, F. Krier, B. Evrard, Continuous production of itraconazole-based solid dispersions by hot melt extrusion: Preformulation, optimization and design space determination, *Int. J. Pharm.* 515 (2016) 114–124. <https://doi.org/10.1016/j.ijpharm.2016.10.003>.
- [12] D.H. Won, M.S. Kim, S. Lee, J.S. Park, S.J. Hwang, Improved physicochemical characteristics of felodipine solid dispersion particles by supercritical anti-solvent precipitation process, *Int. J. Pharm.* 301 (2005) 199–208. <https://doi.org/10.1016/j.ijpharm.2005.05.017>.
- [13] H. Takeuchi, S. Nagira, H. Yamamoto, Y. Kawashima, Solid dispersion particles of amorphous indomethacin with fine porous silica particles by using spray-drying method, *Int. J. Pharm.* 293 (2005) 155–164. <https://doi.org/10.1016/j.ijpharm.2004.12.019>.
- [14] M. Mosharraf, C. Nyström, The effect of particle size and shape on the surface specific dissolution rate of micro-sized practically insoluble drugs, *Int. J. Pharm.* 122 (1995) 35–47. [https://doi.org/10.1016/0378-5173\(95\)00033-F](https://doi.org/10.1016/0378-5173(95)00033-F).

- [15] Z.H. Loh, A.K. Samanta, P.W. Sia Heng, Overview of milling techniques for improving the solubility of poorly water-soluble drugs, *Asian J. Pharm. Sci.* 10 (2014) 255–274. <https://doi.org/10.1016/j.ajps.2014.12.006>.
- [16] H. Rostamian, M.N. Lotfollahi, Production and characterization of ultrafine aspirin particles by rapid expansion of supercritical solution with solid co-solvent (RESS-SC): expansion parameters effects, *Part. Sci. Technol.* 38 (2020) 617–625. <https://doi.org/10.1080/02726351.2019.1573865>.
- [17] M. Vogt, K. Kunath, J.B. Dressman, Dissolution enhancement of fenofibrate by micronization , cogrinding and spray-drying: Comparison with commercial preparations, 68 (2008) 283–288. <https://doi.org/10.1016/j.ejpb.2007.05.010>.
- [18] J. Goole, K. Amighi, 3D printing in pharmaceuticals : A new tool for designing customized drug delivery systems, *Int. J. Pharm.* 499 (2016) 376–394. <https://doi.org/10.1016/j.ijpharm.2015.12.071>.
- [19] M.A. Alhnan, T.C. Okwuosa, M. Sadia, K. Wan, W. Ahmed, Emergence of 3D Printed Dosage Forms : Opportunities and Challenges, *Pharm. Res.* (2016) 1817–1832. <https://doi.org/10.1007/s11095-016-1933-1>.
- [20] L.K. Prasad, H. Smyth, L.K. Prasad, H. Smyth, 3D Printing technologies for drug delivery : a review 3D Printing technologies for drug delivery : a review, 9045 (2016). <https://doi.org/10.3109/03639045.2015.1120743>.
- [21] L.K. Prasad, H. Smyth, 3D Printing technologies for drug delivery: a review, *Drug Dev. Ind. Pharm.* 42 (2016) 1019–1031. <https://doi.org/10.3109/03639045.2015.1120743>.
- [22] J.W. Stansbury, M.J. Idacavage, 3D printing with polymers : Challenges among expanding options and opportunities, *Dent. Mater.* 32 (2015) 54–64. <https://doi.org/10.1016/j.dental.2015.09.018>.
- [23] T.D. Ngo, A. Kashani, G. Imbalzano, K.T.Q. Nguyen, D. Hui, Additive manufacturing ( 3D printing ) : A review of materials , methods , applications and challenges, *Compos. Part B.* 143 (2018) 172–196. <https://doi.org/10.1016/j.compositesb.2018.02.012>.
- [24] B.M. Wu, S.W. Borland, R.A. Giordano, C.L. G., E.M. Sachs, M.J. Cima, Solid free-form fabrication of drug delivery devices, 40 (1996) 77–87.
- [25] N. Sandler, M. Preis, Printed Drug-Delivery Systems for Improved Patient Treatment, *Trends Pharmacol. Sci.* 37 (2016) 1070–1080. <https://doi.org/10.1016/j.tips.2016.10.002>.
- [26] N. Genina, J.P. Boetker, S. Colombo, N. Harmankaya, J. Rantanen, Anti-tuberculosis drug combination for controlled oral delivery using 3D printed compartmental dosage forms : From drug product design to in vivo testing, *J. Control. Release.* 268 (2017) 40–48. <https://doi.org/10.1016/j.jconrel.2017.10.003>.
- [27] A. Maroni, A. Melocchi, F. Parietti, A. Foppoli, L. Zema, A. Gazzaniga, 3D printed multi-compartment capsular devices for two-pulse oral drug delivery, *J. Control. Release.* 268 (2017) 10–18. <https://doi.org/10.1016/j.jconrel.2017.10.008>.
- [28] M. Kyobula, A. Adedeji, M.R. Alexander, E. Saleh, R. Wildman, I. Ashcroft, P.R. Gellert, C.J. Roberts, 3D inkjet printing of tablets exploiting bespoke complex geometries for controlled and tuneable drug release, *J. Control. Release.* 261 (2017) 207–215. <https://doi.org/10.1016/j.jconrel.2017.06.025>.
- [29] A. Goyanes, P. Robles, A. Buanz, A.W. Basit, S. Gaisford, Effect of geometry on drug release from 3D printed tablets, *Int. J. Pharm.* 494 (2015) 657–663. <https://doi.org/10.1016/j.ijpharm.2015.04.069>.

- [30] W. Huang, Q. Zheng, W. Sun, H. Xu, X. Yang, Levofloxacin implants with predefined microstructure fabricated by three-dimensional printing technique, 339 (2007) 33–38. <https://doi.org/10.1016/j.ijpharm.2007.02.021>.
- [31] W. Kempin, V. Domsta, G. Grathoff, I. Brecht, B. Semmling, S. Tillmann, W. Weitschies, A. Seidlitz, Immediate Release 3D-Printed Tablets Produced Via Fused Deposition Modeling of a Thermo-Sensitive Drug, (2018).
- [32] J. Norman, R.D. Madurawe, C.M.V. Moore, M.A. Khan, A. Khairuzzaman, A new chapter in pharmaceutical manufacturing: 3D-printed drug products, *Adv. Drug Deliv. Rev.* 108 (2017) 39–50. <https://doi.org/10.1016/j.addr.2016.03.001>.
- [33] G. Acosta-Vélez and B. M. Wu, 3D Pharming: Direct Printing of Personalized Pharmaceutical Tablets, *Polym. Sci.* 2 (2016) 1–10. <https://doi.org/10.4172/2471-9935.100011>.
- [34] A. Goyanes, M. Kobayashi, R. Martínez-Pacheco, S. Gaisford, A.W. Basit, Fused-filament 3D printing of drug products: Microstructure analysis and drug release characteristics of PVA-based caplets, *Int. J. Pharm.* 514 (2016) 290–295. <https://doi.org/10.1016/j.ijpharm.2016.06.021>.
- [35] H.N. Chia, B.M. Wu, Recent advances in 3D printing of biomaterials, *J. Biol. Eng.* (2015) 1–14. <https://doi.org/10.1186/s13036-015-0001-4>.
- [36] R. Daly, T.S. Harrington, G.D. Martin, I.M. Hutchings, Inkjet printing for pharmaceuticals - A review of research and manufacturing, *Int. J. Pharm.* 494 (2015) 554–567. <https://doi.org/10.1016/j.ijpharm.2015.03.017>.
- [37] W.E. Katstra, R.D. Palazzolo, C.W. Rowe, B. Giritlioglu, P. Teung, M.J. Cima, Oral dosage forms fabricated by Three Dimensional Printing(TM), *J. Control. Release.* 66 (2000) 1–9. [https://doi.org/10.1016/S0168-3659\(99\)00225-4](https://doi.org/10.1016/S0168-3659(99)00225-4).
- [38] D. Dimitrov, K. Schreve, N. De Beer, Advances in three dimensional printing - State of the art and future perspectives, *Rapid Prototyp. J.* 12 (2006) 136–147. <https://doi.org/10.1108/13552540610670717>.
- [39] F. Fina, A. Goyanes, S. Gaisford, A.W. Basit, Selective laser sintering (SLS) 3D printing of medicines, *Int. J. Pharm.* 529 (2017) 285–293. <https://doi.org/10.1016/j.ijpharm.2017.06.082>.
- [40] A. Marro, T. Bandukwala, W. Mak, Three-Dimensional Printing and Medical Imaging: A Review of the Methods and Applications, *Curr. Probl. Diagn. Radiol.* 45 (2016) 2–9. <https://doi.org/10.1067/j.cpradiol.2015.07.009>.
- [41] I. Zein, D.W. Hutmacher, K. Cheng, S. Hin, Fused deposition modeling of novel scaffold architectures for tissue engineering applications, 23 (2002) 1169–1185.
- [42] A. Goyanes, A.B.M. Buanz, G.B. Hatton, S. Gaisford, A.W. Basit, 3D printing of modified-release aminosalicilate (4-ASA and 5-ASA) tablets, *Eur. J. Pharm. Biopharm.* 89 (2015) 157–162. <https://doi.org/10.1016/j.ejpb.2014.12.003>.
- [43] Y. Yang, H. Wang, H. Li, Z. Ou, G. Yang, 3D printed tablets with internal scaffold structure using ethyl cellulose to achieve sustained ibuprofen release, *Eur. J. Pharm. Sci.* 115 (2018) 11–18. <https://doi.org/10.1016/j.ejps.2018.01.005>.
- [44] S. ichiro Kimura, T. Ishikawa, Y. Iwao, S. Itai, H. Kondo, Fabrication of zero-order sustained-release floating tablets via fused depositing modeling 3D printer, *Chem. Pharm. Bull.* 67 (2019) 992–999.

- <https://doi.org/10.1248/cpb.c19-00290>.
- [45] P. Kanaujia, P. Poovizhi, W.K. Ng, R.B.H. Tan, Amorphous formulations for dissolution and bioavailability enhancement of poorly soluble APIs, *Powder Technol.* 285 (2015) 2–15. <https://doi.org/10.1016/j.powtec.2015.05.012>.
  - [46] L.I. Blaabjerg, H. Grohgan, E. Lindenberg, K. Löbmann, A. Müllertz, T. Rades, The influence of polymers on the supersaturation potential of poor and good glass formers, *Pharmaceutics*. 10 (2018) 1–14. <https://doi.org/10.3390/pharmaceutics10040164>.
  - [47] C. Brough, R.O. Williams, Amorphous solid dispersions and nano-crystal technologies for poorly water-soluble drug delivery, *Int. J. Pharm.* 453 (2013) 157–166. <https://doi.org/10.1016/j.ijpharm.2013.05.061>.
  - [48] S. Shah, S. Maddineni, J. Lu, M.A. Repka, Melt extrusion with poorly soluble drugs, *Int. J. Pharm.* 453 (2013) 233–252. <https://doi.org/10.1016/j.ijpharm.2012.11.001>.
  - [49] S. Baghel, H. Cathcart, N.J. O'Reilly, Theoretical and experimental investigation of drug-polymer interaction and miscibility and its impact on drug supersaturation in aqueous medium, *Eur. J. Pharm. Biopharm.* 107 (2016) 16–31. <https://doi.org/10.1016/j.ejpb.2016.06.024>.
  - [50] K. Khougaz, S.D. Clas, Crystallization inhibitor in solid dispersions of MK-0591 and poly(vinylpyrrolidone) polymers, *J. Pharm. Sci.* 89 (2000) 1325–1334. [https://doi.org/10.1002/1520-6017\(200010\)89:10<1325::AID-JPS10>3.0.CO;2-5](https://doi.org/10.1002/1520-6017(200010)89:10<1325::AID-JPS10>3.0.CO;2-5).
  - [51] A.L. Sarode, H. Sandhu, N. Shah, W. Malick, H. Zia, Hot melt extrusion (HME) for amorphous solid dispersions: Predictive tools for processing and impact of drug-polymer interactions on supersaturation, *Eur. J. Pharm. Sci.* 48 (2013) 371–384. <https://doi.org/10.1016/j.ejps.2012.12.012>.
  - [52] K. Adamska, A. Voelkel, Inverse gas chromatographic determination of solubility parameters of excipients, *Int. J. Pharm.* 304 (2005) 11–17. <https://doi.org/10.1016/j.ijpharm.2005.03.040>.
  - [53] A. Forster, J. Hempenstall, I. Tucker, T. Rades, Selection of excipients for melt extrusion with two poorly water-soluble drugs by solubility parameter calculation and thermal analysis, *Int. J. Pharm.* 226 (2001) 147–161. [https://doi.org/10.1016/S0378-5173\(01\)00801-8](https://doi.org/10.1016/S0378-5173(01)00801-8).
  - [54] A. Forster, J. Hempenstall, I. Tucker, T. Rades, The potential of small-scale fusion experiments and the Gordon-Taylor equation to predict the suitability of drug/polymer blends for melt extrusion, *Drug Dev. Ind. Pharm.* 27 (2001) 549–560. <https://doi.org/10.1081/DDC-100105180>.
  - [55] M. Alhijaj, P. Belton, S. Qi, An investigation into the use of polymer blends to improve the printability of and regulate drug release from pharmaceutical solid dispersions prepared via fused deposition modeling (FDM) 3D printing, *Eur. J. Pharm. Biopharm.* 108 (2016) 111–125. <https://doi.org/10.1016/j.ejpb.2016.08.016>.
  - [56] J.R. Hughey, J.M. Keen, D.A. Miller, K. Kolter, N. Langley, J.W. McGinity, The use of inorganic salts to improve the dissolution characteristics of tablets containing Soluplus®-based solid dispersions, *Eur. J. Pharm. Sci.* 48 (2013) 758–766. <https://doi.org/10.1016/j.ejps.2013.01.004>.
  - [57] J. Thiry, F. Krier, B. Evrard, A review of pharmaceutical extrusion: Critical process parameters and scaling-up, *Int. J. Pharm.* 479 (2015) 227–240. <https://doi.org/10.1016/j.ijpharm.2014.12.036>.
  - [58] B.C. Pereira, A. Isreb, R.T. Forbes, F. Dores, R. Habashy, 'Temporary Plasticiser': A novel solution to fabricate 3D printed patient-centred cardiovascular 'Polypill' architectures, *Eur. J. Pharm.*

- Biopharm. 135 (2019) 94–103. <https://doi.org/10.1016/j.ejpb.2018.12.009>.
- [59] S. Palekar, P. Kumar, S.M. Mishra, T. Kipping, K. Patel, Application of 3D printing technology and quality by design approach for development of age-appropriate pediatric formulation of baclofen, *Int. J. Pharm.* 556 (2019) 106–116. <https://doi.org/10.1016/j.ijpharm.2018.11.062>.
- [60] T. Ehtezazi, M. Algellay, Y. Islam, M. Roberts, N.M. Dempster, S.D. Sarker, The Application of 3D Printing in the Formulation of Multilayered Fast Dissolving Oral Films The Application of 3D Printing in the Formulation of Multilayered Fast Dissolving Oral Films, *J. Pharm. Sci.* (2017). <https://doi.org/10.1016/j.xphs.2017.11.019>.
- [61] A. Melocchi, F. Parietti, A. Maroni, A. Foppoli, A. Gazzaniga, L. Zema, Hot-melt extruded filaments based on pharmaceutical grade polymers for 3D printing by fused deposition modeling, *Int. J. Pharm.* 509 (2016) 255–263. <https://doi.org/10.1016/j.ijpharm.2016.05.036>.
- [62] W. Jamróz, M. Kurek, Ł. Ewelina, J. Szafraniec, J. Knapik-kowalczyk, K. Syrek, M. Paluch, R. Jachowicz, 3D printed orodispersible films with Aripiprazole, 533 (2017) 413–420. <https://doi.org/10.1016/j.ijpharm.2017.05.052>.
- [63] G. Kollamaram, D.M. Croker, G.M. Walker, A. Goyanes, A.W. Basit, S. Gaisford, Low temperature fused deposition modeling ( FDM ) 3D printing of thermolabile drugs, *Int. J. Pharm.* 545 (2018) 144–152. <https://doi.org/10.1016/j.ijpharm.2018.04.055>.
- [64] T.C. Okwuosa, D. Stefaniak, B. Arafat, A. Isreb, K. Wan, A Lower Temperature FDM 3D Printing for the Manufacture of Patient-Specific Immediate Release Tablets, *Pharm. Res.* 33 (2016) 2704–2712. <https://doi.org/10.1007/s11095-016-1995-0>.
- [65] J. Zhang, W. Yang, A.Q. Vo, X. Feng, X. Ye, D. Wuk, M.A. Repka, Hydroxypropyl methylcellulose-based controlled release dosage by melt extrusion and 3D printing: Structure and drug release correlation, *Carbohydr. Polym.* 177 (2017) 49–57. <https://doi.org/10.1016/j.carbpol.2017.08.058>.
- [66] A. Isreb, K. Baj, M. Wojsz, M. Isreb, M. Peak, M.A. Alhnan, 3D printed oral theophylline doses with innovative 'radiator-like' design: Impact of polyethylene oxide (PEO) molecular weight, *Int. J. Pharm.* 564 (2019) 98–105. <https://doi.org/10.1016/j.ijpharm.2019.04.017>.
- [67] M. Sadia, A. So, B. Arafat, A. Isreb, W. Ahmed, Adaptation of pharmaceutical excipients to FDM 3D printing for the fabrication of patient-tailored immediate release tablets, *Int. J. Pharm.* 513 (2016) 659–668. <https://doi.org/10.1016/j.ijpharm.2016.09.050>.
- [68] M. Novák, T. Boleslavská, A. Wan, J. Beránek, P. Kova, Virtual Prototyping and Parametric Design of 3D-Printed Tablets Based on the Solution of Inverse Problem, 19 (2018) 3414–3424. <https://doi.org/10.1208/s12249-018-1176-z>.
- [69] C. Korte, J. Quodbach, C. Korte, J. Quodbach, Formulation development and process analysis of drug-loaded filaments manufactured via hot-melt extrusion for 3D-printing of medicines manufactured via hot-melt extrusion for 3D-printing of medicines, *Pharm. Dev. Technol.* 23 (2018) 1117–1127. <https://doi.org/10.1080/10837450.2018.1433208>.
- [70] F.M. Vanin, P.J.A. Sobral, F.C. Menegalli, R.A. Carvalho, A.M.Q.B. Habitante, Effects of plasticizers and their concentrations on thermal and functional properties of gelatin-based films, *Food Hydrocoll.* 19 (2005) 899–907. <https://doi.org/10.1016/j.foodhyd.2004.12.003>.
- [71] K. Pietrzak, A. Isreb, M.A. Alhnan, A flexible-dose dispenser for immediate and extended release 3D printed tablets, *Eur. J. Pharm. Biopharm.* 96 (2015) 380–387.

- <https://doi.org/10.1016/j.ejpb.2015.07.027>.
- [72] M. Jährling, Application report No. AN53134\_E\_04/19K : Use of melt pump to produce filaments for additive manufacturing (3D printing), (2019).
  - [73] T. Wesselink, L. Van Leeuwen, Fused Deposition Modeling Filament Production Apparatus. American Patent No. US20190168436A1., 2019.
  - [74] P. Wang, B. Zou, H. Xiao, S. Ding, C. Huang, Effects of printing parameters of fused deposition modeling on mechanical properties , surface quality , and microstructure of PEEK, *J. Mater. Process. Tech.* 271 (2019) 62–74. <https://doi.org/10.1016/j.jmatprotec.2019.03.016>.
  - [75] V. Zupancic, N. Ograjsek, B. Kotar-jordan, F. Vreced, Physical characterization of pantoprazole sodium hydrates, 291 (2005) 59–68. <https://doi.org/10.1016/j.ijpharm.2004.07.043>.
  - [76] J. Aho, J.P. Bøtker, N. Genina, M. Edinger, L. Arnfast, Roadmap to 3D-Printed Oral Pharmaceutical Dosage Forms : Feedstock Filament Properties and Characterization for Fused Deposition Modeling, *J. Pharm. Sci.* 108 (2019) 26–35. <https://doi.org/10.1016/j.xphs.2018.11.012>.
  - [77] X. Chai, H. Chai, X. Wang, J. Yang, J. Li, Y. Zhao, W. Cai, T. Tao, X. Xiang, Fused Deposition Modeling (FDM) 3D Printed Tablets for Intragastric Floating Delivery of Domperidone OPEN, *Sci. Rep.* 7 (2017). <https://doi.org/10.1038/s41598-017-03097-x>.
  - [78] N.G. Solanki, M. Tahsin, A. V. Shah, A.T.M. Serajuddin, Formulation of 3D Printed Tablet for Rapid Drug Release by Fused Deposition Modeling: Screening Polymers for Drug Release, Drug-Polymer Miscibility and Printability, *J. Pharm. Sci.* 107 (2018) 390–401. <https://doi.org/10.1016/j.xphs.2017.10.021>.
  - [79] A. Goyanes, P. Robles Martinez, A. Buanz, A.W. Basit, S. Gaisford, Effect of geometry on drug release from 3D printed tablets, *Int. J. Pharm.* 494 (2015) 657–663. <https://doi.org/10.1016/j.ijpharm.2015.04.069>.
  - [80] M. Sadia, B. Arafat, W. Ahmed, R.T. Forbes, M.A. Alhnan, Channelled tablets: An innovative approach to accelerating drug release from 3D printed tablets, *J. Control. Release.* 269 (2018) 355–363. <https://doi.org/10.1016/j.jconrel.2017.11.022>.
  - [81] B. Arafat, M. Wojsz, A. Isreb, R.T. Forbes, M. Isreb, Tablet fragmentation without a disintegrant : A novel design approach for accelerating disintegration and drug release from 3D printed cellulosic tablets, 118 (2018) 191–199. <https://doi.org/10.1016/j.ejps.2018.03.019>.
  - [82] A. Isreb, K. Baj, M. Wojsz, M. Isreb, M. Peak, 3D printed oral theophylline doses with innovative ‘ radiator-like ’ design : Impact of polyethylene oxide ( PEO ) molecular weight, *Int. J. Pharm.* 564 (2019) 98–105. <https://doi.org/10.1016/j.ijpharm.2019.04.017>.
  - [83] L. Maggi, R. Bruni, U. Conte, High molecular weight polyethylene oxides ( PEOs ) as an alternative to HPMC in controlled release dosage forms, 195 (2000) 229–238.
  - [84] A. Abdelbary, E.R. Bendas, A.A. Ramadan, D.A. Mostafa, Pharmaceutical and Pharmacokinetic Evaluation of a Novel Fast Dissolving Film Formulation of Flupentixol Dihydrochloride, 15 (2014). <https://doi.org/10.1208/s12249-014-0186-8>.
  - [85] J. Conceição, X. Farto-Vaamonde, A. Goyanes, O. Adeoye, A. Concheiro, H. Cabral-Marques, J.M. Sousa Lobo, C. Alvarez-Lorenzo, Hydroxypropyl- $\beta$ -cyclodextrin-based fast dissolving carbamazepine printlets prepared by semisolid extrusion 3D printing, *Carbohydr. Polym.* 221 (2019)

- 55–62. <https://doi.org/10.1016/j.carbpol.2019.05.084>.
- [86] S.A. Khaled, M.R. Alexander, R.D. Wildman, M.J. Wallace, S. Sharpe, J. Yoo, C.J. Roberts, 3D extrusion printing of high drug loading immediate release paracetamol tablets, *Int. J. Pharm.* 538 (2018) 223–230. <https://doi.org/10.1016/j.ijpharm.2018.01.024>.
- [87] K. Vithani, A. Goyanes, V. Jannin, A.W. Basit, S. Gaisford, B.J. Boyd, A Proof of Concept for 3D Printing of Solid Lipid-Based Formulations of Poorly Water-Soluble Drugs to Control Formulation Dispersion Kinetics, (2019).
- [88] S.A. Khaled, J.C. Burley, M.R. Alexander, J. Yang, C.J. Roberts, 3D printing of five-in-one dose combination polypill with defined immediate and sustained release profiles, *J. Control. Release.* 217 (2015) 308–314. <https://doi.org/10.1016/j.jconrel.2015.09.028>.
- [89] A. Zidan, A. Alayoubi, S. Asfari, J. Coburn, B. Ghamraoui, C.N. Cruz, M. Ashraf, Development of mechanistic models to identify critical formulation and process variables of pastes for 3D printing of modified release tablets, *Int. J. Pharm.* 555 (2019) 109–123. <https://doi.org/10.1016/j.ijpharm.2018.11.044>.
- [90] J. Wang, A. Goyanes, S. Gaisford, A.W. Basit, Stereolithographic (SLA) 3D printing of oral modified-release dosage forms, *Int. J. Pharm.* 503 (2016) 207–212. <https://doi.org/10.1016/j.ijpharm.2016.03.016>.
- [91] E. Andrzejewska, Photopolymerization kinetics of multifunctional monomers, *Prog. Polym. Sci.* 26 (2001) 605–665.
- [92] J. V. Crivello, Photoinitiated Cationic Polymerization., *Annu. Rev. Mater. Sci.* 13 (1983) 173–190. <https://doi.org/10.1146/annurev.ms.13.080183.001133>.
- [93] H. Kadry, S. Wadnap, C. Xu, F. Ahsan, Digital light processing ( DLP ) 3D-printing technology and photoreactive polymers in fabrication of modified-release tablets, *Eur. J. Pharm. Sci.* 135 (2019) 60–67. <https://doi.org/10.1016/j.ejps.2019.05.008>.
- [94] G.F. Acosta-vélez, T.Z. Zhu, C.S. Linsley, B.M. Wu, Photocurable poly ( ethylene glycol ) as a bioink for the inkjet 3D pharming of hydrophobic drugs, *Int. J. Pharm.* 546 (2018) 145–153. <https://doi.org/10.1016/j.ijpharm.2018.04.056>.
- [95] S.F.S. Shirazi, S. Gharekhani, M. Mehrali, H. Yarmand, H.S.C. Metselaar, N.A. Kadri, N.A.A.N.A. Osman, A review on powder-based additive manufacturing for tissue engineering : selective laser sintering and inkjet 3D printing A review on powder-based additive manufacturing for tissue engineering : selective laser sintering and inkjet 3D printing, *Sci. Technol. Adv. Mater.* 16 (2015) 1–20. <https://doi.org/10.1088/1468-6996/16/3/033502>.
- [96] F. Fina, A. Goyanes, C.M. Madla, A. Awad, S.J. Trenfield, J.M. Kuek, P. Patel, S. Gaisford, A.W. Basit, 3D printing of drug-loaded gyroid lattices using selective laser sintering, *Int. J. Pharm.* 547 (2018) 44–52. <https://doi.org/10.1016/j.ijpharm.2018.05.044>.

# ABBREVIATIONS

---



<b>3D</b>	Three-dimensional
<b>API</b>	Active pharmaceutical ingredient
<b>ASD</b>	Amorphous solid dispersion
<b>AV</b>	Acceptance value
<b>BCS</b>	Biopharmaceutics classification system
<b>CAD</b>	Computer-aided design
<b>CBD</b>	Cannabidiol
<b>CD</b>	Cyclodextrin
<b>CH3<math>\beta</math>CD</b>	RAMEB <sup>®</sup>
<b>CM</b>	Continuous manufacturing
<b>DCS</b>	Developability classification system
<b>DMSO</b>	Dimethyl sulfoxide
<b>DPE</b>	Direct powder extrusion 3D printing
<b>DSC</b>	Differential scanning calorimetry
<b>E100</b>	Eudragit <sup>®</sup> E100
<b>EMA</b>	European medicines agency
<b>ENM</b>	Eudragit <sup>®</sup> NM30D
<b>EPO</b>	Eudragit <sup>®</sup> EPO
<b>Eur. Ph.</b>	European Pharmacopoeia
<b>FD</b>	Freeze-drying
<b>FDA</b>	Food and drug administration
<b>FDM</b>	Fused-deposition modeling
<b>GIT</b>	Gastrointestinal tract
<b>GRAS</b>	Generally accepted as safe
<b>HME</b>	Hot-melt extrusion
<b>HPC</b>	Hydroxypropylcellulose
<b>HPLC</b>	High-performance liquid chromatography
<b>HPMC</b>	Hydroxypropyl methylcellulose
<b>HPMCAS</b>	Hypromellose acetate succinate
<b>HP<math>\beta</math>CD</b>	Hydroxypropyl- $\beta$ -cyclodextrin
<b>HP<math>\gamma</math>CD</b>	Hydroxypropyl- $\gamma$ -cyclodextrin
<b>HTS</b>	High-throughput screening
<b>ITZ</b>	Itraconazole
<b>IVIVC</b>	<i>In vitro-in vivo</i> correlations

## ABBREVIATIONS

---

<b>K12PF</b>	Kollidon® 12PF
<b>KVA64</b>	Kollidon® VA64
<b>MS</b>	Mesoporous silica
<b>MS-ALFP</b>	Mesoporous silica Syloid® AL-1FP
<b>MS-Silsol</b>	Mesoporous silica Silsol® SP53D
<b>PAM</b>	Pressure-assisted micro-syringe
<b>PAT</b>	Process analytical technology
<b>PEG</b>	Polyethylene glycol
<b>PEGDA</b>	Polyethylene glycol diacrylate
<b>PEGMA</b>	Polyethylene glycol methacrylate
<b>PEO</b>	Polyox® N10
<b>PVA</b>	Polyvinyl alcohol
<b>PVP</b>	Polyvinylpyrrolidone
<b>PVP/VA</b>	Polyvinylpyrrolidone-vinyl acetate
<b>SA/V</b>	Surface-to-volume
<b>sc-CO<sub>2</sub></b>	Supercritical carbon dioxide
<b>SD</b>	Solid dispersion
<b>SEDDS</b>	Self-emulsifying drug delivery system
<b>SLA</b>	Stereolithography
<b>SLS</b>	Selective laser sintering
<b>SMEDDS</b>	Self-microemulsifying drug delivery system
<b>SNEDDS</b>	Self-nanoemulsifying drug delivery system
<b>SOL</b>	Soluplus®
<b>TCP</b>	Tri-calcium phosphate
<b>T<sub>deg</sub></b>	Degradation temperature
<b>TEC</b>	Triethylcitrate
<b>T<sub>g</sub></b>	Glass transition temperature
<b>TGA</b>	Thermogravimetric analysis
<b>THC</b>	$\Delta^9$ -tetrahydrocannabinol
<b>T<sub>m</sub></b>	Melting temperature
<b>TOF-SIMS</b>	Time-of-flight secondary ion mass spectrometry
<b>TS</b>	Tensile strength
<b>XRPD</b>	X-ray powder diffraction

# CURRICULUM VITAE

---

**Olivier Jennotte**

(07/02/1991, Liège, Belgium)

**Education**

- 2016 – 2014: Master's degree in Pharmaceutical Sciences at Université de Liège, Belgium.
- 2014 – 2009: Bachelor's degree in Pharmaceutical Sciences at Université de Liège, Belgium.
- 2009 – 2003: Languages – Sciences at Collège Saint-Hadelin Visé, Belgium.

**Bibliography**

**Articles in international reviewed journals**

- Koch, N., **Jennotte, O.**, Gasparrini, Y., Vandenbroucke, F., Lechanteur, A., & Evrard, B. (2020). Cannabidiol aqueous solubility enhancement: comparison of three amorphous formulations strategies using different type of polymers. International Journal of Pharmaceutics. doi:10.1016/j.ijpharm.2020.119812.
- **Jennotte, O.**, Koch, N., Lechanteur, A., & Evrard, B. (2020). Three-dimensional printing technology as a promising tool in bioavailability enhancement of poorly water-soluble molecules: a review. International Journal of Pharmaceutics. doi:10.1016/j.ijpharm.2020.119200.
- Koch, N., **Jennotte, O.**, Grignard, B., Lechanteur, A., & Evrard, B. (01 July 2020). Impregnation of mesoporous silica with poor aqueous soluble molecule using pressurized carbon dioxide: is the solubility in the supercritical and subcritical phase a critical parameter? European Journal of Pharmaceutical Sciences, 150, 105332. doi:10.1016/j.ejps.2020.105332.
- Parulski, C., **Jennotte, O.**, Lechanteur, A., & Evrard, B. (August 2021). Challenges of fused deposition modeling 3D printing in pharmaceutical applications: Where are we now? Advanced Drug Delivery Reviews, 175. doi:10.1016/j.addr.2021.05.020.

- Koch, N., **Jennotte, O.**, Ziemons, E., Boussard, G., Lechanteur, A., & Evrard, B. (2022). Influence of API physicochemical properties on amorphization capacity of several mesoporous silica loading methods. *International Journal of Pharmaceutics*. doi:10.1016/j.ijpharm.2021.121372.
- **Jennotte, O.**, Koch, N., Lechanteur, A., & Evrard, B. (2022). Development of amorphous solid dispersions of cannabidiol: Influence of the carrier, the hot-melt extrusion parameters and the use of a crystallization inhibitor. *Journal of Drug Delivery Science and Technology*, 103372. doi:10.1016/j.jddst.2022.103372.
- Parulski, C., Gresse, E., **Jennotte, O.**, Felten, A., Ziemons, E., Lechanteur, A., & Evrard, B. (31 August 2022). Fused deposition modeling 3D printing of solid oral dosage forms containing amorphous solid dispersions: How to elucidate drug dissolution mechanisms through surface spectral analysis techniques? *International Journal of Pharmaceutics*, 626, 122157. doi:10.1016/j.ijpharm.2022.122157.
- Koch, N., **Jennotte, O.**, Toussaint, C., Lechanteur, A., & Evrard, B. (2023). Production challenges of tablets containing lipid excipients: case study using cannabidiol as drug model. *International Journal of Pharmaceutics*, 122639. doi:10.1016/j.ijpharm.2023.122639.

Meeting abstracts, presented at international scientific conferences

- **Jennotte, O.**, Koch, N., Collard, L., Lechanteur, A., & Evrard, B. (26 March 2019). *Hot melt extrusion as a solvent-free technique for the formation of a polymeric amorphous solid dispersion of atorvastatin*. Presented at 3rd European Conference on Pharmaceutics, Bologna, Italy.
- **Jennotte, O.**, Koch, N., Lechanteur, A., & Evrard, B. (06 April 2021). Amorphous solid dispersions of cannabidiol with an increase of the aqueous solubility: influence of the carrier, the hot melt extrusion parameters and the use of a crystallization inhibitor. Presented at The Controlled Release Society BeNeLux&France Early Career Scientists Meeting 2021.
- **Jennotte, O.**, Koch, N., Rosoux, F., Emmerechts Carl, Beeckman Eric, Lechanteur, A., & Evrard, B. (30 March 2022). Formulation and Quality

Consideration of Cannabidiol Printed Tablets Produced by Fused-Deposition Modeling. Presented at 13th World Meeting on Pharmaceutics, Biopharmaceutics and Pharmaceutical Technology.

- **Jennotte, O.**, Lechanteur, A., Koch, N., Evrard, B., Rosoux François, Emmerechts Carl, & Beeckman Eric. (20 March 2023). Formulation and Quality Consideration of Printed Tablets of Cannabidiol Produced by Direct Powder Extrusion. Presented at 4th European Conference on Pharmaceutics.

### Meeting abstracts, presented at national scientific conferences

- **Jennotte, O.**, Koch, N., Collard, L., Lechanteur, A., & Evrard, B. (19 December 2018). Hot melt extrusion as a solvent-free technique for the formation of a polymeric amorphous solid dispersion of atorvastatin. Presented at CIRM Day, Liège, Belgium.
- **Jennotte, O.**, Koch, N., Rocks, N., Lechanteur, A., & Evrard, B. (20 May 2019). Development of new manufacturing processes for amorphous solid dispersions. Presented at 20<sup>th</sup> forum of pharmaceutical sciences, Bruxelles, Belgium.
- **Jennotte, O.**, Koch, N., Lechanteur, A., & Evrard, B. (11 December 2019). Hot-melt extrusion as a solvent-free technique for the formation of a polymeric amorphous solid dispersion of atorvastatin. Presented at Second scientific CIRM day, Liège, Belgium.
- **Jennotte, O.**, Koch, N., Lechanteur, A., & Evrard, B. (02 February 2022). Formulation and Quality Consideration of Cannabidiol Printed Tablets Produced by Fused-Deposition Modeling. Presented at CIRM DAY 2022.

### Grant

2022: 7000 € Research Grant from the « Fonds Leon Fredericq ».